frontiers | Research Topics

Current molecular, immunological, pathological and clinical aspects of pathogenic infections

Edited by
José Luis Muñoz-Carrillo, Oscar Gutierrez-Coronado
and Rommel Chacon-Salinas

Published in
Frontiers in Cellular and Infection Microbiology

ISSN 1664-8714
ISBN 978-2-8325-6815-6
DOI 10.3389/978-2-8325-6815-6

Generative AI statement
Any alternative text (Alt text) provided alongside figures in the articles in this ebook has been generated by Frontiers with the support of artificial intelligence and reasonable efforts have been made to ensure accuracy, including review by the authors wherever possible. If you identify any issues, please contact us.

About Frontiers

Frontiers is more than just an open access publisher of scholarly articles: it is a pioneering approach to the world of academia, radically improving the way scholarly research is managed. The grand vision of Frontiers is a world where all people have an equal opportunity to seek, share and generate knowledge. Frontiers provides immediate and permanent online open access to all its publications, but this alone is not enough to realize our grand goals.

Frontiers journal series

The Frontiers journal series is a multi-tier and interdisciplinary set of open-access, online journals, promising a paradigm shift from the current review, selection and dissemination processes in academic publishing. All Frontiers journals are driven by researchers for researchers; therefore, they constitute a service to the scholarly community. At the same time, the *Frontiers journal series* operates on a revolutionary invention, the tiered publishing system, initially addressing specific communities of scholars, and gradually climbing up to broader public understanding, thus serving the interests of the lay society, too.

Dedication to quality

Each Frontiers article is a landmark of the highest quality, thanks to genuinely collaborative interactions between authors and review editors, who include some of the world's best academicians. Research must be certified by peers before entering a stream of knowledge that may eventually reach the public - and shape society; therefore, Frontiers only applies the most rigorous and unbiased reviews. Frontiers revolutionizes research publishing by freely delivering the most outstanding research, evaluated with no bias from both the academic and social point of view. By applying the most advanced information technologies, Frontiers is catapulting scholarly publishing into a new generation.

What are Frontiers Research Topics?

Frontiers Research Topics are very popular trademarks of the *Frontiers journals series*: they are collections of at least ten articles, all centered on a particular subject. With their unique mix of varied contributions from Original Research to Review Articles, Frontiers Research Topics unify the most influential researchers, the latest key findings and historical advances in a hot research area.

Find out more on how to host your own Frontiers Research Topic or contribute to one as an author by contacting the Frontiers editorial office: frontiersin.org/about/contact

Current molecular, immunological, pathological and clinical aspects of pathogenic infections

Topic editors
José Luis Muñoz-Carrillo — University of Guadalajara, Mexico
Oscar Gutierrez-Coronado — University of Guadalajara, Mexico
Rommel Chacon-Salinas — Departamento de Inmunología, Escuela Nacional de Ciencias Biológicas, Instituto Politécnico Nacional, Mexico

Citation
Muñoz-Carrillo, J. L., Gutierrez-Coronado, O., Chacon-Salinas, R., eds. (2025). *Current molecular, immunological, pathological and clinical aspects of pathogenic infections*. Lausanne: Frontiers Media SA. doi: 10.3389/978-2-8325-6815-6

Table of contents

frontiers | Frontiers in Cellular and Infection Microbiology

TYPE Editorial
PUBLISHED 08 August 2025
DOI 10.3389/fcimb.2025.1665283

OPEN ACCESS

EDITED AND REVIEWED BY
Annemarie H. Meijer,
Leiden University, Netherlands

*CORRESPONDENCE
José Luis Muñoz-Carrillo
mcbjlmc@gmail.com;
jose.munoz@lagos.udg.mx
Oscar Gutiérrez-Coronado
ogutierrez@culagos.udg.mx
Rommel Chacon-Salinas
rchacons@ipn.mx

RECEIVED 13 July 2025
ACCEPTED 25 July 2025
PUBLISHED 08 August 2025

CITATION
Muñoz-Carrillo JL, Gutiérrez-Coronado O and Chacon-Salinas R (2025) Editorial: Current molecular, immunological, pathological and clinical aspects of pathogenic infections.
Front. Cell. Infect. Microbiol. 15:1665283.
doi: 10.3389/fcimb.2025.1665283

Editorial: Current molecular, immunological, pathological and clinical aspects of pathogenic infections

José Luis Muñoz-Carrillo[1,2]*, Oscar Gutiérrez-Coronado[1]* and Rommel Chacon-Salinas[3]*

[1]Laboratorio de Inmunología, Centro Universitario de los Lagos, Universidad de Guadalajara, Lagos de Moreno, Jalisco, Mexico, [2]Escuela de Odontología, Global University, Aguascalientes, Aguascalientes, Mexico, [3]Departamento de Inmunología, Escuela Nacional de Ciencias Biológicas, Instituto Politécnico Nacional, Ciudad de Mexico, Mexico

KEYWORDS

bovine respiratory disease, COVID-19, hepatitis B virus, mycoplasma pneumoniae, periodontitis, puerperal infection, sepsis, type 2 diabetes mellitus

Editorial on the Research Topic
Current molecular, immunological, pathological and clinical aspects of pathogenic infections

Infectious diseases represent a significant risk to human health and have caused approximately more than half of all deaths worldwide (Muñoz-Carrillo et al., 2024). However, the human body possesses mechanisms capable of recognizing and identifying infections caused by pathogens and defending the organism through the early reactions of innate immunity and the late reactions of adaptive immunity (Wang et al., 2024). The innate immune response recognizes pathogen-associated molecular patterns (PAMPs), these PAMPs are recognized by pattern recognition receptors (PRRs), expressed mainly in innate immunity cells; while the adaptive immune response is antigen-specific. In both responses, several immune system cells are activated, playing a key role in establishing the cytokine environment, thereby directing their differentiation, either suppressing or promoting the immune response, which is crucial against pathogen infections (Muñoz-Carrillo et al., 2018). The immune system consists of a series of effector mechanisms capable of destroying pathogenic organisms such as bacteria, fungi, viruses and parasites. These mechanisms consist of (1) preventing the entry of pathogens into the body through physical and chemical barriers; (2) preventing the spread of infections through the complement system and other humoral factors; (3) eliminating pathogens through phagocytosis and cytotoxicity; and (4) activating the adaptive immune system through the synthesis of various cytokines and the presentation of antigens to T and B cells (Muñoz Carrillo et al., 2017). However, sometimes the immune system cannot resolve the various diseases caused by pathogens. Therefore, some type of therapy, whether pharmacological, immunological, etc., is necessary to resolve the disease.

Because diseases caused by pathogens are currently of great interest and importance in the biomedical field, due to the impact they have on the health of the human population, the main aim of this Research Topic was to show recent advances in molecular,

immunological, pathological and clinical aspects of infections and diseases caused by these pathogens. In this context, eleven articles were published in this Research Topic: nine of them were original research articles, one narrative review and one mini review. The most relevant findings from each are described below.

Puerperal infection (PI), responsible for 11% of maternal deaths worldwide, and it is a preventable cause of morbidity and mortality. In the study by Wen et al., the main risk factors and pathogenic bacteria associated with IP were analyzed in 525 women, through a validated predictive model with high precision with an area under the ROC curve of 0.904 (95% CI: 0.871-0.936) in the training set and 0.890 (95% CI: 0.837-0.942) in the test set. Six significant risk factors (*$p<0.05$) were identified: parity, number of vaginal examinations, amount of postpartum bleeding, antibiotics administered one week before admission, induced labor, and indwelling catheter. On the other hand, drug sensitivity map showed that *Escherichia coli* was the main pathogen (89%), with high sensitivity to antibiotics such as Meropenem and Imipenem (100%), Piperacillin tazobactam (97.7%), Ceftazidime (95.5%), and Amoxicillin/Clavulanate (AMC, 93.3%). These findings provide useful guidance for clinical prevention and treatment, reducing the risk of PI by controlling the number of vaginal examinations, postpartum bleeding, and reducing the time of urethral catheter indwelling, with the recommendation to use antibiotics sensitive to *Escherichia coli*.

Bacteremia is the presence of viable bacteria in the blood, a potentially life-threatening condition that can progress to sepsis, characterized primarily by a systemic inflammatory response of the host to bacterial infection. Bacteremia is responsible for approximately 8 million deaths per year worldwide, and the most common pathogenic bacteria involved are *Escherichia coli*, *Klebsiella pneumoniae*, and *Staphylococcus aureus* (Font et al., 2020; Xu et al., 2024). In the study by Zhang et al., the distribution of bacteremia pathogens in elderly patients (≥60 years old) and the impact of gender on this were evaluated, as well as the predictive value of routine blood parameters for diagnosis bacteremia. This study revealed that the main pathogens of bacteremia were *Escherichia coli*, *Klebsiella pneumoniae* and *Streptococcus*, with *Escherichia coli* being significantly ($p=0.021$) more frequent in elderly female patients. Furthermore, analysis of the area under the ROC curve showed that the most effective parameters for predicting bacteremia were the leukocyte count [0.851(95% CI: 0.790 - 0.912)] and the neutrophil-lymphocyte ratio [0.919 (95% CI 0.875 - 0.963)]. These findings support the use of routine blood parameters as useful tools for the early diagnosis of bacteremia in elderly patients.

Periprosthetic joint infection (PJI) is a severe complication characterized by high morbidity, mortality (Abedi et al., 2025), and resistance to antimicrobial treatment (Wouthuyzen-Bakker et al., 2019; Ryan et al., 2024), mainly due to the formation of bacterial biofilms on prosthetic materials, generating chronic infections (Edmiston et al., 2015). These biofilms make it difficult to eradicate the infection, requiring prolonged antibiotic treatment and surgery, including implant removal (Visperas et al., 2022). However, these interventions involve high costs and limited clinical results (Xu et al., 2023). It is noteworthy that factors such as obesity and diabetes increase the incidence of PJI (Kapadia et al., 2016), with obesity being a significant risk factor for treatment failure (Houdek et al., 2015; Watts et al., 2015). In the study by Shi et al., the impact of obesity on the diagnosis of PJI was evaluated through the quantification of levels of biomarkers [C-reactive protein (CRP), erythrocyte sedimentation rate (ESR), fibrinogen, D-dimer, CRP-albumin ratio (CAR), CRP-lymphocyte ratio (CLR), and CRP-monocyte ratio (CMR)] and their diagnostic efficacy. 254 patients were divided into four groups: an obese group (n = 59) and a non-obese group (n = 195) according to their BMI; each of these groups was further divided into a PJI group and an aseptic failure (AF) group. Although biomarker levels were significantly (*$p<0.001$) higher in patients with PJI compared with patients with AF in both the obese and non-obese groups, no differences were observed between obese and non-obese groups. However, the CRP biomarker showed the greatest diagnostic value in obese patients (AUC=0.982); while the CAR biomarker showed the greatest diagnostic value in non-obese patients (AUC=0.935). Therefore, these findings conclude that obesity does not alter biomarker levels, but it does alter the required diagnostic thresholds.

Microorganisms that inhabit the human digestive tract affect enteric health and disorders (Iqbal et al., 2021). Infection of the intestinal tract with an increasingly recognized range of bacterial pathogens can profoundly alter intestinal function, with or without causing overt diarrhea, which has profound effects on intestinal absorption, nutrition and development, as well as on global mortality (Petri et al., 2008), resulting in more than 1.5 billion cases of enteric-related infections (Iqbal et al., 2021). In the study by Zhang et al., the patterns and trends of enteric infections between 1990 and 2021 in 204 countries were analyzed for health policy formulation, medical resource allocation, and optimization of patient care plans. This study revealed a significant burden on global public health. Although standardized prevalence, incidence, mortality, and disability-adjusted life years (DALYs) rates decreased slightly, the most affected groups were women, children under 15 years of age, and the elderly, especially in regions with low socio-demographic index (SDI). In highly developed regions, the disease burden of typhoid fever declined, with unsafe waters identified as the leading risk factor globally in both 1990 and 2021; while rotavirus was the leading cause of death and DALYs. These findings highlight the need for innovative, targeted preventive healthcare strategies to reduce this global burden of disease.

Chronic hepatitis B virus (HBV) infection is a major public health problem, causing considerable morbidity and mortality, with approximately 296 million people chronically infected and more than 820,000 deaths worldwide. Although morbidity and mortality from HBV infection are liver-related, HBV has been considered non-cytopathic and liver injury is mediated primarily by T cells of the immune system (Seto et al., 2018; Jeng et al., 2023). In the study by Meng et al., the efficacy of blocking the Programmed Death-Ligand 1 (PD-L1) protein to restore the humoral immune response against HBV was evaluated in a murine model. Treatment with anti-PD-L1 was observed to significantly enhance the differentiation of T follicular helper (Tfh) cells and germinal

center (GC) B cells, promoting viral clearance. Furthermore, it was observed that plasmacytoid dendritic cells (pDCs) showed the ability to induce immune tolerance and viral persistence, an effect reversed by PD-L1 blockade. These findings point to the PD-L1/pDC axis as a promising therapeutic target in the management and treatment of chronic HBV infection. On the other hand, exosomes are cell-derived nanovesicles that participate in various biological functions, such as the intercellular transport of materials (Liang et al., 2021). Exosomes are associated with immune response, various diseases such as cardiovascular, neurological, and cancer, as well as viral pathogenicity. In this sense, exosomes offer a window into altered states of cells or tissues, and their detection in biological fluids potentially offers a multi-component diagnostic readout (Kalluri and LeBleu, 2020). Exosomes have been shown to be closely involved in the processes of HBV replication and transmission. The mini review by Yuan et al. describes the production process, composition and function of exosomes. Furthermore, the authors delve into the essential role of exosomes in the replication, transmission, and pathological processes of HBV. Therefore, exosomes can act as biomarkers for early detection and have therapeutic potential in the treatment and prevention of HBV.

Central line-associated bloodstream infections represent a significant burden on healthcare, increasing morbidity, mortality, hospitalization time, and associated costs (Odada et al., 2023). A central line-associated bloodstream infection (CLASBI) is defined as a pathogen detected in a blood culture from a patient who had a central line at the time of infection or up to 48 hours before it occurred (Haddadin et al., 2022). In the study by Li et al., the CLABSI pathogenic bacteria characteristic in intensive care unit (ICU) patients were analyzed, and the value of procalcitonin (PCT), lymphocyte ratio (NLR), and platelet to lymphocyte ratio (PLR) in predicting early infections was evaluated. Of 926 patients, 7.88% (73 patients) developed CLABSI, with a predominance of Gram-positive bacteria (60.5%), which showed high resistance to various antibiotics, such as penicillin, erythromycin, clindamycin and oxacillin; but showed sensitivity to vancomycin, linezolid and tetracycline. Peripheral blood levels of PCT, NLR, and PLR were significantly (*$p<0.05$) higher in infected patients, with PCT being the best individual predictor (AUC=0.856). The combination of the three markers achieved an AUC of 0.917, demonstrating significant utility in the early detection and clinical management of CLABSI. These findings demonstrate that CLABSI in the ICU requires careful attention, as Gram-positive bacteria are the main pathogens, and targeted antibiotic therapy based on microbial characteristics is essential for effective treatment. Furthermore, elevated blood levels of NLR, PLR, and PCT can facilitate the diagnosis of CLABSI, guiding early intervention and improving outcomes.

Periodontitis is a multifactorial chronic inflammatory disease associated with the accumulation of dental plaque (biofilm). It is primarily characterized by the progressive destruction of dental supporting tissues. Periodontitis involves the interaction between bacteria, the host immune response, and environmental factors (Kwon et al., 2021), all of which can influence the development and severity of the disease. These factors can be local or systemic, or non-modifiable, such as sex, age, ethnicity, or genetic factors; and modifiable, such as smoking, stress, obesity, and uncontrolled diabetes mellitus (DM) (Moreno Caicedo et al., 2018). DM is a chronic multifactorial disease triggered by various genetic and/or environmental factors (Artasensi et al., 2020). Type 2 diabetes mellitus (T2DM) is the most common type of DM (Majety et al., 2023), characterized by a progressive loss of insulin secretion from β cells, often in the context of insulin resistance (Artasensi et al., 2020). Diverse studies have associated T2DM with periodontitis, suggesting a bidirectional association between both pathologies (Santos et al., 2015; Turner, 2022). On the other hand, COVID-19 disease is caused by SARS-CoV-2, which has caused respiratory illnesses, complications and deaths worldwide (Zhang et al., 2023). Emerging evidence suggests that individuals with underlying comorbidities associated with COVID-19 (Sanyaolu et al., 2025), such as T2DM (Abdi et al., 2020) and periodontitis (Hernández-Vigueras et al., 2021), are at increased risk of disease susceptibility, leading to more severe clinical presentation and even death.

Regarding the association between periodontitis, T2DM, and COVID-19, there is currently insufficient scientific literature on the relationship between these three diseases. In the study by Muñoz-Carrillo et al., an explanation is provided regarding the relationship between these three pathologies, hypothesizing that the three diseases share important cofactors, which are centered on three main axes: 1) a clinicopathological axis; 2) an axis associated with glycemia; and 3) an immune axis associated with inflammation. Clinicopathological axis: T2DM increases susceptibility to developing periodontitis, especially in severe forms, while poor diabetes control is associated with increased morbidity and mortality from COVID-19. Furthermore, periodontitis can worsen the course of COVID-19, increasing the risk of complications such as hospitalization, ventilator support, and death. Axis associated with glycemia: hyperglycemia in patients with T2DM promotes inflammatory mechanisms that worsen insulin resistance and periodontal tissue destruction. Hyperglycemia also facilitates SARS-CoV-2 infection by altering the expression of enzymes that help the virus infect and replicate, exacerbating the inflammatory response. Immune axis associated with inflammation: chronic inflammation is the common denominator between the three diseases. Periodontitis and T2DM generate an exacerbated inflammatory response, characterized by the overproduction of proinflammatory cytokines (such as TNF-α, IL-1β and IL-6) and activation of immune cells. In COVID-19, this inflammation is amplified, causing cytokine storms and tissue damage, which worsens the clinical course of all three pathologies.

Bovine respiratory disease (BRD) and diarrhea are multifactorial diseases (Ferraro et al., 2021; Song et al., 2022), caused mainly by pathogens such as bacteria and viruses (Gandhi et al., 2023), which infect the lower respiratory tract of cattle, with a high morbidity and mortality rate (Urie et al., 2018). Disease control can prevent morbidity and mortality; however, current scientific evidence on the effectiveness of these control practices in achieving this goal is limited (Sanguinetti et al., 2025). The complexity of infectious diarrhea in calves limits the effectiveness of vaccination. In this regard, trained

immunity, which involves immunological memory in innate cells following exposure to pathogens or their antigens to provide increased protection against subsequent exposure to homologous or heterologous infections, offers a promising strategy for preventing unpredictable infections in young animals (Netea et al., 2020). Yeast β-glucan, a cell wall component of fungi (Han et al., 2020), can induce immune memory in innate immune cells (Goh et al., 2023). It has been studied as a prebiotic in animal diets, showing positive effects such as weight gain and reduced diarrhea in calves (Ding et al., 2019; Pornanek and Phoemchalard, 2021). β-glucan has also been observed to stimulate macrophages and immune cells in goats and calves (Angulo et al., 2020). However, its efficacy in preventing diarrhea and BRD in calves is not yet clearly established. In the study by Yan et al., the prophylactic effect of intraperitoneal injection of yeast β-glucan in Holstein calves during their first 74 days of life was evaluated. In 52 healthy newborn Holstein calves, the treatment induced an initial inflammatory response with increased cytokines (IL-1β, IL-6, and TNF-α), immunoglobulins (IgG and IgM), and defensins, improving innate immunity without affecting growth or feed efficiency. Treated calves showed a lower incidence of diarrhea and BRD, especially between 31 and 60 days, as well as a healthier gut microbiota with a higher abundance of *Bifidobacterium*. These results suggest that β-glucan is a promising strategy to prevent infectious diseases in calves.

Sepsis is a serious organ dysfunction caused by an altered immune response to an infection (Cecconi et al., 2018). In its most severe form, sepsis manifests as a drop in blood pressure, which decreases tissue perfusion pressure and causes the hypoxia characteristic of septic shock (Srzić et al., 2022). Sepsis affects more than 30 million people each year and is one of the leading causes of death in critically ill patients worldwide. Furthermore, the cost of sepsis treatment is also the highest among all treatments for the disease (Rocheteau et al., 2015). Despite advances in treatment, its incidence and mortality continue to increase, and its diagnosis and management remain a challenge for healthcare professionals. This is because sepsis is a complex process that affects multiple organs and goes beyond a simple inflammatory or immune response. Its pathogenesis involves inflammatory imbalances, immune dysfunction, mitochondrial damage, coagulopathy, neuroendocrine disorders, endoplasmic reticulum stress, autophagy, and other mechanisms, culminating in organ dysfunction (Huang et al., 2019). In this context, biomarkers for diagnosing sepsis may allow for early intervention that can reduce the risk of death (Faix, 2013). In the study by Chen et al., the potential of S100A8/A9 and resistin as biomarkers to predict mortality in patients with sepsis was evaluated. Serum samples were collected and analyzed from 141 adult sepsis patients (discovery cohort), 43 non-sepsis intensive care units (ICU) patients, 15 healthy volunteers, and 55 sepsis patients along with 17 non-sepsis ICU patients (validation cohort). It was observed that the concentrations of S100A8/A9 and resistin in sepsis patients were noticeably increased relative to non-sepsis patients and healthy controls. In patients with sepsis, elevated serum concentrations of S100A8/A9 (≥ 377.53 ng/mL) were associated with higher survival. In the ICU, the AUC for S100A8/A9 to predict 28-day mortality was 0.617 ($p = 0.032$; 95% CI: 0.513-0.721), and for the organ failure assess (SOFA) score it was 0.750 ($p<0.0001$; 95% CI: 0.660-0.840). In the validation cohort, the AUC were 0.708 ($p=0.032$; 95% CI 0.563–0.854) for S100A8/A9 and 0.698 for SOFA ($p=0.025$; 95% CI 0.550–0.845). On the other hand, in patients with sepsis, serum resistin concentrations were higher in infections caused by gram-negative bacteria than in gram-positive bacteria. Furthermore, resistin levels were predictive of mortality in normal (AUC = 0.810 [$p = 0.034$; 95% CI 0.605–1.00]) and mixed (AUC = 0.708 [$p=0.015$; 95% CI 0.571–0.846]) phenotypes with hyperinflammation. In the normal phenotype, high levels of resistin (≥ 63.695 ng/mL) were associated with lower survival, while in the mixed phenotype with hyperinflammation, elevated levels (≥ 107.64 ng/mL) were related to higher survival. These findings suggest that S100A8/A9 and resistin could be useful for early diagnosis and risk stratification in sepsis, improving clinical decisions in the ICU.

Mycoplasma pneumoniae (MP) is an important bacterium (Waites and Talkington, 2004) that causes respiratory tract infections in children and adults, the severity of which can range from mild to life-threatening (Waites et al., 2017). MP is the pathogen of human bronchitis and atypical pneumonia and is called community-acquired pneumonia (Hu et al., 2023), which can cause acute inflammation of the upper and lower respiratory tract, as well as extrapulmonary syndromes (Jiang et al., 2021), in the skin, brain, kidney, musculoskeletal, digestive system, and even blood system after infection (Hu et al., 2023). Although macrolides are the first-line treatment for MP pneumonia, persistent fever and/or clinical deterioration can sometimes complicate treatment and even lead to severe systemic disease. There is no consensus on the optimal alternatives, doses, or duration of treatment for severe cases. However, tetracyclines and fluoroquinolones have been used as second-line treatments with favorable clinical outcomes in children (Ding et al., 2024). Respiratory symptoms caused by MP result from several pathogenetic mechanisms, such as adhesion to host cells, direct damage (such as cytotoxicity and invasion), immune damage induced by inflammatory response, and immune evasion (Jiang et al., 2021; Hu et al., 2023). In the study by Chen et al., the role of B lymphocytes in the immune response of 202 children diagnosed with MP was analyzed by evaluating the CDR3 repertoires of the B cell receptor (BCR) heavy chain. A significant increase in B lymphocytes and elevated levels of inflammatory markers, such as C-reactive protein (CRP), interleukin (IL)-6, and ferritin, were observed, indicating an active immune response. Immunoglobulin levels were elevated in several patients, indicating immune fluctuations during infection. BCR repertoire analysis revealed increased diversity and altered clonotype distribution in MP patients, with preferential usage of IGHV1-18, IGHV7-4-1, and IGHJ6. MP patients showed a bimodal distribution of CDR3 length, with significantly longer CDR3 regions and clonal expansion with 68 unique MP clonotypes. These findings highlight alterations in the BCR repertoire as key to immunity against MP and potential therapeutic targets.

Author contributions

JM-C: Writing – original draft, Writing – review & editing. OG-C: Writing – original draft, Writing – review & editing. RC-S: Writing – original draft, Writing – review & editing.

Conflict of interest

The authors declare that the research was conducted in the absence of any commercial or financial relationships that could be construed as a potential conflict of interest.

Generative AI statement

The author(s) declare that no Generative AI was used in the creation of this manuscript.

Publisher's note

All claims expressed in this article are solely those of the authors and do not necessarily represent those of their affiliated organizations, or those of the publisher, the editors and the reviewers. Any product that may be evaluated in this article, or claim that may be made by its manufacturer, is not guaranteed or endorsed by the publisher.

References

Abdi, A., Jalilian, M., Sarbarzeh, P. A., and Vlaisavljevic, Z. (2020). Diabetes and COVID-19: A systematic review on the current evidences. *Diabetes Res. Clin. Pract.* 166, 1–14. doi: 10.1016/J.DIABRES.2020.108347

Abedi, A. O., Abedi, A. A., Ferry, T., and Citak, M. (2025). Current applications and the future of phage therapy for periprosthetic joint infections. *Antibiotics* 14, 581. doi: 10.3390/ANTIBIOTICS14060581

Angulo, M., Reyes-Becerril, M., Cepeda-Palacios, R., and Angulo, C. (2020). Oral administration of Debaryomyces hansenii CBS8339-β-glucan induces trained immunity in newborn goats. *Dev. Comp. Immunol.* 105, 1–9. doi: 10.1016/j.dci.2019.103597

Artasensi, A., Pedretti, A., Vistoli, G., and Fumagalli, L. (2020). Type 2 diabetes mellitus: A review of multi-target drugs. *Molecules* 25, 1–20. doi: 10.3390/MOLECULES25081987

Cecconi, M., Evans, L., Levy, M., and Rhodes, A. (2018). Sepsis and septic shock. *Lancet* 392, 75–87. doi: 10.1016/S0140-6736(18)30696-2

Ding, G., Zhang, X., Vinturache, A., van Rossum, A. M. C., Yin, Y., and Zhang, Y. (2024). Challenges in the treatment of pediatric Mycoplasma pneumoniae pneumonia. *Eur. J. Pediatr.* 183, 3001–3011. doi: 10.1007/S00431-024-05519-1

Ding, B., Zheng, J., Wang, X., Zhang, L., Sun, D., Xing, Q., et al. (2019). Effects of dietary yeast beta-1,3-1,6-glucan on growth performance, intestinal morphology and chosen immunity parameters changes in Haidong chicks. *Asian-Australasian J. Anim. Sci.* 32, 1558–1564. doi: 10.5713/AJAS.18.0962

Edmiston, C. E., McBain, A. J., Roberts, C., and Leaper, D. (2015). Clinical and microbiological aspects of biofilm-associated surgical site infections. *Adv. Exp. Med. Biol.* 830, 47–67. doi: 10.1007/978-3-319-11038-7_3

Faix, J. D. (2013). Biomarkers of sepsis. *Crit. Rev. Clin. Lab. Sci.* 50, 23–36. doi: 10.3109/10408363.2013.764490

Ferraro, S., Fecteau, G., Dubuc, J., Francoz, D., Rousseau, M., Roy, J. P., et al. (2021). Scoping review on clinical definition of bovine respiratory disease complex and related clinical signs in dairy cows. *J. Dairy Sci.* 104, 7095–7108. doi: 10.3168/JDS.2020-19471

Font, M. D., Thyagarajan, B., and Khanna, A. K. (2020). Sepsis and Septic Shock – Basics of diagnosis, pathophysiology and clinical decision making. *Med. Clin. North Am.* 104, 573–585. doi: 10.1016/j.mcna.2020.02.011

Gandhi, N. N., Inzana, T. J., and Rajagopalan, P. (2023). Bovine airway models: approaches for investigating bovine respiratory disease. *ACS Infect. Dis.* 9, 1168–1179. doi: 10.1021/ACSINFECDIS.2C00618

Goh, T. W., Kim, H. J., Moon, K., Kim, C. S., and Kim, Y. Y. (2023). Effects of β-glucan with vitamin E supplementation on the growth performance, blood profiles, immune response, fecal microbiota, fecal score, and nutrient digestibility in weaning pigs. *Anim. Biosci.* 36, 642–653. doi: 10.5713/AB.22.0311

Haddadin, Y., Annamaraju, P., and Regunath, H. (2022). Central line–associated blood stream infections. *Heal Infect. Child.* 95–106. doi: 10.1007/978-3-319-98122-2_6

Han, B., Baruah, K., Nguyen, D. V., Williams, D. L., Devriendt, B., Cox, E., et al. (2020). Beta-glucan's varying structure characteristics modulate survival and immune-related genes expression from Vibrio harveyi-infected Artemia franciscana in gnotobiotic conditions. *Fish Shellfish Immunol.* 102, 307–315. doi: 10.1016/j.fsi.2020.04.062

Hernández-Vigueras, S., Aquino-Martínez, R., Hernández-Vigueras, S., and Aquino-Martínez, R. (2021). Potencial Rol de la Periodontitis en la Severidad de COVID-19. *Revisión. Int. J. Odontostomatol* 15, 335–341. doi: 10.4067/S0718-381X2021000200335

Houdek, M. T., Wagner, E. R., Watts, C. D., Osmon, D. R., Hanssen, A. D., Lewallen, D. G., et al. (2015). Morbid obesity: A significant risk factor for failure of two-stage revision total hip arthroplasty for infection. *J. Bone Jt Surg. - Am. Vol* 97, 326–332. doi: 10.2106/JBJS.N.00515

Hu, J., Ye, Y., Chen, X., Xiong, L., Xie, W., and Liu, P. (2023). Insight into the Pathogenic Mechanism of Mycoplasma pneumoniae. *Curr. Microbiol.* 80, 1–13. doi: 10.1007/S00284-022-03103-0

Huang, M., Cai, S., and Su, J. (2019). The pathogenesis of sepsis and potential therapeutic targets. *Int. J. Mol. Sci.* 20, 5376. doi: 10.3390/IJMS20215376

Iqbal, Z., Ahmed, S., Tabassum, N., Bhattacharya, R., and Bose, D. (2021). Role of probiotics in prevention and treatment of enteric infections: a comprehensive review. *3 Biotech.* 11, 242. doi: 10.1007/S13205-021-02796-7

Jeng, W. J., Papatheodoridis, G. V., and Lok, A. S. F. (2023). Hepatitis B. *Lancet* 401, 1039–1052. doi: 10.1016/S0140-6736(22)01468-4

Jiang, Z., Li, S., Zhu, C., Zhou, R., and Leung, P. H. M. (2021). Mycoplasma pneumoniae infections: Pathogenesis and vaccine development. *Pathogens* 10, 1–18. doi: 10.3390/PATHOGENS10020119

Kalluri, R., and LeBleu, V. S. (2020). The biology, function, and biomedical applications of exosomes. *Science (80-)* 367, 1–40. doi: 10.1126/SCIENCE.AAU6977

Kapadia, B. H., Berg, R. A., Daley, J. A., Fritz, J., Bhave, A., and Mont, M. A. (2016). Periprosthetic joint infection. *Lancet* 387, 386–394. doi: 10.1016/S0140-6736(14)61798-0

Kwon, T. H., Lamster, I. B., and Levin, L. (2021). Current concepts in the management of periodontitis. *Int. Dent. J.* 71, 462–476. doi: 10.1111/idj.12630

Liang, Y., Duan, L., Lu, J., and Xia, J. (2021). Engineering exosomes for targeted drug delivery. *Theranostics* 11, 3183–3195. doi: 10.7150/THNO.52570

Majety, P., Lozada Orquera, F. A., Edem, D., and Hamdy, O. (2023). Pharmacological approaches to the prevention of type 2 diabetes mellitus. *Front. Endocrinol. (Lausanne)* 14. doi: 10.3389/FENDO.2023.1118848

Moreno Caicedo, L. F., Amaya Sánchez, S., and Cruz Olivo, E. A. (2018). Factores de riesgo modificables e inmodificables de la periodontitis: revisión narrativa. *Univ Odontol* 37, 1–28. doi: 10.11144/JAVERIANA.UO37-79.FRMI

Muñoz Carrillo, J. L., Castro García, F. P., Gutiérrez Coronado, O., Moreno García, M. A., and Contreras Cordero, J. F. (2017). "Physiology and pathology of innate immune response against pathogens," in *Physiology and Pathology of Immunology*. Ed. R. Nima (IntechOpen, London), 99–134. doi: 10.5772/INTECHOPEN.70556

Muñoz-Carrillo, J. L., Contreras-Cordero, J. F., Gutiérrez-Coronado, O., Villalobos-Gutiérrez, P. T., Ramos-Gracia, L. G., and Hernández-Reyes, V. E. (2018). "Cytokine profiling plays a crucial role in activating immune system to clear infectious pathogens," in *Immune Response Activation and Immunomodulation*. Eds. K. T. Rajeev and S. B. Prakash (IntechOpen, London), 1–30. doi: 10.5772/INTECHOPEN.80843

Muñoz-Carrillo, J. L., Guevara-López, G. W., González-Díaz, C., Palos-Del Toro, E. J., De León-Madrigal, J., Álvarez-Pinto, J. U., et al. (2024). Obesidad y COVID-19: comorbilidad de dos pandemias. *REDNUTRICIÓN* 15, 1252–1261. doi: 10.62640/NT241535R

Netea, M. G., Domínguez-Andrés, J., Barreiro, L. B., Chavakis, T., Divangahi, M., Fuchs, E., et al. (2020). Defining trained immunity and its role in health and disease. *Nat. Rev. Immunol.* 20, 375–388. doi: 10.1038/S41577-020-0285-6

Odada, D., Munyi, H., Gatuiku, J., Thuku, R., Nyandigisi, J., Wangui, A., et al. (2023). Reducing the rate of central line-associated bloodstream infections; a quality improvement project. *BMC Infect. Dis.* 23, 1–8. doi: 10.1186/S12879-023-08744-5

Petri, W. A., Miller, M., Binder, H. J., Levine, M. M., Dillingham, R., and Guerrant, R. L. (2008). Enteric infections, diarrhea, and their impact on function and development. *J. Clin. Invest.* 118, 1277. doi: 10.1172/JCI34005

Pornanek, P., and Phoemchalard, C. (2021). Dietary supplementation of beta-glucan-rich molasses yeast powder on antibody response to swine fever virus and hematology of starter–grower pigs. *Trop. Anim. Health Prod* 53, 1–6. doi: 10.1007/S11250-020-02431-2

Rocheteau, P., Chatre, L., Briand, D., Mebarki, M., Jouvion, G., Bardon, J., et al. (2015). Sepsis induces long-term metabolic and mitochondrial muscle stem cell dysfunction amenable by mesenchymal stem cell therapy. *Nat. Commun.* 6, 1–12. doi: 10.1038/NCOMMS10145

Ryan, S. P., Stambough, J. B., Huddleston, J. I., and Levine, B. R. (2024). Highlights of the 2023 American joint replacement registry annual report. *Arthroplast Today* 26, 1–3. doi: 10.1016/j.artd.2024.101325

Sanguinetti, V. M., Strong, K., Agbese, S. P., Adams, C., Campbell, J., Checkley, S. L., et al. (2025). A systematic review of disease control strategies in beef cow-calf herds, part 2: preweaned calf morbidity and mortality associated with neonatal calf diarrhea and bovine respiratory disease. *Anim. Heal Res. Rev.* 25, 1–22. doi: 10.1017/S1466252325000039

Santos, C. M. M. L., Lira, R., Fischer, R. G., Santos, A. P. P., and Oliveira, B. H. (2015). Systemic antibiotics in periodontal treatment of diabetic patients: A systematic review. *PloS One* 10, 1–11. doi: 10.1371/JOURNAL.PONE.0145262

Sanyaolu, A., Okorie, C., Marinkovic, A., Prakash, S., Balendra, V., Lehachi, A., et al. (2025). COVID-19 management in patients with comorbid conditions. *World J. Virol.* 14, 102674. doi: 10.5501/WJV.V14.I2.102674

Seto, W. K., Lo, Y. R., Pawlotsky, J. M., and Yuen, M. F. (2018). Chronic hepatitis B virus infection. *Lancet* 392, 2313–2324. doi: 10.1016/S0140-6736(18)31865-8

Song, Q., Zhao, X., Cao, C., Duan, M., Shao, C., Jiang, S., et al. (2022). Research advances on interferon (IFN) response during BVDV infection. *Res. Vet. Sci.* 149, 151–158. doi: 10.1016/j.rvsc.2022.04.011

Srzić, I., Adam, V. N., and Pejak, D. T. (2022). Sepsis definition: what's new in the treatment guidelines. *Acta Clin. Croat* 61, 67–72. doi: 10.20471/ACC.2022.61.S1.11

Turner, C. (2022). Diabetes mellitus and periodontal disease: the profession's choices. *Br. Dent. J.* 233, 537–538. doi: 10.1038/S41415-022-5029-5

Urie, N. J., Lombard, J. E., Shivley, C. B., Kopral, C. A., Adams, A. E., Earleywine, T. J., et al. (2018). Preweaned heifer management on US dairy operations: Part V. Factors associated with morbidity and mortality in preweaned dairy heifer calves. *J. Dairy Sci.* 101, 9229–9244. doi: 10.3168/JDS.2017-14019

Visperas, A., Santana, D., Klika, A. K., Higuera-Rueda, C. A., and Piuzzi, N. S. (2022). Current treatments for biofilm-associated periprosthetic joint infection and new potential strategies. *J. Orthop Res.* 40, 1477–1491. doi: 10.1002/JOR.25345

Waites, K. B., and Talkington, D. F. (2004). Mycoplasma pneumoniae and its role as a human pathogen. *Clin. Microbiol. Rev.* 17, 697–728. doi: 10.1128/CMR.17.4.697-728.2004

Waites, K. B., Xiao, L., Liu, Y., Balish, M. F., and Atkinson, T. P. (2017). Mycoplasma pneumoniae from the respiratory tract and beyond. *Clin. Microbiol. Rev.* 30, 747–809. doi: 10.1128/CMR.00114-16

Wang, R., Lan, C., Benlagha, K., Camara, N. O. S., Miller, H., Kubo, M., et al. (2024). The interaction of innate immune and adaptive immune system. *MedComm* 5, 1–37. doi: 10.1002/MCO2.714

Watts, C. D., Wagner, E. R., Houdek, M. T., Lewallen, D. G., and Mabry, T. M. (2015). Morbid obesity: increased risk of failure after aseptic revision TKA. *Clin. Orthop Relat. Res.* 473, 2621–2627. doi: 10.1007/S11999-015-4283-0

Wouthuyzen-Bakker, M., Sebillotte, M., Lomas, J., Taylor, A., Palomares, E. B., Murillo, O., et al. (2019). Clinical outcome and risk factors for failure in late acute prosthetic joint infections treated with debridement and implant retention. *J. Infect.* 78, 40–47. doi: 10.1016/J.JINF.2018.07.014

Xu, Y., Huang, T. B., Schuetz, M. A., and Choong, P. F. M. (2023). Mortality, patient-reported outcome measures, and the health economic burden of prosthetic joint infection. *EFORT Open Rev.* 8, 690–697. doi: 10.1530/EOR-23-0078

Xu, X., Wang, Y., Tao, Y., Dang, W., Yang, B., and Li, Y. (2024). The role of platelets in sepsis: A review. *Biomol BioMed.* 24, 741–752. doi: 10.17305/BB.2023.10135

Zhang, H.P., Sun, Y., Wang, Y.F., Yazici, D., Azkur, D., Ogulur, I., et al. (2023). Recent developments in the immunopathology of COVID-19. *Allergy* 78, 369–388. doi: 10.1111/ALL.15593

frontiers | Frontiers in Cellular and Infection Microbiology

TYPE Original Research
PUBLISHED 12 December 2024
DOI 10.3389/fcimb.2024.1464485

OPEN ACCESS

EDITED BY
José Luis Muñoz-Carrillo,
University of Guadalajara, Mexico

REVIEWED BY
Mingzhe Guo,
University of Nevada, Reno, United States
Mulatu Gashaw,
Jimma University, Ethiopia

*CORRESPONDENCE
Hongbo Qi
qihongbo@cqmu.edu.cn

RECEIVED 13 October 2024
ACCEPTED 25 November 2024
PUBLISHED 12 December 2024

CITATION
Wen Y, Ming X, Yang J and Qi H (2024)
A simple predictive model for puerperal infections: emphasizing risk factors and pathogen analysis.
Front. Cell. Infect. Microbiol. 14:1464485.
doi: 10.3389/fcimb.2024.1464485

A simple predictive model for puerperal infections: emphasizing risk factors and pathogen analysis

Yanqing Wen[1,2], Xin Ming[2,3], Jing Yang[1,4] and Hongbo Qi[1,2]*

[1]Department of Obstetrics and Gynecology, Women and Children's Hospital of Chongqing Medical University, Chongqing, China, [2]Department of Obstetrics and Gynecology, Chongqing Health Center of Women and Children, Chongqing, China, [3]Department of Quality Management Section, Women and Children's Hospital of Chongqing Medical University, Chongqing, China, [4]Department of Obstetrics and Gynecology, Guizhou Provincial People's Hospital, Guizhou, China

Background: Puerperal infection (PI) accounting for approximately 11% of maternal deaths globally is an important preventable cause of maternal morbidity and mortality. This study aims to analyze the high-risk factors and pathogenic bacteria of PI, design a nomogram to predict the risk of PI occurrence, and provide clinical guidance for prevention and treatment to improve maternal outcomes.

Methods: A total of 525 pregnant women were included in the study. The mothers were randomly divided into a training cohort (n=367) and a test cohort (n=158). The performance of our model was assessed using the area under the receiver operating characteristic (ROC) curve, calibration curve, and decision curve analyses. All the women in the group of PI underwent blood culture tests, if the bacteria were detected, drug sensitivity tests were performed. The drug sensitivity spectrum was recorded and analyzed.

Results: Univariate analysis showed that 12 indicators were significantly different ($P < 0.05$). Logistic regression analysis showed 6 factors, such as parity, number of vaginal examinations, amount of postpartum bleeding, antibiotics administered in one week before admission, induced labor, and indwelling catheter were significantly different between the PI group and control group ($P < 0.05$). The area under the ROC curve was 0.904 (95% CI: 0.871-0.936) in the training set and 0.890 (95% CI: 0.837-0.942) in the test set. The calibration curve of the nomogram showed good agreement between prediction and observation. The analysis of the clinical decision curve showed that the nomogram is of practical significance. There were 100 patients with positive blood cultures in the PI group, and *Escherichia.coli* was the main pathogenic bacteria, accounting for 89%. The sensitivity to Meropenem and Imipenem was 100%, to Piperacillin tazobactam 97.75%, to Ceftazidime 95.51%, and to Amoxicillin/Clavulanat (AMC) was 93.26%.

Conclusion: The risk of PI will be significantly reduced by controlling the number of vaginal examinations less than 4 times, postpartum hemorrhage less than 414ml, and reducing the time of urethral catheter indwelling. If PI was clinically diagnosed or highly suspected, it was recommended to use antibiotics that were sensitive to *Escherichia. coli*, such as Piperacillin tazobactam, Ceftazidime, and AMC

KEYWORDS

puerperal infection, pathogenic bacteria, drug sensitivity, nomogram, predictive model

1 Introduction

Puerperal infection (PI) is defined as a local or systemic infection resulting from pathogen invasion of the genital tract, occurring at any time during the 6-week postpartum period. It is a common complication of the puerperium, with an incidence of about 6% (Karsnitz, 2013; Tardieu and Schmidt, 2017; Li et al., 2023). PI is characterized by a brief incubation period, sudden onset, and rapid fluctuations in condition. In severe cases, it may evolve into sepsis, progressing to systemic inflammatory response syndrome and multiple organ dysfunction syndromes, thereby posing a significant threat to maternal well-being (Kobayashi et al., 2017; Li et al., 2023). It was estimated that at least 75,000 maternal deaths from puerperal sepsis occur each year, mostly in low-income countries. Even high-income countries reported relatively high incidences ranging from 0.1 to 0.6 per 1000 deliveries (van Dillen et al., 2010; Acosta et al., 2013). At present, there are many literature reports on PI caused by group A streptococcal infection, especially in developed countries, and it is the main pathogen of PI leading to maternal mortality (Acosta et al., 2014). However, in China, we have found very few cases of puerperal infections caused by group A streptococcal infections. At the same time, bacterial resistance to commonly used antibiotics is increasing at an alarming rate. Therefore, it is important to understand the pathogens of PI and their susceptible antimicrobial spectrum (Song et al., 2020).

Early identification of PI can prevent adverse maternal outcomes, decrease expenses, and enhance the quality of healthcare. However, there is a scarcity of visual forecasting models that can be utilized for PI. The nomogram model has been extensively employed as a calibrated visualization tool in clinical settings to predict various outcomes. This model is based on multivariate analysis and integrates the results of logistic or Cox regression to a great extent to predict the probability of a certain clinical event in patients along with intuitive graphical presentations. It offers clinicians a basis for developing more efficient and personalized treatment plans.

This study aimed to analyze the risk factors of PI and construct a simple and effective multi-factorial prevention model, hoping to provide a reference for the formulation of maternal clinical management rules and infection control strategies. Additionally, this study revealed the most common pathogens and described the sensitivity spectrum of antimicrobial drugs, thereby offering a reliable foundation for the selection of antimicrobial drugs for puerperal infection.

Abbreviations: CQHCWC, Women and Children's Health Hospital of Chongqing Medical University; WBC, white blood cell; N%, neutrophilic granulocyte percentage; HGB, hemoglobin; GDM, Gestational diabetes; GBS, Group B streptococci; ICP, intrahepatic cholestasis of pregnancy; BMI, Body Mass Index; PROM, premature rupture of membranes; PPROM, preterm premature rupture of membranes; AMC, Amoxicillin/clavulanate; Amp/sulb, Ampicillin/sulbactam; MIC, minimum inhibitory concentration; CS, cesarean delivery; PI, puerperal infection.

2 Materials and methods

2.1 Study population

This was a retrospective case-control study including 525 women who gave birth at CQHCWC between January 1, 2022 and September 30, 2023. CQHCWC is a tertiary Class A maternal and infant care center with approximately 20,000 deliveries per year, accepting pregnant women from all regions of Chongqing, as well as from northwest and southwest China, including Guizhou, Sichuan, Tibet, Hubei and other regions. The study population was divided into two groups, one was women who met the criteria for PI, concluding 262 cases, and the other was randomly selected pregnant women who were hospitalized at the same time and gave birth with non-puerperal infection, concluding 263 cases. The overall data is randomly divided into training set (n=367) and verification (n=158) set according to the ratio of 7:3. Throughout this procedure, we establish a random seed to guarantee the randomness and reproducibility of the sampling (Wu et al., 2021).

Pregnant women in the PI group need to meet the following criteria:

1. Time of onset: at the time of delivery or within 42 days postpartum.
2. Fever: temperature ≥38°C during labor or 42 days postpartum, 4-hour intervals, ≥2 times.
3. Clinical signs: abdominal, or uterine, or pelvic pain, or smelly discharge, or poor healing of the incision.
4. Laboratory test: white blood cell count (WBC) $\geq 15\times10^9$/L and neutrophil percentage (N%) ≥ 85%.

Exclusion Criteria of PI group: Confirmed diagnosis of upper respiratory tract infection, urinary tract infection, mastitis.

The normal control group included pregnant women who had normal labor at the same time and had no symptoms of infection.

2.2 Methods

Hospital records for each pregnant woman were reviewed, and medical and obstetric data were extracted. The data collected were as follows:

1. Demographic data: age, weight, height, Body Mass Index (BMI), gestational age, parity, and gravidity.
2. Laboratory data: laboratory results at admission and onset of fever, including WBC, N %, hemoglobin (HGB), blood culture, and drug-sensitive tests, Group B Streptococcus (GBS), albumin.

All the patients in PI group underwent blood culture tests. Both aerobic and anaerobic cultures were performed simultaneously for each patient, with the cultures being incubated for five days. All the isolates were identified at the species level by the MALDI-TOF/TOF

(Bruker, Germany), and routine antimicrobial susceptibility testing was performed by using the BD Phoenix system. At the same time, Escherichia coli ATCC25922 was selected as the standard strains for minimum inhibitory concentration (MIC) detection. All standard strains were purchased from American Type Culture Collection and all antibiotics were purchased from Meilunbio in China.

3. Complications of pregnancy: premature rupture of membranes (PROM), preterm premature rupture of membranes (PPROM), gestational diabetes mellitus (GDM), oligohydramnios, gemellary pregnancy, intrahepatic cholestasis of pregnancy (ICP), gestational hypertension, cervical cerclage, central placenta previa;
4. Perinatal conditions: delivery mode, number of vaginal examinations, amniotic fluid volume, amount of bleeding, antibiotics administered within one week before admission, induced labor, amniotic fluid color, residual placental tissue in the uterine cavity, suturing the uterine cavity to stop bleeding, uterine balloon tamponade, colpoperineal laceration, episiotomy, cervical laceration, forceps delivery, incision hematoma, B-Lynch uterine compression sutures, indwelling catheter.

2.3 Statistical analysis

We used Kolmogorov-Smirnov to test the normality of the continuous variables, and the skewed distribution was expressed as the median and quartile range. Count data were expressed as a rate (%). Clinical characteristics were compared using the Kruskal-Wallis Test (continuous variables) and χ^2 test (categorical variables). LASSO regression was used for feature selection in the training dataset. The nomogram was established as a result of multivariate logistic regression model with Five-fold cross-validation. We utilized a multivariate logistic regression to identify independent predictors, which were subsequently employed in developing a nomogram for predicting the incidence of puerperal infection. Predictor lines were drawn upward to confirm the positioning of the points on the "Total Points" axis, followed by a downward projection onto the lower scales, thereby determining the likelihood of puerperal infection. The Hosmer–Lemeshow test was used to assess goodness of fit. The receiver operating characteristic curve, area under the ROC curve, concordance index, and calibration curve were used to evaluate the predictive accuracy and conformity of the model. The decision curve analysis (DCA) reflected the net benefit of the model for patients. Clinical effectiveness was evaluated by plotting the clinical decision curve. To evaluate both discrimination and calibration, bootstrapping with 1000 resamples was performed.

Statistical analysis was performed with R 4.4.1 software (R Statistical Computing Foundation, Vienna, Austria). All statistical tests were two-sided and a P value <0.05 was considered significant.

2.4 Ethical statement

This survey research was approved by the ethics committee of the Women and Children's Health Hospital of Chongqing Medical University (CQHCWC).

3 Results

3.1 Demographic characteristics

From January 2022 to September 2023, a total of 25,666 pregnant women gave birth at CQHCWC. 525 mothers aged 18 to 41 years were included in the study. We divided the dataset into a training dataset and a test dataset according to 7:3 (367:158 cases). The average BMI of the enrolled mothers was 27.06 ± 3.22 kg/m^2. Overall, 48.5% (178/367) of mothers in the training set and 53.2% (84/158) of mothers in the validation set had a puerperal infection. The p-values of all these factors exceed 0.05, which indicates that there were no statistically significant differences between the training dataset and the validation dataset as shown in Supplementary Table S1. Table 1 shows the baseline characteristics of the normal group and puerperal infection group. Parity, albumin at admission, number of vaginal examinations, amniotic fluid volume, amount of bleeding, PROM, antibiotics administered within one week before admission, induced labor, amniotic fluid color, mode of delivery, suturing the uterine cavity during cesarean section to stop bleeding, and indwelling catheter were statistically significant between the two groups in the training dataset ($P < 0.05$).

3.2 Screening for predictive factors

To prevent overfitting and ensure the stability of the model, the LASSO logistic regression model was ultimately used. The performance was optimal in the training dataset when λ was 0.007 (Figures 1A, B). A total of 12 features were screened, including parity, albumin at admission, number of vaginal examinations, amniotic fluid volume, amniotic fluid color, amount of bleeding, PROM, antibiotics administered in one week before admission, induced labor, suturing the uterine cavity during cesarean section to stop bleeding, mode of delivery, and indwelling catheter, which will be used to construct the predictive model.

3.3 Risk prediction nomogram development

The logistic regression model was constructed based on the above 12 factors. Parity (*OR*: 0.215, *95%CI*: 0.059-0.787), number of vaginal examinations (*OR*: 2.107, *95%CI*: 1.075-4.128), amount of bleeding (*OR*: 1.293, *95%CI*: 1.035-1.617), antibiotics administered

10.3389/fcimb.2024.1464485

TABLE 1 The baseline characteristics of datasets.

Variable	Training dataset			Validation dataset		
	Non-puerperal infection (n=189)	Puerperal infection (n=178)	P value	Non-puerperal infection (n=74)	Puerperal infection (n=84)	P value
Age	29.00 [27.00, 32.00]	29.00 [27.00, 31.00]	0.499	29.00 [27.00, 31.00]	28.50 [27.00, 31.00]	0.690
Weight	67.50 [63.00, 72.00]	67.00 [61.50, 71.50]	0.493	65.85 [60.12, 74.00]	68.00 [62.38, 75.00]	0.239
Height	159.00 [156.00, 162.00]	158.00 [155.00, 161.00]	0.088	159.00 [155.00, 162.00]	158.00 [155.00, 160.00]	0.245
BMI	26.81 [24.97, 28.46]	27.12 [24.62, 29.41]	0.680	26.52 [24.48, 28.56]	27.47 [25.14, 29.49]	0.084
Gestational week	39.14[38.29,39.86]	39.43[38.14,40.29]	0.184	39.07 [38.18, 40.00]	39.36 [38.00, 40.29]	0.573
Gravity	2.00[1.00,3.00]	1.00[1.00,2.00]	0.653	1.00 [1.00, 2.00]	2.00 [1.00, 2.00]	0.421
Parity	0.00[0.00,1.00]	0.00[0.00,0.00]	**<0.001**	0.00 [0.00, 0.00]	0.00 [0.00, 0.00]	0.065
WBC at admission ($10^{9/}$L)	8.70 [7.30, 10.50]	8.80 [7.40, 10.57]	0.577	8.95 [7.43, 11.47]	9.30 [7.65, 11.22]	0.976
N% at admission	76.30 [73.50, 80.30]	76.95 [71.60, 80.45]	0.741	78.00 [72.10, 82.38]	77.25 [72.70, 81.38]	0.499
HGB at admission ($10^{9/}$L)	121.00 [113.00, 129.00]	122.00 [113.00, 128.75]	0.876	124.00 [111.25, 129.75]	120.85 [112.75, 128.00]	0.308
Albumin at admission	37.00 [35.00, 38.00]	36.00 [34.00, 38.00]	**0.004**	37.00 [36.00, 38.75]	36.00 [34.00, 37.00]	**0.002**
Number of vaginal examinations	3.00 [1.00, 5.00]	5.00 [1.00, 8.00]	**<0.001**	4.00 [1.00, 5.00]	5.00 [1.00, 7.25]	**0.029**
Amniotic fluid volume	400.00 [300.00, 500.00]	300.00 [200.00, 500.00]	**<0.001**	400.00 [300.00, 500.00]	300.00 [200.00, 500.00]	0.056
Amount of bleeding (ml)	415.00 [331.00, 498.00]	402.50 [318.50, 490.00]	**<0.001**	325.50 [280.75, 413.75]	445.00 [395.00, 540.00]	**<0.001**
PROM						
No	149 (78.8)	101 (56.7)	**<0.001**	60 (81.1)	50 (59.5)	**0.006**
Yes	40 (21.2)	77 (43.3)		14 (18.9)	34 (40.5)	
GDM						
No	160 (84.7)	149 (83.7)	0.916	61 (82.4)	71 (84.5)	0.890
Yes	29 (15.3)	29 (16.3)		13 (17.6)	13 (15.5)	
GBS						
No	185 (97.9)	172 (96.6)	0.677	74 (100.0)	81 (96.4)	0.290
Yes	4 (2.1)	6 (3.4)		0 (0.0)	3 (3.6)	
Oligohydramnios						
No	179 (94.7)	165 (92.7)	0.562	70 (94.6)	81 (96.4)	0.864
Yes	10 (5.3)	13 (7.3)		4 (5.4)	3 (3.6)	
Gemellary pregnancy						
No	185 (97.9)	169 (94.9)	0.215	72 (97.3)	82 (97.6)	1.000
Yes	4 (2.1)	9 (5.1)		2 (2.7)	2 (2.4)	
ICP						
No	188 (99.5)	171 (96.1)	0.061	74 (100.0)	80 (95.2)	0.163
Yes	1 (0.5)	7 (3.9)		0 (0.0)	4 (4.8)	

(Continued)

10.3389/fcimb.2024.1464485

TABLE 1 Continued

Variable	Training dataset			Validation dataset		
	Non-puerperal infection (n=189)	Puerperal infection (n=178)	P value	Non-puerperal infection (n=74)	Puerperal infection (n=84)	P value
Gestational hypertension						
No	183 (96.8)	176 (98.9)	0.324	69 (93.2)	82 (97.6)	0.344
Yes	6 (3.2)	2 (1.1)		5 (6.8)	2 (2.4)	
Cervical ligation						
No	189 (100.0)	177 (99.4)	0.976	74 (100.0)	84 (100.0)	
Yes	0 (0.0)	1 (0.6)				NA
Central placenta previa						
No	187 (98.9)	176 (98.9)	1.000	73 (98.6)	82 (97.6)	1.000
Yes	2 (1.1)	2 (1.1)		1 (1.4)	2 (2.4)	
Antibiotics administered within 1 week before admission						
No	188 (99.5)	129 (72.5)	**<0.001**	74 (100.0)	63 (75.0)	**<0.001**
Yes	1 (0.5)	49 (27.5)		0 (0.0)	21 (25.0)	
Induced labor						
No	159 (84.1)	92 (51.7)	**<0.001**	63 (85.1)	49 (58.3)	**<0.001**
Yes	30 (15.9)	86 (48.3)		11 (14.9)	35 (41.7)	
Amniotic fluid color						
0	151 (79.9)	120 (67.4)	**<0.001**	60 (81.1)	60 (71.4)	0.383
1	22 (11.6)	15 (8.4)		6 (8.1)	7 (8.3)	
2	13 (6.9)	26 (14.6)		7 (9.5)	13 (15.5)	
3	3 (1.6)	17 (9.6)		1 (1.4)	4 (4.8)	
Mode of labor						
Vaginal	100 (52.9)	40 (22.5)	**<0.001**	47 (63.5)	19 (22.6)	**<0.001**
Cesarean section (CS)	89 (47.1)	138 (77.5)		27 (36.5)	65 (77.4)	
Suturing the uterine cavity during CS to stop bleeding						
No	189 (100.0)	169 (94.9)	**0.005**	74 (100.0)	82 (97.6)	0.533
Yes	0 (0.0)	9 (5.1)		0 (0.0)	2 (2.4)	
Uterine balloon tamponade						
No	188 (99.5)	174 (97.8)	0.333	74 (100.0)	84 (100.0)	NA
Yes	1 (0.5)	4 (2.2)				
Bimanual examination						
No	189 (100.0)	177 (99.4)	0.976	74 (100.0)	84 (100.0)	NA
Yes	0 (0.0)	1 (0.6)				
Incision hematoma						
No	186 (98.4)	172 (96.6)	0.443	74 (100.0)	82 (97.6)	0.533
Yes	3 (1.6)	6 (3.4)		0 (0.0)	2 (2.4)	

(Continued)

10.3389/fcimb.2024.1464485

TABLE 1 Continued

Variable	Training dataset			Validation dataset		
	Non-puerperal infection (n=189)	Puerperal infection (n=178)	P value	Non-puerperal infection (n=74)	Puerperal infection (n=84)	P value
Colpoperineal laceration						
No	170 (89.9)	166 (93.3)	0.341	63 (85.1)	79 (94.0)	0.112
Yes	19 (10.1)	12 (6.7)		11 (14.9)	5 (6.0)	
Episiotomy						
No	178 (94.2)	174 (97.8)	0.143	69 (93.2)	82 (97.6)	0.344
Yes	11 (5.8)	4 (2.2)		5 (6.8)	2 (2.4)	
Cervical laceration						
No	182 (96.3)	175 (98.3)	0.386	68 (91.9)	83 (98.8)	0.085
Yes	7 (3.7)	3 (1.7)		6 (8.1)	1 (1.2)	
Forceps delivery						
No	185 (97.9)	175 (98.3)	1.000	72 (97.3)	82 (97.6)	1.000
Yes	4 (2.1)	3 (1.7)		2 (2.7)	2 (2.4)	
B-Lynch uterine compression sutures						
No	187 (98.9)	174 (97.8)	0.627	74 (100.0)	82 (97.6)	0.533
Yes	2 (1.1)	4 (2.2)		0 (0.0)	2 (2.4)	
Indwelling catheter						
No	171 (90.5)	54 (30.3)	**<0.001**	71 (95.9)	26 (31.0)	**<0.001**
Yes	18 (9.5)	124 (69.7)		3 (4.1)	58 (69.0)	

Bold indicates statistically significant results P < 0.05.

in one week before admission (*OR*:61.303, *95%CI*: 7.491-501.71), induced labor (*OR*: 1.097, *95%CI*: 0.479-2.515), and indwelling catheter (*OR*: 21.726, *95%CI*: 11.010-42.874) were included in the multivariate logistic regression (Table 2). A nomogram for the diagnosis of PI was established based on the LASSO logistic regression model (Figure 2, C-index=0.905),Additionally, we visually deploy the predictive model on shinyapps.io (https://puerperalinfection.shinyapps.io/infection/). We further used RCS regression analysis to find out that the risk of PI increased when the number of vaginal examinations was more than 4 times (Figure 3A) and postpartum bleeding was greater than 414 ml (Figure 3B).

3.4 Model validation

In the training dataset, the AUC was 0.904 (*95% CI*: 0.871-0.936) (Figure 4A), and the calibration curve was close to the ideal diagonal line (Figure 5A). Furthermore, the DCA showed significantly better net benefit in the predictive model (Figure 6A). Moreover, a validation dataset consisting of 158 mothers was used to test the accuracy of the nomogram. The AUC was 0.890 (*95% CI*: 0.837–0.942) (Figure 4B), reflecting a good accuracy of the nomogram. Meanwhile, the model had good consistency and the calibration curve of the validation cohort was also close to the ideal diagonal line (Figure 5B). Additionally, the DCA was employed to visually assess the clinical efficacy of the nomogram prediction model in both the training and validation datasets, as depicted in Figure 6B. The Clinical impact curves (Supplementary Figure S1) in the training and validation datasets are also well-fitted. This evaluation further confirms that the nomogram exhibits optimal predictive capability. The results indicate that the nomogram has a considerable potential for aiding clinical decision-making.

3.5 Drug resistance analysis

Among the 262 PI women, 206 were full-term pregnant at term (≥ 37 weeks) and 42 were non-term pregnant women (< 37 weeks). The positive rate of blood culture in preterm pregnant women was higher than that in full-term pregnant women (χ^2 = 6.254, P = 0.012). 14 women were rehospitalized after discharge for PI (Table 3). The results of blood culture showed that 100 cases were positive, including 89 cases of *Escherichia.coli* (89% of positive blood culture), 3 cases with *Klebsiella pneumoniae*, 2 cases of *Staphylococcus epidermidis* and *Staphylococcus capitis*, and 1 case for each of *Burkholderia cepacia*, *Streptococcus agalactiae*, *Enterococcus faecalis*, and *Streptococcus mitis*. A drug

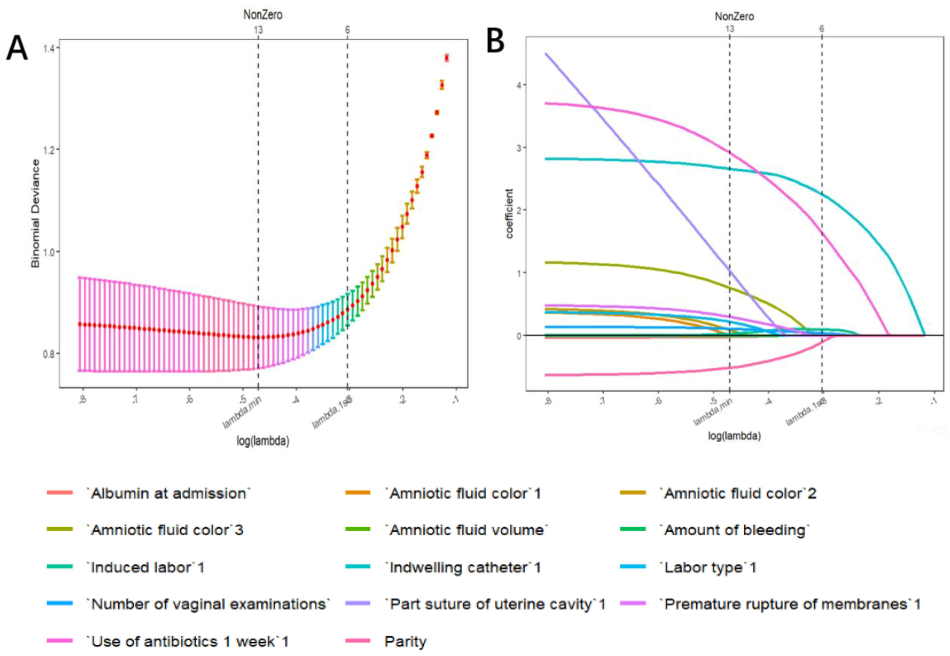

FIGURE 1
Variable selection by the LASSO binary logistic regression model. **(A)** Following verification of the optimal parameter (l) in the LASSO model, the mean squared error changes for the Log (l) value, and the vertical dotted line near Log (l) is drawn based on 1 standard error criteria. **(B)** Six variables with nonzero coefficients were selected by deriving the optimal lambda.

susceptibility test was performed in patients with positive blood cultures. We found that the susceptibility of *Escherichia. coli* to Imipenem and Meropenem was 100%, to Piperacillin/tazobactam was 97.75%, and to Ceftazidime was 95.51% (Figure 7). The susceptibility of *Klebsiella pneumoniae* to Imipenem, Meropenem, Piperacillin/tazobactam, and Ceftazidime was 100% (Figure 8).

4 Discussion

This study has important implications for maternal perinatal health. In the past, due to the lack of good predictive models, obstetricians often started to treat the infection at the onset of PI, and delayed treatment caused great trauma to the mother. On the other hand, some obstetricians used antibiotics without instructions for fear of PI, which increased the risk of drug resistance. To solve this challenging clinical dilemma, we developed a simplified and practical PI prediction model that utilizes LASSO and multivariate regression analyses to select six variables closely associated with PI. These risk factors for PI were parity, number of vaginal examinations, amount of bleeding, antibiotics administered in one week before admission, induced labor, and indwelling catheter. Obstetricians can utilize this nomogram to easily evaluate the risk level and implement targeted prevention and control measures.

The multivariate regression analysis revealed that an increased number of vaginal examinations was an independent risk factor for maternal infection (*OR*: 2.107, *95%CI*: 1.075-4.128). We also observed that conducting vaginal examinations more than 4 times was associated with an increased risk of infection. Similar results were also reported in previous research (Ngonzi et al., 2018; Saeed et al., 2019; Ketema et al., 2020; Oyato et al., 2024). With the increase in a number of vaginal examinations (especially after the membrane is

TABLE 2 Multivariable logistic model of the probability of puerperal infection in the training dataset.

Variables	*B*	*SE*	*P*	*OR*	*95%CI*	
					Low	High
Parity	-0.769	0.331	0.020	0.215	0.059	0.787
Number of vaginal examinations	0.124	0.057	0.030	2.107	1.075	4.128
Amount of bleeding	0.002	0.001	0.024	1.293	1.035	1.617
Antibiotics administered within 1 week before admission	4.116	1.073	<0.001	61.303	7.491	501.71
Induced labor	0.093	0.423	0.826	1.097	0.479	2.515
Indwelling catheter	3.079	0.347	<0.001	21.726	11.010	42.874

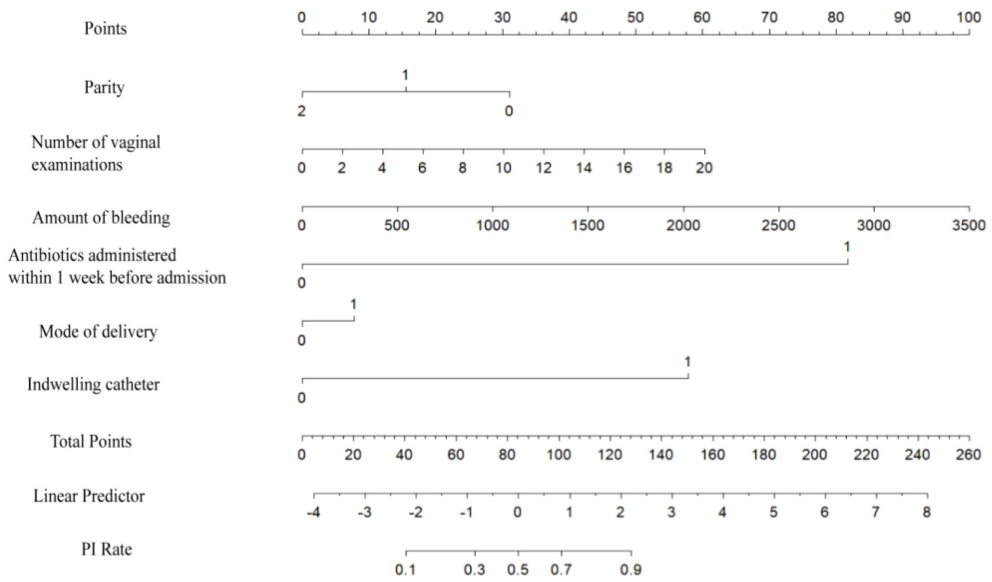

FIGURE 2
Nomogram to estimate the probability of PI. Find the predictor points on the uppermost point scale that correspond to each variable of the pregnant woman and add them up; the total points projected to the bottom scale indicate the probability of PI.

broken), the balance of female vaginal flora may be broken, resulting in weakened defense ability, and pathogenic bacteria may enter the uterine cavity, abdominal cavity, and blood through the cervix, reproductive tract, and wound surface (Oyato et al., 2024). Furthermore, our study showed that indwelling catheter was also a risk factor for PI, which may be because routine catheter indwelling after cesarean section leads to retrograde bacteria and increases the risk of infection. After a cesarean section, the mother should be encouraged to get out of bed in advance and remove the catheter as soon as possible to reduce the risk of infection (Mackeen et al., 2024). Additionally, our study showed that there was an increasing incidence of PI associated with postpartum hemorrhage, and the risk of puerperal infection was elevated when postpartum bleeding exceeded 414 ml. Postpartum hemorrhage causes damage to the maternal reproductive system to a certain extent, resulting in the balance of the body system being broken, and eventually leading to infection (Gonzalez-Brown and Schneider, 2020). After the occurrence of maternal bleeding, timely intervention measures should be taken to control the amount of blood loss within the safe line and minimize the impact of postpartum hemorrhage on the balance of the immune system, thereby reducing the risk of infection. Interestingly, antibiotics administered in 1 week before admission was also an independent risk factor for puerperal infection (Adeyemo et al., 2022). In addition, Miller et al. found that exposure to antibiotics during pregnancy has also been associated with an increased risk of hospitalization infections in children (Miller et al., 2018). Patients who were given antibiotics before delivery had pre-existing infections or had high-risk factors for infection. This might

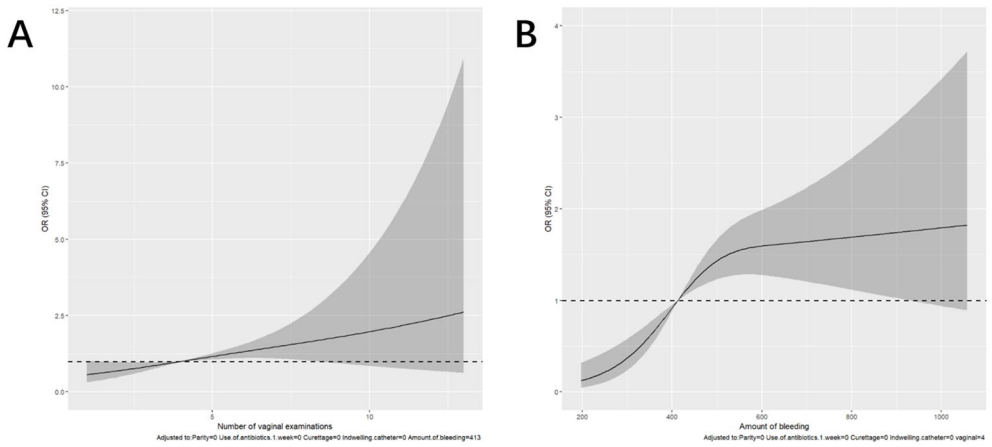

FIGURE 3
Restricted cubic spline (RCS) regression analysis. **(A)** The relationship between the number of vaginal examinations and PI. **(B)** The relationship between the amount of bleeding and PI.

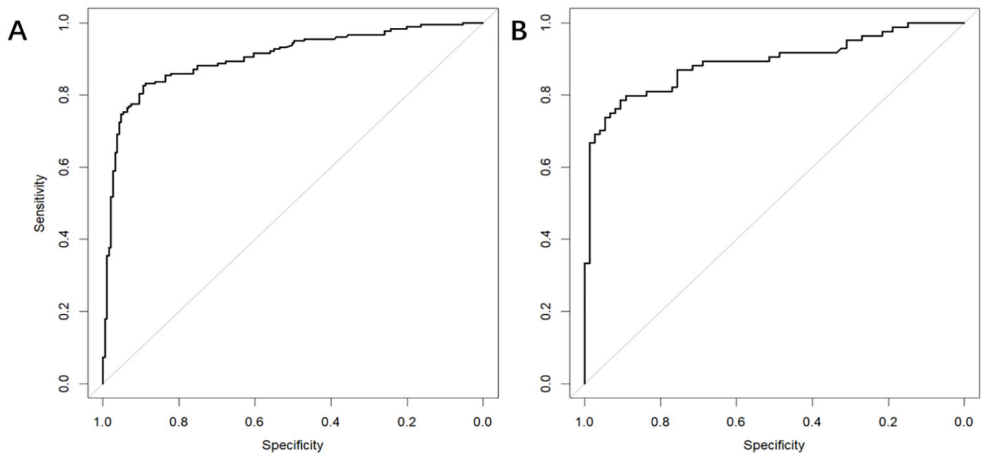

FIGURE 4
The receiver operating characteristic (ROC) curves of nomograms in the training and validation datasets, respectively. **(A)** The AUC value of the training dataset is 0.904, 95% CI: 0.871-0.936 ($p < 0.05$). **(B)** The AUC value of the validation dataset is 0.890, 95% CI: 0.837–0.942 ($p < 0.05$).

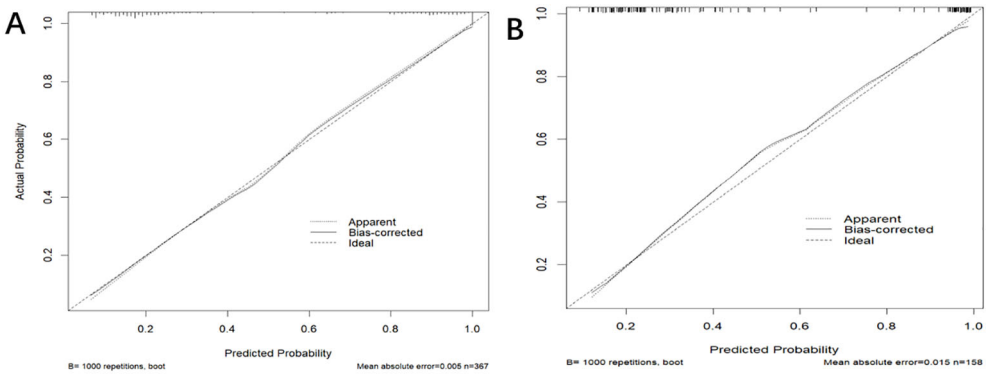

FIGURE 5
The calibration curve of the nomogram for predicting PI in the training dataset **(A)** and validation dataset **(B)**, respectively. Calibration focused on the accuracy of the probability between the predictive model and the actually observed value. The y-axis represents the actual diagnosed cases of puerperal infection, the x-axis represents the predicted risk of puerperal infection, and the solid line represents the prediction of the training dataset and the validation dataset **(B)**.

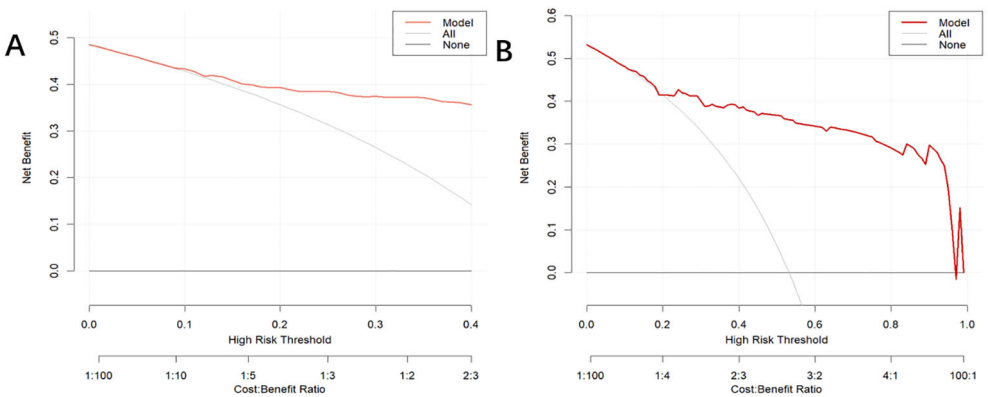

FIGURE 6
Decision curve analysis for the puerperal infection risk nomogram. The y-axis estimates the net benefit, the horizontal solid line represents the probability that the mother does not have a risk of puerperal infection, and the oblique solid line represents the probability of risk that the mother does not have a risk of puerperal infection. **(A)** Training dataset. **(B)** Validation dataset.

TABLE 3 Gestational week and blood culture distribution of puerperal infection group.

The time of onset of fever	Number	Positive blood culture	Negative blood culture	χ^2	P value
≥37week	206	75	131	6.254	0.012
<37week	42	24	18		
Fever recurred after discharge	14	1	13		

be the reason why these patients were at high risk of PI. In these patients, antibiotic choice during and after delivery or the puerperium was important. At present, *Escherichia. coli* is still the main pathogenic bacteria in China, which differs from developed countries. Here we recommended choosing antibiotics that are sensitive to *Escherichia coli*. Our research has found that multiparous women have a lower risk of puerperal infections than primiparous women. This may be due to the shorter duration of labor and the less vaginal examinations in multiparous women.

In the univariate analysis, we found that the CS rate was significantly higher in the PI group than in the control group in both the training and validation sets. The CS rate of all infected patients was 77.5%, of which 11 (4.2%) had bleeding from the placental attachment site, and repeated surgical procedures such as uterine sutures were performed during CS to stop the bleeding. CS and repeated uterine sutures, especially after prolonged labor or induced labor, increased the risk of puerperal infection. This was consistent with previous literature reports. A study from Canada reported that prolonged labor followed by a cesarean section increased the incidence of postpartum sepsis to as high as 30% (Ross et al., 2013). Leth et al. found that the risk of PI seems to be nearly 5-fold increased after cesarean section compared with vaginal

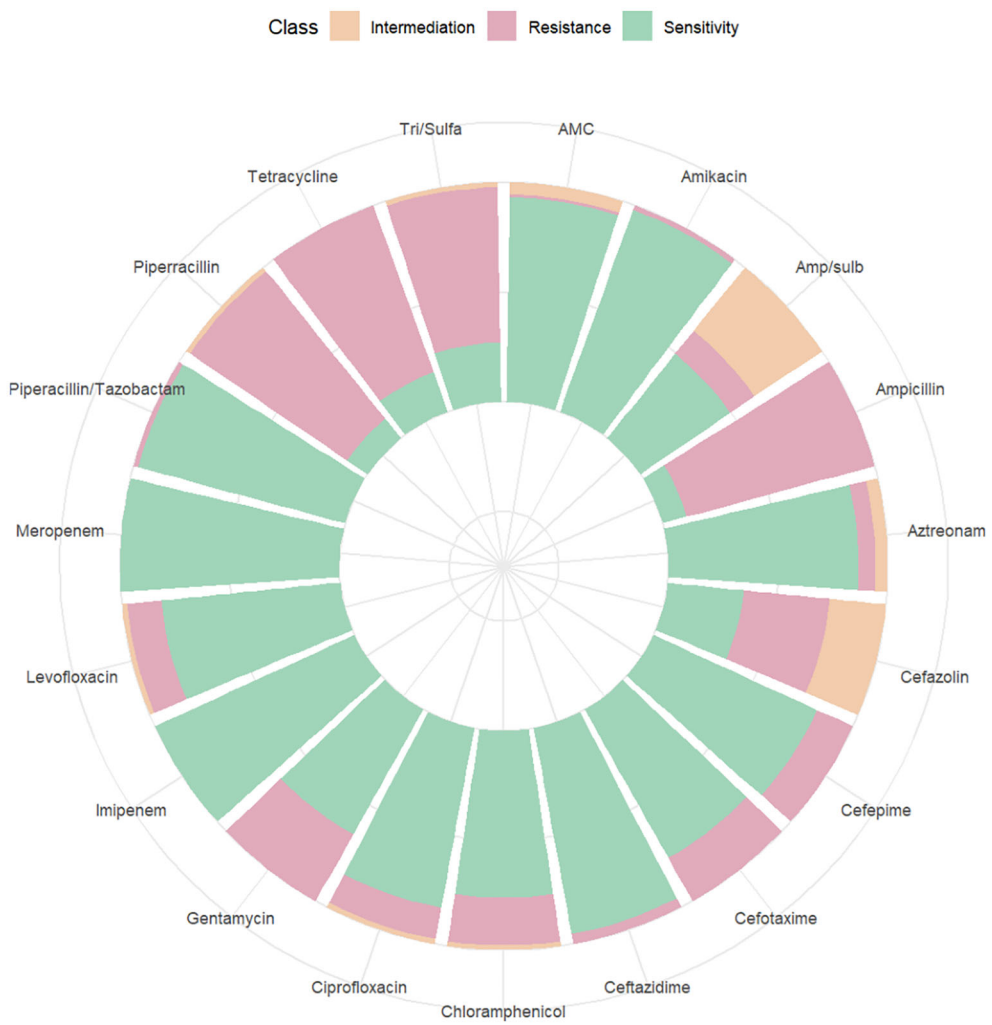

FIGURE 7
Drug sensitivity map of *Escherichia.coli*.

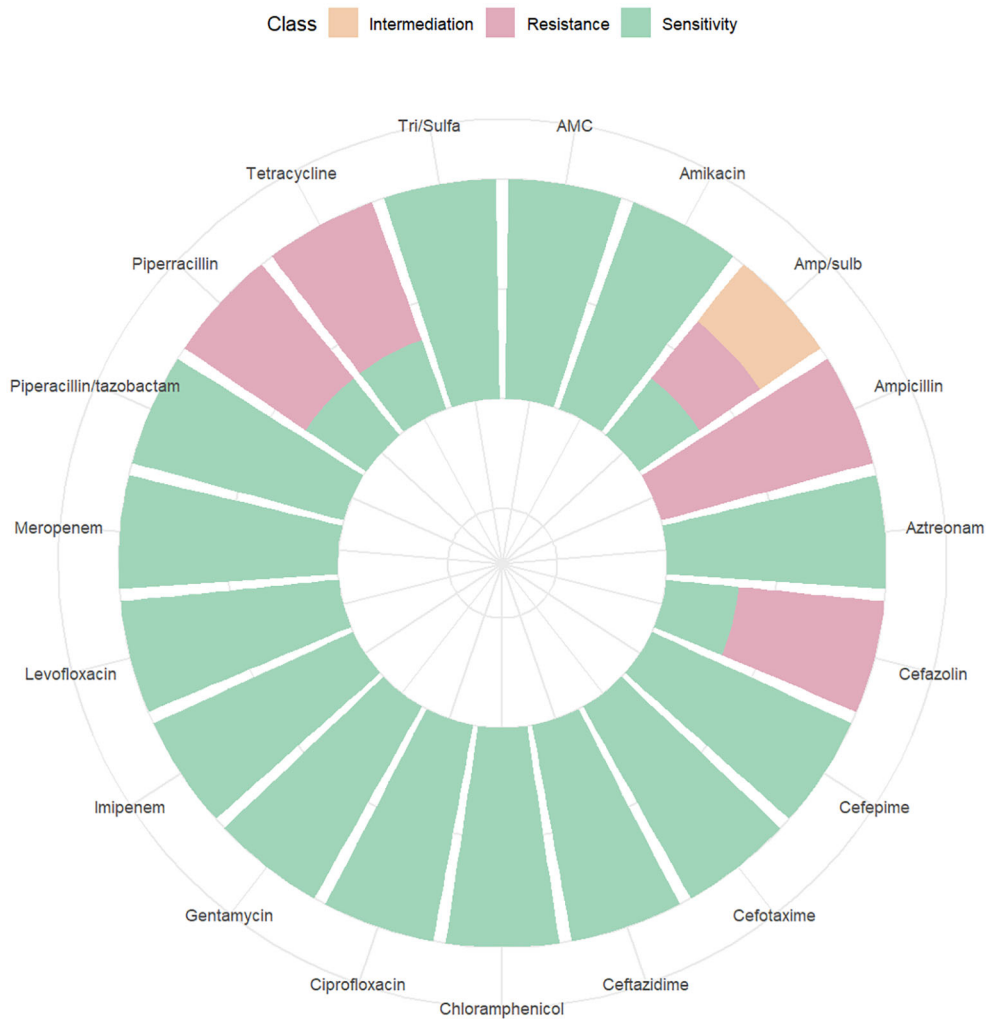

FIGURE 8
Drug sensitivity map of *Klebsiella pneumonia*.

birth (Leth et al., 2009). Also, we found that the infected group had lower amniotic fluid volume than the control group, suggesting that sufficient amniotic fluid may be a protective factor for puerperal infection. PROM might also be one of the reasons for the low volume of amniotic fluid in the infected group. In univariate analysis, PROM was also a risk factor for puerperal infection. PROM increases the risk of retrograde entry into the uterine cavity and is a well-established risk factor for infection. Our study demonstrated that lower levels of albumin upon admission may serve as a potential risk factor for postpartum infection. Albumin plays a pivotal role in both wound healing and immune function (Jiang et al., 2022), thereby suggesting that the association between preoperative hypoalbuminemia and puerperal infection is likely to be multifaceted. One plausible explanation for this intricate relationship could be attributed to the fact that mothers with diminished albumin levels might experience compromised nutritional status along with deficiencies in other essential vitamins and nutrients, leading to increased maternal susceptibility to pathogenic bacteria (Kishawi et al., 2020).

Pathogens are the main culprits responsible for PI, and choosing the right antimicrobial agent is critical to PI outcomes. We found that the main pathogen of PI was *Escherichia.coli*, and we analyzed its antimicrobial susceptibility. The result showed that its sensitivity to carbapenems (Meropenem and Imipenem) were 100%, to the beta-lactam compound drug such as Piperacillin Tazobactam and ceftazidime were over 95%. However, *Escherichia. coli* was less than 50% sensitive to ampicillin-tazobactam and only 11% sensitive to ampicillin. Therefore, prompt antibiotic change should be considered in pregnant women with high fever and suspected sepsis, or with CS after prolonged induction of labor, or with antibiotics administered within one week before termination of pregnancy, or with perioperative fever, and Piperacillin Tazobactam and Ceftazidime were the good choices.

Our nomogram demonstrated a significant level of discrimination (C-index = 0.905), and the decision curve analysis revealed a significantly improved net benefit in the predictive model. This model can be easily recalibrated for individual settings provided that the six predictor variables are available. However, our study was limited to a retrospective single-center and non-randomized controlled study. More prospective, multicenter studies are needed to increase the reliability of the

extrapolation of results. In addition, the data on puerperal infection were not completely obtained as they may be referred to community hospitals. Further external validation is needed to optimize and improve the nomogram.

5 Conclusion

In conclusion, a nomogram that included 6 variables was developed to predict PI risk based on a LASSO and logistic regression analysis, which showed a good performance through internal validation. Based on scoring using the nomogram, we can effectively manage risk factors and implement targeted active surveillance promptly to reduce the occurrence of PI, and decrease costs related to prevention and control. All these indicate that we should strengthen the management of high-risk pregnancies, reduce the frequency of vaginal examination, reduce the amount of postpartum bleeding, and reduce the rate of CS. Once PI occurs, sepsis should be recognized as soon as possible. In addition, antibiotics should be carefully and rationally selected in the clinic to ensure the safety of drug use in patients while improving the therapeutic effect.

Data availability statement

The raw data supporting the conclusions of this article will be made available by the authors, without undue reservation.

Ethics statement

The studies involving humans were approved by the ethics committee of the Women and Children's Health Hospital of Chongqing Medical University (CQHCWC). The studies were conducted in accordance with the local legislation and institutional requirements. Written informed consent for participation was not required from the participants or the participants' legal guardians/next of kin in accordance with the national legislation and institutional requirements.

Author contributions

YW: Conceptualization, Writing – original draft, Writing – review & editing. XM: Conceptualization, Formal analysis, Methodology, Writing – original draft. JY: Data curation, Formal analysis, Writing – original draft. HQ: Funding acquisition, Resources, Supervision, Writing – review & editing.

Funding

The author(s) declare financial support was received for the research, authorship, and/or publication of this article. This work was supported by Sichuan Science and Technology Program (Grant number: 2023YFQ0005). The Key Research Program of Chongqing Science and Technology Bureau (No. CSTB2022TIAD-KPX0156).

Conflict of interest

The authors declare that the research was conducted in the absence of any commercial or financial relationships that could be construed as a potential conflict of interest.

Publisher's note

All claims expressed in this article are solely those of the authors and do not necessarily represent those of their affiliated organizations, or those of the publisher, the editors and the reviewers. Any product that may be evaluated in this article, or claim that may be made by its manufacturer, is not guaranteed or endorsed by the publisher.

Supplementary material

The Supplementary Material for this article can be found online at: https://www.frontiersin.org/articles/10.3389/fcimb.2024.1464485/full#supplementary-material

References

Acosta, C. D., Knight, M., Lee, H. C., Kurinczuk, J. J., Gould, J. B., and Lyndon, A. (2013). The continuum of maternal sepsis severity: incidence and risk factors in a population-based cohort study. *PloS One* 8, e67175. doi: 10.1371/journal.pone.0067175

Acosta, C. D., Kurinczuk, J. J., Lucas, D. N., Tuffnell, D. J., Sellers, S., Knight, M., et al. (2014). Severe maternal sepsis in the UK, 2011-2012: a national case-control study. *PloS Med.* 11, e1001672. doi: 10.1371/journal.pmed.1001672

Adeyemo, M., Oyeneyin, L., Irinyenikan, T., Gbala, M., Akadiri, O., Bakare, B., et al. (2022). Pre-caesarean section vaginal preparation with chlorhexidine solution in preventing puerperal infectious morbidities: A randomized controlled trial. *West Afr J. Med.* 39, 369–374.

Gonzalez-Brown, V., and Schneider, P. (2020). Prevention of postpartum hemorrhage. *Semin. Fetal Neonatal Med.* 25, 101129. doi: 10.1016/j.siny.2020.101129

Jiang, B., Xu, H., Xie, J., Wang, D., Gan, Q., and Zhou, Z. (2022). Are the preoperative albumin levels and the albumin to fibrinogen ratio the risk factors for acute infection after primary total joint arthroplasty? *Front. Surg.* 9. doi: 10.3389/fsurg.2022.1043242

Karsnitz, D. B. (2013). Puerperal infections of the genital tract: a clinical review. *J. Midwif. Womens Health* 58, 632–642. doi: 10.1111/jmwh.12119

Ketema, D. B., Wagnew, F., Assemie, M. A., Ferede, A., Alamneh, A. A., Leshargie, C. T., et al. (2020). Incidence and predictors of surgical site infection following cesarean section in North-west Ethiopia: a prospective cohort study. *BMC Infect. Dis.* 20, 902. doi: 10.1186/s12879-020-05640-0

Kishawi, D., Schwarzman, G., Mejia, A., Hussain, A. K., and Gonzalez, M. H. (2020). Low preoperative albumin levels predict adverse outcomes after total joint arthroplasty. *J. Bone Joint Surg. Am.* 102, 889–895. doi: 10.2106/JBJS.19.00511

Kobayashi, N., Ahmed, S., Sumi, A., Urushibara, N., Kawaguchiya, M., and Aung, M. S. (2017). Collaborative research on puerperal infections in Bangladesh. *Nihon Eiseigaku Zasshi* 72, 106–111. doi: 10.1265/jjh.72.106

Leth, R. A., Moller, J. K., Thomsen, R. W., Uldbjerg, N., and Norgaard, M. (2009). Risk of selected postpartum infections after cesarean section compared with vaginal

birth: a five-year cohort study of 32,468 women. *Acta Obstet. Gynecol. Scand.* 88, 976–983. doi: 10.1080/00016340903147405

Li, P., Li, Y., Zhang, Y., Zhao, L., Li, X., Bao, J., et al. (2023). Incidence, temporal trends and risk factors of puerperal infection in Mainland China: a meta-analysis of epidemiological studies from recent decade, (2010-2020). *BMC Pregnancy Childbirth* 23, 815. doi: 10.1186/s12884-023-06135-x

Mackeen, A. D., Sullivan, M. V., and Berghella, V. (2024). Evidence-based cesarean delivery: preoperative management (part 7). *Am. J. Obstet. Gynecol. MFM* 6, 101362. doi: 10.1016/j.ajogmf.2024.101362

Miller, J. E., Wu, C., Pedersen, L. H., de Klerk, N., Olsen, J., and Burgner, D. P. (2018). Maternal antibiotic exposure during pregnancy and hospitalization with infection in offspring: a population-based cohort study. *Int. J. Epidemiol.* 47, 561–571. doi: 10.1093/ije/dyx272

Ngonzi, J., Bebell, L. M., Fajardo, Y., Boatin, A. A., Siedner, M. J., Bassett, I. V., et al. (2018). Incidence of postpartum infection, outcomes and associated risk factors at Mbarara regional referral hospital in Uganda. *BMC Pregnancy Childbirth* 18, 270. doi: 10.1186/s12884-018-1891-1

Oyato, B. T., Debele, T., Edosa, D., Abasimel, H. Z., Awol, M., Kebede, E. T., et al. (2024). Determinants of puerperal sepsis among postpartum women: a case-control study in East Shoa Zone public hospitals, Central Ethiopia. *BMJ Open* 14, e083230. doi: 10.1136/bmjopen-2023-083230

Ross, L. E., Grigoriadis, S., Mamisashvili, L., Vonderporten, E. H., Roerecke, M., Rehm, J., et al. (2013). Selected pregnancy and delivery outcomes after exposure to antidepressant medication: a systematic review and meta-analysis. *JAMA Psychiatry* 70, 436–443. doi: 10.1001/jamapsychiatry.2013.684

Saeed, K. B., Corcoran, P., O'Riordan, M., and Greene, R. A. (2019). Risk factors for surgical site infection after cesarean delivery: A case-control study. *Am. J. Infect. Control* 47, 164–169. doi: 10.1016/j.ajic.2018.07.023

Song, H., Hu, K., Du, X., Zhang, J., and Zhao, S. (2020). Risk factors, changes in serum inflammatory factors, and clinical prevention and control measures for puerperal infection. *J. Clin. Lab. Anal.* 34, e23047. doi: 10.1002/jcla.23047

Tardieu, S. C., and Schmidt, E. (2017). Group A streptococcus septic shock after surgical abortion: A case report and review of the literature. *Case Rep. Obstet. Gynecol.* 2017, 6316739. doi: 10.1155/2017/6316739

van Dillen, J., Zwart, J., Schutte, J., and van Roosmalen, J. (2010). Maternal sepsis: epidemiology, etiology and outcome. *Curr. Opin. Infect. Dis.* 23, 249–254. doi: 10.1097/QCO.0b013e328339257c

Wu, W. T., Li, Y. J., Feng, A. Z., Li, L., Huang, T., Xu, A. D., et al. (2021). Data mining in clinical big data: the frequently used databases, steps, and methodological models. *Mil Med. Res.* 8, 44. doi: 10.1186/s40779-021-00338-z

frontiers | Frontiers in Cellular and Infection Microbiology

TYPE Original Research
PUBLISHED 16 January 2025
DOI 10.3389/fcimb.2024.1472765

OPEN ACCESS

EDITED BY
José Luis Muñoz-Carrillo,
University of Guadalajara, Mexico

REVIEWED BY
Shiori Kitaya,
Kanazawa University Hospital, Japan
César Iván Romo Sáenz,
Autonomous University of Nuevo León,
Mexico

*CORRESPONDENCE
Shi-Yan Zhang
myebox@139.com

RECEIVED 06 August 2024
ACCEPTED 26 December 2024
PUBLISHED 16 January 2025

CITATION
Zhang S-Y, Zhuo Y, Li B-R, Jiang Y-Y, Zhang J, Cai N and Yang L (2025) Identifying key blood markers for bacteremia in elderly patients: insights into bacterial pathogens. *Front. Cell. Infect. Microbiol.* 14:1472765. doi: 10.3389/fcimb.2024.1472765

Identifying key blood markers for bacteremia in elderly patients: insights into bacterial pathogens

Shi-Yan Zhang*, Ying Zhuo, Bu-Ren Li, Ying-Ying Jiang, Jie Zhang, Na Cai and Lin Yang

Department of Clinical Laboratory, Fuding Hospital, Fujian University of Traditional Chinese Medicine, Fuding, Fujian, China

Background: This study aimed to assess the distribution of bacteremia pathogens in elderly patients, examine the impact of gender on pathogen distribution, and evaluate the predictive value of routine blood parameters for diagnosing bacteremia.

Methods: A retrospective analysis was conducted on 151 elderly patients (≥60 years old) admitted to Fuding Hospital, Fujian University of Traditional Chinese Medicine between October 2022 and June 2023. Comprehensive routine blood tests and blood cultures were performed. The diagnostic efficacy of routine blood parameters, including white blood cell (WBC), neutrophil-to-lymphocyte ratio (NLR), platelet-lymphocyte ratio (PLR), and red blood cell distribution width (RDW), was evaluated using receive operating characteristic (ROC) curve analysis. Patients were categorized into either the culture-positive group (82 cases) or the culture-negative group (69 cases) according to blood culture results.

Results: No significant differences in age and gender were found between the culture-positive and culture-negative groups. The primary bacterial pathogens of bacteremia in the elderly were *Escherichia coli*, *Klebsiella pneumoniae* and *Streptococcus*. Elderly female patients demonstrated a significantly higher culture positivity rate for *E. coli* compared to their male counterparts (P = 0.021). The areas under the ROC curve (AUC) for the four parameters were as follows: WBC, 0.851 (95% confidence interval (CI) 0.790 - 0.912); NLR, 0.919 (95% CI 0.875 - 0.963); PLR, 0.609 (95% CI 0.518 - 0.700); and RDW was 0.626 (95% CI 0.563 - 0.717).

Conclusions: *E. coli* was identified as the predominant pathogenic microorganism causing bacteremia in the elderly, with a significantly higher culture positivity rate among female patients. Routine blood parameters (WBC, NLR, PLR, and RDW) demonstrated a predictive potential for diagnosing bacteremia in elderly patients.

KEYWORDS

elderly, blood culture, neutrophil-to-lymphocyte ratio, ROC analysis, *Escherichia coli*, bacteremia

Background

Bacteremia, which can progress to sepsis, is a life-threatening organ dysfunction caused by a disorder in the host's response to infection, resulting in high morbidity and mortality worldwide (Font et al., 2020; Jirak et al., 2022; Xu et al., 2024). Globally, bacteremia is responsible for approximately 8 million deaths annually, as pathogenic bacteria invade the bloodstream, multiply, and trigger a systemic inflammatory response that often escalates rapidly (Fernando et al., 2018). The most common bacterial causes of bacteremia worldwide include *Escherichia coli*, *Klebsiella pneumoniae*, and *Staphylococcus aureus*, representing both Gram-negative and Gram-positive pathogens (Gatica et al., 2023). Regionally, studies from Asia, particularly China, have highlighted the predominance of Gram-negative bacteria, such as *E. coli* and *K. pneumoniae* as the primary pathogens causing bacteremia in elderly patients. In Chinese investigations, *E. coli* accounted for 47% of bloodstream infections, with *K. pneumoniae* contributing to over 15% (Fu et al., 2024; Li et al., 2024). Similarly, in the United States, *E. coli* has been identified as the leading cause of community-onset bacteremia in seniors, with an estimated 53,476 cases annually among noninstitutionalized elderly individuals (Jackson et al., 2005). These findings highlight the global and regional dominance of these pathogens, particularly in hospitalized or immunocompromised elderly populations.

Bacteremia in elderly patients is particularly concerning due to their reduced immunity and often insidious disease progression, which often results in subtle clinical symptoms, delayed diagnosis, poor prognosis, and higher long-term mortality (Hernández-Quiles et al., 2022). Early detection and intervention are critical in this population to reduce mortality. Currently, the clinical "gold standard" for diagnosing bacteremia is a laboratory blood culture. However, this method has several limitations, including a prolonged processing time (5-7 days), risk of contamination, and potential false-negative results, which can delay treatment and increase mortality (Bonnet et al., 2024).

In recent years, medical practitioners have explored more rapid biomarkers for diagnosing bacteremia, including procalcitonin (PCT), C-reactive protein (CRP), and interleukin-6 (IL-6) (Bonnet et al., 2024). Although these biomarkers can aid in early detection, their moderate diagnostic accuracy, high cost, and lengthy turnaround time limit their widespread application. In contrast, routine blood parameters, which are cost-effective, easy to perform, and readily available in primary healthcare settings, have been proposed as practical tools for predicting bacteremia in high-risk populations (Berhane et al., 2019). Numerous global studies have highlighted the value of routine blood parameters, including white blood cell count (WBC), neutrophil-to-lymphocyte ratio (NLR), platelet-lymphocyte ratio (PLR), and red blood cell distribution width (RDW), in identifying patients at risk of bacteremia and predicting poor outcomes (Agnello et al., 2021). These biomarkers are cost-effective, easily accessible, and hold potential for detecting bacteremia and assessing its severity, especially in resource-limited settings.

Despite these global and regional findings, there is limited understanding of how routine blood parameters correlate with bacteremia in elderly patients, particularly in the Chinese population. In China, few studies have specifically investigated the relationship between routine blood parameters and bacteremia pathogens in elderly patients. Therefore, this study aims to address this gap by investigating the association between routine blood parameters (WBC, NLR, PLR, and RDW) and bacteremia in elderly patients in a Chinese hospital setting. It also examines the distribution of bacterial pathogens in elderly bacteremia patients and evaluates the potential of these routine blood markers as predictive tools for early diagnosis.

Materials and methods

Patient characteristics

The clinical and laboratory data of 151 consecutive inpatients aged over 60 years who underwent blood culture testing were retrospectively analyzed between October 2022 and June 2023 at the Department of Clinical Laboratory, Fuding Hospital, Fujian University of Traditional Chinese Medicine. The study focused on elderly patients presenting with suspected bacteremia. The patients were categorized into two groups: the bacteremia group (n = 82), consisting of patients with confirmed positive blood culture results, and the control group (n = 69), consisting of patients with negative blood culture results but similar clinical presentations to ensure a valid comparison.

Inclusion and exclusion criteria

Inclusion criteria

Patients diagnosed with bacteremia based on positive blood culture results, including those who developed sepsis or septic shock during hospitalization, as defined by the Surviving Sepsis Campaign Guidelines (Evans et al., 2021).

Exclusion criteria

1. Antibiotic exposure: Patients who received antibiotics more than 24 hours prior to screening were excluded to prevent false-negative blood culture results caused by prior antimicrobial therapy.
2. Pregnant women: Excluded to eliminate the confounding effects of pregnancy-related physiological changes on hematological indices.
3. Immune-compromised patients: Patients receiving radiation therapy, cytotoxic drugs, or organ transplants, as well as those with AIDS or inherited immunodeficiency diseases, were excluded due to altered immune responses that could affect pathogen detection and biomarker reliability.
4. Chronic kidney and liver disease: Patients with chronic kidney disease (baseline serum creatinine ≥2 mg/dL) or

chronic liver failure (Child-Pugh grade C) were excluded because these conditions influence inflammatory markers.
5. Long-term treatment cases: Patients with bacterial endocarditis requiring prolonged antibiotic treatment were excluded to focus on acute bacteremia cases.
6. Hematologic and systemic conditions: Patients with conditions affecting hematological indices were excluded, including: Hematologic diseases (e.g., anemia, leukemia); tumors; autoimmune diseases; trauma.

Ethical approval and compliance

The study protocol was approved by the Medical Ethics Committee of Fuding Hospital, Fujian University of Traditional Chinese Medicine (Approval No.: Fuding Hospital 2022325). All procedures were conducted in accordance with relevant guidelines and regulations. Due to the retrospective nature of the study, the requirement for written informed consent was waived by the ethics committee.

Laboratory analysis

Blood samples (2.0 mL) were drawn from the median elbow vein of patients prior to initiating treatment, using EDTA as an anticoagulant. Prior to venipuncture, the skin was disinfected thoroughly with 75% alcohol followed by iodine solution to minimize contamination. Complete blood cell counts were analyzed using the SYSMEX XE 2100 fully automated hematology analyzer (Sysmex, Japan) and associated reagents. NLR and PLR were calculated based on neutrophil count, lymphocyte count, and platelet count obtained from routine blood tests. All procedures followed standard operating procedures (SOPs), with in-house quality control conducted to ensure accuracy and reproducibility.

Two sets of bilateral double vials were collected for blood culture, with both aerobic and anaerobic cultures performed simultaneously. Blood samples were obtained via peripheral venous puncture, injected directly into Bactec vials, and incubated at 37°C for up to 7 days in a Bactec incubator (BD Diagnostics, Franklin Lakes, NJ, USA). Positive cultures were immediately Gram-stained and subcultured on solid media for further analysis. Microbial identification was conducted using the VITEK 2 Compact system (bioMérieux, France) for identifying *Enterobacteriaceae* and other Gram-negative bacteria, supplemented by the Vitek mass spectrometry system for precise bacterial species identification. These systems provide high reliability, with pathogen detection accuracy exceeding 95%.

A positive blood culture result from a single vial was considered indicative of bacterial presence. For isolates such as coagulase-negative *Staphylococcus*, *Propionibacterium*, and *Corynebacterium*, the same strain needed to be consistently isolated from multiple samples or repeatedly at the same time; otherwise, it was considered a contaminant from skin colonization.

The study focused on bacterial pathogens isolated from blood cultures. Fungi, *Mycoplasma, Chlamydia, parasites*, and viruses were excluded to maintain the study's focus on bacterial infections and ensure consistency in statistical analysis.

Statistical analysis

Data normality was assessed using the Shapiro-Wilk test. Non-normally distributed variables were presented as median and quartiles (P25-P75) and analyzed using nonparametric tests: the Mann-Whitney U test for two-group comparisons and the Kruskal-Wallis H test for multiple groups. Normally distributed data were reported as mean ± standard deviation, and the t-test was employed for mean comparisons between groups. Categorical variables were measured using the chi-square test (χ^2) or Fisher's exact tests, as appropriate, and were reported as count (%). Receiver operating characteristic (ROC) curve analysis was conducted for blood routine parameters. The area under the ROC curve (AUC) was calculated along with the standard error and 95% confidence interval (CI). Sensitivity, specificity, accuracy, positive predictive value, and negative predictive value were derived from the ROC curves. Statistical analyses were performed using SPSS 22.0 software (IBM SPSS, Armonk, NY, USA). A P-value of <0.05 was considered statistically significant.

Results

The Shapiro-Wilk test was used to assess data normality within each group. In all groups, the *P*-value were less than 0.05, indicating non-normal distribution. Consequently, the data were summarized as medians and interquartile ranges. No statistically significant differences in age or gender were observed between the two groups ($P > 0.05$). Detailed results are presented in Table 1.

Analysis of WBC, NLR, PLR, and RDW measurements

The positive group demonstrated significantly higher WBC, NLR, PLR, and RDW values compared to the negative control

TABLE 1 Clinical baseline parameters of blood culture positive and negative groups [median (P25-P75)].

Groups (cases)	Age (years)	Male (%)	Female (%)
Positive (82)	73.0 (70.0–80.3)	38 (46.3)	44 (53.7)
Negative (69)	72.0 (68.5–75.5)	34 (49.3)	35 (50.7)
Mann-Whitney U/ χ^2 test	-1.793	0.129	
P-value	0.073	0.719	

Age is presented as median (25th percentile - 75th percentile). Gender distribution (Male and Female) is presented as number of cases (percentage). Mann-Whitney U test was used for age comparisons, and the Chi-square (χ^2) test was used for gender comparisons.

TABLE 2 Comparison of blood cell parameters between the two groups [median (P25-P75)].

Parameter	Positive group (n=82)	Negative group (n=69)	Z-value	P-value
WBC (10^9/L)	10.93 (7.32 – 16.23)	5.96 (4.80–7.18)	-10.407	0.000
Neutrophils (10^9/L)	8.58 (5.67 – 14.75)	3.69 (2.76–4.54)	-8.407	0.000
Lymphocytes 10^9/L)	1.00 (0.59 - 1.49)	1.70 (1.38–2.18)	-6.307	0.000
RDW (%)	13.70 (13.00-15.00)	12.90 (12.30- 14.00)	-2.676	0.007
NLR	10.52 (5.50–18.44)	2.01 (1.36–3.07)	-8.853	0.000
PLR	188.61 (97.64–250.00)	135.86 (97.66–187.50)	-2.312	0.021

Non-parametric comparisons between the two groups was performed using the Mann-Whitney U test. WBC, White blood cells; NLR, Neutrophil-to-lymphocyte ratio; PLR, Platelet-to-lymphocyte ratio; RDW, Red cell distribution width.

group, with statistically significant differences ($P < 0.05$). Detailed results are presented in Table 2.

Distribution and composition of bacterial pathogens

A total of 82 bacterial strains were isolated from the blood samples of 82 hospitalized elderly patients. The prevalence of Gram-negative bacteria was significantly higher among elderly female patients with bacteremia (61 cases, 74.4%) compared to their male counterparts (21 cases, 25.6%) ($P = 0.021$) (Table 3). Fungal infections were excluded from the analysis.

The distribution of bacterial pathogens included 42 strains of *E. coli*, 15 strains of *K. pneumoniae*, 10 strains of *Streptococcus*, and 9 strains of *Staphylococcus aureus*. Additionally, six strains of other bacteria accounted for 7.3% of the isolates, comprising 2 strains of *Enterococcus faecium*, 2 strains of *Bacteroides fragilis*, 1 strain of *Proteus mirabilis*, and 1 strain of *Moraxella osloensis.* Detailed data are presented in Table 4 and Figure 1.

Tables 1–4 present detailed statistical analyses comparing the study groups and summarizing key outcomes. These tables highlight the characteristics of the groups, statistical significance, counts of various cell types, and the effectiveness of routine blood parameters. Specially, Table 4 demonstrates the results of the Kruskal-Wallis H test, which examines differences among various

TABLE 3 Distribution of pathogenic bacteria between male and female groups (n, %).

Pathogen (Strains)	Male (n = 37)	Female (n = 45)	χ^2	*P*- value
Gram-stain (n = 82)				
Positive (n = 21)	14 (37.8)	7 (15.6)	5.292	0.021a
Negative (n = 61)	23 (62.2)	38 (84.4)		
Escherichia coli (n = 42)				
Positive	13 (35.1)	29 (64.4)	6.981	0.008a
Negative	24 (64.9)	16 (35.6)		
Klebsiella pneumoniae (n = 15)				
Positive	9 (24.3)	6 (13.3)	1.641	0.200a
Negative	28 (75.7)	39 (86.7)		
Streptococcus (n = 10)				
Positive	7 (18.9)	3 (6.7)	–	0.089b
Negative	30 (81.1)	42 (93.3)		
Staphylococcus (n = 9)				
Positive	5(13.5)	4 (8.9)	–	0.725b
Negative	32 (86.5)	41 (91.1)		
Other bacteria (n = 6)				
Positive	3 (8.1)	3 (6.7)	–	1.000b
Negative	34 (91.9)	42 (93.3)		

aChi-square test. bFisher's exact test. Other bacteria include *Enterococcus faecium* (2 strains), *Bacteroides fragilis* (2 strains), *Proteus mirabilis* (1 strain), *Moraxella osloensis* (1 strain).

TABLE 4 Kruskal-Wallis H test of routine blood parameters across different pathogens.

Pathogen (Strains)	Number Rank Average			
	WBC	NLR	PLR	RDW
Escherichia coli (42)	43.79	38.90	41.48	40.90
Klebsiella pneumoniae (15)	43.90	48.80	39.60	36.23
Streptococcus (10)	32.30	37.50	43.00	35.70
Staphylococcus (9)	33.06	42.78	44.11	57.61
Other bacteria (6)	47.50	46.17	40.00	44.33
H-value	3.544	2.447	0.267	5.618
p-value	0.471	0.654	0.992	0.230

The non-parametric test Kruskal-Wallis H test was used to compare the five groups of routine blood parameters across different pathogens. No statistically significant differences were observed for any parameter (all $P > 0.05$). As a result, the Bonferroni method was not applied for *post-hoc* pairwise comparisons. WBC, White blood cell count; NLR, Neutrophil-to-lymphocyte ratio; PLR, Platelet-to-lymphocyte ratio; RDW, Red cell distribution width. Other bacteria: *Enterococcus faecium* (2 strains), *Bacteroides fragilis* (2 strains), *Proteus mirabilis* (1 strain), *Moraxella osloensis* (1 strain).

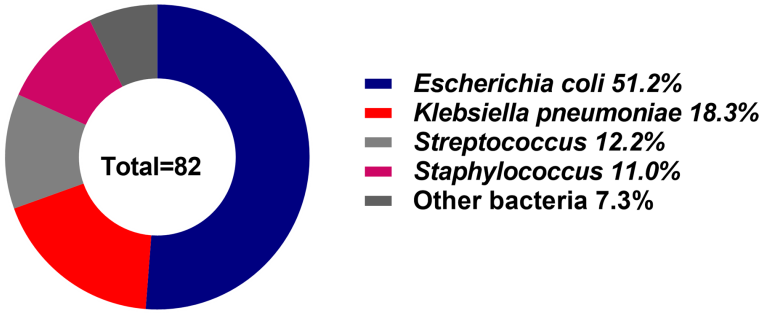

FIGURE 1
Distribution of bacterial pathogens in elderly patients with bacteremia. *Escherichia coli* was the most prevalent pathogen (51.2%), followed by *Klebsiella pneumoniae* (18.3%), *Streptococcus* (12.2%), and others (18.3%).

TABLE 5 Area under the receiver operating characteristic (ROC) curve and related parameters.

Item	WBC	NLR	PLR	RDW
Optimal Cutoff	8.0	4.0	205.9	13.0
Youden index (%)	61.3	69.4	26.7	30.2
Sensitivity (%)	74.4	85.4	42.7	78.0
Specificity (%)	87.0	84.1	84.1	52.2
Accuracy (%)	80.1	84.8	61.6	66.2
PPV (%)	87.1	86.4	76.1	66.0
NPV (%)	74.1	82.9	55.2	66.7
AUC (95%CI)	0.851 (0.790-0.912)	0.919 (0.875-0.963)	0.609 (0.518-0.700)	0.626 (0.536-0.717)
Standard Error	0.031	0.022	0.046	0.046
P- value	0.000	0.000	0.021	0.008

AUC, Area under the receiver operating characteristic (ROC) curve; 95%CI, 95% confidence interval; WBC, White blood cells; NLR, Neutrophil-to-lymphocyte ratio; PLR, Platelet-to-lymphocyte ratio; RDW, Red cell distribution width; PPV, Positive predictive value; NPV, Negative predictive value.

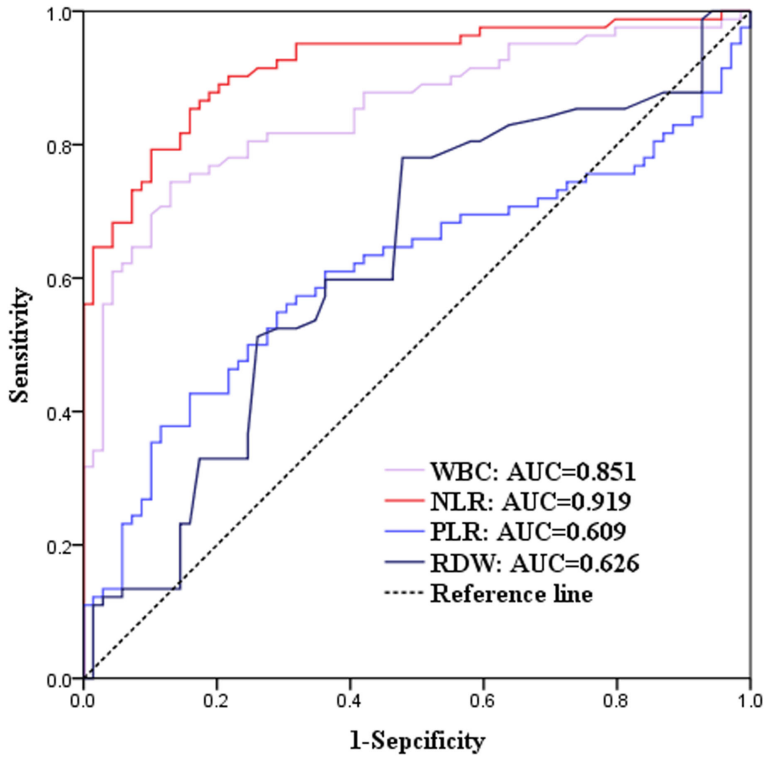

FIGURE 2
Receiver operating characteristic (ROC) curves for blood parameters. The area under the curve (AUC) values were: White blood cell (WBC): 0.851; Neutrophil-to-lymphocyte ratio (NLR): 0.919; Platelet-to-lymphocyte ratio (PLR): 0.609; Red blood cell distribution width (RDW): 0.626. Optimal cutoff values, sensitivity, and specificity derived from the ROC analysis highlight the diagnostic performance of each parameter.

pathogens and their associations with routine blood parameters. Additionally, Table 5 and Figure 2 illustrate the ROC curve analysis, providing optimal cutoff values, sensitivities, specificities, accuracies, and predictive values for different blood cell parameters.

Discussion

This retrospective study of 82 elderly patients with bacteremia and 69 controls identified *E. coli* (51.2%), *K. pneumoniae* (18.3%), and *Streptococcus* (12.2%) as the most prevalent bacteria pathogens (Figure 1). These findings align with previous studies, including those by Guarno et al. (Guarino et al., 2023) and Daniela Dambroso et al (Dambroso-Altafini et al., 2022), which highlighted reported Gram-negative bacteria, particularly *E. coli* and *K. pneumoniae*, as leading causes of bloodstream infections. Similarly, a Japanese study (Matono et al., 2022) reported comparable trends, identifying *E. coli* (28/58, 48%) and *K. pneumoniae* (6/58,10%) as the predominant pathogens.

Our findings reflect global trends where *E. coli* predominates in elderly individuals due to its frequent colonization of the gastrointestinal tract, a critical infection focus for bloodstream infections. Disruptions in intestinal barrier integrity facilitate the translocation of gut-resident *E. coli* into the bloodstream, contributing to systemic infections (Tao et al., 2024; Wu et al., 2024). Identifying key infection foci, such as the gastrointestinal and urinary tracts, is vital for improving clinical management and preventing sepsis progression. In our study, *E. coli* demonstrated a significantly higher positivity rate in elderly women compared to men (64.4% vs. 35.1%, $P = 0.008$) (Table 3). This gender disparity is likely attributed to anatomical factors, including a shorter urethra in females, which increases their susceptibility to urinary tract infections (UTIs)—a common source of *E. coli* bacteremia in this population (Poolman and Wacker, 2016; Plasencia and Ashraf, 2024; Zhan et al., 2024).

Beyond UTIs, *E. coli* can invade human tissues, causing severe infections and high mortality (Fay et al., 2020). It remains the leading cause of bacteremia globally and a major contributor to sepsis-related hospitalizations and deaths among elderly patients (Bonten et al., 2021). Mortality rates in this population range from 15% to 30%, highlighting the critical need for early detection and timely intervention (Tocut et al., 2022).

The analysis of blood cell parameters showed significant increases in leukocyte count, NLR, PLR, and RDW among bacteremia patients. Among these, NLR demonstrated the highest predictive value, with a sensitivity of 85.4% and specificity of 84.1% (Figure 2). Elevated WBC, PLR, and RDW were also significantly associated with bacteremia. These findings underscore the potential of routine blood parameters as rapid, cost-effective, and accessible diagnostic tools, especially in resource-limited settings where immediate blood culture results are unavailable.

While WBC is traditionally used as an indicator of bacterial infection, its diagnostic accuracy may be influenced by conditions

such as hematological diseases, non-infectious inflammatory conditions, surgery, and trauma (Wu et al., 2023). RDW, a marker for red blood cell size variability, is primarily used to diagnose anemia (Liu et al., 2023). However, in conditions like sepsis, oxidative stress and inflammation disrupt erythrocyte maturation, resulting in elevated RDW levels (Jain et al., 2022). A study by Dogan P et al. reported that an RDW cutoff of >19.50% had a sensitivity of 87% and specificity of 81% for predicting late-onset Gram-negative sepsis. In contrast, our study identified an RDW cutoff of >13.0%, achieving a sensitivity of 78.0% and specificity of 52.2%, likely reflecting differences in patient populations.

Our study highlights the value of NLR as a reliable indicator of systemic inflammatory response and a strong predictor of bacteremia (Agnello et al., 2021). Routine blood parameters, including NLR, PLR, and RDW, represent valuable diagnostic tools due to their accessibility, cost-effectiveness, and rapid turnaround time. Clinically, these parameters can aid in the early identification of bacteremia in elderly patients, particularly in resource-limited settings where immediate blood culture results may not be available. Furthermore, While this study focus on the diagnostic performance of blood parameters and pathogen distribution, further research should investigate the relationship between clinical outcomes, blood parameters, and drug susceptibility patterns of the detected pathogens. Additionally, identifying infection foci, particularly in sepsis cases, may further improve clinical management and outcome prediction. Future studies addressing these aspects will provide a more comprehensive understanding of bacteremia and its clinical implications.

Conclusion

Our cross-sectional study identified *E. coli* as the predominant pathogen in elderly patients with bacteremia, with a higher positivity rate in females. This finding underscores the importance of investigating urinary and gastrointestinal infection foci in this demographic. Routine blood parameters, particularly WBC, NLR, PLR, and RDW, showed significant predictive value for diagnosing bacteremia. These accessible and cost-effective markers can facilitate early detection and timely treatment, particularly in resource-limited settings, improving outcomes for at-risk elderly patients. Future research should examine the relationship between blood parameters, clinical outcomes, and pathogen drug susceptibility to enhance diagnostic accuracy and optimize treatment strategies.

Limitations

This study focused exclusively on bacterial pathogens, excluding others such as fungi, *Mycoplasma*, *Chlamydia*, parasites, and viruses. Future research should adopt a multi-center design with larger sample sizes to offer a more comprehensive understanding of geriatric bacteremia. Additionally, further investigations are needed to explore microorganism distribution and enhance the predictive utility of routine blood parameters.

Data availability statement

The raw data supporting the conclusions of this article will be made available by the authors, without undue reservation.

Ethics statement

The study was approved by the Medical Ethics Committee of Fuding Hospital, Fujian University of Traditional Chinese Medicine (Approval Number: Fuding Hospital 2022325). All procedures involving human participants adhered to the ethical standards of the institutional and/or national research committee, as well as the 1964 Helsinki Declaration and its subsequent amendments or comparable ethical guidelines. Informed consent was waived due to the retrospective nature of the study.

Author contributions

S-YZ: Conceptualization, Formal analysis, Methodology, Software, Writing – original draft, Writing – review & editing. YZ: Conceptualization, Writing – original draft, Writing – review & editing. B-RL: Conceptualization, Writing – original draft, Writing – review & editing. Y-YJ: Writing – review & editing. JZ: Writing – review & editing. NC: Software, Writing – review & editing. LY: Software, Writing – review & editing.

Funding

The author(s) declare financial support was received for the research, authorship, and/or publication of this article. Financial support from the 2022 Ningde City Natural Science Foundation (health field), China, Grant/Award Number: 2022J54.

Acknowledgments

We express our gratitude to the staff of the Department of Clinical Laboratory, Fuding Hospital, Fujian University of Traditional Chinese Medicine for their dedication and assistance in data collection and analysis.

Conflict of interest

The authors declare that the research was conducted in the absence of any commercial or financial relationships that could be construed as a potential conflict of interest.

Publisher's note

References

Agnello, L., Giglio, R. V., Bivona, G., Scazzone, C., Gambino, C. M., Iacona, A., et al. (2021). The value of a complete blood count (CBC) for sepsis diagnosis and prognosis. *Diagn. (Basel. Switzerland).* 11:1–19. doi: 10.3390/diagnostics11101881

Berhane, M., Melku, M., Amsalu, A., Enawgaw, B., Getaneh, Z., and Asrie, F. (2019). The role of neutrophil to lymphocyte count ratio in the differential diagnosis of pulmonary tuberculosis and bacterial community-acquired pneumonia: a cross-sectional study at ayder and mekelle hospitals, Ethiopia. *Clin. Lab.* 65. doi: 10.7754/Clin.Lab.2018.180833

Bonnet, E., Maulin, L., Senneville, E., Castan, B., Fourcade, C., Loubet, P., et al. (2024). Clinical practice recommendations for infectious disease management of diabetic foot infection (DFI)–2023 SPILF. *Infect. Dis. Now.* 54, 104832. doi: 10.1016/j.idnow.2023.104832

Bonten, M., Johnson, J. R., van den Biggelaar, A. H. J., Georgalis, L., Geurtsen, J., de Palacios, P. I., et al. (2021). Epidemiology of escherichia coli bacteremia: A systematic literature review. *Clin. Infect. Dis.* 72, 1211–1219. doi: 10.1093/cid/ciaa210

Dambroso-Altafini, D., Menegucci, T. C., Costa, B. B., Moreira, R. R. B., Nishiyama, S. A. B., Mazucheli, J., et al. (2022). Routine laboratory biomarkers used to predict Gram-positive or Gram-negative bacteria involved in bloodstream infections. *Sci. Rep.* 12, 15466. doi: 10.1038/s41598-022-19643-1

Evans, L., Rhodes, A., Alhazzani, W., Antonelli, M., Coopersmith, C. M., French, C., et al. (2021). Surviving sepsis campaign: international guidelines for management of sepsis and septic shock 2021. *Intensive Care Med.* 47, 1181–1247. doi: 10.1007/s00134-021-06506-y

Fay, K., Sapiano, M. R. P., Gokhale, R., Dantes, R., Thompson, N., Katz, D. E., et al. (2020). Assessment of health care exposures and outcomes in adult patients with sepsis and septic shock. *JAMA Netw. Open* 3, e206004. doi: 10.1001/jamanetworkopen.2020.6004

Fernando, S. M., Rochwerg, B., and Seely, A. J. E. (2018). Clinical implications of the third international consensus definitions for sepsis and septic shock (Sepsis-3). *Cmaj* 190, E1058–e1059. doi: 10.1503/cmaj.170149

Font, M. D., Thyagarajan, B., and Khanna, A. K. (2020). Sepsis and Septic Shock - Basics of diagnosis, pathophysiology and clinical decision making. *Med. Clin. North Am.* 104, 573–585. doi: 10.1016/j.mcna.2020.02.011

Fu, Y., Zhao, F., Lin, J., Li, P., and Yu, Y. (2024). Antibiotic susceptibility patterns and trends of the gram-negative bacteria isolated from the patients in the emergency departments in China: results of SMART 2016-2019. *BMC Infect. Dis.* 24, 501. doi: 10.1186/s12879-024-09294-0

Gatica, S., Fuentes, B., Rivera-Asín, E., Ramírez-Céspedes, P., Sepúlveda-Alfaro, J., Catalán, E. A., et al. (2023). Novel evidence on sepsis-inducing pathogens: from laboratory to bedside. *Front. Microbiol.* 14, 1198200. doi: 10.3389/fmicb.2023.1198200

Guarino, M., Perna, B., Cesaro, A. E., Maritati, M., Spampinato, M. D., Contini, C., et al. (2023). 2023 update on sepsis and septic shock in adult patients: management in the emergency department. *J. Clin. Med.* 12, 3188. doi: 10.3390/jcm12093188

Hernández-Quiles, R., Merino-Lucas, E., Boix, V., Fernández-Gil, A., Rodríguez-Díaz, J. C., Gimeno, A., et al. (2022). Bacteraemia and quick Sepsis Related Organ Failure Assessment (qSOFA) are independent risk factors for long-term mortality in very elderly patients with suspected infection: retrospective cohort study. *BMC Infect. Dis.* 22, 248. doi: 10.1186/s12879-022-07242-4

Jackson, L. A., Benson, P., Neuzil, K. M., Grandjean, M., and Marino, J. L. (2005). Burden of community-onset escherichia coli bacteremia in seniors. *J. Infect. Dis.* 191, 1523–1529. doi: 10.1086/jid.2005.191.issue-9

Jain, K., Sharma, D., Patidar, M., Nandedkar, S., Pathak, A., and Purohit, M. (2022). Red cell distribution width as a predictor of mortality in patients with clinical sepsis: experience from a single rural center in central India. *Clin. Pathol.* 15, 2632010x221075592. doi: 10.1177/2632010X221075592

Jirak, P., Haertel, F., Mirna, M., Rezar, R., Lichtenauer, M., Paar, V., et al. (2022). A comparative analysis of novel biomarkers in sepsis and cardiovascular disease. *Appl. Sci.* 12, 1419. doi: 10.3390/app12031419

Li, B. R., Zhuo, Y., Jiang, Y. Y., and Zhang, S. Y. (2024). Random forest differentiation of Escherichia coli in elderly sepsis using biomarkers and infectious sites. *Sci. Rep.* 14, 12973. doi: 10.1038/s41598-024-63944-6

Liu, L., Fu, Q., Zhang, D., Chen, D., Wang, F., Guo, R., et al. (2023). Analysis of mean corpuscular volume and red cell distribution width in patients with aplastic anemia. *Hemoglobin*. 47, 31–35. doi: 10.1080/03630269.2023.2206575

Matono, T., Yoshida, M., Koga, H., and Akinaga, R. (2022). Diagnostic accuracy of quick SOFA score and inflammatory biomarkers for predicting community-onset bacteremia. *Sci. Rep.* 12, 11121. doi: 10.1038/s41598-022-15408-y

Plasencia, J. T., and Ashraf, M. S. (2024). Management of bacteriuria and urinary tract infections in the older adult. *Urol. Clin. North Am.* 51, 585–594. doi: 10.1016/j.ucl.2024.07.002

Poolman, J. T., and Wacker, M. (2016). Extraintestinal pathogenic escherichia coli, a common human pathogen: challenges for vaccine development and progress in the field. *J. Infect. Dis.* 213, 6–13. doi: 10.1093/infdis/jiv429

Tao, Y. L., Wang, J. R., Liu, M., Liu, Y. N., Zhang, J. Q., Zhou, Y. J., et al. (2024). Progress in the study of the correlation between sepsis and intestinal microecology. *Front. Cell Infect. Microbiol.* 14, 1357178. doi: 10.3389/fcimb.2024.1357178

Tocut, M., Zohar, I., Schwartz, O., Yossepowitch, O., and Maor, Y. (2022). Short- and long-term mortality in patients with urosepsis caused by Escherichia coli susceptible and resistant to 3rd generation cephalosporins. *BMC Infect. Dis.* 22, 571. doi: 10.1186/s12879-022-07538-5

Wu, H., Li, M., Shou, C., Shi, F., Song, X., Hu, Q., et al. (2024). Pathogenic spectrum and drug resistance of bloodstream infection in patients with acute myeloid leukaemia: a single centre retrospective study. *Front. Cell Infect. Microbiol.* 14, 1390053. doi: 10.3389/fcimb.2024.1390053

Wu, Y., Wang, G., Huang, Z., Yang, B., Yang, T., Liu, J., et al. (2023). Diagnostic and therapeutic value of biomarkers in urosepsis. *Ther. Adv. Urol.* 15, 17562872231151852. doi: 10.1177/17562872231151852

Xu, X., Wang, Y., Tao, Y., Dang, W., Yang, B., and Li, Y. (2024). The role of platelets in sepsis: A review. *Biomol. Biomed.* 24, 741–752. doi: 10.17305/bb.2023.10135

Zhan, Z. S., Shi, J., Zheng, Z. S., Zhu, X. X., Chen, J., Zhou, X. Y., et al. (2024). Epidemiological insights into seasonal, sex–specific and age–related distribution of bacterial pathogens in urinary tract infections. *Exp. Ther. Med.* 27, 140. doi: 10.3892/etm.2024.12428

frontiers | Frontiers in Cellular and Infection Microbiology

TYPE Original Research
PUBLISHED 18 February 2025
DOI 10.3389/fcimb.2025.1483503

OPEN ACCESS

EDITED BY
José Luis Muñoz-Carrillo,
University of Guadalajara, Mexico

REVIEWED BY
Matthew Gavino Donadu,
University of Sassari, Italy
Victor Asensi,
University of Oviedo, Spain

*CORRESPONDENCE
Tao Li
qdult@qdu.edu.cn
Ying-ze Zhang
yzling_liu@163.com

RECEIVED 20 August 2024
ACCEPTED 23 January 2025
PUBLISHED 18 February 2025

CITATION
Shi W-p, Jiang Y-p, Wu T-y, Wang Y-z, Zhang Y-z and Li T (2025) Does obesity affect the diagnostic value of various biomarkers for periprosthetic joint infections? A single center retrospective study. *Front. Cell. Infect. Microbiol.* 15:1483503. doi: 10.3389/fcimb.2025.1483503

Does obesity affect the diagnostic value of various biomarkers for periprosthetic joint infections? A single center retrospective study

Wei-peng Shi[1], Ya-ping Jiang[2], Ting-yu Wu[1], Ying-zhen Wang[1], Ying-ze Zhang[1,3]* and Tao Li[1]*

[1]Department of Orthopaedic Surgery, The Affiliated Hospital of Qingdao University, Qingdao, China,
[2]Department of Oral Implantology, The Affiliated Hospital of Qingdao University, Qingdao, China,
[3]Department of Orthopaedics, The Third Hospital of Hebei Medical University, Shijiazhuang, China

Objective: The aim of this study was to examine the impact of obesity on the diagnosis of periprosthetic joint infections (PJI) by assessing the levels and diagnostic efficacy of biomarkers.

Methods: A total of 254 patients were divided into obese group (n=59) and non-obese group (n=195) according to BMI. Each group was further divided into the PJI group and the AF group. Data on CRP, ESR, fibrinogen, D-dimer, CRP-albumin ratio (CAR), CRP-lymphocyte ratio (CLR), and CRP-monocyte ratio (CMR) were collected from all patients. ROC curve was performed to evaluate the diagnostic values of these biomarkers.

Results: The levels of biomarkers were significantly higher in PJI patients compared to the AF patients in both the obese and non-obese groups ($P < 0.001$), but the levels of biomarkers were similar between the obese and non-obese groups. In the obese group, CRP exhibited the highest diagnostic value (AUC=0.982). In the non-obese group, CAR demonstrated the highest diagnostic value (AUC =0.935). Subgroup analysis showed no significant differences in biomarker levels ($P > 0.05$).

Conclusions: Obesity did not affect biomarker levels in patients with PJI. But for obese patients, the diagnostic thresholds for CRP and ESR are higher, and clinical diagnosis should be careful to avoid false positives. CRP and CAR were identified as the most effective biomarkers for diagnosing PJI in the obese and non-obese groups, respectively.

KEYWORDS

obesity, periprosthetic joint infection, CRP, CAR, ESR

Introduction

With the global population increasing and population aging progressing, the number of total joint arthroplasties (TJAs) is expected to surpass 4 million per year in the UK and the United States by 2030 (Kapadia et al., 2016). TJA is a common treatment for end-stage osteoarthritis, effectively reducing pain and promoting joint function recovery. However, periprosthetic joint infection (PJI), although rare with an incidence of only 0.5-2% (Whitehouse et al., 2016; Gundtoft et al., 2017; Koh et al., 2017), poses a severe and devastating complication following TJA, imposing significant burdens on patients and society both in terms of health and economic impact. The incidence of PJI is projected to rise due to the increasing prevalence of obesity, diabetes, and other comorbidities (Kapadia et al., 2016). Numerous studies have already demonstrated that obesity/morbid obesity is a significant risk factor for TJA failure (Houdek et al., 2015; Watts et al., 2015; Kapadia et al., 2016; Roth et al., 2019).

Since the 1980s, the body mass index (BMI) and obesity rates among the Chinese population have been steadily increasing (Wang et al., 2021). Obesity not only serves as a significant risk factor for cardiovascular and kidney diseases (Wang et al., 2021) but also impacts the levels of various serum inflammatory biomarkers (Cohen et al., 2021). Adipose cells play a role in synthesizing the pro-inflammatory cytokine IL-6, which subsequently leads to increased production of C-reactive protein (CRP) by the liver (Laaksonen et al., 2004; Cohen et al., 2021). Obese individuals have been found to exhibit higher levels of fibrinogen compared to those with normal body weight, with an increase of 93.5 mg/dl (95% CI, 72.9-114.1) based on reference values from individuals with normal body weight (Nguyen et al., 2009). Leff et al. have discovered that obese patients who exceed their ideal weight by 45 kg exhibit significantly higher average erythrocyte sedimentation rates (ESR) compared to patients with normal weight (17 mm/h vs. 4 mm/h, P=0.015) (Leff and Akre, 1986). PJI and aseptic failure (AF) share certain clinical symptoms, such as pain and joint swelling. Therefore, accurately distinguishing between PJI and AF holds crucial importance for guiding targeted treatments in the future. PET-CT is an important tool for diagnosing PJI, and whole-body PET/CT may detect other infectious lesions, which can have an impact on subsequent treatment strategies (Roschke et al., 2021). A study reported abnormalities in 99mTC labeled scintigraphy in patients with early prosthetic infections, but the study did not discuss the low specificity of the test (Matthews et al., 2009). However, these technological methods are expensive and difficult to widely use in primary hospitals. There is currently a lack of research regarding the impact of obesity on the levels of various biomarkers and the diagnostic capability for PJI patients. Hence, our study aimed to incorporate the CAR, CLR, and the newly introduced CMR alongside traditional biomarkers (CRP and ESR) and fibrinolytic biomarkers (fibrinogen and D-dimer), all of which have demonstrated promising diagnostic value in previous studies conducted by our research team (Shi et al., 2022; Shi et al., 2023) and by others (Pevzner et al., 2011).

The primary research objectives of this study were as follows: (1) to investigate the impact of obesity on the levels of serum inflammatory biomarkers in PJI patients; (2) to determine the optimal diagnostic biomarkers for PJI patients in both the obese and non-obese groups; (3) to explore the possibility of identifying an ideal biomarker that could be universally applied to both groups of patients; (4) and to assess the diagnostic value of various biomarkers in subgroup analyses of obese and non-obese patients.

By addressing these objectives, we aimed to enhance our understanding of the relationship between obesity and serum inflammatory biomarkers in PJI patients, identify effective diagnostic biomarkers tailored to the specific needs of obese and non-obese patients, and evaluate the diagnostic performance of these biomarkers within subgroups.

Methods

Study population

This single-center retrospective study was conducted in accordance with the principles outlined in the Declaration of Helsinki. Approval for the study was obtained from the Institutional Review Board (IRB) of the Affiliated Hospital of Qingdao University. Data were collected from the electronic case system of patients who underwent total knee or hip revision surgery at our institution between June 2013 and April 2023. To ensure accuracy, certain exclusion criteria were applied. Patients with periprosthetic fractures and dislocation were initially excluded. Additionally, patients with the following conditions were excluded from the study: (1) malignant tumors; (2) hematological diseases (thrombocytopenia, thrombosis, etc.); (3) autoimmune diseases (rheumatoid arthritis, systemic lupus erythematosus, ankylosing spondylitis, etc.); (4) infections in other body parts; (5) recent use of anticoagulants or antibiotics; and (6) missing data. After the screening process, a total of 254 patients were included in the final analysis. Considering that all patients were of Chinese descent, those with a BMI greater than 28 kg/m^2 were classified as obese, while the remaining patients were classified as non-obese. Following the criteria set forth by the 2018 International Consensus Conference (ICM) (Parvizi et al., 2018), each patient group was further divided into the PJI group and the AF group.

Data extraction

The baseline data for all the included patients primarily consisted of age, gender, height, weight, and the affected joints. On the day of admission or early morning of the following day, a specialist nurse collected fasting venous blood samples from the patients, which were then promptly sent to the laboratory for testing within 1 hour. The collected blood samples were used to measure serum levels of CRP, ESR, neutrophils, lymphocytes, monocytes, and albumin. Additionally, relevant biomarker ratios were

calculated based on these measurements. Moreover, in order to further improve the accuracy of diagnosis, during the surgical procedure, synovial fluid or pus samples were obtained from patients who were either suspected or confirmed to have PJI. These samples were subjected to culture under both aerobic and anaerobic conditions. Concurrently, histopathological examinations were conducted on the tissues or bones surrounding the prosthesis.

Statistical analyses

All statistical analyses in this study were performed using SPSS version 26.0 (IBM Inc., Armonk, NY, USA). Continuous variables were presented as mean ± standard deviation (SD), while categorical variables were expressed as percentages (%). Student's t-test was employed to compare normally distributed continuous variables between two groups, whereas the Mann-Whitney U test was used for non-normally distributed continuous variables. The chi-square test was applied to analyze categorical variables. Statistical significance was defined as P<0.05. Receiver operating characteristic (ROC) curves were constructed to calculate the area under the curve (AUC) for each biomarker, determining their diagnostic value. The 95% confidence intervals (CI), sensitivity, specificity, positive predictive value (PPV), and negative predictive value (NPV) were also calculated based on the Youden index. The diagnostic value of each biomarker was categorized into five levels based on the AUC: excellent (0.900-1.000), good (0.800-0.899), fair (0.700-0.799), poor (0.600-0.699), and no diagnostic ability (0.500-0.599). All figures were generated using GraphPad Prism 8.0.2 (GraphPad Software Inc., San Diego, CA, USA).

Results

Demographic characteristics of obese and non-obese patients

A total of 254 patients were included in the study, comprising 59 obese patients and 195 non-obese patients. The results indicated that the obese group had a higher proportion of PJI patients compared to the non-obese group, suggesting that obesity was indeed a risk factor for PJI. There were no significant differences in age and gender distribution between the PJI and AF groups, regardless of whether patients were obese or non-obese (P>0.05). In the obese group, a statistically higher proportion of patients with knee infections (p=0.023), whereas in the non-obese group, the proportions of knee and hip joint infections were similar (Table 1).

Comparison of the levels of biomarkers in the obese and non-obese patients

Compared with the AF group, the PJI group showed significantly elevated serum levels and ratios of various biomarkers (CAR, CLR, and CMR) in both the obese and non-obese groups (P<0.001). Detailed results can be found in Table 2 and Figures 1, 2.

In the obese group, the AUC (95% CI) values for the seven biomarkers were as follows: CRP - 0.982 (0.945, 1.000), fibrinogen - 0.858 (0.755, 0.961), D-dimer - 0.830 (0.727, 0.934), ESR - 0.928 (0.865, 1.000), CAR - 0.978 (0.940, 1.000), CLR- 0.973 (0.933, 1.000), and CMR - 0.959 (0.911, 1.000). CRP exhibited the highest diagnostic value, with an optimal cutoff value of 8.38, a sensitivity of 96.6%, and a specificity of 100.0%. CAR had the second-highest diagnostic value, with an optimal cutoff value of 0.26, a sensitivity of 89.7%, and a specificity of 100.0%. Based on a further calculation using the Youden index, the PPV for the seven biomarkers or ratios was 100.0%, 85.7%, 80.0%, 95.3%, 100.0%, 96.6%, and 93.3%, respectively. The NPV was 96.7%, 80.7%, 71.9%, 80.0%, 90.6%, 93.3%, and 93.1%, respectively (Table 3; Figure 3A).

In the non-obese group, the ROC analysis indicated that CAR had the highest diagnostic value for PJI with an AUC of 0.935 (95% CI: 0.894, 0.977), followed by CRP with an AUC of 0.932 (95% CI: 0.889, 0.975). The subsequent biomarkers in terms of diagnostic value were CLR (AUC=0.929, 95% CI: 0.866, 0.973), CMR (AUC=0.918, 95% CI: 0.872, 0.965), ESR (AUC=0.914, 95% CI: 0.872, 0.956), fibrinogen (AUC=0.892, 95% CI: 0.843, 0.940), and D-dimer (AUC=0.769, 95% CI: 0.690, 0.847) (Table 3; Figure 3B).

Two important findings should be noted. Firstly, the optimal cutoff values of the two traditional biomarkers (CRP and ESR) were higher in the obese group compared to the non-obese group (8.38

TABLE 1 Demographic characteristics of obesity and non-obesity patients.

	Obese		P value	Non-obese		P value
	PJI (n=30)	AF (n=29)		PJI (n=61)	AF (n=134)	
Age(y)	64.40 ± 9.85	65.34 ± 8.12	0.689	64.98 ± 8.62	65.32 ± 9.77	0.825
Gender (female, %)	16 (53.33)	17 (58.62)	0.683	31 (50.82)	70 (52.24)	0.854
Joint			<0.001			<0.001
Knee	24	8		27	27	
Hip	6	29		34	107	

PJI, periprosthetic joint infections, AF, aseptic failure.

TABLE 2 Comparison of the levels of biomarkers in the obesity and non-obesity patients.

	Obese		P value	Non-obese		P value
	PJI (n=30)	AF (n=29)		PJI (n=61)	AF (n=134)	
CRP (mg/L)	35.98 ± 35.80	2.95 ± 2.49	<0.001	44.91 ± 54.08	3.54 ± 5.15	<0.001
Fibrinogen(g/L)	4.75 ± 1.29	3.16 ± 0.73	<0.001	4.83 ± 1.55	3.04 ± 0.85	<0.001
D-dimer(ng/mL)	1137.59 ± 771.08	461.43 ± 266.77	<0.001	1177.64 ± 1025.90	500.12 ± 299.30	<0.001
ESR (mm/h)	49.84 ± 27.46	11.57 ± 8.42	<0.001	45.20 ± 25.07	13.52 ± 11.06	<0.001
CAR	1.16 ± 1.43	0.07 ± 0.07	<0.001	1.31 ± 1.61	0.09 ± 0.15	<0.001
CLR	35.04 ± 61.47	1.74 ± 1.76	<0.001	34.10 ± 52.81	2.32 ± 5.53	<0.001
CMR	60.72 ± 52.11	6.89 ± 6.71	<0.001	77.61 ± 129.47	9.78 ± 26.25	<0.001

CRP, C-reactive protein, ESR, erythrocyte sedimentation rate, CAR, CRP-albumin ratio, CLR, CRP-lymphocyte ratio, CMR, CRP-monocyte ratio.

vs. 7.36 for CRP; 29.00 vs. 16.95 for ESR). This finding suggested that obesity could affect the diagnostic thresholds for CRP and ESR in PJI. Secondly, D-dimer showed the lowest sensitivity and poor specificity in both the obese and non-obese groups.

Comparison of biomarkers in the subgroups

The subgroup analysis based on culture results, affected joints, and acute/chronic infections aimed to investigate whether various biomarkers still had diagnostic value in different situations within the obesity and non-obesity groups. The results indicated that there were relative differences in the levels of various biomarkers in each subgroup, regardless of obesity status. However, these differences were not statistically significant (P>0.05), suggesting that the diagnostic value of the biomarkers might not vary significantly across different subgroups (Table 4).

Discussion

We conducted a comprehensive comparison of the diagnostic value of traditional inflammatory biomarkers (CRP and ESR), fibrinolytic biomarkers (fibrinogen and D-dimer), and previously established biomarkers (CAR, CLR, and CMR) in PJI patients, considering their obesity status. Our study findings revealed that the levels of serum inflammatory markers in obese PJI patients did not show a significant increase compared to the AF group. Among all biomarkers, CRP and CAR emerged as the most effective indicators for diagnosing PJI in obese and non-obese patients, respectively. Notably, the optimal cutoff value for CRP was higher in the obese group than in the non-obese group, while no significant difference was observed in CAR between the two groups. These results highlighted the importance of considering patients' BMI when using CRP as a diagnostic indicator for PJI to avoid false positive results. Furthermore, it is noteworthy that all biomarkers performed poorly in subgroup analyses of obese and non-obese patients, indicating limited diagnostic ability in these specific populations.

CRP, as a widely studied traditional inflammatory biomarker, is known to be an acute-phase protein synthesized by liver cells in response to inflammation triggered by various factors, such as infection or obesity. Recent research has highlighted the complex relationship between obesity and chronic inflammation, with studies such as demonstrating that elevated CRP levels are not only indicative of acute infections but also reflect chronic inflammatory states associated with obesity. These findings further underscore the importance of developing tailored diagnostic thresholds for obese patients (Marongiu et al., 2020). Previous studies have demonstrated a positive association between CRP concentration and increasing BMI. For instance, Nguyen et al. have observed that as BMI increases, CRP concentration rises from 0.11 ± 0.03 mg/dl to 0.73 ± 0.09 mg/dl, with the strongest association seen in individuals with a BMI > 40 kg/m^2 (Nguyen et al., 2009). Similarly, Visser et al. have reported elevated odds ratios (OR) for elevated CRP in obese males (OR: 2.13, 95% CI: 1.56-2.91) and females (OR: 6.21, 95% CI: 4.94-7.81) (Visser et al., 1999). Cohen et al. have also demonstrated significantly increased OR for elevated CRP across all BMI groups compared to individuals with normal BMI, irrespective of gender (Houdek et al., 2015). Furthermore, ESR levels have been found to be elevated in obese patients (Houdek et al., 2015). Given this existing research, it would be reasonable to expect higher CRP and ESR levels in obese PJI patients compared to non-obese PJI patients.

Probasco and his colleagues found that elevated CRP and ESR levels in preoperative inflammation are positively correlated with BMI, and they believed that traditional biomarkers should be used with caution in the diagnosis of obesity PJI (Probasco et al., 2020). However, in our study, we did not observe a significant difference in CRP and ESR levels between the obese and non-obese groups. Several factors may contribute to these unexpected findings. Firstly, obesity is characterized by chronic inflammation, and while inflammatory biomarkers may increase in obese patients, PJI represents a more acute and severe form of inflammation that can have a greater impact on markers like CRP and ESR. Secondly, the sample size of obese PJI patients in our study was relatively small compared to previous studies, which may have introduced greater variability and potential errors. Future large-scale research is

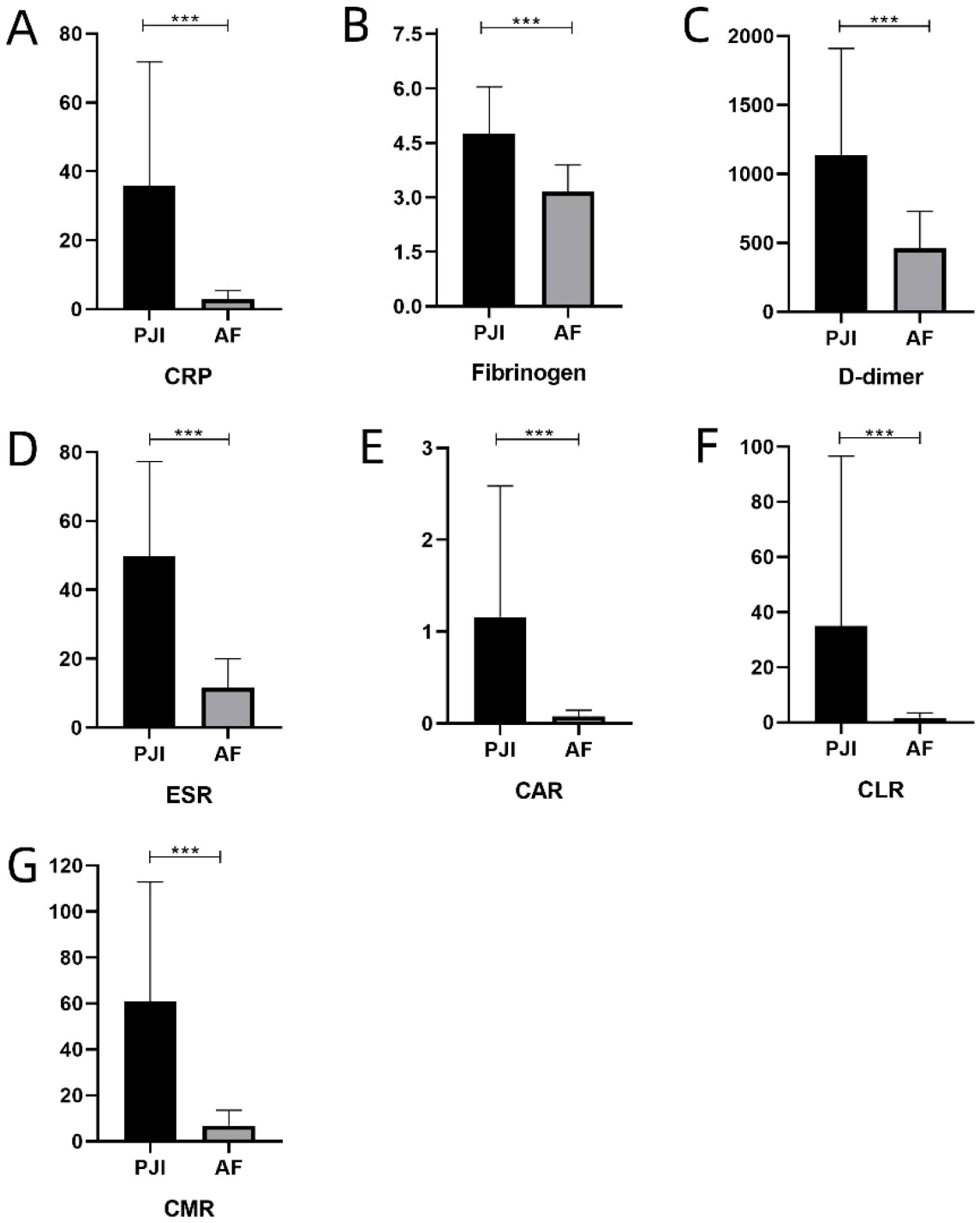

FIGURE 1
(A-G) represents the levels of various serum inflammatory biomarkers in obese patients, respectively. C-reactive protein, ESR, erythrocyte sedimentation rate, CAR, CRP-albumin ratio, CLR, CRP-lymphocyte ratio, CMR, CRP-monocyte ratio. ***: P<0.001.

needed to confirm these conclusions regarding inflammation. Additionally, it is important to consider that BMI is influenced by race (Issa et al., 2014), and variations in grouping criteria can also lead to discrepancies in results.

While the levels of CRP and ESR in obese PJI patients were not found to be significantly higher than those in non-obese groups, this study identified higher optimal cutoff values for diagnosing PJI using CRP and ESR. Moreover, both sensitivity and specificity were higher compared to our previous studies (Shi et al., 2021). Although these results should be interpreted cautiously due to the limited sample size, they indicated that traditional biomarkers still held considerable diagnostic value in

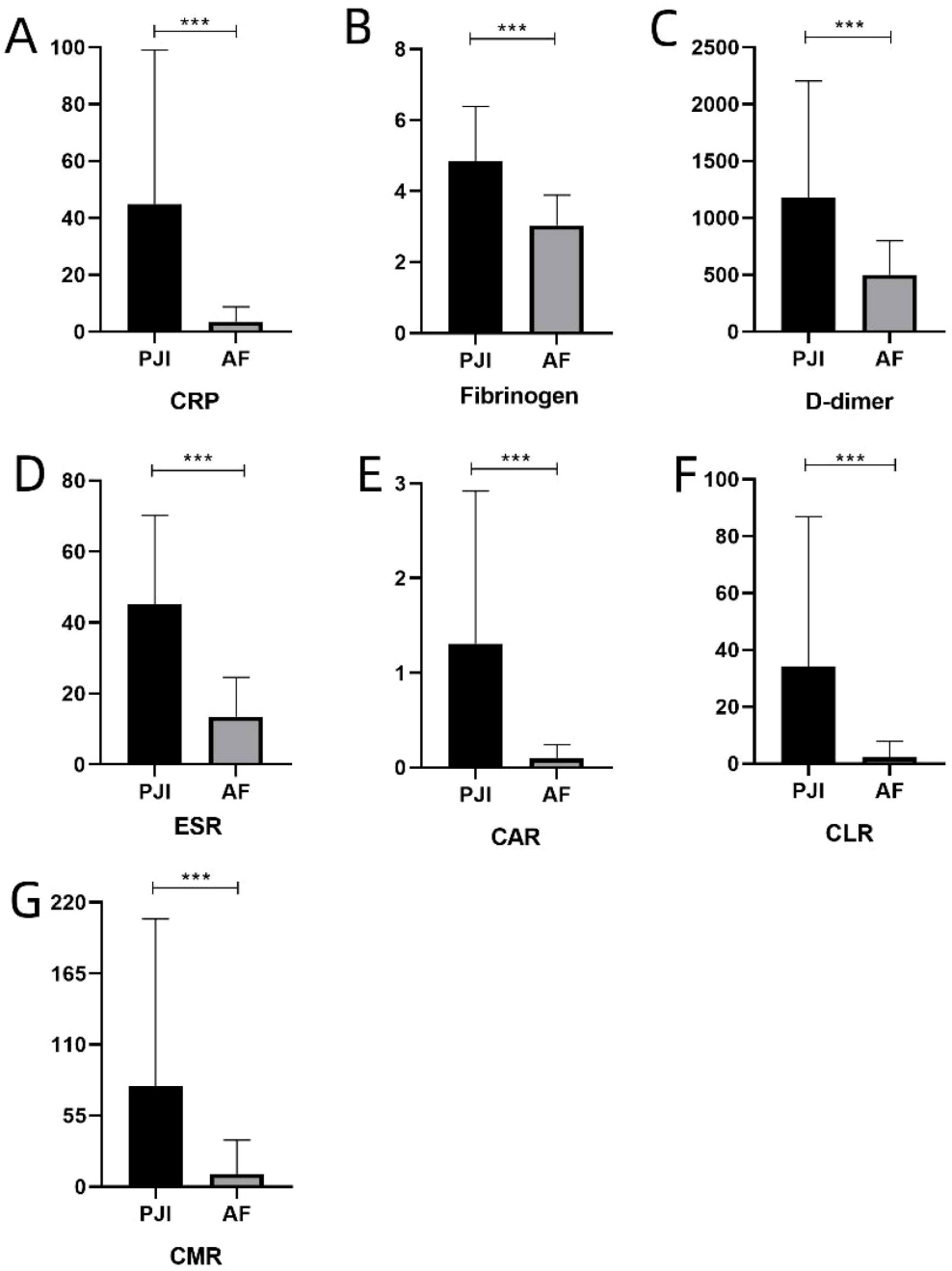

FIGURE 2
(A-G) represents the levels of various serum inflammatory biomarkers in non-obese patients, respectively. C-reactive protein, ESR, erythrocyte sedimentation rate, CAR, CRP-albumin ratio, CLR, CRP-lymphocyte ratio, CMR, CRP-monocyte ratio. ***: P<0.001.

obese PJI patients. Currently, clinical practice does not differentiate between obese and non-obese PJI patients, and using lower cutoff values for CRP and ESR may result in the overtreatment of obese individuals. On the other hand, the CAR, which is previously discovered in our study, demonstrated good performance in both obese and non-obese PJI patients. Importantly, there was no significant difference in the optimal cutoff value between the two patient groups. Thus, we recommend considering the correlation between CRP and CAR to enhance the accuracy of PJI diagnosis.

A recent study has highlighted that hip and knee infections are distinct issues. Specifically, in obese and severely obese patients with hip infection, higher rates of polymicrobial infection and Enterococcus are observed, while severely obese patients show a

10.3389/fcimb.2025.1483503

TABLE 3 The diagnostic value of biomarkers in the obese and non-obese PJI patients.

	Obese							
	AUC	95%CI	Youden index	Optimal cutoff value	Sensitivity (%)	Specificity (%)	PPV (%)	NPV (%)
CRP (mg/L)	0.982	(0.945,1.000)	0.966	8.38	96.6	100.0	100.0	96.7
Fibrinogen (g/L)	0.858	(0.755,0.961)	0.720	3.73	82.8	89.3	85.7	80.7
D-dimer (ng/mL)	0.830	(0.727,0.934)	0.511	690.00	69.0	82.1	80.0	71.9
ESR (mm/h)	0.928	(0.865,1.000)	0.723	29.00	75.9	96.4	95.3	80.0
CAR	0.978	(0.940,1.000)	0.897	0.26	89.7	100.0	100.0	90.6
CLR	0.973	(0.933,1.000)	0.895	5.46	93.1	96.4	96.6	93.3
CMR	0.959	(0.911,1.000)	0.860	17.63	93.1	92.9	93.3	93.1
	Non-obese							
	AUC	95%CI	Youden index	Optimal cutoff value	Sensitivity (%)	Specificity (%)	PPV (%)	NPV (%)
CRP (mg/L)	0.932	(0.889,0.975)	0.733	7.36	83.3	90.0	76.1	92.2
Fibrinogen (g/L)	0.892	(0.843,0.940)	0.649	3.36	90.7	74.2	60.0	93.3
D-dimer (ng/mL)	0.769	(0.690,0.847)	0.411	685.00	61.1	80.0	55.9	82.1
ESR (mm/h)	0.914	(0.872,0.956)	0.703	16.95	94.4	75.8	65.1	96.0
CAR	0.935	(0.894,0.977)	0.748	0.27	81.5	93.3	83.3	91.9

CRP, C-reactive protein, ESR, erythrocyte sedimentation rate, CAR, CRP-albumin ratio, CLR, CRP-lymphocyte ratio, CMR, CRP-monocyte ratio, PPV, positive predictive value, NPV, negative predictive value.

higher incidence of Gram-negative infections. However, this phenomenon is not observed in knee infections (Lowik et al., 2019). The underlying reason may be attributed to the increase in bacterial colonization on the hip skin, particularly in the groin, as BMI rises (OR=1.15, 95% CI: 1.03-1.29, P=0.01) (Boni et al., 2018). Conversely, in our present study, we observed a higher proportion of knee infections in the obese group. We speculated that this could be due to the hip joint's proximity to the perineum, leading to more meticulous disinfection by medical professionals. Additionally, the knee joint is more exposed and poses an increased risk of postoperative infection. Another contributing factor could be the small sample size and inherent data biases, which may have resulted in contradictory outcomes.

Furthermore, another study has proposed that obese PJI patients (BMI > 35 kg/m^2) exhibit a higher rate of positive intraoperative cultures, likely due to challenges in disinfection and lower tissue

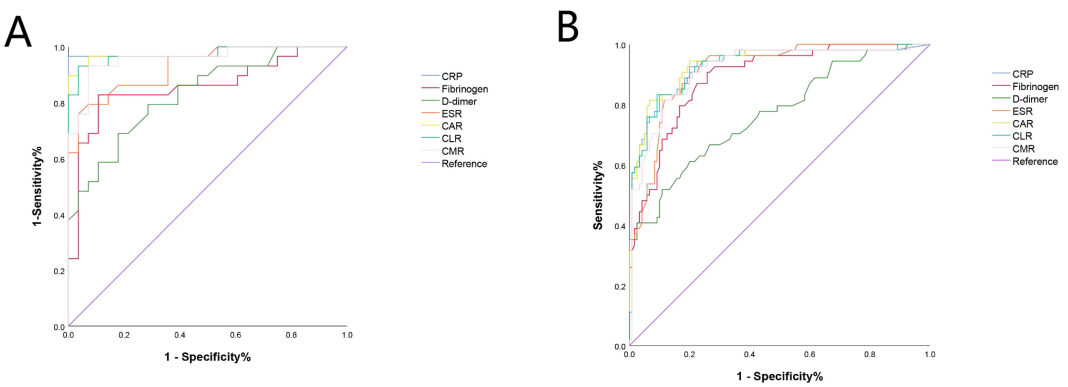

FIGURE 3
The ROC of CRP, Fibrinogen, D-dimer, ESR, CAR, CLR and CMR in obese and non-obese patients. **(A)** In the obese group, the ROC analysis indicated that CRP had the highest diagnostic value for PJI with an AUC of 0.982, followed by CAR with an AUC of 0.978. **(B)** In the non-obese group, the ROC analysis indicated that CAR had the highest diagnostic value for PJI with an AUC of 0.935, followed by CRP with an AUC of 0.932. CRP, C-reactive protein, ESR, erythrocyte sedimentation rate, CAR, CRP-albumin ratio, CLR, CRP-lymphocyte ratio, CMR, CRP-monocyte ratio.

10.3389/fcimb.2025.1483503

TABLE 4 Comparison of biomarkers in the obese and non-obese PJI subgroups.

	Obese								
	Culture positive PJI (n=21)	Culture negative PJI (n=9)	P value	Acute PJI (n=3)	Chronic PJI (n=27)	P value	Knee PJI (n=24)	Hip PJI (n=6)	P value
CRP (mg/L)	35.81 ± 38.15	36.78 ± 31.74	0.967	24.27 ± 10.45	37.28 ± 37.46	0.196	35.81 ± 32.20	36.68 ± 51.60	0.970
Fibrinogen(g/L)	4.74 ± 1.05	4.79 ± 1.81	0.935	4.29 ± 0.60	4.80 ± 1.34	0.292	4.75 ± 1.18	4.76 ± 1.79	0.997
D-dimer (ng/mL)	1262.00 ± 846.11	861.11 ± 505.98	0.127	1553.33 ± 1938.10	1089.62 ± 585.04	0.719	1231.30 ± 823.74	778.33 ± 385.61	0.068
ESR (mm/h)	50.21 ± 27.48	49.00 ± 29.05	0.917	36.03 ± 12.22	51.38 ± 28.37	0.146	51.01 ± 26.74	45.18 ± 32.43	0.697
CAR	1.15 ± 1.55	1.17 ± 1.16	0.982	0.62 ± 0.31	1.21 ± 1.49	0.094	1.07 ± 1.06	1.51 ± 2.55	0.697
CLR	34.38 ± 68.70	36.60 ± 43.51	0.916	15.00 ± 10.91	37.27 ± 64.45	0.124	37.83 ± 66.61	23.90 ± 36.35	0.500
CMR	62.21 ± 57.00	57.24 ± 41.28	0.792	52.13 ± 29.70	61.67 ± 54.35	0.661	65.50 ± 55.44	41.59 ± 32.64	0.194
	Non-obese								
	Culture positive PJI(n=42)	Culture negative PJI (n=19)	P value	Acute PJI (n=8)	Chronic PJI (n=53)	P value	Knee PJI (n=27)	Hip PJI (n=34)	P value
	51.56 ± 57.96	30.23 ± 42.03	0.111	44.98 ± 53.53	44.90 ± 54.67	0.997	41.27 ± 55.62	47.45 ± 53.52	0.686
	4.93 ± 1.62	4.61 ± 1.39	0.428	5.09 ± 1.10	4.79 ± 1.61	0.523	4.65 ± 1.78	4.97 ± 1.35	0.448
	1129.21 ± 921.81	1285.88 ± 1252.62	0.648	1082.86 ± 962.56	1191.46 ± 1043.75	0.790	1400.00 ± 1325.37	1029.39 ± 752.75	0.243
	45.55 ± 26.41	44.44 ± 22.55	0.867	48.09 ± 23.88	44.75 ± 25.44	0.724	45.73 ± 26.58	44.76 ± 24.16	0.885

CRP, C-reactive protein, ESR, erythrocyte sedimentation rate, CAR, CRP-albumin ratio, CLR, CRP-lymphocyte ratio, CMR, CRP-monocyte ratio, PJI, periprosthetic joint infections, AF, aseptic failure.

concentration of cefazolin in obese individuals (Font-Vizcarra et al., 2011; Pevzner et al., 2011). In our present study, the culture-positive rate in the obese group was 70.0% (21/30), while it was 68.9% (42/61) in the non-obese group. However, it is important to note that our study was retrospective and unable to accurately determine whether each patient received antibiotic treatment before surgery, unlike the prospective study that excludes patients who have received antibiotic treatment within 2 weeks prior to surgery. Therefore, confounding factors cannot be entirely excluded, potentially accounting for the different findings between the two studies.

Our study represented the first attempt to classify PJI patients based on BMI and assess the diagnostic value of traditional biomarkers, fibrinolytic biomarkers, and other inflammatory markers. However, it is crucial to acknowledge the limitations of this study. Firstly, it was a retrospective study conducted at a single center, which inevitably introduced inherent data biases. Secondly, the study focused on Chinese individuals, and racial differences may result in variations in the definition of "obesity." Therefore, further validation of our research findings is necessary for other ethnic populations. Thirdly, the lack of a gold standard for PJI diagnosis introduces the possibility of misclassification of patients. Fourthly, the sample size in our study, particularly for PJI patients in the obese group, was limited. Thus, larger sample sizes and prospective studies are needed to ensure the reliability of our conclusions.

Conclusions

In conclusion, among the biomarkers studied, CRP and CAR demonstrated the highest diagnostic value in the obese and non-obese groups, respectively. While the subgroup analysis did not yield optimal results, these findings do not diminish the promising potential of CRP and CAR as diagnostic biomarkers for PJI patients with varying BMI levels.

Data availability statement

The raw data supporting the conclusions of this article will be made available by the authors, without undue reservation.

Ethics statement

The studies involving humans were approved by Institutional Review Board (IRB) of The Affiliated Hospital of Qingdao University. The studies were conducted in accordance with the local legislation and institutional requirements. The participants provided their written informed consent to participate in this study. Written informed consent was obtained from the individual(s) for the publication of any potentially identifiable images or data included in this article.

Author contributions

W-PS: Data curation, Writing – original draft. Y-PJ: Data curation, Writing – review & editing. T-YW: Methodology, Writing – review & editing. Y-ZW: Project administration, Writing – review & editing. Y-ZZ: Conceptualization, Supervision, Writing – review & editing. TL: Project administration, Supervision, Validation, Writing – review & editing.

Funding

The author(s) declare financial support was received for the research, authorship, and/or publication of this article. National Natural Science Foundation of China; Grant number: 82272489, 82203588; TaiShan Scholars Project Special Fund; Grant number: NO. tsqn202306396; Qingdao Traditional Chinese Medicine Science and Technology Project; Grant number: 2021-zyym28; Science and technology Development Project of Shandong Geriatric Society; Grant number: LKJGG2021W082.

Conflict of interest

The authors declare that the research was conducted in the absence of any commercial or financial relationships that could be construed as a potential conflict of interest.

Publisher's note

All claims expressed in this article are solely those of the authors and do not necessarily represent those of their affiliated organizations, or those of the publisher, the editors and the reviewers. Any product that may be evaluated in this article, or claim that may be made by its manufacturer, is not guaranteed or endorsed by the publisher.

References

Boni, L., Kuster, S. P., Bartik, B., Zbinden, R., Zingg, P. O., and Achermann, Y. (2018). Association of cutibacterium avidum colonization in the groin with obesity: A potential risk factor for hip periprosthetic joint infection. *Clin. Infect. Dis.* 67, 1878–1882. doi: 10.1093/cid/ciy379

Cohen, E., Margalit, I., Shochat, T., Goldberg, E., and Krause, I. (2021). Markers of chronic inflammation in overweight and obese individuals and the role of gender: A cross-sectional study of a large cohort. *J. Inflammation Res.* 14, 567–573. doi: 10.2147/JIR.S294368

Font-Vizcarra, L., Tornero, E., Bori, G., Bosch, J., Mensa, J., and Soriano, A. (2011). Relationship between intraoperative cultures during hip arthroplasty, obesity, and the risk of early prosthetic joint infection: a prospective study of 428 patients. *Int. J. Artif. Organs.* 34, 870–875. doi: 10.5301/ijao.5000026

Gundtoft, P. H., Pedersen, A. B., Varnum, C., and Overgaard, S. (2017). Increased mortality after prosthetic joint infection in primary THA. *Clin. Orthop. Relat. Res.* 475, 2623–2631. doi: 10.1007/s11999-017-5289-6

Houdek, M. T., Wagner, E. R., Watts, C. D., Osmon, D. R., Hanssen, A. D., Lewallen, D. G., et al. (2015). Morbid obesity: a significant risk factor for failure of two-stage revision total hip arthroplasty for infection. *J. Bone Joint Surg. Am.* 97, 326–332. doi: 10.2106/JBJS.N.00515

Issa, K., Banerjee, S., Kester, M. A., Khanuja, H. S., Delanois, R. E., and Mont, M. A. (2014). The effect of timing of manipulation under anesthesia to improve range of motion and functional outcomes following total knee arthroplasty. *J. Bone Joint Surg. Am.* 96, 1349–1357. doi: 10.2106/JBJS.M.00899

Kapadia, B. H., Berg, R. A., Daley, J. A., Fritz, J., Bhave, A., and Mont, M. A. (2016). Periprosthetic joint infection. *Lancet* 387, 386–394. doi: 10.1016/S0140-6736(14)61798-0

Koh, C. K., Zeng, I., Ravi, S., Zhu, M., Vince, K. G., and Young, S. W. (2017). Periprosthetic joint infection is the main cause of failure for modern knee arthroplasty: an analysis of 11,134 knees. *Clin. Orthop. Relat. Res.* 475, 2194–2201. doi: 10.1007/s11999-017-5396-4

Laaksonen, D. E., Niskanen, L., Nyyssonen, K., Punnonen, K., Tuomainen, T. P., Valkonen, V. P., et al. (2004). C-reactive protein and the development of the metabolic syndrome and diabetes in middle-aged men. *Diabetologia* 47, 1403–1410. doi: 10.1007/s00125-004-1472-x

Leff, R. D., and Akre, S. P. (1986). Obesity and the erythrocyte sedimentation rate. *Ann. Intern. Med.* 105, 143. doi: 10.7326/0003-4819-105-1-143_2

Lowik, C., Zijlstra, W. P., Knobben, B., Ploegmakers, J., Dijkstra, B., de Vries, A. J., et al. (2019). Obese patients have higher rates of polymicrobial and Gram-negative early periprosthetic joint infections of the hip than non-obese patients. *PloS One* 14, e215035. doi: 10.1371/journal.pone.0215035

Marongiu, G., Contini, A., Cozzi Lepri, A., Donadu, M., Verona, M., and Capone, A. (2020). The treatment of acute diaphyseal long-bones fractures with orthobiologics and pharmacological interventions for bone healing enhancement: a systematic review of clinical evidence. *Bioengineering (Basel)* 7 (1), 22. doi: 10.3390/bioengineering7010022

Matthews, P. C., Berendt, A. R., McNally, M. A., and Byren, I. (2009). Diagnosis and management of prosthetic joint infection. *BMJ* 338, 0. doi: 10.1136/bmj.b1773

Nguyen, X. M., Lane, J., Smith, B. R., and Nguyen, N. T. (2009). Changes in inflammatory biomarkers across weight classes in a representative US population: a link between obesity and inflammation. *J. Gastrointest. Surg.* 13, 1205–1212. doi: 10.1007/s11605-009-0904-9

Parvizi, J., Tan, T. L., Goswami, K., Higuera, C., Della Valle, C., and Chen, A. F. (2018). The 2018 definition of periprosthetic hip and knee infection: an evidence-based and validated criteria. *J. Arthroplasty.* 33, 0. doi: 10.1016/j.arth.2018.02.078

Pevzner, L., Swank, M., Krepel, C., Wing, D. A., Chan, K., and Edmiston, C. J. (2011). Effects of maternal obesity on tissue concentrations of prophylactic cefazolin during cesarean delivery. *Obstet. Gynecol.* 117, 877–882. doi: 10.1097/AOG.0b013e31820b95e4

Probasco, W. V., Cefalu, C. J., Lee, R., Lee, D., Gu, A., and Dasa, V. (2020). Prevalence of idiopathically elevated ESR and CRP in patients undergoing primary total knee arthroplasty as a function of body mass index. *J. Clin. Orthop. Trauma* 11, S722–S728. doi: 10.1016/j.jcot.2020.05.031

Roschke, E., Kluge, T., Stallkamp, F., Roth, A., Zajonz, D., and Hoffmann, K. T. (2021). Use of PET-CT in diagnostic workup of periprosthetic infection of hip and knee joints: significance in detecting additional infectious focus. *Int. Orthop.* 46, 0. doi: 10.1007/s00264-021-05218-8

Roth, A., Khlopas, A., George, J., Churchill, J. L., Molloy, R., Mont, M. A., et al. (2019). The effect of body mass index on 30-day complications after revision total hip and knee arthroplasty. *J. Arthroplasty.* 34, S242–S248. doi: 10.1016/j.arth.2019.02.005

Shi, W., Jiang, Y., Tian, H., Wang, Y., Zhang, Y., Yu, T., et al. (2023). C-reactive protein-to-albumin ratio (CAR) and C-reactive protein-to-lymphocyte ratio (CLR) are valuable inflammatory biomarker combination for the accurate prediction of periprosthetic joint infection. *Infect. Drug Resist.* 16, 477–486. doi: 10.2147/IDR.S398958

Shi, W., Jiang, Y., Wang, Y., Zhang, C., Yu, T., and Li, T. (2022). The diagnostic value of various inflammatory biomarkers for diagnosing periprosthetic joint infection is gender-specific. *J. Inflammation Res.* 15, 3975–3982. doi: 10.2147/JIR.S364309

Shi, W., Wang, Y., Zhao, X., Yu, T., and Li, T. (2021). CRP/albumin has a promising prospect as a new biomarker for the diagnosis of periprosthetic joint infection. *Infect. Drug Resist.* 14, 5145–5151. doi: 10.2147/IDR.S342652

Visser, M., Bouter, L. M., McQuillan, G. M., Wener, M. H., and Harris, T. B. (1999). Elevated C-reactive protein levels in overweight and obese adults. *JAMA* 282, 2131–2135. doi: 10.1001/jama.282.22.2131

Wang, L., Zhou, B., Zhao, Z., Yang, L., Zhang, M., Jiang, Y., et al. (2021). Body-mass index and obesity in urban and rural China: findings from consecutive nationally representative surveys during 2004-18. *Lancet* 398, 53–63. doi: 10.1016/S0140-6736(21)00798-4

Watts, C. D., Wagner, E. R., Houdek, M. T., Lewallen, D. G., and Mabry, T. M. (2015). Morbid obesity: increased risk of failure after aseptic revision TKA. *Clin. Orthop. Relat. Res.* 473, 2621–2627. doi: 10.1007/s11999-015-4283-0

Whitehouse, M. R., Parry, M. C., Konan, S., and Duncan, C. P. (2016). Deep infection after hip arthroplasty: staying current with change. *Bone Joint J.* 98-B, 27–30. doi: 10.1302/0301-620X.98B1.36294

frontiers | Frontiers in Cellular and Infection Microbiology

TYPE Original Research
PUBLISHED 20 March 2025
DOI 10.3389/fcimb.2025.1527765

OPEN ACCESS

EDITED BY
José Luis Muñoz-Carrillo,
University of Guadalajara, Mexico

REVIEWED BY
Abubakar Nazir,
King Edward Medical University, Pakistan
Tirupataiah Sirupangi,
Baylor College of Medicine, United States

*CORRESPONDENCE
Hui Liang
lianghui8689@smu.edu.cn
Jieyan Wang
993368974@qq.com

†Theses authors have contributed equally to this work

RECEIVED 13 November 2024
ACCEPTED 26 February 2025
PUBLISHED 20 March 2025

CITATION
Zhang Y, Zhang Y, Chen Z, Jia Z, Yu Y, Wang J and Liang H (2025) Global burden, subtype, risk factors and etiological analysis of enteric infections from 1990-2021: population based study.
Front. Cell. Infect. Microbiol. 15:1527765.
doi: 10.3389/fcimb.2025.1527765

Global burden, subtype, risk factors and etiological analysis of enteric infections from 1990-2021: population based study

Youao Zhang[1,2†], Yuran Zhang[2†], Zhifeng Chen[2], Zixuan Jia[3], Yulan Yu[2], Jieyan Wang[1*] and Hui Liang[1*]

[1]Department of Urology, People's Hospital of Longhua, Shenzhen, Guangdong, China, [2]Nanfang Hospital, The First Clinical Medical College of Southern Medical University, Guangzhou, Guangdong, China, [3]School of Chinese Medicine, Southern Medical University, Guangzhou, China

Background: Enteric infections represent a prevalent global health issue and contribute significantly to the global disease burden. This study aims to investigate the patterns and trends of enteric infections from 1990 to 2021, providing valuable insights for health policy formulation, medical resource allocation, and the optimization of patient management plans.

Methods: We analyzed the Global Burden of Disease (GBD) 2021 for 21 regions and 204 countries to understand better the health burden using prevalence, incidence, mortality, and disability-adjusted life years (DALYs), subtype, risk factors, and etiology. We tested correlations with the Socio-demographic Index (SDI), and using decomposition analysis to dissect the reasons behind changes in epidemiological indicators of the disease.

Results: In 2021, the age-standardized rates of prevalence, incidence, deaths, and DALYs per 100,000 population for enteric infections were 879.58, 577.21, 17.83, and 1020.15, respectively. Compared to 1990, these rates exhibited -0.18, -0.12, -0.73, and -0.72 changes. Gender and age analyses revealed a higher burden among females, those under 15 years old, and the elderly. Regions with low SDI had higher epidemiological indicators. The burden of Typhoid fever declines in high-development regions. Unsafe water sources were identified as the primary risk factor globally in both 1990 and 2021. Rotavirus was the leading cause of deaths and DALYs.

Conclusion: This study highlights the complex epidemiological landscape of enteric infections, revealing variations in burden, risk factors, and etiological characteristics across age, gender, and geographical regions. It underscores the urgent need for healthcare professionals and policymakers to develop innovative prevention and healthcare strategies based on the current and evolving burden of enteric infections, to alleviate the global disease burden.

KEYWORDS

enteric infections, global burden of disease, epidemiology, trend analysis, risk factors, etiological analysis

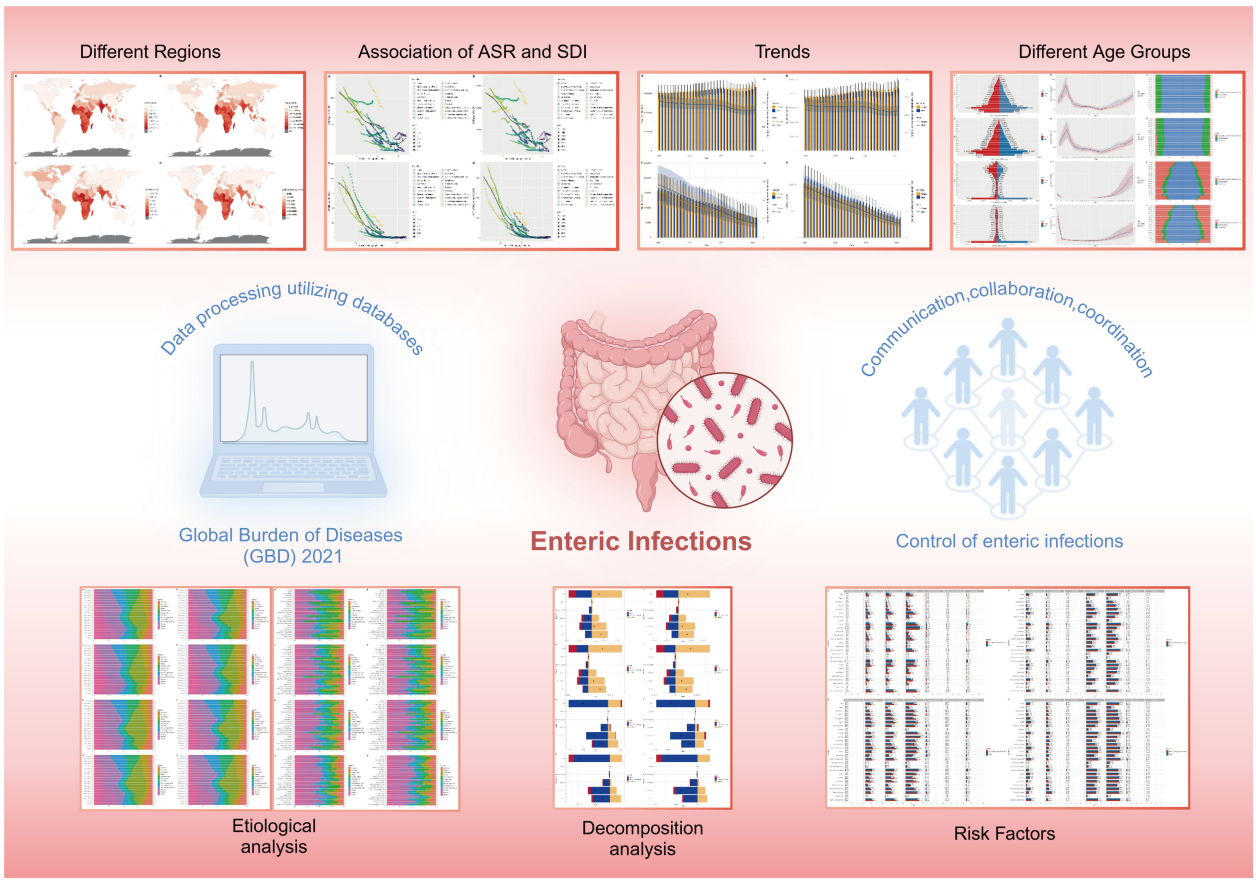

GRAPHICAL ABSTRACT

Introduction

Enteric infections, as a category of diseases significantly affecting global public health, encompass gastrointestinal inflammation caused by various pathogens (Torgerson et al., 2015). These infections not only lead to a decrease in patients' quality of life and increasing the risk of death (Hoivik et al., 2012), but also impose a significant economic burden at the social and family levels (Boccuzzi, 2003). Diarrheal diseases, a common symptom of gastrointestinal infections caused by diverse pathogens, pose a significant risk of dehydration and are the seventh leading cause of death in low-income countries according to the 2021 WHO statistics (World Health Organization, 2021). Typhoid fever, transmitted via contaminated food or water, can lead to severe fever, fatigue, and mortality. In low-income and middle-income countries, the average total cost of inpatient treatment per person ranges from $201 to $976 (Debellut et al., 2024). Paratyphoid A and B have clinical presentations similar to typhoid but are milder and shorter in duration. Invasive non-typhoidal Salmonella (iNTS) is a major health problem in low-income and underdeveloped countries in Africa and Asia that lack proper sanitation facilities (Hajra et al., 2023).

Therefore, the purpose of this analysis is to characterize the global burden of enteric infections and subtype in 21 regions and 204 countries and territories worldwide. The 2021 GBD conducted an in-depth assessment of the health hazards, with the support of more than 11,500 collaborators from 164 countries (GBD 2021 Causes of Death Collaborators, 2024; GBD 2021 Diseases and Injuries Collaborators, 2024; Sun et al., 2024; Tuo et al., 2024; Yang et al., 2024). Therefore, the GBD study is a reliable tool for understanding and assessing the current burden of enteric infections.

Methods

Data source

The present study extracted global incidence, prevalence, mortality, and DALYs (one DALY represents the loss of one year of full health due to premature death or disability), along with their 95% uncertainty intervals (UI), spanning from 1990 to 2021 from the GBD database (https://vizhub.healthdata.org/gbd-results/). Data on sex, age groups, population, and SDI were also included for comprehensive analysis.

SDI analysis

The SDI was employed as a metric to assess the socio-economic status of countries, with a higher score indicating more robust socio-economic development. Regions were stratified into five quintiles based on the GBD studies: High SDI (>0.81), High-middle SDI (0.70–0.81), Middle SDI (0.61–0.69), Low-middle SDI (0.46–0.60), and Low SDI (<0.46) (GBD 2021 Causes of Death Collaborators, 2024; GBD 2021 Diseases and Injuries Collaborators, 2024). To examine the correlation between SDI and the burden of enteric infections, locally estimated scatterplot smoothing (loess) models were applied, utilizing the geom_smooth function within the ggplot2 package.

Decomposition analysis

To quantify the driving factors behind the changes in the number of enteric infections, we estimated the relative contributions of aging, population growth, and epidemiological shifts. For this decomposition analysis, we employed the classic method developed by Das Gupta (1978), which utilizes algebraic decomposition techniques to break down the overall changes into the standardized impacts of each factor, thereby identifying the contribution of each component.

Statistics analysis

Age-standardized prevalence rates (ASPR), age-standardized incidence rates (ASIR), age-standardized mortality rates (ASMR), and ASR of DALYs were expressed as predicted values per 100,000 population, including their 95% UI. All analytical procedures and graphical representations were executed using the statistical software R (version 4.4.1).

Results

Global level

Enteric infections

In 2021, the global prevalence was 67,826,600, with an ASPR of 879.58. Between 1990 and 2021, the ASPR decreased by 0.18, and the ASIR decreased by 0.12. The number of incident cases was 4,448,407,870 with an ASIR of 57,721.08. From 1990 to 2021, the number of deaths was 1,336,220 with an ASMR of 17.83; the ASMR decreased by 0.73 over this period. The global DALYs totaled 71,929,008 with an ASR of 1,020.15, and the ASR of DALYs decreased by 0.72 from 1990 to 2021 (Table 1).

Diarrheal diseases

In 2021, the global prevalence was 67,276,401 with an ASPR of 872.02; from 1990 to 2021, the ASPR decreased by 0.16. The number of incident cases was 4,438,577,275 with an ASIR of 57,586.1; the ASIR decreased by 0.12 from 1990 to 2021. The number of deaths was 1,165,398 with an ASMR of 15.42; the ASMR decreased by 0.75 during the same period. The global DALYs totaled 58,983,817 with an ASR of 834.18, and the ASR of DALYs decreased by 0.75 from 1990 to 2021 (Supplementary Table S1).

Typhoid fever

In 2021, the global prevalence was 452,343 with an ASPR of 6.23. From 1990 to 2021, the ASPR decreased by 0.7. The number of incident cases was 715,455 with an ASIR of 98.56, and the ASIR decreased by 0.7 over this period. The number of deaths was 93,333 with an ASMR of 1.31, which decreased by 0.59 from 1990 to 2021. The global DALYs were 7,087,733 with an ASR of DALYs of 101.09, and the ASR of DALYs decreased by 0.59 during this period (Supplementary Table S2).

Paratyphoid fever

In 2021, the global prevalence was 94,953 with an ASPR of 1.28. Between 1990 and 2021, the ASPR decreased by 0.79. The number of incident cases was 2,166,063 with an ASIR of 29.21; the ASPR decreased by 0.79 from 1990 to 2021. The number of deaths was 14,127 with an ASMR of 0.19, and the ASMR decreased by 0.72 over the same period. The global DALYs totaled 1,011,842 with an ASR of DALYs of 14.16, which decreased by 0.73 from 1990 to 2021 (Supplementary Table S3).

iNTS

In 2021, the global prevalence was 11,847, with an ASPR of 0.17. From 1990 to 2021, the ASPR increased by 0.21. The number of incident cases was 509,976 with an ASIR of 7.21; the ASIR increased by 0.2 over the same period. The number of deaths was 62,018 with an ASMR of 0.88, and the ASMR increased by 0.02 from 1990 to 2021. The global DALYs were 4,740,235, with an ASR of DALYs of 69.14, and the ASR of DALYs increased by 0.12 during this period (Supplementary Table S4).

Regional level

Enteric infections

In 2021, the ASPR was highest in Low SDI regions, reaching 1774.15. Geographically, the South Asia region exhibited the highest ASPR at 1878.93 (Table 1; Figure 1A). From 1990 to 2021, the slowest decline was observed in Low SDI regions, with a decrease of 0.14. Geographically, the High-income Asia Pacific region showed the most significant upward trend, at 0.28 (Table 1). The ASIR was highest in Low SDI regions, at 115140.51, with South Asia again exhibiting the highest ASIR at 121872.67 (Table 1; Figure 1B). Between 1990 and 2021, the slowest decline was observed in Low SDI regions, with a downward trend of 0.09. Geographically, the High-income Asia Pacific region showed the most significant upward trend, at 0.35 (Table 1). The ASMR was highest in Low SDI regions, at 75.25. Geographically, the Western Sub-Saharan Africa region had the highest ASMR at 65.53 (Table 1; Figure 1C). Between 1990 and 2021, the fastest increase was

observed in High SDI regions, with an upward trend of 0.25. Geographically, the High-income North America region showed the most significant upward trend, at 3.85 (Table 1). The ASR of DALYs was highest in Low SDI regions, at 2999.43. Geographically, the Western Sub-Saharan Africa region had the highest ASR of DALYs at 3383.88 (Table 1; Figure 1D). Between 1990 and 2021, the slowest decline was observed in High SDI regions, with a downward trend of 0.3. Geographically, Western Europe showed the most significant upward trend, at 0.05 (Table 1).

Diarrheal diseases

In 2021, the ASPR was highest in Low SDI regions, at 1763.73. Geographically, the South Asia region had the highest ASPR at 1857.37. Between 1990 and 2021, the slowest decline was observed in Low SDI regions, with a downward trend of 0.13. Geographically, the High-income Asia Pacific region showed the most significant upward trend, at 0.28 (Supplementary Table S1). The ASIR was highest in Low SDI regions, at 114948.62. Geographically, the South Asia region had the highest ASIR at 121489.61. Between 1990 and 2021, the slowest decline was observed in Low SDI regions, with a downward trend of 0.08. Geographically, the High-income Asia Pacific region showed the most significant upward trend, at 0.35 (Supplementary Table S1). The ASMR was highest in Low SDI regions, at 69.75. Geographically, the Eastern Sub-Saharan Africa region had the highest ASMR at 59.99. Between 1990 and 2021, the fastest increase was observed in High SDI regions, with an upward trend of 0.35. Geographically, the High-income North America region showed the most significant upward trend, at 4.36 (Supplementary Table S1). The ASR of DALYs was highest in Low SDI regions, at 2605.84. Geographically, the Western Sub-Saharan Africa region had the highest ASR of DALYs at 2769.81. Between 1990 and 2021, the slowest decline was observed in High SDI regions, with a downward trend of 0.27. Geographically, Western Europe showed the most significant upward trend, at 0.08 (Supplementary Table S1).

Typhoid fever

The ASPR was highest in Low-middle SDI regions, at 12.09. Geographically, the South Asia region had the highest ASPR at 17.01. Between 1990 and 2021, the slowest decline was observed in High-middle SDI regions, with a downward trend of 0.54. Geographically, Australasia showed the least decline, at 0.01 (Supplementary Table S2). The ASIR was highest in Low-middle SDI regions, at 191.27. Geographically, the South Asia region had the highest ASIR at 269.08. Between 1990 and 2021, the slowest decline was observed in High-middle SDI regions, with a downward trend of 0.54. Geographically, Australasia showed the least decline, at 0.01 (Supplementary Table S2). The ASMR was highest in Low-middle SDI regions, at 2.52. Geographically, the Oceania region had the highest ASMR at 3.48. Between 1990 and 2021, the slowest decline was observed in High-middle SDI regions, with a downward trend of 0.57. Geographically, Australasia showed the most significant upward trend, at 0.71 (Supplementary Table S2). The ASR of DALYs was highest in Low-middle SDI regions, at 188.51. Geographically, the South Asia region had the highest ASR of DALYs at 260.27. Between 1990 and 2021, the slowest decline was observed in High-middle SDI regions, with a downward trend of 0.58. Geographically, Southern Sub-Saharan Africa showed the most significant upward trend, at 0.03 (Supplementary Table S2).

Paratyphoid fever

In 2021, the ASPR was highest in Low-middle SDI regions, at 2.93. Geographically, the South Asia region had the highest ASPR at 4.85. Between 1990 and 2021, the slowest decline was observed in High SDI regions, with a downward trend of 0.33. Geographically, Australasia showed the most significant upward trend, at 0.62 (Supplementary Table S3). The ASIR was highest in Low-middle SDI regions, at 66.83. Geographically, the South Asia region had the highest ASIR at 110.56. Between 1990 and 2021, the slowest decline was observed in High SDI regions, with a downward trend of 0.34. Geographically, Australasia showed the most significant upward trend, at 0.61 (Supplementary Table S3). The ASMR was highest in Low-middle SDI regions, at 0.44. Geographically, the South Asia region had the highest ASMR at 0.73. Between 1990 and 2021, the slowest decline was observed in High-middle SDI regions, with a downward trend of 0.67. Geographically, High-income North America showed the most significant upward trend, at 0.73 (Supplementary Table S3). The ASR of DALYs was highest in Low-middle SDI regions, at 30.99. Geographically, the South Asia region had the highest ASR of DALYs at 51.64. Between 1990 and 2021, the slowest decline was observed in High-middle SDI regions, with a downward trend of 0.69. Geographically, High-income North America showed the most significant upward trend, at 0.54 (Supplementary Table S3).

iNTS

In 2021, the ASPR was highest in Low SDI regions, at 0.48. Geographically, the Western Sub-Saharan Africa region had the highest ASPR at 1.1. Between 1990 and 2021, the fastest increase was observed in High SDI regions, with an upward trend of 0.18. Geographically, Western Europe showed the most significant upward trend, at 0.68 (Supplementary Table S4). The ASIR was highest in Low SDI regions, at 20.91. Geographically, the Western Sub-Saharan Africa region had the highest ASIR at 47.54. Between 1990 and 2021, the fastest increase was observed in High SDI regions, with an upward trend of 0.17. Geographically, Western Europe showed the most significant upward trend, at 0.66 (Supplementary Table S4). The ASMR was highest in Low SDI regions, at 3.3. Geographically, the Western Sub-Saharan Africa region had the highest ASMR at 6.88. Between 1990 and 2021, the slowest decline was observed in Low SDI regions, with a downward trend of 0.31. Geographically, the Caribbean showed the most significant upward trend, at 0.01 (Supplementary Table S4). The ASR of DALYs was highest in Low SDI regions, at 234.06. Geographically, the Western Sub-Saharan Africa region had the highest ASR of DALYs at 486.81. Between 1990 and 2021, the slowest decline was observed in Low SDI regions, with a downward trend of 0.24. Geographically, Oceania showed the most significant upward trend, at 0.06 (Supplementary Table S4).

TABLE 1 Prevalent cases, age-standardized prevalence rates, incident cases, age-standardized incidence rates, death cases, age-standardized mortality rates, DALYs, and age-standardized rates of DALYs for enteric infections in 1990 and 2021 for both sexes and rate change of age-standardized rates by GBD.

		1990		2021		1990–2021
		All-ages cases	Age-standardized rates per 100,000	All-ages cases	Age-standardized rates per 100,000	Rate change in age-standardized rates
		N (95%UI)		N (95%UI)		N (95%UI)
Global	Prevalence	61055404 (54000541 to 68729603)	1043.56 (925.18 to 1171.6)	67826600 (61771775 to 74750450)	879.58 (801.36 to 972.25)	-0.18 (-0.22 to -0.13)
	Incidence	3758659175 (3260094453 to 4255859151)	65466.27 (56954.84 to 73982.41)	4448407870 (3965332197 to 4991900224)	57721.08 (51210.03 to 64765.61)	-0.12 (-0.18 to -0.06)
	Deaths	3214610 (2574183 to 4002667)	60.58 (46.34 to 79.9)	1336220 (978118 to 1797317)	17.83 (13.38 to 23.5)	-0.73 (-0.77 to -0.68)
	DALYs	214438908 (173838488 to 252010744)	3337.13 (2684.15 to 3994.3)	71929008 (58296705 to 88193657)	1020.15 (822.7 to 1259.39)	-0.72 (-0.77 to -0.67)
Socio-demographic Index (SDI)						
High SDI	Prevalence	2551657 (2142234 to 3028519)	326.97 (269.31 to 394.92)	2767787 (2453972 to 3109622)	278.39 (235.41 to 326.08)	-0.15 (-0.19 to -0.11)
	Incidence	161510412 (133525808 to 191309059)	20689.81 (16749.3 to 24983.77)	173794217 (150709751 to 197313883)	17498.72 (14477.63 to 20576.96)	-0.15 (-0.19 to -0.11)
	Deaths	8064 (7098 to 9151)	0.84 (0.73 to 0.97)	27117 (22704 to 29833)	1.16 (1 to 1.26)	0.25 (0.07 to 0.41)
	DALYs	609189 (494654 to 742900)	77.57 (61.87 to 95.79)	731654 (631981 to 856337)	57.86 (47.68 to 71.48)	-0.3 (-0.39 to -0.23)
High-middle SDI	Prevalence	4085310 (3466586 to 4816257)	410.07 (344.78 to 486.18)	2745044 (2388543 to 3140651)	247.23 (209.74 to 289.69)	-0.4 (-0.44 to -0.36)
	Incidence	256269268 (212672970 to 302880831)	25845.86 (21357.63 to 30597.41)	180727882 (154454773 to 209294829)	16245.72 (13536.94 to 19130.51)	-0.37 (-0.41 to -0.33)
	Deaths	51860 (40808 to 62563)	5.26 (4.09 to 6.33)	18631 (13740 to 23200)	1.3 (1.01 to 1.59)	-0.77 (-0.81 to -0.74)
	DALYs	4232752 (3520463 to 4982910)	420.6 (349.94 to 498.14)	877647 (720773 to 1069220)	84.66 (70 to 102.51)	-0.82 (-0.84 to -0.78)
Middle SDI	Prevalence	18100901 (15818203 to 20694988)	970.33 (857.36 to 1097.96)	16130490 (14571235 to 18003830)	684.38 (614.99 to 767.47)	-0.31 (-0.34 to -0.26)
	Incidence	1116840410 (955571259 to 1281310554)	60646.64 (52576.63 to 68929.37)	1068928569 (943201109 to 1209397348)	45293.11 (39773.15 to 51308.45)	-0.26 (-0.3 to -0.21)
	Deaths		41.96 (28.5 to 58.22)		8.76 (5.79 to 12.13)	-0.8 (-0.84 to -0.76)

(Continued)

10.3389/fcimb.2025.1527765

TABLE 1 Continued

		1990		2021		1990–2021
		All-ages cases	Age-standardized rates per 100,000	All-ages cases	Age-standardized rates per 100,000	Rate change in age-standardized rates
		N (95%UI)		N (95%UI)		N (95%UI)
Socio-demographic Index (SDI)						
		558050 (424745 to 706972)		188350 (121962 to 266788)		
	DALYs	38118303 (30474442 to 45305880)	1972.46 (1539.6 to 2372.74)	8890401 (6992304 to 11176121)	426.35 (340.12 to 529.48)	-0.8 (-0.83 to -0.77)
Low-middle SDI	Prevalence	23906860 (21237278 to 26668660)	1752.18 (1587.72 to 1935.52)	26447136 (24067904 to 29066200)	1391.11 (1273.51 to 1522.18)	-0.23 (-0.27 to -0.19)
	Incidence	1469161007 (1275921726 to 1651651578)	110887.41 (98232.61 to 124029.01)	1735881923 (1544016836 to 1948698545)	91250.49 (81752.09 to 102132.36)	-0.19 (-0.23 to -0.14)
	Deaths	1623455 (1308956 to 2067629)	185.39 (136.59 to 261.93)	554032 (388724 to 819133)	42.1 (27.89 to 63.93)	-0.78 (-0.83 to -0.72)
	DALYs	102147738 (85140005 to 120396465)	6982.21 (5654.75 to 8895.33)	25272138 (20143943 to 32252792)	1482.56 (1168.18 to 1949.54)	-0.81 (-0.84 to -0.77)
Low SDI	Prevalence	12379983 (11164337 to 13664446)	2018.19 (1851.61 to 2198.63)	19703744 (18022741 to 21450172)	1774.15 (1648.72 to 1906.17)	-0.14 (-0.18 to -0.1)
	Incidence	752987003 (662421461 to 845942634)	125371.61 (112564.78 to 139219.26)	1286917992 (1146820963 to 1436705137)	115140.51 (104963.9 to 126783.5)	-0.09 (-0.13 to -0.03)
	Deaths	971623 (769772 to 1199430)	226.43 (166.82 to 311.5)	547373 (414232 to 713744)	75.25 (50.89 to 110.13)	-0.68 (-0.76 to -0.6)
	DALYs	69215477 (53961045 to 83956627)	9231.04 (7207.31 to 11730.12)	36111927 (27436121 to 45426990)	2999.43 (2315.53 to 3859.13)	-0.7 (-0.77 to -0.63)
GBD Regions						
Andean Latin America	Prevalence	637098 (587004 to 692561)	1438.45 (1338.61 to 1549.33)	225849 (198333 to 258588)	347.21 (306.64 to 396.98)	-0.76 (-0.78 to -0.73)
	Incidence	37003808 (33077888 to 41140431)	83887.59 (75901.95 to 92599.28)	15483051 (13322848 to 18133567)	23820.04 (20605.46 to 27817.86)	-0.72 (-0.74 to -0.69)
	Deaths	10189 (8652 to 12022)	24.64 (20.18 to 29.42)	1717 (1202 to 2643)	2.92 (2.03 to 4.47)	-0.88 (-0.92 to -0.84)
	DALYs	859437 (739200 to 998145)	1722.02 (1478.56 to 1997.06)	106991 (80792 to 142675)	172.7 (129.89 to 229.98)	-0.9 (-0.92 to -0.87)

(Continued)

10.3389/fcimb.2025.1527765

TABLE 1 Continued

		1990		2021		1990–2021
		All-ages cases	Age-standardized rates per 100,000	All-ages cases	Age-standardized rates per 100,000	Rate change in age-standardized rates
		N (95%UI)		N (95%UI)		N (95%UI)
GBD Regions						
Australasia	Prevalence	54259 (46462 to 62444)	275.84 (234.87 to 318.67)	28194 (24877 to 31910)	86 (74.09 to 100.08)	-0.69 (-0.71 to -0.66)
	Incidence	3633258 (3089858 to 4214597)	18410.12 (15461.84 to 21460.9)	1852252 (1607504 to 2114402)	5649.98 (4834.1 to 6567.15)	-0.69 (-0.72 to -0.67)
	Deaths	144 (130 to 156)	0.68 (0.62 to 0.75)	300 (247 to 334)	0.5 (0.42 to 0.55)	-0.29 (-0.36 to -0.21)
	DALYs	9454 (7556 to 12101)	48.26 (38.35 to 61.59)	7528 (6479 to 8784)	19.75 (16.68 to 23.93)	-0.6 (-0.63 to -0.56)
Caribbean	Prevalence	205617 (182351 to 231442)	545.92 (487.37 to 610.99)	197728 (172514 to 226101)	431.58 (375.13 to 496.73)	-0.21 (-0.26 to -0.17)
	Incidence	13526296 (11668609 to 15430483)	35922.73 (31233.84 to 40827.91)	13633676 (11685295 to 16054870)	29747.59 (25321.07 to 35131.8)	-0.17 (-0.23 to -0.12)
	Deaths	14784 (12439 to 17311)	37.84 (32.09 to 44.4)	5867 (4156 to 7944)	14.02 (9.89 to 18.88)	-0.63 (-0.74 to -0.52)
	DALYs	1218184 (1013446 to 1427693)	2924.35 (2452.1 to 3433.32)	432887 (308278 to 575802)	1090.49 (769.64 to 1461.56)	-0.63 (-0.74 to -0.51)
Central Asia	Prevalence	371269 (336412 to 410692)	426.91 (386.5 to 473.53)	136164 (115852 to 158872)	141.7 (120.12 to 165.64)	-0.67 (-0.7 to -0.64)
	Incidence	22127122 (19231924 to 25016511)	25482 (22210.82 to 28897.23)	8500235 (7102605 to 9994522)	8829.8 (7339.39 to 10394.51)	-0.65 (-0.68 to -0.62)
	Deaths	14303 (12955 to 15923)	15.52 (14.08 to 17.26)	1929 (1428 to 2578)	1.96 (1.46 to 2.62)	-0.87 (-0.91 to -0.83)
	DALYs	1295085 (1171023 to 1440412)	1384.22 (1252.12 to 1538.59)	179360 (135239 to 237289)	181.19 (136.74 to 239.6)	-0.87 (-0.9 to -0.83)
Central Europe	Prevalence	59402 (48041 to 71969)	61.08 (49.9 to 73.7)	31447 (27856 to 35322)	31.03 (25.9 to 36.63)	-0.49 (-0.52 to -0.46)
	Incidence	3524216 (2801998 to 4306524)	3606.12 (2852.61 to 4421.83)	1918889 (1671273 to 2151872)	1940.64 (1588.77 to 2317.59)	-0.46 (-0.49 to -0.43)
	Deaths	1101 (1003 to 1210)	1.11 (1 to 1.23)	2587 (2291 to 2857)	1.38 (1.23 to 1.52)	0.18 (0.04 to 0.32)
	DALYs	85107 (77245 to 94006)	92.63 (83.37 to 102.36)	58242 (52321 to 64426)	53.61 (47.2 to 60.41)	-0.44 (-0.53 to -0.35)
Central Latin America	Prevalence	1685320 (1475073 to 1930555)	922.97 (824.47 to 1033.36)	821783 (731603 to 924682)	336.52 (298.71 to 379.58)	-0.64 (-0.65 to -0.62)

(Continued)

10.3389/fcimb.2025.1527765

TABLE 1 Continued

		1990		2021		1990–2021
		All-ages cases	Age-standardized rates per 100,000	All-ages cases	Age-standardized rates per 100,000	Rate change in age-standardized rates
		N (95%UI)		N (95%UI)		N (95%UI)
GBD Regions						
	Incidence	106731052 (91671723 to 122913384)	58634.62 (51678.52 to 66144.45)	54272972 (47604897 to 62316837)	22249.12 (19462.14 to 25539.5)	-0.62 (-0.64 to -0.6)
	Deaths	57020 (53692 to 60966)	35.7 (33.87 to 37.7)	12001 (10339 to 14016)	5.29 (4.52 to 6.22)	-0.86 (-0.88 to -0.83)
	DALYs	4383927 (4102666 to 4728530)	2095.79 (1973.25 to 2244.48)	585977 (491974 to 708152)	265.96 (220.2 to 324.16)	-0.88 (-0.9 to -0.85)
Central Sub-Saharan Africa	Prevalence	1076393 (988522 to 1171299)	1480.01 (1370.45 to 1598.41)	1944566 (1788238 to 2126501)	1387.7 (1298 to 1486.26)	-0.07 (-0.12 to -0.01)
	Incidence	64737365 (57444092 to 72181916)	90480.93 (81487.72 to 100113.35)	133600151 (119153900 to 151351998)	94579.16 (86007.3 to 105129.88)	0.04 (-0.03 to 0.13)
	Deaths	85579 (62473 to 104671)	148.47 (100.81 to 202.43)	35116 (23282 to 50781)	43.08 (25.65 to 67.35)	-0.73 (-0.82 to -0.64)
	DALYs	6703204 (4870684 to 8229530)	7184.05 (5299.52 to 8890.93)	2394531 (1678182 to 3358268)	1728.05 (1182.63 to 2452.9)	-0.78 (-0.84 to -0.71)
East Asia	Prevalence	4892517 (4147855 to 5808512)	413.68 (349.66 to 491.17)	1523826 (1294326 to 1772754)	116.74 (97.8 to 137.63)	-0.72 (-0.74 to -0.69)
	Incidence	297864969 (246384420 to 352693370)	25263.17 (20941.29 to 29838.11)	101274027 (85606904 to 118448050)	7713.32 (6387.53 to 9177.52)	-0.69 (-0.72 to -0.67)
	Deaths	95230 (70931 to 117616)	9.01 (6.5 to 11.39)	5893 (4191 to 9552)	0.44 (0.33 to 0.63)	-0.95 (-0.97 to -0.94)
	DALYs	7989901 (6186017 to 9826256)	681.69 (526.2 to 838.12)	406593 (329152 to 510531)	36.88 (29.99 to 45.96)	-0.95 (-0.96 to -0.93)
Eastern Europe	Prevalence	740072 (608559 to 880252)	398.84 (327.17 to 474.49)	350071 (288904 to 422655)	214.2 (171.28 to 262.11)	-0.46 (-0.51 to -0.41)
	Incidence	45627064 (36790586 to 55097865)	24587.31 (19703.28 to 29834.95)	21782627 (17510047 to 26437234)	13426.49 (10585.13 to 16628.67)	-0.45 (-0.5 to -0.4)
	Deaths	2100 (2024 to 2182)	1.16 (1.12 to 1.21)	585 (545 to 623)	0.26 (0.24 to 0.27)	-0.79 (-0.8 to -0.77)
	DALYs	235178 (206399 to 272360)	136.26 (120.42 to 155.99)	61076 (47513 to 77854)	38.44 (29.69 to 49.29)	-0.72 (-0.76 to -0.68)
Eastern Sub-Saharan Africa	Prevalence	5119633 (4664167 to 5639418)	2183.19 (2022.55 to 2381.52)	7720002 (7085740 to 8421769)	1787.88 (1666.27 to 1916.12)	-0.19 (-0.23 to -0.15)

(Continued)

10.3389/fcimb.2025.1527765

TABLE 1 Continued

		1990		2021		1990–2021
		All-ages cases	Age-standardized rates per 100,000	All-ages cases	Age-standardized rates per 100,000	Rate change in age-standardized rates
		N (95%UI)		N (95%UI)		N (95%UI)
GBD Regions						
	Incidence	308972113 (274106477 to 347935023)	133773.19 (120477.21 to 149066.93)	504500793 (449626298 to 568451319)	116696.88 (106204.64 to 129070.34)	-0.13 (-0.18 to -0.08)
	Deaths	317581 (231951 to 413916)	180.6 (113.91 to 263.03)	164018 (117642 to 218541)	62.72 (37.23 to 84.34)	-0.67 (-0.78 to -0.49)
	DALYs	23878766 (16853365 to 31040384)	8098.06 (5797.76 to 10825.01)	11045655 (8363694 to 14313440)	2523.08 (1853.83 to 3295.26)	-0.71 (-0.79 to -0.6)
High-income Asia Pacific	Prevalence	696565 (568274 to 836214)	458.84 (373.48 to 556.14)	829379 (728360 to 942444)	585.88 (486.35 to 692.85)	0.28 (0.18 to 0.37)
	Incidence	41653270 (33869000 to 49621246)	27758.11 (22376.07 to 33584.45)	53657289 (46068548 to 61883794)	37568.18 (30699.1 to 44976.2)	0.35 (0.28 to 0.44)
	Deaths	1644 (1318 to 1943)	1.08 (0.87 to 1.26)	4841 (3697 to 6024)	0.8 (0.64 to 1)	-0.27 (-0.38 to -0.11)
	DALYs	122703 (96255 to 156214)	83.7 (64.81 to 107.43)	157361 (127042 to 198469)	85.92 (63.03 to 115.97)	0.02 (-0.09 to 0.12)
High-income North America	Prevalence	410367 (329027 to 515651)	160.16 (126.76 to 203.36)	71763 (64432 to 79478)	18.67 (16.47 to 21.07)	-0.88 (-0.9 to -0.87)
	Incidence	26187750 (20691270 to 32549003)	10166.2 (7966.47 to 12788)	4348391 (3822662 to 4943141)	1125.19 (978.91 to 1297.34)	-0.89 (-0.9 to -0.87)
	Deaths	959 (874 to 1014)	0.28 (0.26 to 0.29)	10322 (8838 to 11150)	1.49 (1.3 to 1.6)	3.85 (3.51 to 4.08)
	DALYs	81130 (64472 to 100818)	30.54 (23.92 to 38.41)	180935 (164342 to 191982)	32.31 (29.91 to 34.2)	0.02 (-0.19 to 0.27)
North Africa and Middle East	Prevalence	3221544 (2798552 to 3668830)	686.35 (598.76 to 779.37)	2874392 (2409657 to 3421853)	456.42 (385.05 to 541.43)	-0.34 (-0.4 to -0.28)
	Incidence	193045883 (161958092 to 225157945)	41622.41 (35195.23 to 48177.47)	192887301 (158892555 to 234109970)	30655.52 (25356.16 to 36889.09)	-0.26 (-0.33 to -0.19)
	Deaths	101940 (78959 to 127704)	21.87 (16.67 to 27.16)	18339 (13735 to 24094)	3.53 (2.62 to 4.75)	-0.85 (-0.88 to -0.81)
	DALYs	9063178 (7068838 to 11340027)	1745.34 (1343.31 to 2182.98)	1656313 (1271459 to 2170155)	280.4 (216.48 to 367.29)	-0.85 (-0.88 to -0.81)

(Continued)

10.3389/fcimb.2025.1527765

TABLE 1 Continued

		1990		2021		1990–2021
		All-ages cases	Age-standardized rates per 100,000	All-ages cases	Age-standardized rates per 100,000	Rate change in age-standardized rates
		N (95%UI)		N (95%UI)		N (95%UI)
GBD Regions						
Oceania	Prevalence	88853 (81463 to 97451)	1144.13 (1055.39 to 1240.41)	148580 (136730 to 162855)	1014.26 (942.88 to 1094.23)	-0.15 (-0.19 to -0.1)
	Incidence	5484843 (4914907 to 6137868)	72521.57 (65043.68 to 80161.63)	10063172 (9077770 to 11227900)	68839.7 (62561.85 to 75931.16)	-0.06 (-0.12 to 0)
	Deaths	3757 (2615 to 5047)	79.04 (48.81 to 109.52)	4027 (2769 to 5418)	43.48 (27.78 to 62.25)	-0.5 (-0.59 to -0.4)
	DALYs	267031 (190767 to 363055)	2926.72 (2062.22 to 3889.14)	269613 (184474 to 376343)	1780.07 (1253.7 to 2384.7)	-0.49 (-0.6 to -0.38)
South Asia	Prevalence	24678581 (21701853 to 27927901)	1971.36 (1770.28 to 2195.22)	34162384 (31044486 to 37491065)	1878.93 (1716.49 to 2049.84)	-0.09 (-0.14 to -0.04)
	Incidence	1550617053 (1320986591 to 1762161539)	128123.11 (112430.41 to 144337.51)	2215979139 (1971336860 to 2476296089)	121872.67 (108949 to 135347.48)	-0.06 (-0.12 to 0.01)
	Deaths	1664505 (1330406 to 2176400)	230.96 (169.95 to 330.02)	650729 (430032 to 1010207)	52.25 (34.34 to 81.39)	-0.79 (-0.84 to -0.72)
	DALYs	97275211 (80465643 to 117199267)	7630.49 (6111.88 to 9999.63)	26267550 (20172537 to 35803484)	1688.36 (1282.69 to 2324.84)	-0.8 (-0.84 to -0.76)
Southeast Asia	Prevalence	7141453 (6258765 to 8098329)	1369.55 (1218.49 to 1531.94)	5449156 (4951789 to 6076444)	829.83 (747.92 to 929)	-0.41 (-0.44 to -0.38)
	Incidence	423236909 (362813623 to 483950260)	82572.88 (72303.9 to 93680.92)	358637500 (313989689 to 402974774)	54498.27 (47651.09 to 61254.88)	-0.34 (-0.37 to -0.31)
	Deaths	346228 (240210 to 488465)	98.38 (57.22 to 152.66)	88987 (53789 to 116713)	16.32 (9.52 to 21.72)	-0.84 (-0.9 to -0.76)
	DALYs	22490665 (16325875 to 28930584)	4208.73 (2932.65 to 5788.35)	4232029 (3283180 to 5305626)	702.82 (539.9 to 881.87)	-0.85 (-0.88 to -0.8)
Southern Latin America	Prevalence	320724 (268393 to 380934)	634.7 (534.37 to 749.55)	118878 (99858 to 138670)	191.76 (158.87 to 226.28)	-0.7 (-0.72 to -0.68)
	Incidence	20533698 (17182877 to 24543776)	40675.52 (34101.07 to 48467.86)	7912146 (6527708 to 9292111)	12762.35 (10398.97 to 15130.27)	-0.69 (-0.71 to -0.67)
	Deaths	1638 (1547 to 1719)	3.49 (3.29 to 3.67)	1267 (1122 to 1403)	1.53 (1.36 to 1.69)	-0.57 (-0.61 to -0.53)

(Continued)

10.3389/fcimb.2025.1527765

TABLE 1 Continued

		1990		2021		1990–2021
		All-ages cases	Age-standardized rates per 100,000	All-ages cases	Age-standardized rates per 100,000	Rate change in age-standardized rates
		N (95%UI)		N (95%UI)		N (95%UI)
GBD Regions						
	DALYs	130865 (116790 to 146123)	258.17 (230.11 to 288.49)	41123 (36017 to 47869)	65.46 (56.41 to 77.33)	-0.75 (-0.78 to -0.72)
Southern Sub-Saharan Africa	Prevalence	1573635 (1401466 to 1761372)	2707.46 (2432.39 to 2994.73)	1372608 (1255656 to 1500758)	1688.18 (1552.89 to 1834.68)	-0.38 (-0.41 to -0.34)
	Incidence	96530924 (84596034 to 109166428)	166237.52 (148057.31 to 188063.74)	89893938 (79721355 to 102583407)	110703.56 (98915.34 to 125610.4)	-0.33 (-0.37 to -0.28)
	Deaths	38729 (32139 to 47502)	82.24 (60.05 to 116.63)	24462 (17182 to 33542)	40.58 (26.73 to 58.19)	-0.52 (-0.6 to -0.4)
	DALYs	2875263 (2497611 to 3307024)	4453.58 (3800.92 to 5350.47)	1451876 (1163483 to 1831288)	1941.05 (1555.22 to 2486.17)	-0.57 (-0.64 to -0.49)
Tropical Latin America	Prevalence	1263454 (1081971 to 1474675)	777.8 (675.36 to 894.8)	604160 (525832 to 693384)	284.37 (244.36 to 330.11)	-0.63 (-0.66 to -0.61)
	Incidence	78226903 (64938932 to 92548183)	48190.25 (40896.06 to 56253.16)	41643472 (35593321 to 48562339)	19491.36 (16521.16 to 22919.92)	-0.6 (-0.62 to -0.57)
	Deaths	38029 (33520 to 42625)	27.72 (25.04 to 30.59)	6243 (5475 to 6721)	2.71 (2.37 to 2.92)	-0.9 (-0.91 to -0.89)
	DALYs	3154322 (2730620 to 3582444)	2006.05 (1745.51 to 2268.63)	244093 (216599 to 276067)	116.69 (102.98 to 133.14)	-0.94 (-0.95 to -0.93)
Western Europe	Prevalence	1408001 (1183959 to 1689714)	438.6 (355.04 to 539.24)	1683577 (1496791 to 1899296)	416.16 (345.33 to 490.54)	-0.05 (-0.11 to 0.01)
	Incidence	92167543 (76349297 to 110346130)	28505.1 (22757.4 to 34939.87)	102588935 (89592335 to 116188594)	25442.59 (20832.64 to 30200.77)	-0.11 (-0.15 to -0.07)
	Deaths	2980 (2680 to 3170)	0.52 (0.47 to 0.56)	13318 (10985 to 14776)	1.12 (0.95 to 1.23)	0.96 (0.81 to 1.09)
	DALYs	216573 (163747 to 282965)	63.23 (45.71 to 84.64)	358703 (300485 to 429953)	68.24 (52.83 to 88.15)	0.05 (-0.01 to 0.13)
Western Sub-Saharan Africa	Prevalence	5410647 (4885111 to 5933268)	2363.89 (2169.09 to 2568.62)	7532094 (6865406 to 8320158)	1482.84 (1372.3 to 1604.33)	-0.38 (-0.41 to -0.35)
	Incidence	327227137 (288708266 to 366253411)	144649.34 (130049.86 to 162001.6)	513977912 (454637135 to 578613767)	101090.39 (91655.59 to 111930.73)	-0.3 (-0.34 to -0.26)
	Deaths		188.92 (127.39 to 258.31)		65.53 (45.98 to 88.84)	-0.68 (-0.75 to -0.59)

(Continued)

10.3389/fcimb.2025.1527765

TABLE 1 Continued

GBD Regions		1990		2021		1990–2021
		All-ages cases	Age-standardized rates per 100,000	All-ages cases	Age-standardized rates per 100,000	Rate change in age-standardized rates
		N (95%UI)		N (95%UI)		N (95%UI)
	DALYs	416168 (304048 to 507528)	9643.34 (6926.45 to 11864.65)	283674 (203307 to 375380)	3383.88 (2464.9 to 4393.17)	-0.68 (-0.75 to -0.6)
		32103726 (23334866 to 38990208)		21790570 (15281983 to 29569603)		

DALYs, Disability-adjusted life years; GBD, Global Burden of Disease.

National and territorial level

Enteric infections

In 2021, India had the highest number of prevalence cases, totaling 29,470,511 (Supplementary Table S5). South Sudan had the highest ASPR at 2888.11 (Supplementary Table S6; Figure 1A). Between 1990 and 2021, North Korea experienced the fastest increase, with an upward trend of 2.68 (Supplementary Table S7). India had the highest number of incidence cases with 1,898,215,166 (Supplementary Table S5). South Sudan had the highest ASIR at 175498.06 (Supplementary Table S6; Figure 1B). Between 1990 and 2021, North Korea experienced the fastest increase, with an upward trend of 2.6 (Supplementary Table S7). Regarding deaths, India had the highest number with 552,102 (Supplementary Table S5). South Sudan had the highest ASMR at 168.95 (Supplementary Table S6; Figure 1C). Between 1990 and 2021, India experienced the fastest increase, with an upward trend of 15.37 (Supplementary Table S7). Furthermore, India also had the highest number of DALYs with 20,822,873 (Supplementary Table S5). Chad had the highest ASR of DALYs at 7791.23 (Supplementary Table S6; Figure 1D). Between 1990 and 2021, Sweden experienced the fastest increase, with an upward trend of 1.14 (Supplementary Table S7).

Diarrheal diseases

In 2021, India had the highest number of prevalence cases with 29,167,174 (Supplementary Table S8). South Sudan had the highest ASPR at 2881.95 (Supplementary Table S9). Between 1990 and 2021, North Korea experienced the fastest increase, with an upward trend of 2.69 (Supplementary Table S10). India had the highest number of incidence cases with 1,892,784,379 (Supplementary Table S8). South Sudan had the highest ASIR at 175395.84 (Supplementary Table S9). Between 1990 and 2021, North Korea experienced the fastest increase, with an upward trend of 2.6 (Supplementary Table S10). India also had the highest number of deaths with 496,725 (Supplementary Table S8). South Sudan had the highest ASMR at 166.68 (Supplementary Table S9). Between 1990 and 2021, Sweden experienced the fastest increase, with an upward trend of 16.15 (Supplementary Table S10). India had the highest number of DALYs with 16,762,076 (Supplementary Table S8). Chad had the highest ASR of DALYs at 7341.22 (Supplementary Table S9). Between 1990 and 2021, Sweden experienced the fastest increase, with an upward trend of 1.16 (Supplementary Table S10).

Typhoid fever

In 2021, a study conducted at the country and regional level found that India had the highest number of prevalence cases, incidence and deaths, with 234,912, 3,715,087 and 41,586 respectively (Supplementary Table S11). Burkina Faso had the highest ASPR at 20.76 (Supplementary Table S12). Between 1990 and 2021, Australia experienced the fastest increase, with an upward trend of 0.87 (Supplementary Table S1). Burkina Faso had the highest ASIR at 328.48 (Supplementary Table S12). Between 1990 and 2021, Australia experienced the fastest increase, with an upward

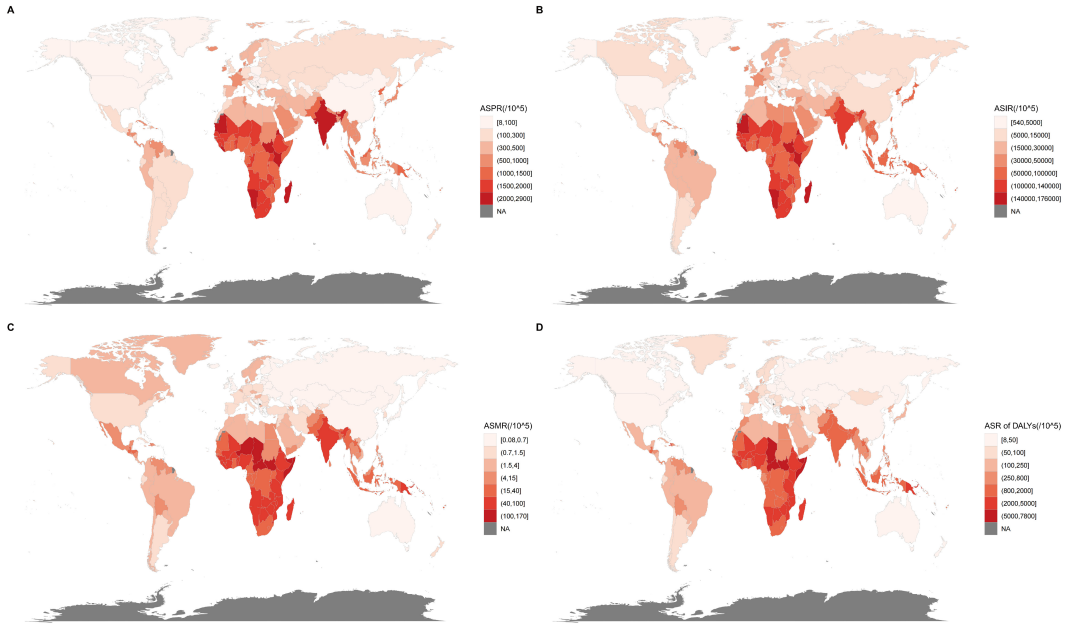

FIGURE 1
Global distribution of enteric infections disease burden in 2021. **(A)** ASPR of enteric infections; **(B)** ASIR of enteric infections; **(C)** ASMR of enteric infections; **(D)** ASR of DALYs of enteric infections. ASPR, Age-standardized prevalence rates; ASIR, Age-standardized incidence rates; ASMR, Age-standardized mortality rates; ASR, Age-standardized rate; DALYs, Disability-adjusted life years.

trend of 0.86 (Supplementary Table S1). Bhutan had the highest ASMR at 5.61 (Supplementary Table S12). Denmark experienced the fastest increase, with an upward trend of 58.98 between 1990 and 2021 (Supplementary Table S13). India had the highest number of DALYs with 3,117,354 (Supplementary Table S11). Bhutan had the highest ASR of DALYs at 434.23 (Supplementary Table S12). Between 1990 and 2021, Denmark experienced the fastest increase, with an upward trend of 21.28 (Supplementary Table S13).

Paratyphoid fever

In 2021, India had the highest number of prevalence cases with 73,385 (Supplementary Table S14). India had the highest ASPR at 5.46 (Supplementary Table S15). Between 1990 and 2021, Kenya experienced the fastest increase, with an upward trend of 3.71 (Supplementary Table S16). India had the highest number of incidence cases with 1,673,611 (Supplementary Table S14). India also had the highest ASIR at 124.45 (Supplementary Table S15). Between 1990 and 2021, Kenya experienced the fastest increase, with an upward trend of 3.7 (Supplementary Table S16). India had the highest number of deaths with 9,893 (Supplementary Table S14). Pakistan had the highest ASMR at 1.05 (Supplementary Table S15). Between 1990 and 2021, Denmark experienced the fastest increase, with an upward trend of 275.01 (Supplementary Table S16). India also had the highest number of DALYs with 695,210 (Supplementary Table S14). Pakistan had the highest ASR of DALYs at 72.66 (Supplementary Table S15). Between 1990 and 2021, Denmark experienced the fastest increase, with an upward trend of 125.61 (Supplementary Table S16).

iNTS

In 2021, Nigeria had the highest number of prevalence cases with 3,844 (Supplementary Table S17). Mali had the highest ASPR at 1.74 (Supplementary Table S18). Between 1990 and 2021, the United Kingdom experienced the fastest increase, with an upward trend of 1.75 (Supplementary Table S19). Nigeria had the highest number of incidence cases with 164,230 (Supplementary Table S17). Mali had the highest ASIR at 76.24 (Supplementary Table S18). Between 1990 and 2021, the United Kingdom experienced the fastest increase, with an upward trend of 1.74 (Supplementary Table S19). Nigeria also had the highest number of deaths with 21,614 (Supplementary Table S17). Mali had the highest ASMR at 13.26 (Supplementary Table S18). Between 1990 and 2021, The Bahamas experienced the fastest increase, with an upward trend of 14.25 (Supplementary Table S19). Nigeria had the highest number of DALYs with 1,754,290 (Supplementary Table S17). Mali had the highest ASR of DALYs at 859.23 (Supplementary Table S18). Between 1990 and 2021, The Bahamas experienced the fastest increase, with an upward trend of 13.47 (Supplementary Table S19).

Age, sex, and subtype analysis

In 2021, among enteric infections, the 10-14 year age group exhibited the highest prevalence and incidence rates, while mortality rate was highest among those aged 90 and above, and DALYs rate was highest in children under 5. Females under 90 had

a higher burden of prevalence and incidence compared to males; however, for those aged over 90, both mortality and DALYs rates were lower in females than in males. Due to the large number and variety of pathogens causing diarrheal diseases, only three subtypes, typhoid fever, paratyphoid fever, and iNTS, were included for comparison (Figure 2). Typhoid fever had higher rates across all epidemiological indicators, with the largest proportion of cases seen in children under 5 for prevalence and incidence, iNTS in those over 85 for deaths and DALYs, and Paratyphoid fever had the lowest proportion under 10 years old. Regional distribution of subtypes varied, with the highest proportion of Typhoid fever in prevalence in North Africa and the Middle East having, the highest incidence rates in Eastern Sub-Saharan Africa, and the highest rates of deaths and DALYs in Southeast Asia (Supplementary Figure S1).

Overall temporal trends

Globally, prevalence and incidence rose from 1990 to 2011, then declined until 2015. deaths and DALYs consistently declined, with a moderated decrease between 2003 and 2006(Supplementary Figure S2). In High SDI regions, prevalence and incidence rates shifted from a decline to an increase in 2019, while High-middle, Middle, and Low-middle SDI regions saw this change in 2000, 2016, and 2020, respectively. Low SDI regions had two periods of increase, from 2005 to 2009 and from 2018 to 2020. Except for High SDI peaking in 1991, all SDI regions showed a downward trend in deaths and DALYs. Among the 21 GBD regions, Southern Sub-Saharan Africa had the steepest decline in prevalence and Incidence rates, with females showing a significant increase in the rate of decline from 2004, and both genders showing an increase in 2019. Central Latin America saw a sharp decline in deaths and DALYs after an increase from 1995 to 2000 (Supplementary Figure S3).

Association between ASR and SDI

This section primarily depicts the relationship between the four epidemiological indicators and the SDI. From 1990 to 2021, in the global context and across the 21 GBD regions, ASPR and ASIR declined with increasing SDI, but then rose again in High SDI regions. ASMR and ASR of DALYs also decreased with increasing SDI and remained at very low levels from High-middle SDI regions onwards (Figure 3). Analyzing 204 countries and regions in 2021, the overall trend is similar to that of the global and 21 GBD regions (Supplementary Figure S4).

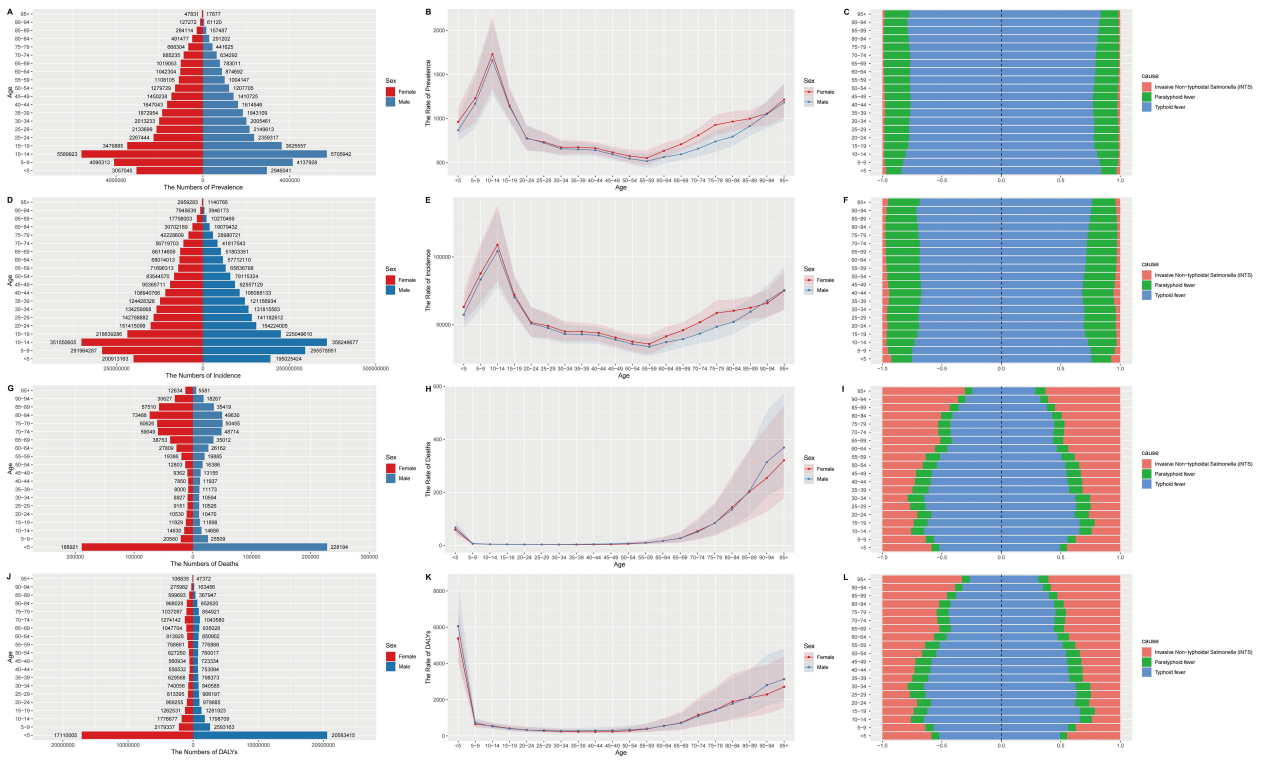

FIGURE 2
Sex, age-structured, and subtype analysis of enteric infections disease burden in 2021. **(A)** The number of prevalence; **(B)** The rate of prevalence; **(C)** The subtype of prevalence in different age groups; **(D)** The number of incidence; **(E)** The rate of incidence; **(F)** The subtype of incidence in different age groups; **(G)** The number of deaths; **(H)** The rate of deaths; **(I)** The subtype of deaths in different age groups; **(J)** The number of DALYs; **(K)** The rate of DALYs; **(L)** The subtype of DALYs in different age groups. DALYs, disability-adjusted life years.

Risk factors analysis

Globally, unsafe water source was the largest contributor to DALYs and deaths, with contribution rates of 58% and 59.9% respectively in 2021. In the 5 SDI regions, Low SDI regions had the largest proportion, with deaths and DALYs reaching 65.4% and 63.8%, while in High SDI regions, deaths and DALYs were only 7.7% and 10% respectively. Among the 21 GBD regions, the Caribbean had the largest proportion, with DALYs reaching up to 73.5%, while Western Europe had the lowest proportion, with Deaths at only 3.6% (Figures 4A, B). Other significant factors include unsafe sanitation, child wasting, child underweight, and child stunting, all of which were most prevalent in Low SDI regions (Figure 4). In 1990, the overall situation was similar to 2021, but each factor accounted for a significantly higher proportion (Figures 4C, D).

Etiological analysis

In 2021, Norovirus emerged as the primary cause of death from enteric infections across all age groups, peaking at 46.33 per 100,000 among individuals over 95. Rotavirus was identified as the main contributor to DALYs in children under 5, with a rate of 1741.65 per 100,000 in 2021, a significant decrease from the 1990 rate of 9398.04 per 100,000 (Figure 5; Supplementary Tables S20-S32). In 2021, Rotavirus was the leading cause of enteric infection fatalities globally, causing 92,607 deaths, with the highest number of total cases in Western Sub-Saharan Africa at 37,189 individuals. Among the five SDI regions, the Low SDI region experienced the highest number of Rotavirus-related deaths. In 1990, the Low-middle SDI region and South Asia had the highest death tolls, with 162,007 and 124,198 fatalities respectively. While Rotavirus has always been the most dangerous pathogen, Shigella was the third leading cause in 1990 with 17,500,460 cases, rising to the second-highest cause in 2021. (Supplementary Figure S5, Supplementary Tables S33-S45 for the global, 5 SDI regions and 21 GBD regions, and Supplementary Tables S46-S58 for 204 countries and territories).

Overall, there has been a significant decrease in the number of deaths and DALYs caused by various pathogens over the past 32 years. Globally, the number of deaths attributed to Rotavirus decreased from 392, 148 in 1990 to 92, 607 in 2021, and DALYs decreased from 32, 857,936 to 7, 279, 772, indicating a significant reduction in the number of cases.

Decomposition analysis

From 1990 to 2021, the increase in prevalence and incidence globally and in High SDI, Low-middle SDI, and Low SDI regions was primarily due to population growth. In High-middle SDI and Middle

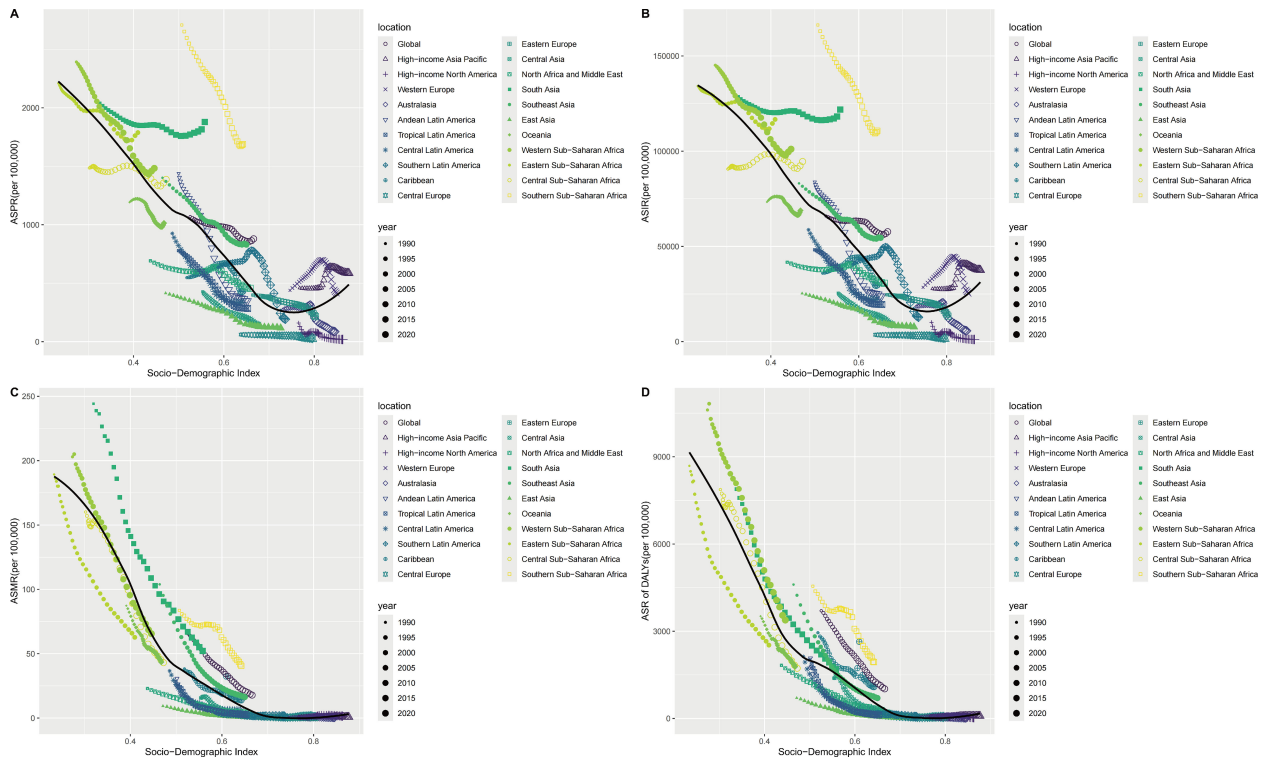

FIGURE 3
The association of the SDI and ASPR, ASIR ASMR, ASR of DALYs of enteric infections, globe and regions from 1990 to 2021. **(A)** The association of the SDI and ASPR; **(B)** The association of the SDI and ASIR; **(C)** The association of the SDI and ASMR; **(D)** The association of the SDI and ASR of DALYs. SDI, Socio-demographic index; ASPR, Age-standardized prevalence rates; ASIR, Age-standardized incidence rates; ASMR, Age-standardized mortality rates; ASR, Age-standardized rates; DALYs, Disability-adjusted life years.

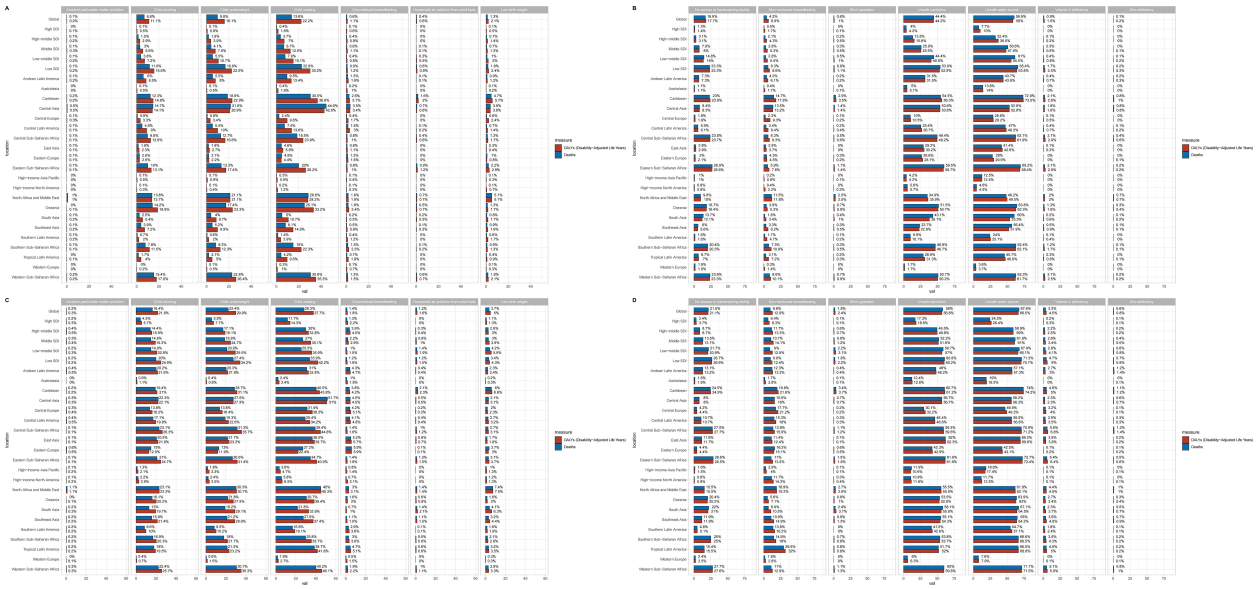

FIGURE 4
The enteric infections DALYs and deaths attributable to risk factors compared in 2021 and 1990, globally and by 21 GBD regions. **(A, B)** DALYs and deaths attributable to risk factors in 2021; (C&D) DALYs and deaths attributable to risk factors in 1990. DALYs, Disability-adjusted life years.

SDI regions, there was a decrease, mainly due to epidemiological changes. The reduction in deaths and DALYs across all four SDI regions (except High SDI) was primarily due to epidemiological changes. In High SDI regions, the increase was attributed to aging for deaths in males (45.62%) and epidemiological changes for deaths in females (44.17%). The increase in DALYs was attributed to population growth (Figure 6; Supplementary Table S59).

Discussion

Enteric infections represent a significant public health challenge worldwide, with a substantial disease burden that has attracted considerable research and attention. This study comprehensively estimated the prevalence, incidence, deaths, and DALYs of enteric infections across 21 global regions, 204 countries and territories, and age groups, as well as risk factors, providing a detailed picture of the disease burden of enteric infections. The main findings are as follows:

Regional variability and risk factors

High-ranking regions for ASPR and ASIR are Low SDI and South Asia, while ASMR and ASR of DALYs are highest in Low SDI and Western Sub-Saharan Africa. America than in South Asia and in sub-Saharan Africa, but higher than in high-income regions. Unsafe water sources contribute significantly to high DALYs and deaths in Low SDI regions, accounting for up to 65.4% and 63.8% respectively. Limited water infrastructure and the use of contaminated drinking water are significant factors (Bain et al., 2014). Inadequate water facilities increase exposure to contaminated sources. In rural Bangladesh, the risk of neonatal death is 3.12 times higher in households without toilets than in those with toilets (Rahman et al., 1985). In many developing areas, untreated water from wells and rivers is used for drinking, bathing, and irrigation (Laffite et al., 2016), leading to severe fecal contamination, especially in rainy and dry seasons (Kayembe et al., 2018).In Latin America and the Caribbean, as well as in East Asia and the Pacific region, the reduction in temperature-attributable enteric infection deaths caused by viral pathogens has led to a net decrease in overall temperature-related enteric infection mortality (Verlicchi et al., 2010).

ASMR and ASR of DALYs decreased with increasing SDI, but the regions with the fastest growth in ASMR and the slowest decrease in ASR of DALYs were High SDI regions, specifically High-income North America and Western Europe. In these high-income areas, policies and facilities have reduced the impact of unsafe water resources on enteric infection-related diseases, but hospital wastewater may become a new source of infection (Boillot et al., 2008; Verlicchi et al., 2010), with its complex mixture of chemicals and biological substances potentially promoting the spread of bacteria and their antibiotic resistance genes (Cosgrove, 2006).

From 1990 to 2021, the global and 21 GBD regions showed a downward trend in ASPR and ASIR with increasing SDI, reflecting the positive impact of socio-economic development on health status improvement. Notably, in 2021, High-income Asia Pacific ranked high in ASPR and ASIR, which, in addition to unsafe water resources, may also reflect the high sensitivity or high-risk exposure of specific populations in the region, such as the elderly, chronic disease patients, or immigrant groups, to enteric infections. The systemic inflammation that occurs during aging can lead to dysbiosis (Li et al., 2016), and the microbiota that was dominant in

FIGURE 5
Etiological analysis of enteric infections for both sexes among all age groups in 1990 and 2021. **(A)** Etiological analysis of males in deaths (2021), **(B)** Etiological analysis of females in deaths (2021); **(C)** Etiological analysis of males in DALYs (2021); **(D)** Etiological analysis of females in DALYs (2021); **(E)** Etiological analysis of males in deaths (1990), **(F)** Etiological analysis of females in deaths (1990); **(G)** Etiological analysis of males in DALYs (1990); **(H)** Etiological analysis of females in DALYs (1990). DALYs, Disability-adjusted life years.

youth can become pathogen-rich, such as Enterobacteriaceae (Fransen et al., 2017), increasing the risk of disease. The high-fat and high-sugar dietary habits common in High-income Asia Pacific may promote dysbiosis (Randeni et al., 2024). Also, physical activity, stress levels, sleep patterns, medication use, and even mental state can affect the gut microbiome (Mundula et al., 2022; Mundula et al., 2023). Over the past three decades, environmental issues and international travel have significantly increased transmission risk and infection prevalence of enteric diseases (Love et al., 2024). So the incidence of disease increases significantly for those who have traveled to South Asian countries such as India, Nepal, and Bhutan (Kuenzli et al., 2017).

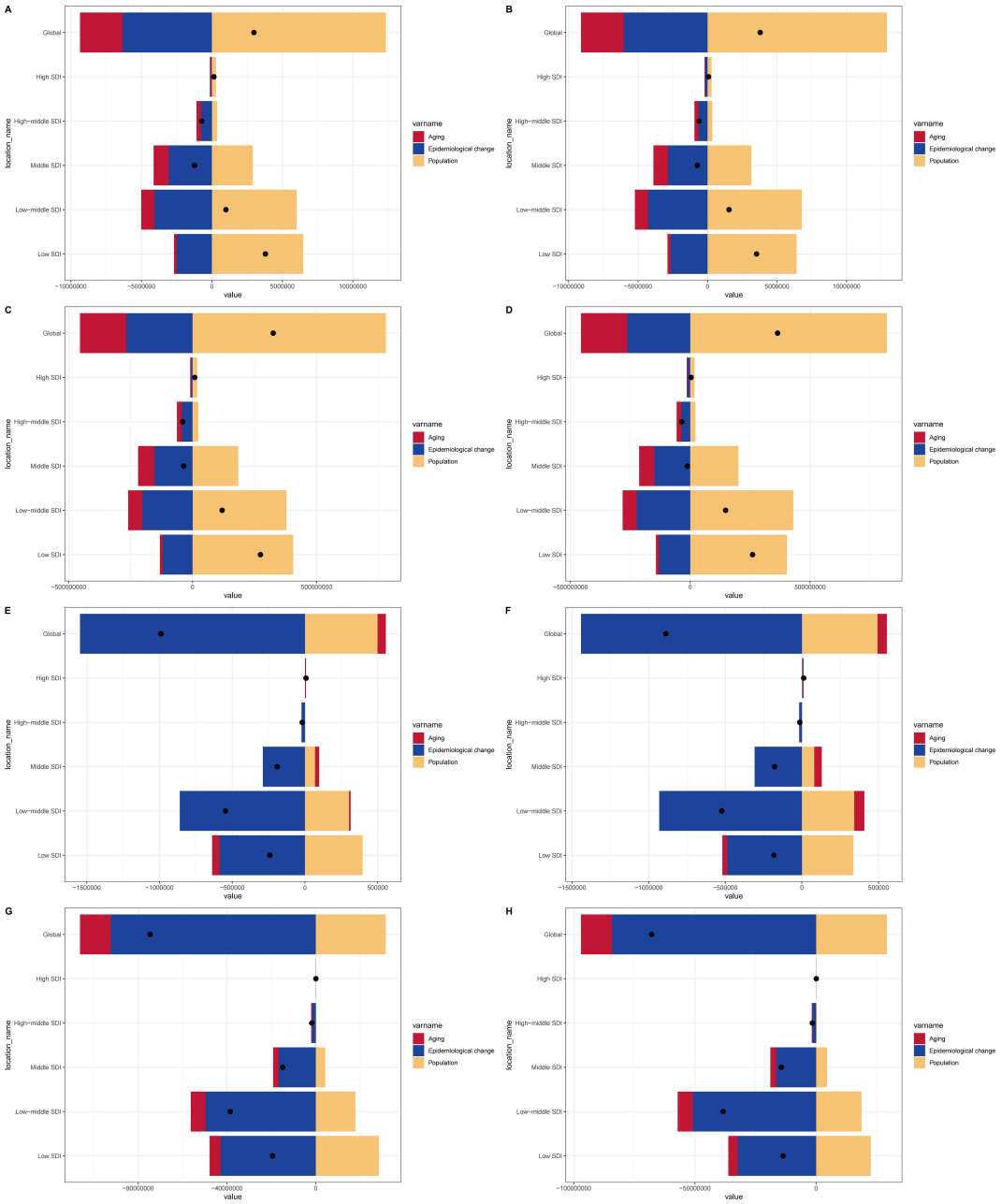

FIGURE 6
Changes in prevalence, incidence, deaths, and DALYs for both sexes according to population-level determinants of population growth, aging, and epidemiological change from 1990 to 2021 in the globe and SDI regions. **(A)** Changes in prevalence of males; **(B)** Changes in prevalence of females; **(C)** Changes in incidence of males; **(D)** Changes in incidence of females; **(E)** Changes in deaths of males; **(F)** Changes in deaths of females; **(G)** Changes in DALYs of males; **(H)** Changes in DALYs of females. SDI, Socio-demographic index; DALYs, Disability-adjusted life years.

Subtype analysis

In 2021, typhoid fever was the leading cause of high intestinal infections (prevalence and incidence) in Central Latin America and Southeast Asia (Supplementary Figure S1). A systematic review and meta-analysis of case-control studies assessing the association between typhoid and WASH as well as food exposure suggested that poor sanitation and untreated water had the strongest correlation with typhoid risk (Brockett et al., 2020). Moreover, warm and humid climates likely contribute to pathogen survival and growth, with higher temperatures enhancing their proliferation (Lal et al., 2012). Furthermore, Salmonella typhi has developed strong drug resistance (Browne et al., 2020). From a low base in 1990, the prevalence of fluoroquinolone-resistant Salmonella typhi surged, reaching an overall prevalence of 95.2% in South Asia by 2019 (Zakir et al., 2021; GRAM Typhoid Collaborators for 2024, 2024). Since 2016, Pakistan has experienced an outbreak of typhoid caused by extensively drug-

resistant (XDR) S., which may be closely related to international air travel (Walker et al., 2023).

It is noteworthy that in High-income North America and High-income Asia Pacific regions, typhoid fever accounts for the smallest proportion of enteric infection deaths and DALYs; instead, iNTS has become the main cause of death, mainly related to the difficulty in treating iNTS and its multiple complications (Supplementary Figure S1). A meta-analysis indicated that a significant proportion of patients with non-typhoidal Salmonella invasive diseases have life-threatening complications such as encephalopathy and pleuropulmonary infections. Among the 84 studies it summarized, 66 (78.6%) had a high overall bias risk, 18 (21.4%) were at moderate risk, none were at low risk, and about 15% of patients with non-typhoidal Salmonella invasive diseases eventually died (Marchello et al., 2022), highlighting the deadliness of iNTS.

Age and gender analysis

Age and gender both influence the gut microbiota (Singh and Manning, 2016). According to age analysis, the burden is heavier on infants, adolescents, and the elderly (Figure 2). The richness of the microbial community increases with age in children, but it is still lower than the diversity of the adult microbiota at the age of 5 (Roswall et al., 2021). Additionally, the mode of birth, microbiota-directed food, and other factors may be related to the gut microbiota in early life (Gehrig et al., 2019). Furthermore, whether mothers wash their hands before breastfeeding and after cleaning the child, the child's use of toilet facilities and the child's hygiene habits such as washing hands before meals and not putting hands in the mouth can also be contributing factors.

Elderly individuals often acquire frailness-associated bacteria like low Bifidobacterium (Pang et al., 2023). Long-term medication use can lead to abnormal microbiomes and metabolomes in the elderly (Forslund et al., 2021; Li et al., 2024), contributing to higher death rates, along with physical decline and hospital-acquired infections (Taylor and Oppenheim, 1998). Malnutrition, including child wasting, stunting, underweight, and unsafe sanitation significantly increase the risk of intestinal infections in children, with 48.7% of malnourished children in southern Ethiopia affected by parasitic infections (Yoseph and Beyene, 2020).

The greater burden of prevalence and incidence in females than in males may be largely influenced by cultural customs. In rural communities in West Bengal, India, logistic regression analysis showed that boys had 4.2 times more opportunity to spend more money on medical treatment and were 4.9 times more likely to receive early medical care than girl, with the highest gender bias among mothers with higher education (Bhan et al., 2005).

Etiological analysis

In the field of enteric infections, there have been significant changes in the distribution of causes and the resulting deaths and DALYs in recent years. From 1990 to 2021, Norovirus, Enterotoxigenic E. coli, and Cryptosporidium have continued to pose threats worldwide, but Rotavirus has always dominated, especially in causing deaths from intestinal infections in children.

However, it is noteworthy that over the past 32 years, there has been a significant decrease in the number of deaths and DALYs caused by various etiologies of enteric infections. Taking Rotavirus as an example, the global deaths it caused dropped from 392,147 in 1990 to 92,607 in 2021, and DALYs decreased from 32,857,936 to 7,279,772, mainly due to the widespread vaccination against Rotavirus and the strengthening of global healthcare (Soares-Weiser et al., 2019). Since 2006, vaccines such as RotaTeq, Rotarix, and Rotavac, which have been proven to significantly prevent Rotavirus infection have gradually been approved and launched (Wiedermann and Kollaritsch, 2006). Governments and research institutions around the world are also continuously exploring the development and application of new Rotavirus vaccines to achieve better prevention outcomes (ACIP recommends new vaccine to prevent rotavirus. An update from CDC, 2006).

Overall and future trends analysis

From 1990 to 2021, global prevalence and incidence of enteric infections saw turning points in 2011 and 2015, likely due to increased vaccine R&D investments by WHO and governments, especially the broader use of vaccines like Rotavirus (Muhsen et al., 2015; Enane et al., 2016; Kobayashi et al., 2018).

In high SDI regions, the downward trend in prevalence and incidence rates for both males and females reversed to an upward trend in 2019 (Leung et al., 2003). The emergence of COVID-19 in 2019 was primarily a respiratory infection, often accompanied by gastrointestinal involvement, and up to half of patients' gastrointestinal symptoms preceded respiratory symptoms, which complicated the treatment of intestinal infections (Jin et al., 2022). COVID-19 or antiviral treatments may also cause liver damage, adding to the challenge of managing enteric infections (Chen et al., 2020). Despite this, deaths and DALYs showed a downward trend across all SDI regions, except for high SDI. This could be attributed to advancements in medical technology and increased medical resources, significantly improving treatment outcomes for intestinal infectious diseases (Zhou et al., 2023; Cheng et al., 2024). Early detection, diagnosis, and treatment have also reduced the disease's impact on patients, thereby reducing DALYs (Zhou et al., 2023; Cheng et al., 2024).

Limitations

However, this study also has limitations. First, the GBD database primarily compiles data from national and regional reports and publications, rather than direct national reports, which may lead to issues with data completeness, timeliness, and quality, especially in low-income areas where there may be a lack of

access to raw data, potentially hindering GBD researchers in their estimations. Additionally, differences in disease management across countries and regions, including diagnosis, recording, and reporting, may affect the results.

Data availability statement

The original contributions presented in the study are included in the article/Supplementary Material. Further inquiries can be directed to the corresponding authors.

Author contributions

YZ: Conceptualization, Data curation, Formal Analysis, Funding acquisition, Investigation, Methodology, Software, Writing – original draft, Writing – review & editing. YRZ: Conceptualization, Formal Analysis, Investigation, Validation, Writing – original draft, Writing – review & editing. ZC: Formal Analysis, Investigation, Resources, Writing – original draft, Writing – review & editing. ZJ: Visualization, Writing – original draft, Writing – review & editing. YY: Data curation, Writing – original draft, Writing – review & editing. JW: Funding acquisition, Supervision, Writing – original draft, Writing – review & editing. HL: Supervision, Writing – review & editing.

Funding

The author(s) declare that financial support was received for the research and/or publication of this article. This study was supported by Special Fund Project for Science and Technology Innovation Strategy of Guangdong Province (Grant number pdjh2023b0107), Shenzhen Science and Technology Planning Project (No. JCYJ20220530165014033), Medical research project of Shenzhen Longhua Medical Association (2023LHMA10) and Shenzhen Medical Key Discipline (No. MKD202007090201), Special Fund for Science and Technology Innovation in Longhua District, Shenzhen (11501A20240704D87ABF8).

Acknowledgments

We appreciate the excellent works by the Global Burden of Diseases, Injuries, and Risk Factors Study (GBD) 2021 collaborators.

Conflict of interest

The authors declare that the research was conducted in the absence of any commercial or financial relationships that could be construed as a potential conflict of interest.

Generative AI statement

The author(s) declare that no Generative AI was used in the creation of this manuscript.

Publisher's note

All claims expressed in this article are solely those of the authors and do not necessarily represent those of their affiliated organizations, or those of the publisher, the editors and the reviewers. Any product that may be evaluated in this article, or claim that may be made by its manufacturer, is not guaranteed or endorsed by the publisher.

Supplementary material

The Supplementary Material for this article can be found online at: https://www.frontiersin.org/articles/10.3389/fcimb.2025.1527765/full#supplementary-material

References

(2006). ACIP recommends new vaccine to prevent rotavirus. An update from CDC. (Chinese Center For Disease Control And Prevention) 105, 20.

Bain, R., Cronk, R., Hossain, R., Bonjour, S., Onda, K., Wright, J., et al. (2014). Global assessment of exposure to faecal contamination through drinking water based on a systematic review. *Trop. Med. Int. Health* 19, 917–927. doi: 10.1111/tmi.2014.19.issue-8

Bhan, G., Bhandari, N., Taneja, S., Mazumder, S., and Bahl, R. (2005). The effect of maternal education on gender bias in care-seeking for common childhood illnesses. *Soc. Sci. Med.* 60, 715–724. doi: 10.1016/j.socscimed.2004.06.011

Boccuzzi, S. J. (2003). "Indirect health care costs," in *Cardiovascular Health Care Economics*. Ed. W. S. Weintraub (Humana Press, Totowa, NJ), 63–79.

Boillot, C., Bazin, C., Tissot-Guerraz, F., Droguet, J., Perraud, M., Cetre, J. C., et al. (2008). Daily physicochemical, microbiological and ecotoxicological fluctuations of a hospital effluent according to technical and care activities. *Sci. Total Environ.* 403, 113–129. doi: 10.1016/j.scitotenv.2008.04.037

Brockett, S., Wolfe, M. K., Hamot, A., Appiah, G. D., Mintz, E. D., and Lantagne, D. (2020). Associations among water, sanitation, and hygiene, and food exposures and typhoid fever in case-control studies: A systematic review and meta-analysis. *Am. J. Trop. Med. Hyg* 103, 1020–1031. doi: 10.4269/ajtmh.19-0479

Browne, A. J., Hamadani, B. H. K., Kumaran, E. A. P., Rao, P., Longbottom, J., Harriss, E., et al. (2020). Drug-resistant enteric fever worldwide, 1990 to 2018: a systematic review and meta-analysis. *BMC Med.* 18, 22. doi: 10.1186/s12916-019-1443-1

Chen, N., Zhou, M., Dong, X., Qu, J., Gong, F., Han, Y., et al. (2020). Epidemiological and clinical characteristics of 99 cases of 2019 novel coronavirus pneumonia in Wuhan, China: a descriptive study. *Lancet* 395, 507–513. doi: 10.1016/S0140-6736(20)30211-7

Cheng, Z., Wang, T., Jiao, Y., Qi, J., Zhang, X., Zhou, S., et al. (2024). Burden of digestive system diseases in China and its provinces during 1990-2019: Results of the 2019 Global Disease Burden Study. *Chin. Med. J. (Engl)* 137, 2182–2189. doi: 10.1097/CM9.0000000000003277

Cosgrove, S. E. (2006). The relationship between antimicrobial resistance and patient outcomes: mortality, length of hospital stay, and health care costs. *Clin. Infect. Dis.* 42, S82–S89. doi: 10.1086/499406

Das Gupta, P. (1978). A general method of decomposing a difference between two rates into several components. *Demography* 15, 99–112. doi: 10.2307/2060493

Debellut, F., Friedrich, A., Baral, R., Pecenka, C., Mugisha, E., and Neuzil, K. M. (2024). The cost of typhoid illness in low- and middle-income countries, a scoping review of the literature. *PloS One* 19, e0305692. doi: 10.1371/journal.pone.0305692

Enane, L. A., Gastañaduy, P. A., Goldfarb, D. M., Pernica, J. M., Mokomane, M., Moorad, B., et al. (2016). Impact of rotavirus vaccination on hospitalizations and deaths from childhood gastroenteritis in Botswana. *Clin. Infect. Dis.* 62 Suppl 2, S168–S174. doi: 10.1093/cid/civ1210

Forslund, S. K., Chakaroun, R., Zimmermann-Kogadeeva, M., Markó, L., Aron-Wisnewsky, J., Nielsen, T., et al. (2021). Combinatorial, additive and dose-dependent drug–microbiome associations. *Nature* 600, 500–505. doi: 10.1038/s41586-021-04177-9

Fransen, F., van Beek, A. A., Borghuis, T., Aidy, S. E., Hugenholtz, F., van-der-Gaast-de-Jongh, C., et al. (2017). Aged Gut Microbiota Contributes to Systemical Inflammaging after Transfer to Germ-Free Mice. *Front. Immunol.* 8, 1385. doi: 10.3389/fimmu.2017.01385

GBD 2021 Causes of Death Collaborators. (2024). Global burden of 288 causes of death and life expectancy decomposition in 204 countries and territories and 811 subnational locations, 1990-2021: a systematic analysis for the Global Burden of Disease Study 2021. *Lancet* 403, 2100–2132. doi: 10.1016/S0140-6736(24)00367-2

GBD 2021 Diseases and Injuries Collaborators. (2024). Global incidence, prevalence, years lived with disability (YLDs), disability-adjusted life-years (DALYs), and healthy life expectancy (HALE) for 371 diseases and injuries in 204 countries and territories and 811 subnational locations, 1990-2021: a systematic analysis for the Global Burden of Disease Study 2021. *Lancet* 403, 2133–2161. doi: 10.1016/S0140-6736(24)00757-8

Gehrig, J. L., Venkatesh, S., Chang, H. W., Hibberd, M. C., Kung, V. L., Cheng, J., et al. (2019). Effects of microbiota-directed foods in gnotobiotic animals and undernourished children. *Science* 365. doi: 10.1126/science.aau4732

GRAM Typhoid Collaborators for 2024. (2024). Estimating the subnational prevalence of antimicrobial resistant Salmonella enterica serovars Typhi and Paratyphi A infections in 75 endemic countries, 1990-2019: a modelling study. *Lancet Glob Health* 12, e406–e418. doi: 10.1016/S2214-109X(23)00585-5

Hajra, D., Nair, A. V., and Chakravortty, D. (2023). Decoding the invasive nature of a tropical pathogen of concern: The invasive non-Typhoidal Salmonella strains causing host-restricted extraintestinal infections worldwide. *Microbiol. Res.* 277, 127488. doi: 10.1016/j.micres.2023.127488

Hoivik, M. L., Moum, B., Solberg, I. C., Cvancarova, M., Hoie, O., Vatn, M. H., et al. (2012). Health-related quality of life in patients with ulcerative colitis after a 10-year disease course: results from the IBSEN study. *Inflammation Bowel Dis.* 18, 1540–1549. doi: 10.1002/ibd.21863

Jin, S., Lu, X., and Xu, C. (2022). COVID-19 induces gastrointestinal symptoms and affects patients' prognosis. *J. Int. Med. Res.* 50, 3000605221129543. doi: 10.1177/03000605221129543

Kayembe, J. M., Thevenon, F., Laffite, A., Sivalingam, P., Ngelinkoto, P., Mulaji, C. K., et al. (2018). High levels of faecal contamination in drinking groundwater and recreational water due to poor sanitation, in the sub-rural neighbourhoods of Kinshasa, Democratic Republic of the Congo. *Int. J. Hyg Environ. Health* 221, 400–408. doi: 10.1016/j.ijheh.2018.01.003

Kobayashi, M., Adachi, N., Miyazaki, M., and Tatsumi, M. (2018). Decline of rotavirus-coded hospitalizations in children under 5 years: A report from Japan where rotavirus vaccines are self-financed. *Vaccine* 36, 2727–2732. doi: 10.1016/j.vaccine.2017.10.033

Kuenzli, E., Juergensen, D., Kling, K., Jaeger, V. K., DeCrom, S., Steffen, R., et al. (2017). Previous exposure in a high-risk area for travellers' diarrhoea within the past year is associated with a significant protective effect for travellers' diarrhoea: a prospective observational cohort study in travellers to South Asia. *J. Travel Med.* 24. doi: 10.1093/jtm/tax056

Laffite, A., Kilunga, P. I., Kayembe, J. M., Devarajan, N., Mulaji, C. K., Giuliani, G., et al. (2016). Hospital effluents are one of several sources of metal, antibiotic resistance genes, and bacterial markers disseminated in sub-saharan urban rivers. *Front. Microbiol.* 7. doi: 10.3389/fmicb.2016.01128

Lal, A., Hales, S., French, N., and Baker, M. G. (2012). Seasonality in human zoonotic enteric diseases: A systematic review. *PloS One* 7, e31883. doi: 10.1371/journal.pone.0031883

Leung, W. K., To, K. F., Chan, P. K., Chan, H. L., Wu, A. K., Lee, N., et al. (2003). Enteric involvement of severe acute respiratory syndrome-associated coronavirus infection. *Gastroenterology* 125, 1011–1017. doi: 10.1016/j.gastro.2003.08.001

Li, T., Ding, N., Guo, H., Hua, R., Lin, Z., Tian, H., et al. (2024). A gut microbiota-bile acid axis promotes intestinal homeostasis upon aspirin-mediated damage. *Cell Host Microbe* 32, 191–208.e199. doi: 10.1016/j.chom.2023.12.015

Li, H., Qi, Y., and Jasper, H. (2016). Preventing age-related decline of gut compartmentalization limits microbiota dysbiosis and extends lifespan. *Cell Host Microbe* 19, 240–253. doi: 10.1016/j.chom.2016.01.008

Love, N. K., Jenkins, C., McCarthy, N., Baker, K. S., Manley, P., and Wilson, D. (2024). International travel as a risk factor for gastrointestinal infections in residents of North East England. *Epidemiol. Infect.* 152, e97. doi: 10.1017/S0950268824000827

Marchello, C. S., Birkhold, M., Crump, J. A., Martin, L. B., Ansah, M. O., Breghi, G., et al. (2022). Complications and mortality of non-typhoidal salmonella invasive disease: a global systematic review and meta-analysis. *Lancet Infect. Dis.* 22, 692–705. doi: 10.1016/S1473-3099(21)00615-0

Muhsen, K., Rubenstein, U., Kassem, E., Goren, S., Schachter, Y., Kremer, A., et al. (2015). A significant and consistent reduction in rotavirus gastroenteritis hospitalization of children under 5 years of age, following the introduction of universal rotavirus immunization in Israel. *Hum. Vaccin Immunother.* 11, 2475–2482. doi: 10.1080/21645515.2015.1056951

Mundula, T., Baldi, S., Gerace, E., and Amedei, A. (2023). Role of the intestinal microbiota in the genesis of major depression and the response to antidepressant drug therapy: A narrative review. *Biomedicines* 11. doi: 10.3390/biomedicines11020550

Mundula, T., Russo, E., Curini, L., Giudici, F., Piccioni, A., Franceschi, F., et al. (2022). Chronic systemic low-grade inflammation and modern lifestyle: the dark role of gut microbiota on related diseases with a focus on COVID-19 pandemic. *Curr. Med. Chem.* 29, 5370–5396. doi: 10.2174/0929867329666220430131018

Pang, S., Chen, X., Lu, Z., Meng, L., Huang, Y., Yu, X., et al. (2023). Longevity of centenarians is reflected by the gut microbiome with youth-associated signatures. *Nat. Aging* 3, 436–449. doi: 10.1038/s43587-023-00389-y

Rahman, M., Wojtyniak, B., Rahaman, M. M., and Aziz, K. M. S. (1985). Impact of environmental sanitation and crowding on infant mortality in rural Bangladesh. *Lancet* 2, 28–30. doi: 10.1016/S0140-6736(85)90068-6

Randeni, N., Bordiga, M., and Xu, B. (2024). A comprehensive review of the triangular relationship among diet-gut microbiota-inflammation. *Int. J. Mol. Sci.* 25. doi: 10.3390/ijms25179366

Roswall, J., Olsson, L. M., Kovatcheva-Datchary, P., Nilsson, S., Tremaroli, V., Simon, M. C., et al. (2021). Developmental trajectory of the healthy human gut microbiota during the first 5 years of life. *Cell Host Microbe* 29, 765–776.e763. doi: 10.1016/j.chom.2021.02.021

Singh, P., and Manning, S. D. (2016). Impact of age and sex on the composition and abundance of the intestinal microbiota in individuals with and without enteric infections. *Ann. Epidemiol.* 26, 380–385. doi: 10.1016/j.annepidem.2016.03.007

Soares-Weiser, K., Bergman, H., Henschke, N., Pitan, F., and Cunliffe, N. (2019). Vaccines for preventing rotavirus diarrhoea: vaccines in use. *Cochrane Database Syst. Rev.* 2019. doi: 10.1002/14651858.CD008521.pub5

Sun, P., Yu, C., Yin, L., Chen, Y., Sun, Z., Zhang, T., et al. (2024). Global, regional, and national burden of female cancers in women of child-bearing age, 1990-2021: analysis of data from the global burden of disease study 2021. *EClinicalMedicine* 74, 102713. doi: 10.1016/j.eclinm.2024.102713

Taylor, M. E., and Oppenheim, B. A. (1998). Hospital-acquired infection in elderly patients. *J. Hosp Infect.* 38, 245–260. doi: 10.1016/S0195-6701(98)90074-3

Torgerson, P. R., Devleesschauwer, B., Praet, N., Speybroeck, N., Willingham, A. L., Kasuga, F., et al. (2015). World Health Organization Estimates of the Global and Regional Disease Burden of 11 Foodborne Parasitic Diseases, 2010: A Data Synthesis. *PloS Med.* 12, e1001920. doi: 10.1371/journal.pmed.1001920

Tuo, Y., Li, Y., Li, Y., Ma, J., Yang, X., Wu, S., et al. (2024). Global, regional, and national burden of thalassemia, 1990-2021: a systematic analysis for the global burden of disease study 2021. *EClinicalMedicine* 72, 102619. doi: 10.1016/j.eclinm.2024.102619

Verlicchi, P., Galletti, A., Petrovic, M., and Barceló, D. (2010). Hospital effluents as a source of emerging pollutants: An overview of micropollutants and sustainable treatment options. *J. Hydrology* 389, 416–428. doi: 10.1016/j.jhydrol.2010.06.005

Walker, J., Chaguza, C., Grubaugh, N. D., Carey, M., Baker, S., Khan, K., et al. (2023). Assessing the global risk of typhoid outbreaks caused by extensively drug resistant Salmonella Typhi. *Nat. Commun.* 14, 6502. doi: 10.1038/s41467-023-42353-9

Wiedermann, U., and Kollaritsch, H. (2006). Vaccines against traveler's diarrhoea and rotavirus disease - a review. *Wien Klin Wochenschr* 118, 2–8. doi: 10.1007/s00508-006-0671-5

World Health Organization. (2021). "World health statistics 2021," in *The top 10 causes of death*. (World Health Organization).

Yang, K., Yang, X., Jin, C., Ding, S., Liu, T., Ma, B., et al. (2024). Global burden of type 1 diabetes in adults aged 65 years and older, 1990-2019: population based study. *Bmj* 385, e078432. doi: 10.1136/bmj-2023-078432

Yoseph, A., and Beyene, H. (2020). The high prevalence of intestinal parasitic infections is associated with stunting among children aged 6-59 months in Boricha Woreda, Southern Ethiopia: a cross-sectional study. *BMC Public Health* 20, 1270. doi: 10.1186/s12889-020-09377-y

Zakir, M., Khan, M., Umar, M. I., Murtaza, G., Ashraf, M., and Shamim, S. (2021). Emerging trends of multidrug-resistant (MDR) and extensively drug-resistant (XDR) salmonella typhi in a tertiary care hospital of Lahore, Pakistan. *Microorganisms* 9. doi: 10.3390/microorganisms9122484

Zhou, J. L., Bao, J. C., Liao, X. Y., Chen, Y. J., Wang, L. W., Fan, Y. Y., et al. (2023). Trends and projections of inflammatory bowel disease at the global, regional and national levels, 1990-2050: a bayesian age-period-cohort modeling study. *BMC Public Health* 23, 2507. doi: 10.1186/s12889-023-17431-8

frontiers | Frontiers in Immunology

TYPE Original Research
PUBLISHED 24 April 2025
DOI 10.3389/fimmu.2025.1545667

Check for updates

OPEN ACCESS

EDITED BY
Rommel Chacon-Salinas,
Instituto Politécnico Nacional, Mexico

REVIEWED BY
Gina Stella Garcia-Romo,
National Autonomous University of Mexico, Mexico
Raúl Antonio Maqueda-Alfaro,
National Polytechnic Institute of Mexico (CINVESTAV), Mexico

*CORRESPONDENCE
Jianjie Wang
jmsdxjianjie@163.com
Qingyang Dong
dongqy_meta@126.com

†These authors have contributed equally to this work

RECEIVED 15 December 2024
ACCEPTED 07 April 2025
PUBLISHED 24 April 2025

CITATION
Meng D, Wang J, Du L, Hu X, Liu Y, Zhang P, Wang J and Dong Q (2025) PD-L1 in plasmacytoid dendritic cells promote HBV persistence through disrupting humoral immune response. *Front. Immunol.* 16:1545667. doi: 10.3389/fimmu.2025.1545667

PD-L1 in plasmacytoid dendritic cells promote HBV persistence through disrupting humoral immune response

Danyang Meng[1,2†], Jinhao Wang[2†], Lianqun Du[2†], Xiaojun Hu[2], Ying Liu[2], Pengcheng Zhang[2], Jianjie Wang[1*] and Qingyang Dong[2*]

[1]School of Basic Medicine, Jiamusi University, Jiamusi, Heilongjiang, China, [2]Military Medical Sciences Academy, Academy of Military Sciences, Tianjin, China

Objective: To investigate the efficacy of PD-L1 blockade in restoring humoral immune response against HBV.

Methods: HBV-persistent C57BL/6J mice were established through hydrodynamic tail vein injection of 10 μg pAAV-HBV1.2 plasmid. Subsequently, mice treated i.p. with anti-PD-L1 and/or anti-CTLA-4 at specified time points, with dosages of 500 μg, 250 μg, and 250 μg, respectively. Additionally, 5×10^5 magnetic bead-purified plasmacytoid dendritic cells (pDCs) were adoptively transferred i.v. into the acute mouse model followed by anti-PD-L1 treatment. Quantitative real-time PCR was employed to assess the expression levels of costimulatory and tolerogenic molecules in two dendritic cell subsets. Serum HBsAg and HBsAb were measured using ELISA. Flow cytometry was utilized to quantify T follicular helper (Tfh) cells, regulatory T cells (Treg), and germinal center (GC) B cells.

Results: PD-L1 blockade markedly enhanced the differentiation of Tfh cells and GC B cells in HBV-persistent C57BL/6J mice, thereby promoting HBV clearance. Additionally, pDCs exhibited an increased capacity to induce immune tolerance, with pDCs isolated from HBV carriers inducing viral persistence. This persistence was effectively counteracted by treatment with anti-PD-L1.

Conclusion: pDCs mediate the dysregulation of the humoral immune response to HBV through PD-L1 in chronic hepatitis B infection, highlighting a promising target for the management of chronic HBV.

KEYWORDS

humoral immune deficiencies, pDCs, PD-L1, CHB, Tfh, GC B cell

Introduction

CHB (Chronic hepatitis B) infection remains a global health challenge, affecting approximately 256 million individuals and resulting in 1.1 million deaths annually, primarily from cirrhosis and hepatocellular carcinoma (1). Current therapies, including long-term nucleos(t)ide analogues (NUCs) and PEGylated interferon α (IFNα), are effective in suppressing HBV replication but rarely achieve a functional cure (2, 3). In the absence of treatment, 15–40% of individuals with chronic HBV infection progress to cirrhosis or develop liver cancer (4). Extended or indefinite treatment not only incurs significant costs but also limits accessibility, underscoring the urgent need for more effective and less toxic therapeutic strategies.

Recent advances in immunology have promoted the development of immunotherapeutic strategies targeting various diseases. In CHB patients, the immune landscape is characterized by an absence of neutralizing antibodies (5) and a deficiency of functional virus-induced immune cells response such as T cells (6), macrophages (7), natural killer (NK) cells (8), and dendritic cells (DC) (9). These deficits contribute to HBV-specific immune tolerance. Additionally, anti-HBs can directly bind viral particles and, with the aid of NK cells, destroy virus-infected cells through antibody-dependent cellular cytotoxicity (ADCC), thereby facilitating intracellular viral clearance (10).

Regulatory T cells (Tregs) inhibit T follicular helper (Tfh) cells differentiation via CTLA-4, disrupting humoral immunity and contributing to chronic HBV infection. Blocking of CTLA-4 can restore normal differentiation of Tfh cells and GC B cells, promoting HBV clearance (10, 11). Additionally, blocking PD-1 has been shown to enhance Tfh cell responses in seasonal influenza vaccination (12). Nevertheless, the role of PD-1/PD-L1 pathway in modulating dysregulated humoral responses in CHB infection warrants further investigation.

Our research focuses on the impact of PD-L1 blocking on HBV clearance and the restoration of humoral responses in CHB infection. Utilizing nontransgenic hydrodynamic transfection mouse models, we found that treatment with anti-PD-L1 significantly boosts Tfh-dependent humoral immune responses against hepatitis B surface antigens (HBsAg), thus promoting the elimination of HBV. This mechanism is critically dependent on pDCs, highlighting a novel therapeutic avenue in the management of chronic HBV infection.

Results

Acute and chronic HBV transfection mouse models

In this study, we first established acute and chronic HBV transfection models in C57BL/6N and C57BL/6J respectively by administering 10 μg of the pAAV-HBV1.2 plasmid per mouse through hydrodynamic injection, as described previously (10) (Figure 1A). Serological analysis revealed that C57BL/6N mice exhibited a rapid decline in HBsAg positivity, coupled with a significantly higher positive rate of HBsAb compared to the B6J transfection model within 7 weeks post transfection (Figures 1B, C). These results mean that we successfully conducted chronic HBV transfected model in C57BL/6J.

PD-L1 blockade promote viral clearance in HBV-persistent B6J mice

The PD-1/PD-L1 axis serves as a pivotal immune checkpoint, and blockade of this pathway has been shown to enhance humoral immune responses (13). Based on HBV-persistent B6J Mice, we assessed the impact of anti-PD-L1 treatment on viral clearance (Figure 1D). Serological analyses revealed a rapid decline in HBsAg positivity rates combined with enhanced HBsAb response following anti-PD-L1 treatment in HBV-persistent B6J mice, paralleling those observed in HBV transfected B6N mice (Figures 1E, F). Given that HBV transfection-induced humoral immune responses were previously established only in liver draining lymph nodes and spleen (10), we examined splenic Tfh ($CD4^+B220^-CXCR5^{hi}PD\text{-}1^{hi}$) and GC B ($B220^+GL7^+Fas^+$) in HBV transfected mice via flow cytometry (Supplementary Figure 1). The results indicated that both Tfh and GC B cells underwent significant expansion following anti-PD-L1 treatment (Figures 1G, H). Collectively, these findings suggested that anti-PD-L1 therapy could restore humoral immune responses and facilitated the clearance of HBV in chronic HBV transfection mice.

Blocking PD-L1 promote HBV clearance in HBV carrier mice

To evaluate the therapeutic efficacy of anti-PD-L1 in HBV carrier B6J mice, we employed C57BL/6J mice, establishing the model by administering the pAAV-HBV1.2 plasmid. On day 18 post-transfection (D18), mice with high HBsAg were identified as HBV carriers and subjected to anti-PD-L1 treatment (Figure 2A). Serological evaluations revealed that anti-PD-L1 treatment substantially promoted HBsAg clearance and HBsAb production (Figures 2B, C). Further analysis of humoral immune response indicated that differentiation of Tfh and GC B cells were restored following anti-PD-L1 treatment in HBV carriers (Figures 2D, E). Intriguingly, a significant reduction in Treg was also noted post-treatment (Figure 2F and Supplementary Figure 2). These findings collectively affirm that anti-PD-L1 therapy not only restore dysregulated anti-HBV humoral responses but also concurrently suppressed Treg differentiation in HBV carriers, highlighting its potential as a viable therapeutic strategy for managing chronic HBV infection.

The therapeutic effect of anti-PD-L1 is independent of $CD8^+$ T cells

In context of CHB pathogenesis, $CD8^+$ T cell exhaustion plays a pivotal role, and treatment with anti-PD-L1 has been shown to alleviate this exhaustion, thereby promoting antigen clearance (14). To investigate whether the efficacy of anti-PD-L1 extends beyond the

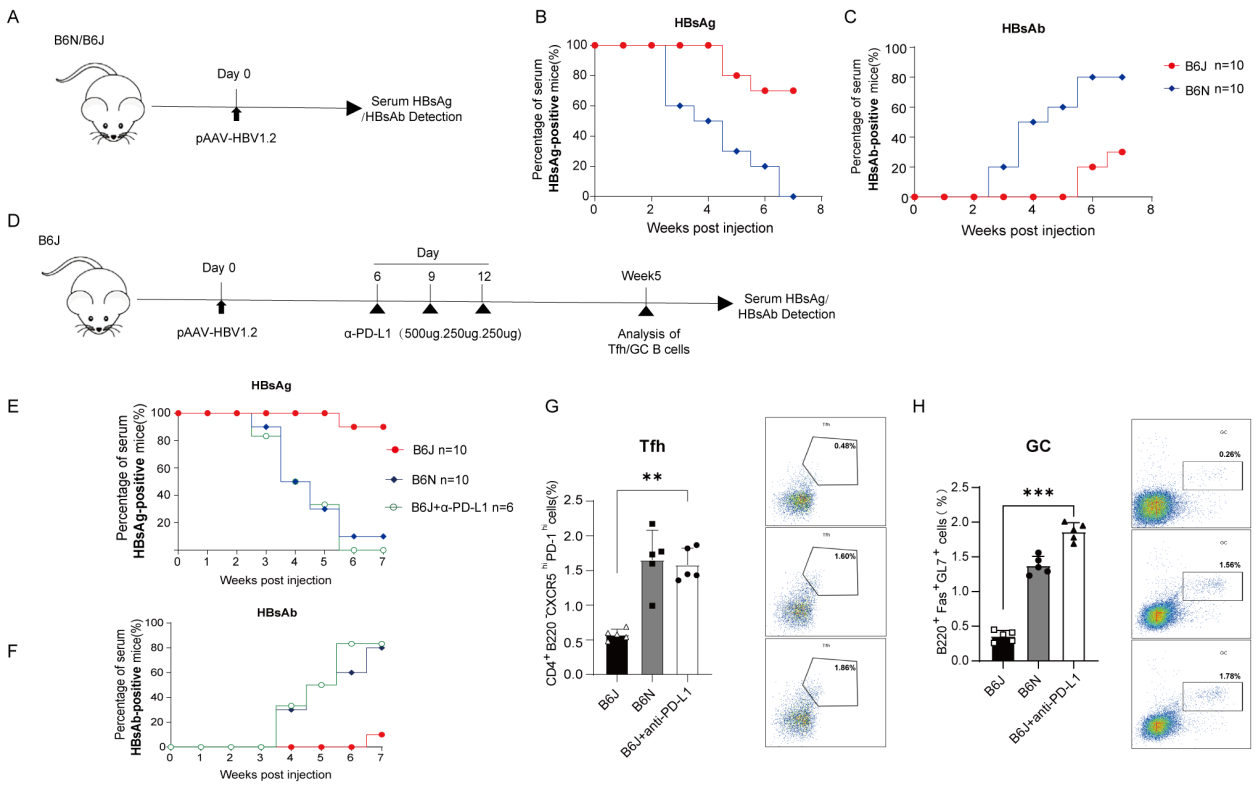

FIGURE 1
Enhanced HBV clearance in HBV persistent B6J mice treated with PD-L1 mAb. **(A)** Schematic representation of HBV transfection experiments in the study. **(B, C)** The positive rates of mice with detectable circulating HBsAg **(B)** and HBsAb **(C)** are shown. Data are from 10 mice and were replicated in at least two independent experiments. **(D)** Schematic representation of the PD-L1 monoclonal antibody (mAb) treatment experiments. B6J mice transfected with HBV received intraperitoneal injections of 500 μg PD-L1 mAb or an isotype control antibody on day 6 post-transfection. Subsequent administrations of 250 μg were performed on days 9 and 12. Serum samples were collected on a weekly basis, and splenic Tfh cells along with GC B cells were analyzed at the designated time points. **(E, F)** Evaluation of serum HBsAg and HBsAb via ELISA. Data are from 6–10 mice and were replicated in at least two independent experiments. **(G, H)** Percentages of splenic Tfh cells **(G)** and GC B cells **(H)** in B6J HBV-transfected mice treated with PD-L1mAb or isotype control were measured at week 5 post-injection, and untreated B6N transfection mice served as positive control. Data are from 5 mice and were replicated in at least two independent experiments. The data shown are mean ± s.e.m. Statistical analysis was performed using one-way Anova. **p < 0.01; ***p < 0.001.

modulation of $CD8^+$ T cell exhaustion, we first utilized CD8 knockout (CD8KO) mice to conduct HBV transfection and test of HBsAg showed significant HBV persistence without anti-PD-L1 treatment (Figures 3A, B). Then we treated CD8 KO transfected mice with anti-PD-L1 as described (Figure 3A), and serological evaluations indicated that, despite the absence of $CD8^+$ T cells, anti-PD-L1 treatment significantly enhanced the clearance of HBsAg and production of HBsAb (Figures 3C, D). Concurrently, blockade of PD-L1 markedly augmented the differentiation of Tfh and GC B cells in CD8KO transfection mice (Figures 3E, F). Collectively, these findings demonstrate that the therapeutic effects of anti-PD-L1 on HBV-persistent mice are independent of $CD8^+$T cells but are primarily mediated through restoration of humoral immune response to HBV.

The efficacy of anti-PD-1 and/or anti-CTLA-4 on HBV clearance

Building on our previous findings that anti-CTLA-4 treatment facilitates HBV clearance by restoring dysregulated humoral immune responses in chronic HBV infection, we investigated the potential synergistic effects of dual blockade with anti-PD-L1 and anti-CTLA-4 (Figure 4A). Serological tests revealed no significant differences in the positivity rates of HBsAg and HBsAb between treatments with either anti-CTLA-4 or anti-PD-L1 alone, and combined therapy did not demonstrate a clear advantage over monotherapy (Figures 4B, C). Similarly, analyses of Tfh and GC B cell showed that combined therapy did not offer a clear benefit over monotherapy (Figures 4D, E). These results suggested that both agents may promote humoral immunity recovery via overlapping signaling pathways, with anti-PD-L1 potentially acting upstream of Treg.

pDCs possess enhanced potential to drive immune tolerance

DCs, crucial antigen-presenting cells, include subtypes such as conventional DCs (cDCs) and plasmacytoid DCs (pDCs). We initially assessed the expression levels of costimulatory and

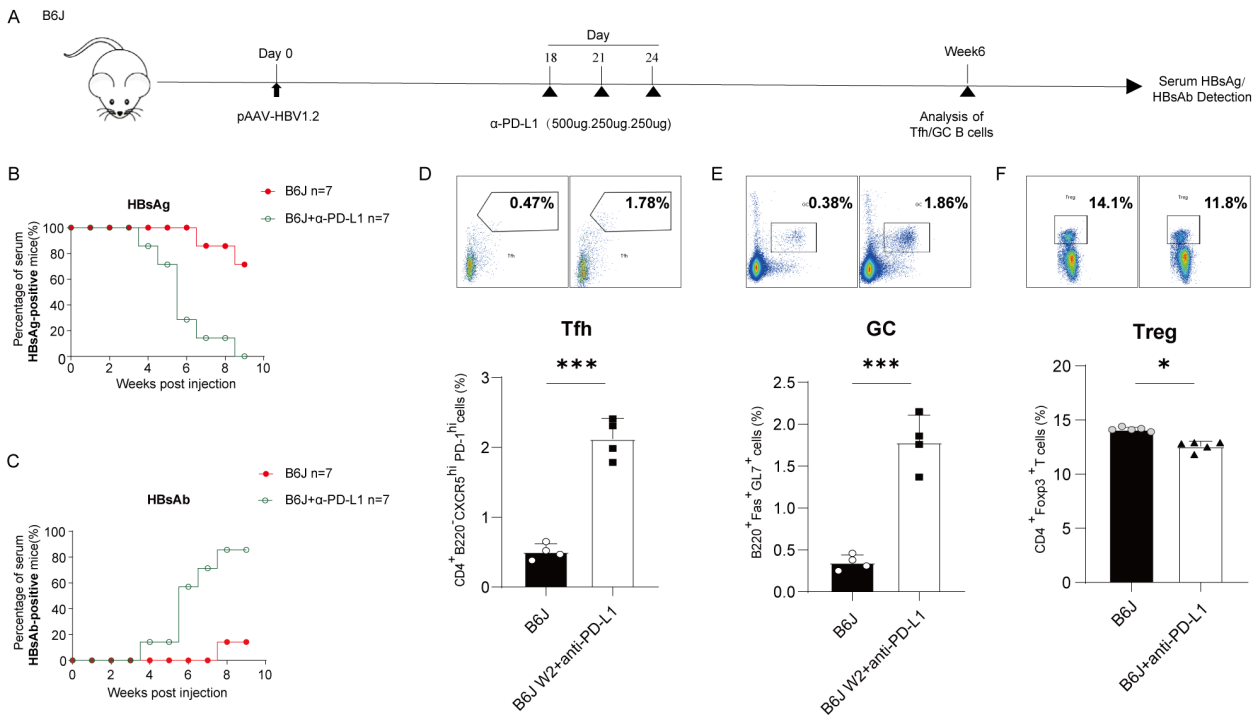

FIGURE 2
Treatment of PD-L1 mAb promote HBV clearance in HBV carrier mice. **(A)** Schematic representation of PD-L1 mAb treatment in the HBV carrier mice. Mice exhibiting high HBsAg detected by ELISA on day 18 post-transfection were classified as carriers and received treatment with PD-L1 mAb at indicated time course as described above. Serum samples were collected on a weekly basis, and proportions of splenic Tfh cells and GC B cells were analyzed three weeks post-treatment. **(B, C)** Positive rates of serum HBsAg and HBsAb were assessed via ELISA at designated times post-HBV transfection. Data are from 7 mice and were replicated in at least two independent experiments. **(D-F)** Percentages of splenic Tfh cells **(D)**, GC B cells **(E)**, and Treg **(F)** in HBV carrier mice treated with PD-L1mAb or isotype control were measured via flow cytometry three weeks post-treatment. Data are from 4–5 mice(D-E, n=4; F, n=5)and were replicated in at least two independent experiments. The data shown are mean ± s.e.m. Statistical analyses were performed using a two-tailed unpaired t-test. *p < 0.05; ***p < 0.001.

tolerogenic molecules in splenic cDCs and pDCs of C57BL/6J mice. Our results revealed negligible differences in the expression of CD80/86 and IL-10 between the two DC subtypes (Figures 5A, B); however, pDCs exhibited enhanced expression of TGF-β and IDO (Figure 5C). Interestingly, this expression profile exhibited organ-specific variation, as hepatic pDCs showed selective upregulation of TGF-β without IDO elevation when compared to their cDCs (Supplementary Figures S3A, B). DC-T co-culture experiments demonstrated that splenic pDCs from B6J mice exhibited a significantly higher capacity to induce Treg differentiation compared to cDCs (Figure 5D), prompting further investigation into the role of splenic pDCs in HBV persistent mice. Subsequent analysis showed a higher proportion of splenic pDCs in the chronic HBV transfection mice compared to the acute model (Figure 5E and Supplementary Figure 4). Further examinations of IL-10 and TGF-β, which are critical for immune tolerance (15, 16), demonstrated that splenic pDCs from HBV carrier mice had a significantly greater capacity to express these molecules compare to B6N transfection mice (Figures 5F, G). Collectively, these results suggest that splenic pDCs in HBV persistent mice have enhanced ability to induce immune tolerance, highlighting their potential role in chronic HBV infection.

Splenic pDCs from HBV persistent mice results in dysregulation of humoral immune response

To elucidate the role of pDCs in the pathogenesis of chronic HBV infection, we conducted adoptive transfer of DCs. Initially, splenic pDCs or cDCs from the B6J carriers were transferred to B6N mice one day before HBV transfection as described (Figure 6A). The results indicate that, compared to splenic cDCs, pDCs significantly inhibit the clearance of HBsAg (Figure 6B). Additionally, transplantation outcomes for hepatic DC subpopulations show that neither pDCs nor cDCs from carriers inhibit the clearance of HBsAg (Supplementary Figure 3C). These findings suggest that splenic pDCs in carrier mice possess a marked ability to suppress HBsAg clearance. Subsequent experiments involving the transplantation of pDCs examined their impact on the humoral immune response, revealing that pDCs significantly inhibit the differentiation of Tfh and GC B cells (Figures 6C, D). To fully characterize the expression of co-stimulatory molecules in pDCs, we sorted splenic pDCs from B6J and B6N mice at D0 and W2 post transfection and analyzed the mRNA levels of CD80, CD86, and PD-L1. The results revealed no significant differences in

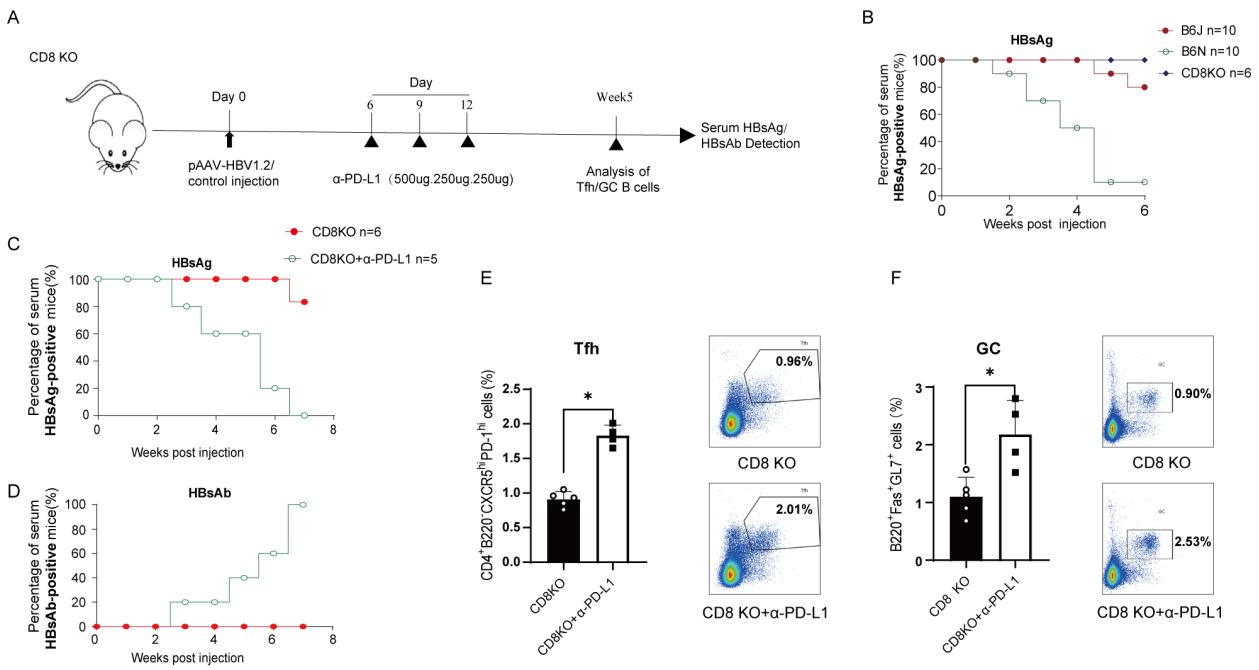

FIGURE 3
Enhancement of HBV clearance by PD-L1 mAb in CD8KO mice. **(A)** Schematic representation of the PD-L1 mAb treatment in CD8KO HBV transfection mice. CD8KO mice were hydrodynamically injected with 10 μg of the pAAV-HBV1.2 plasmid per mouse at day 0, and then treated intraperitoneally with 500 μg PD-L1 mAb or isotype control on day 6 post-transfection. Subsequent administrations of 250 μg were performed on days 9 and 12. Serum samples were collected on a weekly basis, and the proportions of splenic Tfh cells and GC B cells were analyzed at week 5. **(B)** Evaluation of serum HBsAg by ELISA at specified times post-HBV transfection in B6J, B6N, and CD8KO mice. Data are from 6–10 mice and were replicated in at least two independent experiments. **(C, D)** Positive rates of serum HBsAg and HBsAb were measured via ELISA. Data are from 5–6 mice and were replicated in at least two independent experiments. **(E, F)** Proportions of splenic Tfh cells **(E)** and GC B cells **(F)** in CD8KO HBV-transfected mice treated with PD-L1 mAb or isotype control were measured via flow cytometry 3 weeks post-treatment. Data are from 4–5 mice and were replicated in at least two independent experiments. The data shown are mean ± s.e.m. Statistical analysis was conducted using a two-tailed unpaired t-test. *$p < 0.05$.

these markers between groups, although PD-L1 mRNA showed an upward trend post-modeling (Supplementary Figure 5A). To further validate these findings, we conducted flow cytometry analysis to confirm the expression of PD-L1 on pDCs in the spleen. The results indicated PD-L1$^+$ pDCs remained unchanged in acute HBV mice. However, in carrier mice, the frequency of PD-L1$^+$pDCs was significantly elevated (Supplementary Figures S5B, C). Collectively, these results demonstrated that splenic pDCs significantly influence humoral immune responses and the clearance of HBV, underscoring their critical role in the dynamics of HBV infection.

Anti-PD-L1 interventions counteract the suppressive impact of pDCs on humoral immune response

To further determine whether pDCs exert their suppressive effects via PD-L1, we transferred pDCs isolated from HBV carriers into B6N mice one day prior to HBV transfection, followed by interventions of anti–PD-L1 as described (Figure 6E). Serological analysis revealed that anti-PD-L1 effectively reversed the pDCs-mediated inhibition of HBV clearance (Figure 6F). Moreover, treatment with anti-PD-L1 restored the impaired differentiation of Tfh and GC B cells that result from the carriers' pDCs (Figures 6G, H). Taken together, these findings delineate a mechanism that pDCs promote humoral immune dysregulation through the PD-1/PD-L1 axis in chronic HBV infection.

Discussion

Investigations into immune checkpoints have elucidated mechanisms of immune tolerance prevalent in tumors and chronic diseases (17). Crucially, restoring defective immune response is a pivotal therapeutic strategy for HBV clearance in CHB patients. Previous studies have demonstrated that inhibition of CTLA-4 on Tregs enhances the humoral response in chronic HBV infection, thereby facilitating the elimination of HBV (10). Extending these findings, our research identifies the PD-L1 in pDCs as a critical contributor to humoral immune deficiency, likely through its role in promoting Treg differentiation. These insights significantly advance our understanding of humoral immune dysregulation in chronic HBV infection and propose novel therapeutic avenues for its management.

The dysfunction of cytotoxic T cells is widely recognized as a primary mechanism underlying chronic viral infection. Blocking of the PD-1/PD-L1 signaling pathway has been shown to reinvigorate

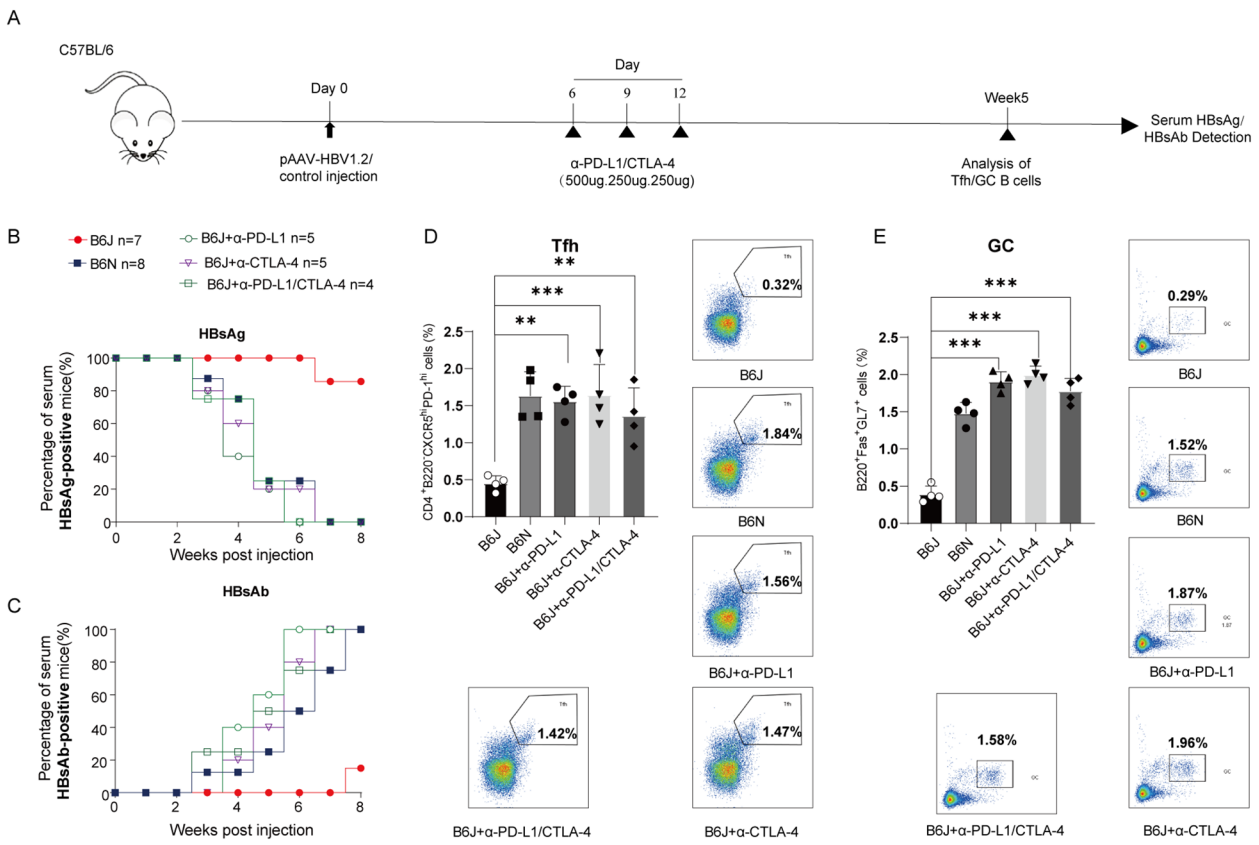

FIGURE 4
Combination therapy of CTLA-4 mAb and PD-L1 mAb. **(A)** Schematic representation of the combined CTLA-4 mAb and PD-L1 mAb treatment in B6J HBV persistent mice. B6J mice were hydrodynamically injected with 10 μg of the pAAV-HBV1.2 plasmid per mouse at day 0 and subsequently treated intraperitoneally with 500 μg of PD-L1 mAb and/or CTLA-4 mAb on day 6 post-transfection, followed by additional doses of 250 μg on days 9 and 12. Serum samples were collected weekly, and the proportions of Tfh cells and GC B cells were analyzed at week 5 post-injection. **(B, C)** Positive rates of serum HBsAg and HBsAb were measured via ELISA. Data are from 4–8 mice and were replicated in at least two independent experiments. **(D, E)** Percentages of splenic Tfh cells **(D)** and GC B cells **(E)** in B6J HBV persistent mice treated with PD-L1 mAb and/or CTLA-4 mAb, and untreated B6N transfection mice served as positive control. Data are from 4 mice and were replicated in at least two independent experiments. The data shown are mean ± s.e.m. Statistical analysis was performed using one-way Anova. **p < 0.01; ***p < 0.001.

exhausted CD8$^+$ T cells in both tumor and chronic viral infections, thereby restoring their cytotoxic capabilities (12, 14, 18, 19). Additionally, PD-1 blocking has also been implicated in enhancing the humoral immune response (13, 20). In our studies conducted on a chronic HBV transfection mouse model, we demonstrate that treatment with anti-PD-L1 effectively restored the differentiation of Tfh and GC B cells to facilitate clearance of HBV, which is independent of CD8$^+$T cell. Furthermore, the PD-1 pathway is integral to promoting Treg cell differentiation and sustaining immune tolerance (21). Our results further indicate that blocking PD-L1 inhibits Treg differentiation. The outcomes of combined treatment with anti-CTLA-4 and anti-PD-L1 suggest that both regulate the humoral immune response to HBV, implying that the restoration of humoral immunity in chronic HBV following PD-L1 blockade may be due to the inhibition of Treg differentiation.

Treg differentiation is influenced by various cellular interactions, with DCs playing a pivotal role in providing the necessary signals for Treg differentiation and survival (22, 23). A comparative analysis of tolerogenic molecules within two DC subsets revealed that pDCs express markedly higher levels of TGF-β and IDO than cDCs, suggesting that pDCs possess superior tolerogenic capabilities. In HBV-persistent B6J mice, the proportion of splenic pDCs was substantially higher than that of B6N acute mice, paralleling with more IL-10 and TGF-β, which are critical for immune tolerance. Adoptive transfer experiments demonstrated that splenic pDCs from HBV carriers hindered HBV clearance in the acute model. Importantly, co-treatment with anti-PD-L1 reversed the suppressive effect of pDCs from carrier mice on HBV clearance, suggesting that pDCs mediate inhibition of humoral immune response predominantly through the PD-1/PD-L1 pathway.

While our findings confirm that pDCs induced dysregulation of humoral immunity via PD-L1, resulting in HBV persistence, it is crucial to acknowledge that these results were derived using non-transgenic hydrodynamic transfection mouse models and comprehensive clinical studies are necessary to validate these observations. Future research should employ pDC-specific depletion models, such as BDCA2-DTR mice or anti-PDCA1 antibodies, to explore whether the removal of PD-L1$^+$ pDCs can restore humoral immune responses and promote the clearance of HBsAg. Additionally, studies could investigate the antiviral capabilities of pDCs.

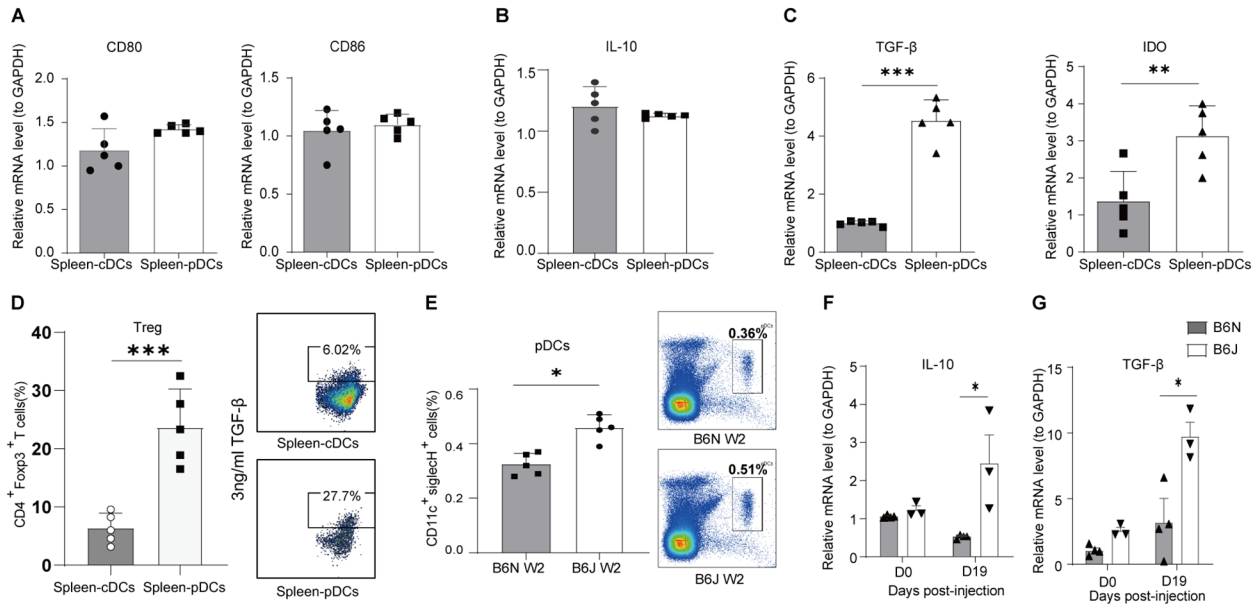

FIGURE 5
Differential expression of co-stimulatory and tolerogenic molecules in splenic cDCs and pDCs. Splenic pDCs and cDCs were sorted by BD FACSAria. **(A-C)** *CD80/86, IL-10, TGF-β and IDO* gene expression of splenic cDCs and pDCs cells from naïve B6J mice, Data are from 5 mice and were replicated in at least two independent experiments. **(D)** Percentage of Treg in DC-T co-culture Assay. Data are from 5 mice and were replicated in at least two independent experiments. **(E)** Percentage of splenic pDCs in B6N and B6J HBV transfection mice, measured two weeks post-injection, Data are from 5 mice and were replicated in at least two independent experiments. **(F, G)** IL-10 and TGF-β gene expression of splenic pDCs from B6J and B6N transfection mice at day 0 and days 19. Data are from 3–4 mice and were replicated in at least two independent experiments. The data shown are mean ± s.e.m. A 2-tailed unpaired t test was used to compare experimental groups. *p < 0.05, **p < 0.01, ***p < 0.001.

Methods

Mice

Male C57BL/6N (B6N) and C57BL/6J (B6J) mice were acquired from Charles River (Beijing), while CD8KO mice were kindly provided by Professor Lilin Ye. All mice were 6 weeks old and maintained at the SPF animal facility of the Tianjin Institute of Environmental and Operational Medicine. The Institutional Animal Care and Use Committee (IACUC) at this institute approved all experimental procedures involving mice.

Hydrodynamic injection and serological test

Mice received hydrodynamic tail vein injections of 10 μg of the HBV expression plasmid pAAV-HBV1.2 (genotype A), a contribution from Dr. Pei-Jer Chen. Hydrodynamic tail vein injections has been described previously16. Serum samples were collected at designated intervals post-injection for the analysis of HBsAg and anti-HBs using ELISA kits as described (KeHua, Shanghai, China).

Cut-off value (COV) determination

Negative Control (NC): Mean optical density (OD) of triplicate negative controls (NCx) was calculated as, NCx=(NC1 + NC2 + NC3)/3. If NCx < 0, it was set to 0. Positive Control (PC): OD value of positive control. Assay Validity Requirements: NCx ≤ 0.100;PC > 1.000. Blank control (for dual-wavelength reading) < 0.040; for single-wavelength reading ≤ 0.080. COV=NCx+0.100. Sample OD (S) and S/COV ratio were calculated. Positive: S/COV > 1.0;Negative: S/COV < 1.0.

Lymphocyte isolation

Spleen tissues were disaggregated through a 70 μm nylon mesh (Falcon; BD Biosciences) using the rounded end of a 2 ml syringe plunger to achieve single cell suspensions. Spleen samples required further erythrocytes lysis using ACK buffer (R1010, Solarbio, China) and washed with stain buffer.

Dendritic cell (DC) and T cell co-culture assay

$CD4^+CD25^-$ naïve T cells were purified from spleens of B6J mice via FACS. Sorted DCs (2.5×10^4 cells/well) and naïve T cells (1.5×10^5 cells/well) were co-cultured in 96-well plates precoated with anti-CD3 and anti-CD28 mAbs. TGF-β (3ng/ml) were added to the cultures to induce Treg differentiation. On day 3 of co-culture, 50% of the medium was replaced, and 20 U/mL recombinant IL-2 (rIL-2) (PeproTech ®) was supplemented. After an additional 48 hours, cells were harvested, stained with CD4 (clone GK1.5) and Foxp3 (Invitrogen), and analyzed by flow cytometry.

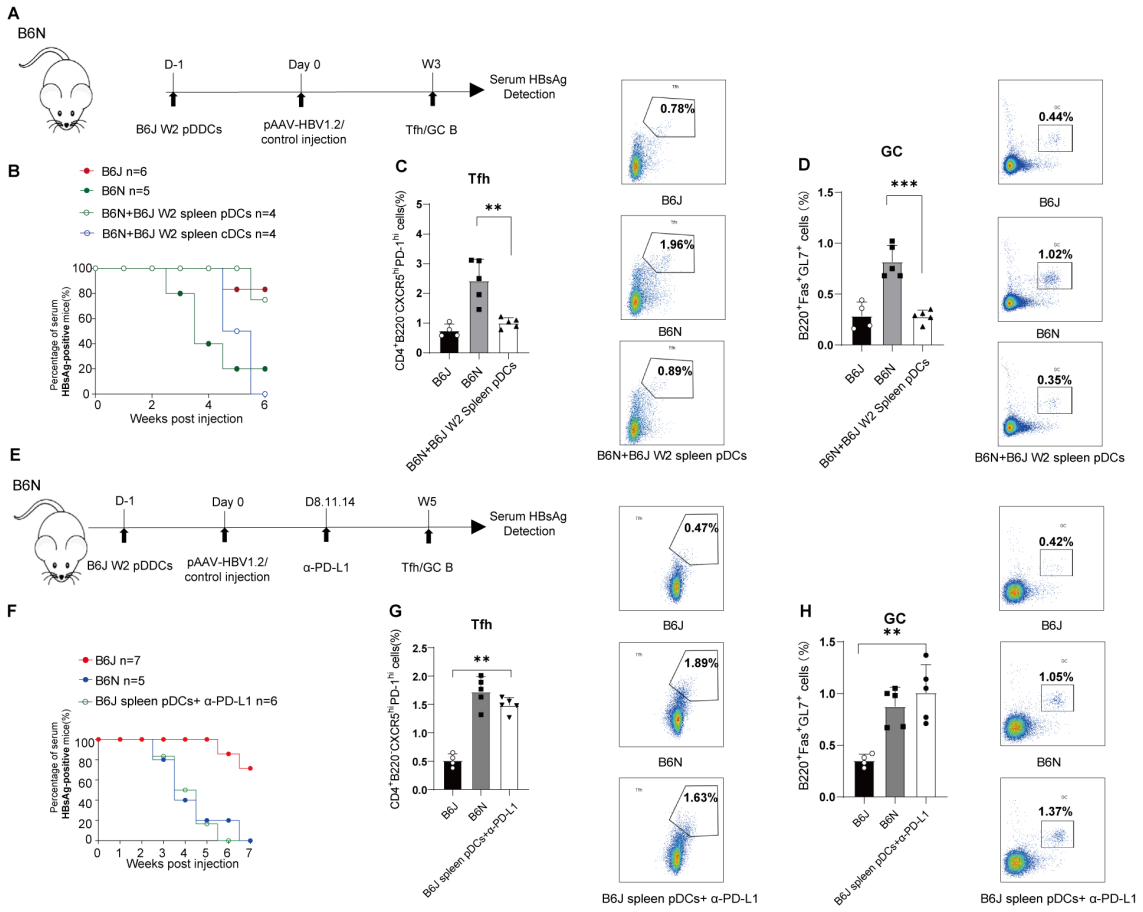

FIGURE 6
pDCs results in dysregulation of humoral immune response through PD-L1. **(A)** 5×10^5 magnetic bead (MACS)-purified pDCs from B6J carriers were adoptively transferred to B6N which were challenged with 10ug pAAV-HBV1.2 plasmid 1 days later. B6N and B6J HBV transfection mice were conducted as control. Serum were collected weekly, and proportions of splenic Tfh cells and GC B cells were analyzed in three weeks post-injection. **(B)** Serum HBsAg examined by ELISA at specified times post-HBV transfection. Data are from 4–6 mice and were replicated in at least two independent experiments. **(C-D)** Frequencies of splenic Tfh cells **(C)** and GC B cells **(D)** of HBV-transfected recipients and control were measured three weeks post-injection. Data are from 4–5 mice and were replicated in at least two independent experiments. **(E)** 5×10^5 MACS-purified splenic pDCs from B6J carriers were adoptively transferred to B6N which were challenged with 10ug pAAV-HBV1.2 plasmid 1 days later and subsequently treated with 500 μg PD-L1 mAb on day 8, followed by 250 μg PD-L1 mAb on days 11 and 14. Serum and splenic Tfh/GC B cells were analyzed at the indicated time. B6N and B6J HBV transfection mice were conducted as control. **(F)** Serum HBsAg measured by ELISA at specified times post-HBV transfection. Data are from 5–7 mice and were replicated in at least two independent experiments. **(G-H)** Frequencies of splenic Tfh cells **(G)** and GC B cells **(H)** in recipients and control were measured three weeks post-treatment. Data are from 4–5 mice and were replicated in at least two independent experiments. The data shown are mean ± s.e.m; statistical comparisons were made using one-way Anova. **p < 0.01, ***p < 0.001.

Flow cytometry

Following isolation, lymphocytes were stained at 4°C for 30 minutes with antibodies against CD16/32(clone 93), Fas (clone 15A7), PD-1(clone J43), GL-7(clone GL7) sourced from eBioscience. Antibodies against CD3(clone 145-2C11), CD4(clone GK1.5), CD11c (clone N418), SiglecH (clone551), B220(clone RA3-6B2), CD45(clone 30-F11) (clone M5/114.15.2) sourced from Biolegend.

For Tfh staining

The cells were first labeled with Biotin Rat Anti-Mouse CD185 (CXCR5) (BD Clone 2G8) and CD16/32 for 1.5 h at room temperature. Then the cells were washed with stain buffer and stained with PE Streptavidin (Invitrogen), CD4, B220 and PD-1.

A Celesta Cell Analyzer (BD Biosciences) was used for data acquisition, and analysis was conducted using FlowJo software.

For Treg staining

For the labeling of Treg cells, Fixation/permeabilization kit (eBioscience) is used to membrane permeabilization. First, CD4 and CD16/32 is used for surface molecule labeling, then follow the reagent kit instructions for intracellular Foxp3 (Invitrogen)staining.

Antibody treatments

In vivo blockade of PD-L1 was performed using PD-L1 blocking antibodies (Clone 10F.9G2, BioXcell) or IgG, injected intraperitoneally at specified times after pAAV/HBV1.2 hydrodynamic injection. The initial dose was 500 ug per mouse, followed by two doses of 250 ug each.

In vivo blockade of CTLA-4 was performed using CTLA-4 blocking antibodies (Clone 9D9, BioXcell) or IgG, injected intraperitoneally at specified times after pAAV/HBV1.2 hydrodynamic injection. The initial dose was 500 ug per mouse, followed by two doses of 250 ug each.

Real-time quantitative

RNA was extracted using RNeasy mini kits (Qiagen), treated with DNase I (Thermo Fisher Scientific), and reverse transcribed with the Revert Aid First Strand cDNA Synthesis Kit (Thermo Fisher Scientific). Gene expressions were quantified by an ABI Q5 using specific primers and normalized to GAPDH. The primers were as follows:

mGAPDH forward 5′-AGGTCGGTGTGAACGGATTTG-3′, reverse5′ -TGTAGACCATGTAGTTGAGGTCA -3′;
mCD80 forward 5′-ACCCCCAACATAACTGAGTCT-3′, reverse5′-TTCCAACCAAGAGAAGCGAGG-3′;
mCD86 forward 5′-TGTTTCCGTGGAGACGCAAG-3′, reverse5′-TTGAGCCTTTGTAAATGGGCA-3′;
mIL-10 forward 5′-GCTCTTACTGACTGGCATGAG-3′, reverse5′-CGCAGCTCTAGGAGCATGTG-3′;
mIDO forward 5′-GCTTTGCTCTACCACATCCAC-3′, reverse5′-CAGGCGCTGTAACCTGTGT-3′;
mTGF-b forward 5′-TACCTGAACCCGTGTTGCTCTC-3′, reverse5′-GTTGCTGAGGTATCGCCAGGAA-3′

Adoptive-transfer study

pDCs were harvested from the spleens of designated mice utilizing a Plasmacytoid Dendritic Cell Isolation Kit (Miltenyi Biotec). A total of 5 × 10^5 pDCs were administered intravenously to recipient mice.

Statistical analysis

Data analyses were conducted using Prism (GraphPad) employing t-tests (unpaired or paired as appropriate) or one-way ANOVA with significance thresholds set at $^{*}p < 0.05$, $^{**}p < 0.01$, and $^{***}p < 0.001$. Data are presented as mean ± s.e.m. The process of group assignment and subsequent evaluation of results was conducted under conditions of blindness to ensure impartiality. There were no exclusionary criteria set forth, and all collected samples were incorporated into the analysis without exception.

Data availability statement

The raw data supporting the conclusions of this article will be made available by the authors, without undue reservation.

Ethics statement

The animal study was approved by Ethics Committee of Environmental and Operational Medicine Research Department. The study was conducted in accordance with the local legislation and institutional requirements.

Author contributions

DM: Writing – original draft, Investigation, Methodology, Writing – review & editing. JHW: Writing – review & editing. LD: Writing – original draft. XH: Writing – review & editing. YL: Writing – review & editing. PZ: Writing – review & editing. JJW: Writing – review & editing, Conceptualization, Funding acquisition, Investigation. QD: Writing – original draft, Conceptualization, Funding acquisition, Writing – review & editing.

Funding

The author(s) declare that financial support was received for the research and/or publication of this article. This project was supported by the National Natural Science Foundation of China (81901577).

Acknowledgments

The authors thank professor Lilin Ye for generously providing CD8KO mice; Li Tang for generously providing pAAV-HBV 1.2 plasmids.

Conflict of interest

The authors declare that the research was conducted in the absence of any commercial or financial relationships that could be construed as a potential conflict of interest.

Generative AI statement

The author(s) declare that no Generative AI was used in the creation of this manuscript.

Publisher's note

Supplementary material

The Supplementary Material for this article can be found online at: https://www.frontiersin.org/articles/10.3389/fimmu.2025.1545667/full#supplementary-material

SUPPLEMENTARY FIGURE 1
Gating strategies for Tfh and GC. **(A)** Gating strategy to determine the GC B cells in the spleen, using B220, GL-7 and FAS. **(B)** Gating strategy to determine the Tfh cells in the spleen, using B220, CD4, CXCR5 and PD-1.

SUPPLEMENTARY FIGURE 2
Gating strategy for Treg. Gating strategy to determine the Treg in the spleen, using CD3e, CD4 and Foxp3.

SUPPLEMENTARY FIGURE 3
Tolerogenic capability of liver cDCs and pDCs. **(A, B)** CD80/86, IL-10, TGF-β and IDO gene expression of liver cDCs and pDCs from naïve B6J mice. Data are from 3 mice and were replicated in at least two independent experiments. **(C)** Serum HBsAg examined by ELISA at specified times post-HBV transfection. Data are from 3–5 mice and were replicated in at least two independent experiments. The data shown are mean ± s.e.m. An unpaired t test was used to compare experimental groups, ***$p < 0.001$.

SUPPLEMENTARY FIGURE 4
Gating strategies for pDCs. Gating strategy to determine the pDCs in the spleen, using CD11c and SiglecH.

SUPPLEMENTARY FIGURE 5
Tolerogenic capability of splenic pDCs. **(A)** *CD80/86, CD86* and *PD-L1* gene expression of splenic pDCs from mice at D0 and W2 post transfection. Data are from 4 mice and were replicated in at least two independent experiments. **(B, C)** Percentage of PD-L1^{+}pDCs in spleen of mice at D0 and W2 post transfection. Data are from 5–7 mice and were replicated in at least two independent experiments. The data shown are mean ± s.e.m. An unpaired t test was used to compare experimental groups, **$p < 0.01$.

References

1. World Health Organization. Hepatitis B(2024). Available online at: https://www.who.int/news-room/fact-sheets/detail/hepatitis-b (Accessed December 10, 2024).

2. Omata M, Cheng AL, Kokudo N, Kudo M, Lee JM, Jia J, et al. Asia-pacific clinical practice guidelines on the management of hepatocellular carcinoma: A 2017 update. *Hepatol Int*. (2017) 11:317–70. doi: 10.1007/s12072-017-9799-9

3. Tseng CH, Chen TH, Wu JL, Lee TY, Borghi JA, Lin JT, et al. Serious adverse events after cessation of nucleos(T)Ide analogues in individuals with chronic hepatitis B: A systematic review and meta-analysis. *JHEP Rep*. (2023) 5:100617. doi: 10.1016/j.jhepr.2022.100617

4. Hsu YC, Huang DQ, Nguyen MH. Global burden of hepatitis B virus: current status, missed opportunities and a call for action. *Nat Rev Gastroenterol Hepatol*. (2023) 20:524–37. doi: 10.1038/s41575-023-00760-9

5. Zhang S, Zhao J, Zhang Z. Humoral immunity, the underestimated player in hepatitis B. *Cell Mol Immunol*. (2018) 15:645–8. doi: 10.1038/cmi.2017.132

6. Gehring AJ, Protzer U. Targeting innate and adaptive immune responses to cure chronic hbv infection. *Gastroenterology*. (2019) 156:325–37. doi: 10.1053/j.gastro.2018.10.032

7. Faure-Dupuy S, Delphin M, Aillot L, Dimier L, Lebossé F, Fresquet J, et al. Hepatitis B virus-induced modulation of liver macrophage function promotes hepatocyte infection. *J Hepatol*. (2019) 71:1086–98. doi: 10.1016/j.jhep.2019.06.032

8. Rehermann B. Pathogenesis of chronic viral hepatitis: differential roles of T cells and Nk cells. *Nat Med*. (2013) 19:859–68. doi: 10.1038/nm.3251

9. Yonejima A, Mizukoshi E, Tamai T, Nakagawa H, Kitahara M, Yamashita T, et al. Characteristics of impaired dendritic cell function in patients with hepatitis B virus infection. *Hepatology*. (2019) 70:25–39. doi: 10.1002/hep.30637

10. Wang X, Dong Q, Li Q, Li Y, Zhao D, Sun J, et al. Dysregulated response of follicular helper T cells to hepatitis B surface antigen promotes Hbv persistence in mice and associates with outcomes of patients. *Gastroenterology*. (2018) 154:2222–36. doi: 10.1053/j.gastro.2018.03.021

11. Wing JB, Ise W, Kurosaki T, Sakaguchi S. Regulatory T cells control antigen-specific expansion of tfh cell number and humoral immune responses via the coreceptor Ctla-4. *Immunity*. (2014) 41:1013–25. doi: 10.1016/j.immuni.2014.12.006

12. Huang Q, Wu X, Wang Z, Chen X, Wang L, Lu Y, et al. The primordial differentiation of tumor-specific memory Cd8(+) T cells as bona fide responders to Pd-1/Pd-L1 blockade in draining lymph nodes. *Cell*. (2022) 185:4049–66.e25. doi: 10.1016/j.cell.2022.09.020

13. Herati RS, Knorr DA, Vella LA, Silva LV, Chilukuri L, Apostolidis SA, et al. Pd-1 directed immunotherapy alters Tfh and humoral immune responses to seasonal influenza vaccine. *Nat Immunol*. (2022) 23:1183–92. doi: 10.1038/s41590-022-01274-3

14. Bengsch B, Martin B, Thimme R. Restoration of Hbv-specific Cd8+ T cell function by Pd-1 blockade in inactive carrier patients is linked to T cell differentiation. *J Hepatol*. (2014) 61:1212–9. doi: 10.1016/j.jhep.2014.07.005

15. Chen ZM, O'Shaughnessy MJ, Gramaglia I, Panoskaltsis-Mortari A, Murphy WJ, Narula S, et al. Il-10 and Tgf-beta induce alloreactive Cd4+Cd25- T cells to acquire regulatory cell function. *Blood*. (2003) 101:5076–83. doi: 10.1182/blood-2002-09-2798

16. Akdis CA, Akdis M. Mechanisms of immune tolerance to allergens: role of Il-10 and Tregs. *J Clin Invest*. (2014) 124:4678–80. doi: 10.1172/jci78891

17. Tison A, Garaud S, Chiche L, Cornec D, Kostine M. Immune-checkpoint inhibitor use in patients with cancer and pre-existing autoimmune diseases. *Nat Rev Rheumatol*. (2022) 18:641–56. doi: 10.1038/s41584-022-00841-0

18. Barber DL, Wherry EJ, Masopust D, Zhu B, Allison JP, Sharpe AH, et al. Restoring function in exhausted cd8 T cells during chronic viral infection. *Nature*. (2006) 439:682–7. doi: 10.1038/nature04444

19. Urbani S, Amadei B, Tola D, Pedrazzi G, Sacchelli L, Cavallo MC, et al. Restoration of Hcv-specific T cell functions by Pd-1/Pd-L1 blockade in Hcv infection: effect of viremia levels and antiviral treatment. *J Hepatol*. (2008) 48:548–58. doi: 10.1016/j.jhep.2007.12.014

20. Shi J, Hou S, Fang Q, Liu X, Liu X, Qi H. Pd-1 controls follicular T helper cell positioning and function. *Immunity*. (2018) 49:264–74.e4. doi: 10.1016/j.immuni.2018.06.012

21. Leung CS, Yang KY, Li X, Chan VW, Ku M, Waldmann H, et al. Single-cell transcriptomics reveal that Pd-1 mediates immune tolerance by regulating proliferation of regulatory T cells. *Genome Med*. (2018) 10:71. doi: 10.1186/s13073-018-0581-y

22. Lan Q, Zhou X, Fan H, Chen M, Wang J, Ryffel B, et al. Polyclonal Cd4+Foxp3+ Treg cells induce Tgfβ-dependent tolerogenic dendritic cells that suppress the murine lupus-like syndrome. *J Mol Cell Biol*. (2012) 4:409–19. doi: 10.1093/jmcb/mjs040

23. Cifuentes-Rius A, Desai A, Yuen D, Johnston APR, Voelcker NH. Inducing immune tolerance with dendritic cell-targeting nanomedicines. *Nat Nanotechnol*. (2021) 16:37–46. doi: 10.1038/s41565-020-00810-2

frontiers | Frontiers in Cellular and Infection Microbiology

TYPE Original Research
PUBLISHED 30 April 2025
DOI 10.3389/fcimb.2025.1525758

OPEN ACCESS

EDITED BY
José Luis Muñoz-Carrillo,
University of Guadalajara, Mexico

REVIEWED BY
Benjamin M. Liu,
George Washington University, United States
Nazan Tuna,
Namik Kemal University, Türkiye

*CORRESPONDENCE
Keyu Sun
zhu97b3@126.com
Jiqin Wang
57658382@qq.com

†These authors share first authorship

RECEIVED 10 November 2024
ACCEPTED 01 April 2025
PUBLISHED 30 April 2025

CITATION
Li Y, Li Y, Wang J and Sun K (2025) Pathogenic bacteria features of central line-associated bloodstream infections in ICU patients: focus on the early predictive value of neutrophil-to-lymphocyte and platelet-to-lymphocyte ratios.
Front. Cell. Infect. Microbiol. 15:1525758.
doi: 10.3389/fcimb.2025.1525758

Pathogenic bacteria features of central line-associated bloodstream infections in ICU patients: focus on the early predictive value of neutrophil-to-lymphocyte and platelet-to-lymphocyte ratios

Yuzhen Li†, Yanyan Li†, Jiqin Wang* and Keyu Sun*

Department of Emergency, Minhang Hospital, Fudan University, Shanghai, China

Objective: Explore and analyze CLABSI pathogenic bacteria characteristics in ICU patients and the value of PCT, NLR, PLR in early infection prediction.

Methods: 926 ICU patients with central venous catheters in Minhang Hospital from January 2021 to December 2023 were enrolled. They were grouped by co-infection status. PCT, NLR and PLR levels were measured, patient data analyzed, pathogenic bacteria characteristics summarized, and their predictive value evaluated via ROC curve.

Results: From January 2021 to December 2023, among the 926 patients with CVC, 73 were diagnosed with CLABSI, with an infection rate of 7.88%. A total of 81 strains of pathogenic bacteria were isolated, including 60.50% (49/81) Gram - positive bacteria, 35.80% (29/81) Gram - negative bacteria, and 3.70% (3/81) fungi. The main Gram - positive bacteria exhibited high resistance to penicillin, erythromycin, clindamycin, and oxacillin, with a resistance rate exceeding 70%, yet were sensitive to vancomycin, linezolid, and tetracycline. The main Gram - negative bacteria had high resistance to piperacillin, piperacillin/tazobactam, Aztreonam, and gentamicin, with a resistance rate over 70%, and were more sensitive to cefoperazone/sulbactam, imipenem, and amikacin. Age, the site of catheterization, the duration of catheterization, and the employment of double - cavity catheters were all factors that exerted an influence on CLABSI among ICU patients (with $p < 0.05$). The levels of peripheral blood NLR, PLR, and PCT in the infected group were higher than those in the non - infected group ($p < 0.05$). The areas under the curve (AUCs) of peripheral blood NLR, PLR, and PCT were 0.814, 0.798, and 0.856, respectively, with the largest AUC for PCT. When the cut - off

point was 2.75 ng/ml, the Youden index was the largest. The AUCs of the combination of peripheral blood NLR and PLR, NLR and PCT, PLR and PCT, and all three combined were 0.877, 0.903, 0.857, and 0.917.

Conclusion: The early prediction of CLABSI in ICU patients by means of PCT, NLR, and PLR is of remarkable significance. It can provide a precious reference for clinical diagnostic and treatment strategies.

KEYWORDS

central line-associated bloodstream infection (CLABSI), pathogenic bacteria, drug resistance, neutrophil to lymphocyte ratio(NLR), platelet to lymphocyte ratio(PLR), procalcitonin(PCT)

1 Introduction

As a commonly used diagnosis and treatment method in intensive care units (ICUs), central venous catheters (CVC) are widely used in hemodynamic monitoring, parenteral nutrition, hemofiltration, fluid resuscitation, etc. However, as a foreign body, it is easily colonized by microorganisms, which may lead to central line-associated bloodstream infection (CLABSI), thereby increasing mortality, morbidity and healthcare costs (van der Kooi et al., 2023; Teja et al., 2024; Xu et al., 2024).

Patients with CLABSI typically present without characteristic clinical features. Generally, fever is the most prominent initial sign. Redness, swelling, pain, and suppuration at the intubation site are highly specific manifestations. Other clinical presentations include hemodynamic instability, catheter malfunction, and sudden-onset sepsis, among others (Singer et al., 2016). If the infection fails to be effectively managed, it can give rise to severe complications, thereby impacting the patients' quality of life, prolonging hospitalization, and even resulting in death (Badia-Cebada et al., 2022). At present, bacterial culture remains the gold - standard for diagnosing CLABSI. Nevertheless, its low positive culture rate and long processing time limit its guiding value in early - stage clinical treatment (Liu et al., 2021; Ruiz-Ruigómez and Aguado, 2021). The neutrophil to lymphocyte ratio (NLR) and platelet to lymphocyte ratio (PLR) are effective indicators in blood biochemical indicators that can evaluate the inflammatory state of the body. The detection is simple and easy to obtain. Currently, they have been applied in the diagnosis and prognosis of diseases including systemic lupus erythematosus and influenza (Luo et al., 2022; Zinellu et al., 2022). Serum procalcitonin (PCT) is widely applied in bacterial infectious diseases. It is not influenced by other diseases and has relatively high diagnostic specificity, and its value has already been recognized (Zhang et al., 2022; Bajić et al., 2023). This study analyzed the pathogenic bacteria and drug - resistance status of patients with CLABSI and explored the diagnostic value of peripheral blood NLR, PLR, and PCT for such infections, aiming to provide a reference for early clinical diagnosis and treatment.

2 Subjects and methods

2.1 Subjects

A total of 926 patients with CVC in the ICU of the Minhang Hospital were enrolled as the research subjects. Inclusion criteria were as follows (Figure 1): (1) Patients with CVC within the ICU of the hospital; (2) Those having indwelling CVC for over 48 hours; (3) In the situation of multiple catheter - related infections in one patient, only the first instance was chosen; (4) Patients with reports of microbiological examinations related to the catheter. Exclusion criteria were: (1) Patients who had been clearly diagnosed with sepsis prior to catheterization; (2) Patients who developed a hematoma during the puncture procedure; (3) Nosocomial infections due to non - catheter - associated factors. The diagnostic criteria for central venous catheter - related infections referred to the Clinical Practice Guidelines for the Diagnosis and Management of CLABSI in the United States (Hentrich et al., 2014). This study was reviewed and approved by the hospital's medical ethics committee.

2.2 Methods

Cases were retrieved through the hospital's medical record query system. Two staff members were assigned to fill in the form, while another two were responsible for the review process. The statistical content covered various aspects: patients' basic information (including gender, age, body mass index, and past medical history), details of the catheter (such as type, indwelling site, duration of indwelling, and the time interval from catheter insertion to the onset of infection), results of pathogen detection and drug - sensitivity tests. For the infected group, the NLR, PLR, and PCT values were selected within 48 hours before blood culture and catheter culture were performed when infection was suspected. For patients in the non - infected group, the results of blood routine examinations and PCT tests were selected on the day

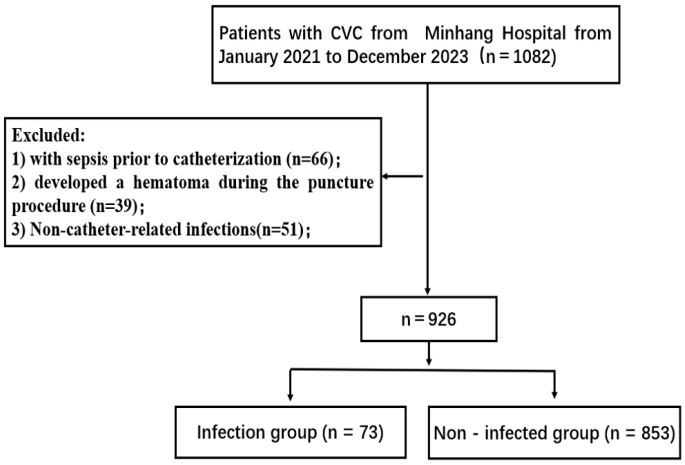

FIGURE 1
The flow of patient selection.

of CVC removal. Blood routine examination items include neutrophils, platelets, and lymphocytes, among others. Based on these elements, the NLR and PLR are calculated.

2.3 Statistical analysis

The SPSS21.0 software was employed for data analysis. The counting data were expressed in the form of case numbers or percentages, and either the χ^2 test or the Fisher's exact probability method was utilized. Measurements following a normal distribution were presented as ($\bar{x} \pm s$), while those with a non - normal distribution were presented as P_{50} (P_{25}, P_{75}). An independent - sample T - test was conducted for inter - group comparison. The receiver operating characteristic (ROC) curve of subject characteristics was drawn to analyze the value of serological indices in diagnosing CLABSI. The test level $\alpha = 0.05$ for both - sided tests, and a p - value less than 0.05 was considered statistically significant.

3 Results

3.1 Infection rate and related conditions

A total of 926 patients with a central venous catheter in the ICU were investigated from January 2021 to December 2023. Among them, 73 patients developed CLABSI, resulting in an infection rate of 7.88%. Among the infected patients, 45 were male and 28 were female. Fifty patients were 60 years old or older, while 23 were younger than 60. There were 30 patients with a catheter indwelling time of 14 days or more, and 43 patients with a catheter indwelling time of less than 14 days. Multiple logistic regression analysis indicated that age, catheterization site, catheterization time, and the application of a double - luminal catheter were independent influencing factors for CLABSI ($P < 0.05$), as presented in Tables 1, 2.

3.2 Distribution of pathogenic bacteria

In this study, 73 patients with CLABSI had 81 pathogenic bacteria strains detected. Gram - positive bacteria accounted for 60.50% (49/81), gram - negative ones for 35.80% (29/81), and fungi for 3.70% (3/81). The specific proportion of each is shown in Figure 2.

3.3 Drug resistance of major Gram - positive bacteria

Among the pathogens related to CLABSI in the intensive care unit, gram - positive bacteria exhibited high resistance to penicillin, erythromycin, clindamycin, and oxacillin, with a resistance rate exceeding 70%. In contrast, vancomycin, linezolid, and tetracycline demonstrated low drug resistance, having a resistance rate of less than 20%, as presented in Table 3.

3.4 Drug resistance of major Gram - negative bacteria

Among the pathogens of CLABSI in intensive care units, the principal Gram - negative bacteria exhibited high resistance to cefepime, piperacillin, aztreonam, and gentamicin, with the drug resistance rate exceeding 70%. In contrast, cefoperazone/sulbactam, imipenem, and amikacin demonstrated low drug resistance, having resistance rates lower than 20%, as presented in Table 4.

TABLE 1 Univariate analysis of the CLABSI.

Project	Infected Group (n = 73)	Non-infected group (n = 853)	χ^2 - value	*P* - value
Gender (Male/Female)	45/28	465/388	1.382	0.240
Age (in years)	61.18 ± 8.39	60.59 ± 8.82	0.579	0.577
BMI (kg/m²)	21.73 ± 3.84	22.40 ± 3.65	0.896	0.462
Catheter Indwelling Time (days)			6.280	0.012
<14d	43	620		
≥14d	30	233		
Indwelling Catheter Position			7.476	0.006
Non - femoral Vein	28	469		
Femoral Vein	45	384		
Use of Double - lumen Catheters			7.868	0.005
Yes	39	314		
No	34	539		
History of Diabetes Mellitus			3.212	0.073
No	54	703		
Yes	19	150		

BMI, body mass index.

3.5 The levels of peripheral blood PCT, NLR, and PLR of patients in both the infected and non - infected groups were compared

The peripheral blood PCT levels of patients in the infected and non - infected groups differed statistically ($P < 0.001$). When the NLR and PLR levels of the two groups were compared, it was found that the NLR and PLR in the infected group were significantly higher than those in the non - infected group ($p < 0.001$) (Table 5).

3.6 Value of peripheral blood PCT, NLR, and PLR levels in the diagnosis of CLABSI individually and in combination

The AUC of the levels of PCT, NLR, and PLR in peripheral blood for diagnosing CLABSI were 0.856, 0.814, and 0.798 respectively. The AUC for PCT diagnosis was the largest. When the cut - off point was 2.75 ng/ml, the Youden index reached its maximum. In the combined diagnosis, the AUCs of peripheral blood PLR combined with NLR, PLR combined with PCT, NLR combined with PCT, and the combination of all three in diagnosing CLABSI were 0.877, 0.857, 0.903, and 0.917 respectively. Among these combinations, the combination of all three had the highest diagnostic efficiency, as presented in Table 6 and Figure 3.

4 Discussion

In this study, it has been determined that the risk factors for CLABSI within ICUs include an age of ≥60 years, femoral vein catheterization, a catheter placement time of ≥14 days, and the use of double - lumen catheters. This finding coincides with certain research on CLABSI (Chua et al., 2014; Cheng et al., 2019; de Grooth et al., 2020; Pitiriga et al., 2020). It suggests that the patient's age, the site of catheterization, the duration, and the type of catheter all increase the incidence of CLABSI in ICUs to varying degrees.

TABLE 2 Multivariate logistic regression analysis of the infection in CLABSI.

Associated Factors and Variable Assignment	*β*	*S.E*	*Wald* χ^2	*P - value*	*OR*	*95%CI*
Age	1.965	0.827	4.968	0.029	6.287	2.891, 37.834
Tube Placement Location	3.217	0.587	11.223	0.012	14.926	3.897, 52.437
Indwelling Time of Catheter	1.447	0.430	12.320	0.007	4.503	1.116, 19.228
Use of Double - lumen Catheters	3.762	0.536	11.874	0.009	15.327	4.396, 59.671

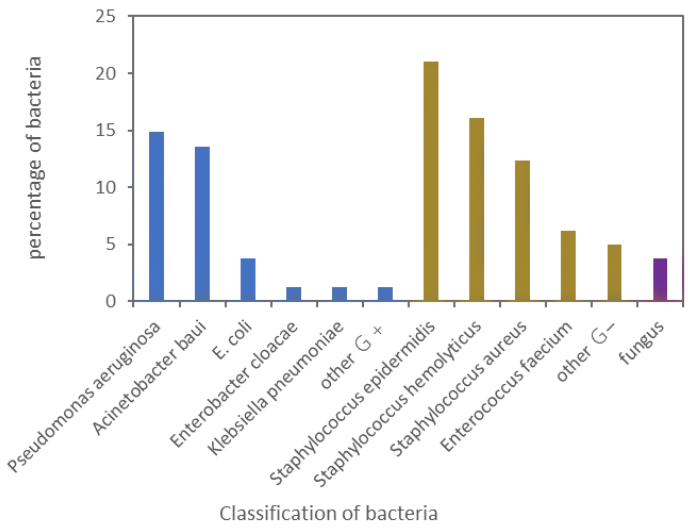

FIGURE 2
Constituent ratio of the pathogens isolated from the patients with CLABSI.

Consequently, for clinical catheterization, the internal jugular vein or subclavian vein should be selected whenever feasible. Additionally, the catheter should be removed as soon as possible, and the single - cavity catheter should be preferred.

In this study, through analyzing the distribution of pathogens related to CLABSI, it was found that among 926 patients in the ICU, 73 suffered from CLABSI, with an infection rate of 7.88%. In the United States, approximately 16,000 cases of CLABSI occur in ICUs, and around 400 - 5,000 patients die annually due to catheter infection (Chua et al., 2014). In this research, a total of 81 strains of pathogenic bacteria were identified in 73 patients with CLABSI. Among them, gram - positive bacteria accounted for 60.50%, gram - negative bacteria for 35.80%, and fungi for 3.70%. The most common gram - positive bacteria was Staphylococcus epidermidis (20.99%), and the most prevalent gram - negative bacteria was Pseudomonas aeruginosa (14.82%). Pinto et al. (2022) investigated patients in three large hospitals and revealed that the positive rate of Staphylococcus epidermidis was 36.21%, and among gram - negative bacteria, the positive rate of Pseudomonas aeruginosa was the highest. This is similar to the results of this study and relevant literature (Barrigah-Benissan et al., 2023; Rha et al., 2023; Tabah et al., 2023), indicating that gram - positive bacteria are the principal pathogens in patients with CLABSI in the ICU, which has guiding significance for clinical drug use.

In the present study, through the monitoring of the drug resistance profiles of the principal pathogens in patients diagnosed with Central Venous Catheter-Related Bloodstream Infections (CLABSI), several notable findings were obtained. It was observed that Gram-positive bacteria manifested a high level of resistance to penicillin, erythromycin, clindamycin, and oxacillin, with the resistance rates surpassing 70%. In contrast, their

TABLE 3 Drug Resistance of Major Gram - positive Bacteria in CLABSI in the Intensive Care Unit [Strains (%)].

Antibacterial drug	Staphylococcus aureus (n = 10)		Staphylococcus hemolyticus (n = 13)		Staphylococcus epidermidis (n = 17)	
	N	Drug Resistance Rate (%)	N	Drug Resistance Rate (%)	N	Drug Resistance Rate (%)
Levofloxacin	3	30.00	5	38.46	6	35.29
Ciprofloxacin	5	50.00	8	61.54	7	41.18
Linezolid	1	10.00	2	15.38	0	0.00
Oxacillin	9	90.00	12	92.31	16	94.12
Vancomycin	0	0.00	0	0.00	0	0.00
Clindamycin	8	80.00	11	84.62	14	82.35
Tetracycline	4	40.00	4	30.77	9	52.94
Erythromycin	9	90.00	12	92.31	16	94.12
Penicillin	8	80.00	10	76.92	15	88.24

TABLE 4 Drug resistance of major Gram-negative bacteria in CLABSI in intensive care unit [strains (%)].

Antibacterial Drug	Acinetobacter baumannii (n = 11)		Pseudomonas aeruginosa (n = 12)	
	N	Drug Resistance Rate (%)	N	Drug Resistance Rate (%)
Levofloxacin	6	54.55	6	50.00
Ciprofloxacin	5	45.45	5	41.67
Amikacin	2	18.18	2	16.67
Gentamicin	9	81.82	9	75.00
Meropenem	4	36.36	5	41.67
Imipenem	0	0.00	0	0.00
Aztreonam	8	72.73	9	75.00
Piperacillin	9	81.82	11	91.67
Cefoperazone - Sulbactam	1	9.09	1	8.33
Cefotaxime	6	54.55	8	66.67
Cefepime	10	90.91	11	91.67
Ceftazidime	5	45.45	8	66.67

resistance to vancomycin, linezolid, and tetracycline was relatively low, as evidenced by the resistance rates remaining below 20%. Regarding Gram-negative bacteria, these pathogens demonstrated a pronounced resistance to cefepime, piperacillin, aztreonam, and gentamicin, where the resistance rates exceeded 70%. However, they exhibited a low resistance to Cefoperazone-Sulbactam, imipenem, and amikacin, with the resistance rates being less than 20%. Previous studies (Ohnuma et al., 2023) have suggested that vancomycin could be considered as the preferred therapeutic option for treating Gram-positive bacterial infections in the context of CLABSI, especially in regions characterized by a low prevalence of CLABSI and a relatively low susceptibility to vancomycin. Concurrently, within the scope of this study, it was found that the resistance rate of amoxicillin in the drug-susceptibility testing was the highest among the antibiotics tested, followed by that of ampicillin. For Gram-negative bacteria, imipenem was identified as the antibiotic to which they exhibited the highest sensitivity, followed by tobramycin. Nevertheless, it should be noted that these Gram-negative bacteria still displayed a relatively high resistance rate to aztreonam and ceftriaxone. This comprehensive understanding of the drug resistance patterns of the main pathogens in CLABSI patients can provide valuable insights for guiding the rational selection of antibiotics in clinical practice, aiming to improve the treatment outcomes and mitigate the impact of antibiotic resistance.

In this study, NLR, PLR, and PCT were selected as predictors for CLABSI. NLR serves as an indicator reflecting the levels of neutrophils and lymphocytes within the body. During sepsis and other systemic infections, the activation of extracellular regulatory kinase and other substances can be observed, and the enhanced expression of anti - apoptotic proteins leads to the delay of neutrophil apoptosis. A higher count of neutrophils implies a more severe inflammatory response within the body and a more intense systemic inflammatory reaction. Meanwhile, the large consumption of lymphocytes can directly reflect the degree of inflammation in the body and provide auxiliary evidence for the early diagnosis of bacterial bloodstream infections. (Buonacera et al., 2022; Li et al., 2022; Wang et al., 2023). PLR is an index that reflects the levels of platelets and lymphocytes. Besides their hemostatic and thrombosis - promoting functions, platelets also

TABLE 5 Peripheral Blood PCT, NLR and PLR Levels in Patients of the Infected and Uninfected Groups.

Index	Non-infected Group (n = 853)	Infected Group (n = 73)	*t* value	*P* value
PCT, median (Q1, Q3)	0.43 (0.29, 0.67)	5.87 (4.83, 7.70)	-30.024	<0.001
PLR, median (Q1, Q3)	121.71 (98.04, 141.79)	168.35 (143.24, 217.39)	-10.177	<0.001
NLR, median (Q1, Q3)	2.28 (1.87, 2.96)	6.80 (2.90, 9.60)	-8.827	<0.001

TABLE 6 Diagnostic value of peripheral blood PCT, NLR and PLR in CLABSI.

Index	AUC	Cut - off value	Sensitivity (%)	Specificity (%)	95% *CI*	*P* value
PCT	0.856	2.75	74.14	96.53	0.762-0.949	<0.001
PLR	0.798	130.24	92.66	50.92	0.700-0.895	<0.001
NLR	0.814	2.87	81.52	62.27	0.724-0.901	<0.001
PCT+NLR	0.903	—	85.27	91.36	0.849-0.975	<0.001
PCT+PLR	0.857	—	81.55	76.27	0.757-0.954	<0.001
PLR+NLR	0.877	—	88.93	75.07	0.804-0.948	<0.001
PCT+NLR+PLR	0.917	—	85.26	92.90	0.827-0.978	<0.001

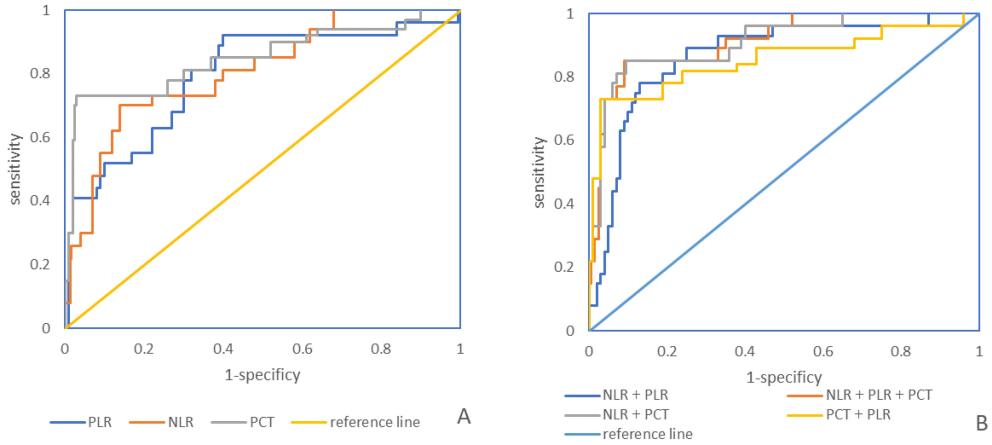

FIGURE 3
(A). ROC curve of peripheral blood PCT, NLR, and PLR levels individually for the diagnosis of CLABSI; **(B)**. ROC curve of peripheral blood PCT, NLR, and PLR levels in combination for the diagnosis of CLABSI.

possess a certain pathogen - killing effect. In the process of systemic inflammatory response, endotoxin can trigger platelet activation and the secretion of pro - inflammatory factors such as chemokines and nitric oxide. These molecules attach to and bind with neutrophils, activate them, and result in the production of reactive oxygen species, cytokines, and other substances to eliminate pathogenic microorganisms. Hence, the level of endotoxin can also indicate the degree of inflammation in the body (Kim et al., 2019; Kriplani et al., 2022; Kearney et al., 2023). The results of this study demonstrated that NLR and PLR were significantly elevated in the infected group compared to the uninfected group, indicating that the levels of NLR and PLR increase with CLABSI. PCT, a protein consisting of 116 amino acid residues, is a precursor of calcitonin. Studies (Lee et al., 2022; Bajić et al., 2023; Oussalah et al., 2023) have revealed that PCT can be released in large quantities during infectious diseases, and its appearance time precedes that of other cytokines, enabling it to better reflect the body's inflammatory response syndrome. The results of this study indicated that patients with CLABSI had a substantial increase in PCT, which was significantly higher than that of the uninfected group. In this study, the diagnostic AUC of each index was > 0.7, validating that each index has significant value in the early diagnosis of CLABSI. Among the indicators in this study, the PCT level has the highest diagnostic value. The possible reason is that routine blood indexes such as neutrophils, lymphocytes, and platelets can be influenced by numerous factors, whereas the PCT level only changes significantly in the context of infectious diseases, endowing it with higher diagnostic specificity and efficacy for infectious diseases (Centor and Gilbert, 2022; Schuetz, 2022). In this study, the combined - diagnosis AUC of multiple indicators was greater than that of any single indicator. Therefore, the combined detection of multiple indicators can be used to enhance the diagnostic efficiency of CLABSI in clinical practice.

The limitations of this paper are summarized as follows: (1) Sample size limitation: The study included only 73 cases in the infection group (infection rate: 7.88%), which is relatively small and may affect statistical power and the stability of results. (2) Limitations of retrospective design: The study is based on retrospective data, which may be subject to selection bias (e.g., non-randomized grouping), information bias (e.g., incomplete data recording), or inadequate control of confounding factors (e.g., lack of detailed records on antibiotic use history and immunosuppressive status). (3) External validity of single-center study: The research was conducted exclusively at Minhang Hospital. Results may be influenced by specific medical environments, operational norms, or regional pathogen distributions, making it difficult to generalize to other medical institutions or regions.

CLABSI in ICU requires close attention. Key risk factors include age, catheter site, insertion duration, and double-cavity catheter use. Gram-positive bacteria are the primary pathogens, and targeted antibiotic therapy based on microbial characteristics is critical for effective treatment. Elevated peripheral blood NLR, PLR, and PCT levels can aid CLABSI diagnosis (individually or combined), guiding early intervention and improving outcomes.

Data availability statement

The original contributions presented in the study are included in the article/supplementary material. Further inquiries can be directed to the corresponding authors.

Ethics statement

The studies involving humans were approved by the Human Research and Ethics Committee of the Minhang Hospital. The studies were conducted in accordance with the local legislation and institutional requirements. The participants provided their written informed consent to participate in this study. Written informed

consent was obtained from the individual(s) for the publication of any potentially identifiable images or data included in this article.

Author contributions

YZL: Conceptualization, Data curation, Formal Analysis, Investigation, Methodology, Project administration, Resources, Software, Supervision, Visualization, Writing – original draft. YYL: Conceptualization, Data curation, Formal Analysis, Investigation, Methodology, Project administration, Resources, Software, Validation, Writing – original draft. JW: Conceptualization, Data curation, Formal Analysis, Investigation, Methodology, Project administration, Resources, Supervision, Visualization, Writing – original draft. KS: Conceptualization, Data curation, Formal Analysis, Investigation, Methodology, Project administration, Resources, Software, Supervision, Validation, Writing – review & editing.

Funding

The author(s) declare that no financial support was received for the research and/or publication of this article. This research was supported by the National Clinical Key Specialty Construction Project(NO.Z155080000004) and the Minhang District Central Hospital, level project(NO.2020MHJC07).

Conflict of interest

The authors declare that the research was conducted in the absence of any commercial or financial relationships that could be construed as potential conflicts of interest.

Generative AI statement

The author(s) declare that no Generative AI was used in the creation of this manuscript.

Publisher's note

All claims expressed in this article are solely those of the authors and do not necessarily represent those of their affiliated organizations, or those of the publisher, the editors and the reviewers. Any product that may be evaluated in this article, or claim that may be made by its manufacturer, is not guaranteed or endorsed by the publisher.

References

Badia-Cebada, L., Peñafiel, J., Saliba, P., Andrés, M., Càmara, J., Domenech, D., et al. (2022). Trends in the epidemiology of catheter-related bloodstream infections; towards a paradigm shift, Spain, 2007 to 2019. *Euro Surveill.* 27, 2100610. doi: 10.2807/1560-7917.ES.2022.27.19.2100610

Bajić, D., Matijašević, J., Andrijević, L., Zarić, B., Lalić-Popović, M., Andrijević, I., et al. (2023). Prognostic role of monocyte distribution width, CRP, procalcitonin and lactate as sepsis biomarkers in critically ill COVID-19 patients. *J. Clin. Med.* 12, 1197. doi: 10.3390/jcm12031197

Barrigah-Benissan, K., Ory, J., Simon, C., Loubet, P., Martin, A., Beregi, J. P., et al. (2023). Clinical factors associated with peripherally inserted central catheters (PICC) related bloodstream infections: a single centre retrospective cohort. *Antimicrob Resist. Infect. Control.* 12, 5. doi: 10.1186/s13756-023-01209-z

Buonacera, A., Stancanelli, B., Colaci, M., and Malatino, L. (2022). Neutrophil to lymphocyte ratio: an emerging marker of the relationships between the immune system and diseases. *Int. J. Mol. Sci.* 23, 3636. doi: 10.3390/ijms23073636

Centor, R. M., and Gilbert, D. N. (2022). Annals on call - procalcitonin in the diagnosis of bacterial infection. *Ann. Intern Med.* 175, OC1. doi: 10.7326/A21-0006

Cheng, S., Xu, S., Guo, J., He, Q., Li, A., Huang, L., et al. (2019). Risk factors of central venous catheter-related bloodstream infection for continuous renal replacement therapy in kidney intensive care unit patients. *Blood Purif.* 48, 175–182. doi: 10.1159/000495024

Chua, H. R., Schneider, A. G., Sherry, N. L., Lotfy, N., Chan, M. J., Galtieri, J., et al. (2014). Initial and extended use of femoral versus nonfemoral double-lumen vascular catheters and catheter-related infection during continuous renal replacement therapy. *Am. J. Kidney Dis.* 64, 909–917. doi: 10.1053/j.ajkd.2014.04.022

de Grooth, H. J., Timsit, J. F., Mermel, L., Mimoz, O., Buetti, N., du Cheyron, D., et al. (2020). Validity of surrogate endpoints assessing central venous catheter-related infection: evidence from individual- and study-level analyses. *Clin. Microbiol Infect.* 26, 563–571. doi: 10.1016/j.cmi.2019.09.022

Hentrich, M., Schalk, E., Schmidt-Hieber, M., Chaberny, I., Mousset, S., Buchheidt, D., et al. (2014). Central venous catheter-related infections in hematology and oncology: 2012 updated guidelines on diagnosis, management and prevention by the Infectious Diseases Working Party of the German Society of Hematology and Medical Oncology. *Ann. Oncol.* 25, 936–947. doi: 10.1093/annonc/mdt545

Kearney, N., McCourt, C., Hambly, R., Hughes, R., O'Kane, D., and Kirby, B. (2023). Association of biologic treatment in hidradenitis suppurativa with reduced neutrophil-lymphocyte ratio and platelet-lymphocyte ratio. *JAMA Dermatol.* 159, 222–224. doi: 10.1001/jamadermatol.2022.5710

Kim, Y. J., Kang, J., Ryoo, S. M., Ahn, S., Huh, J. W., and Kim, W. Y.. (2019). Platelet-lymphocyte ratio after granulocyte colony stimulating factor administration: an early prognostic marker in septic shock patients with chemotherapy-induced febrile neutropenia. *Shock.* 52, 160–165. doi: 10.1097/SHK.0000000000001256

Kriplani, A., Pandit, S., Chawla, A., de la Rosette, J. J. M. C. H., Laguna, P., Jayadeva Reddy, S., et al. (2022). Neutrophil-lymphocyte ratio (NLR), platelet-lymphocyte ratio (PLR) and lymphocyte-monocyte ratio (LMR) in predicting systemic inflammatory response syndrome (SIRS) and sepsis after percutaneous nephrolithotomy (PNL). *Urolithiasis.* 50, 341–348. doi: 10.1007/s00240-022-01319-0

Lee, E. H., Lee, K. H., Song, Y. G., and Han, S. H.. (2022). Discrepancy of C-reactive protein, procalcitonin and interleukin-6 at hospitalization: infection in patients with normal C-reactive protein, procalcitonin and high interleukin-6 values. *J. Clin. Med.* 11, 7324. doi: 10.3390/jcm11247324

Li, D., Li, J., Zhao, C., Liao, X., Liu, L., Xie, L., et al. (2022). Diagnostic value of procalcitonin, hypersensitive C-reactive protein and neutrophil-to-lymphocyte ratio for bloodstream infections in pediatric tumor patients. *Clin. Chem. Lab. Med.* 61, 366–376. doi: 10.1515/cclm-2022-0801

Liu, B. M., Carlisle, C. P., Fisher, M. A., and Shakir, S. M.. (2021). The brief case: capnocytophaga sputigena bacteremia in a 94-year-old male with type 2 diabetes mellitus, pancytopenia, and bronchopneumonia. *J. Clin. Microbiol.* 59, e0247220. doi: 10.1128/JCM.02472-20

Luo, S., Yang, W. S., Shen, Y. Q., Chen, P., Zhang, S. Q., Jia, Z., et al. (2022). The clinical value of neutrophil-to-lymphocyte ratio, platelet-to-lymphocyte ratio, and D-dimer-to-fibrinogen ratio for predicting pneumonia and poor outcomes in patients with acute intracerebral hemorrhage. *Front. Immunol.* 13, 1037255. doi: 10.3389/fimmu.2022.1037255

Ohnuma, T., Chihara, S., Costin, B., Treggiari, M. M., Bartz, R. R., Raghunathan, K., et al. (2023). Association of appropriate empirical antimicrobial therapy with in-hospital mortality in patients with bloodstream infections in the US. *JAMA Netw Open* 6, e2249353. doi: 10.1001/jamanetworkopen.2022.49353

Oussalah, A., Callet, J., Manteaux, A. E., Thilly, N., Jay, N., Guéant, J. L., et al. (2023). Usefulness of procalcitonin at admission as a risk-stratifying biomarker for 50-day in-hospital mortality among patients with community-acquired bloodstream infection: an observational cohort study. *Biomark Res.* 11, 4. doi: 10.1186/s40364-023-00450-3

Pinto, M., Borges, V., Nascimento, M., Martins, F., Pessanha, M. A., Faria, I., et al. (2022). Insights on catheter-related bloodstream infections: a prospective observational

study on the catheter colonization and multidrug resistance. *J. Hosp Infect.* 123, 43–51. doi: 10.1016/j.jhin.2022.01.025

Pitiriga, V., Kanellopoulos, P., Bakalis, I., Kampos, E., Sagris, I., Saroglou, G., et al. (2020). Central venous catheter-related bloodstream infection and colonization: the impact of insertion site and distribution of multidrug-resistant pathogens. *Antimicrob Resist. Infect. Control.* 9, 189. doi: 10.1186/s13756-020-00851-1

Rha, B., See, I., Dunham, L., Kutty, P. K., Moccia, L., Apata, I. W., et al. (2023). Vital signs: health disparities in hemodialysis-associated staphylococcus aureus bloodstream infections - United States, 2017-2020. *MMWR Morb Mortal Wkly Rep.* 72, 153–159. doi: 10.15585/mmwr.mm7206e1

Ruiz-Ruigómez, M., and Aguado, J. M. (2021). Duration of antibiotic therapy in central venous catheter-related bloodstream infection due to Gram-negative bacilli. *Curr. Opin. Infect. Dis.* 34, 681–685. doi: 10.1097/QCO.0000000000000763

Schuetz, P. (2022). How to best use procalcitonin to diagnose infections and manage antibiotic treatment. *Clin. Chem. Lab. Med.* 61 (5), 822-828. doi: 10.1515/cclm-2022-1072

Singer, M., Deutschman, C. S., Seymour, C. W., Shankar-Hari, M., Annane, D., Bauer, M., et al. (2016). The third international consensus definitions for sepsis and septic shock (Sepsis-3). *JAMA.* 315, 801–810. doi: 10.1001/jama.2016.0287

Tabah, A., Buetti, N., Staiquly, Q., Ruckly, S., Akova, M., Aslan, A. T., et al. (2023). Epidemiology and outcomes of hospital-acquired bloodstream infections in intensive care unit patients: the EUROBACT-2 international cohort study. *Intensive Care Med.* 49, 178–190. doi: 10.1007/s00134-022-06944-2

Teja, B., Bosch, N. A., Diep, C., Pereira, T. V., Mauricio, P., Sklar, M. C., et al. (2024). Complication rates of central venous catheters: A systematic review and meta-analysis. *JAMA Intern Med.* 184, 474–482. doi: 10.1001/jamainternmed.2023.8232

van der Kooi, T. I. I., Smid, E. A., Koek, M. B. G., Geerlings, S. E., Bode, L. G. M., Hopmans, T. E. M., et al. (2023). The effect of an intervention bundle to prevent central venous catheter-related bloodstream infection in a national programme in the Netherlands. *J. Hosp Infect.* 131, 194–202. doi: 10.1016/j.jhin.2022.11.006

Wang, R. H., Wen, W. X., Jiang, Z. P., Chen, P., Zhang, S. Q., Jia, Z., et al. (2023). The clinical value of neutrophil-to-lymphocyte ratio (NLR), systemic immune-inflammation index (SII), platelet-to-lymphocyte ratio (PLR) and systemic inflammation response index (SIRI) for predicting the occurrence and severity of pneumonia in patients with intracerebral hemorrhage. *Front. Immunol.* 14, 1115031. doi: 10.3389/fimmu.2023.1115031

Xu, H., Hyun, A., Mihala, G., Rickard, C. M., Cooke, M. L., Lin, F., et al. (2024). The effectiveness of dressings and securement devices to prevent central venous catheter-associated complications: A systematic review and meta-analysis. *Int. J. Nurs. Stud.* 149, 104620. doi: 10.1016/j.ijnurstu.2023.104620

Zhang, R. M., Tan, K., Fu, S., and Deng, J. K. (2022). Limited value of procalcitonin, C-reactive protein, white blood cell, and neutrophil in detecting bacterial coinfection and guiding antibiotic use among children with enterovirus infection. *World J. Pediatr.* 18, 230–233. doi: 10.1007/s12519-021-00504-2

Zinellu, A., Zinellu, E., Mangoni, A. A., Pau, M. C., Carru, C., Pirina, P., et al. (2022). Clinical significance of the neutrophil-to-lymphocyte ratio and platelet-to-lymphocyte ratio in acute exacerbations of COPD: present and future. *Eur. Respir. Rev.* 31, 220095. doi: 10.1183/16000617.0095-2022

frontiers | Frontiers in Cellular and Infection Microbiology

TYPE Review
PUBLISHED 08 May 2025
DOI 10.3389/fcimb.2025.1527217

OPEN ACCESS

EDITED BY
Eileen Uribe-Querol,
Universidad Nacional Autónoma de México, Mexico

REVIEWED BY
Pavlo Petakh,
Uzhhorod National University, Ukraine
Suchetha Aghanashini,
Rajiv Gandhi University of Health Sciences, India

*CORRESPONDENCE
José Luis Muñoz-Carrillo
mcbjlmc@gmail.com
Oscar Gutiérrez-Coronado
ogutierrez@culagos.udg.mx

RECEIVED 13 November 2024
ACCEPTED 16 April 2025
PUBLISHED 08 May 2025

CITATION
Muñoz-Carrillo JL, Palomeque-Molina PI, Villacis-Valencia MS, Gutiérrez-Coronado O, Chávez-Ruvalcaba F, Vázquez-Alcaraz SJ, Villalobos-Gutiérrez PT and Palomeque-Molina J (2025) Relationship between periodontitis, type 2 diabetes mellitus and COVID-19 disease:
a narrative review.
Front. Cell. Infect. Microbiol. 15:1527217.
doi: 10.3389/fcimb.2025.1527217

Relationship between periodontitis, type 2 diabetes mellitus and COVID-19 disease: a narrative review

José Luis Muñoz-Carrillo[1,2]*, Paulo Israel Palomeque-Molina[3], Marcelo Stalin Villacis-Valencia[3], Oscar Gutiérrez-Coronado[1]*, Francisca Chávez-Ruvalcaba[4], Silverio Jafet Vázquez-Alcaraz[5], Paola Trinidad Villalobos-Gutiérrez[1] and Josue Palomeque-Molina[6]

[1]Laboratorio de Inmunología, Centro Universitario de los Lagos, Universidad de Guadalajara, Lagos de Moreno, Jalisco, Mexico, [2]Escuela de Odontología, Global University, Aguascalientes, Aguascalientes, Mexico, [3]Facultad de Ciencias de La Salud, Escuela de Odontología, Universidad Internacional del Ecuador, Quito, Ecuador, [4]Licenciatura en Nutrición, Universidad Autónoma de Zacatecas, Zacatecas, Zacatecas, Mexico, [5]Departamento de Odontología Conservadora, Escuela de Odontología, Universidad Complutense de Madrid, Madrid, Spain, [6]Departamento de Pediatría, Hospital Homero Castanier Crespo, Azogues, Ecuador

Inflammation plays a fundamental role in the development and bidirectional association of di-verse diseases, such as periodontitis and type 2 diabetes mellitus (T2DM), which generates important clinical complications, where chronic exposure to high levels of blood glucose affects the repair process of periodontal tissues. Likewise, it has been observed that comorbidity, between these two diseases, influences the development of the COVID-19 disease towards a more severe course. However, there is currently very little scientific evidence on the relationship between periodontitis, T2DM and COVID-19 disease. This narrative review aims to provide an understanding of the current and most relevant aspects of the relationship between periodontitis, T2DM and COVID-19 disease. A narrative review was performed through a systematic search of published studies, without date restrictions, indexed in the electronic databases of PubMed, for the inclusion of articles in English, and LILACS for the inclusion of articles in Spanish. This review included different articles, which addressed the most important aspects to present a current perspective on the relationship and influence between periodontitis, T2DM and COVID-19 disease. Comorbidity between periodontitis and T2DM represents a greater risk of developing a more severe course of COVID-19 disease, because these three diseases share three important axes: a clinicopathological axis; an axis associated with glycemia, and an immunological axis associated with inflammation.

KEYWORDS

COVID-19, inflammation, periodontitis, SARS-CoV-2, type 2 diabetes mellitus

1 Introduction

At a clinical level, periodontal health is characterized by the absence of inflammation (Chapple et al., 2018). Under these conditions, the periodontal tissue is capable of adequately defending itself, through various mechanisms of the immune system, against the presence of bacteria present in the oral cavity. Periodontal disease develops when the balance between these defense mechanisms that control infection and the subgingival biofilm is lost, triggering the innate (inflammation) and adaptive immune response of the host (Mira et al., 2017). Periodontal disease can be divided into four stages based on the type of lesion: 1) initial and 2) early lesions; which are part of gingivitis; and the 3) established and 4) advanced lesions that are part of periodontitis (Muñoz-Carrillo et al., 2019). In this context, periodontitis is an immunoinflammatory disease that mainly affects the periodontal tissues that support the teeth, causing their progressive destruction, which ultimately results in tooth loss (Kedlaya et al., 2023). On the other hand, there are risk factors that influence the development and severity of periodontal disease, which can be local and systemic. Likewise, these factors can also be modifiable, such as smoking, stress, obesity, and uncontrolled diabetes mellitus, among others; and non-modifiable such as sex, age, ethnicity or genetic factors (Moreno Caicedo et al., 2018).

Diabetes mellitus is a syndrome that involves a wide variety of genetic, epigenetic and pathophysiological abnormalities, which can be influenced by environmental factors, such as infections, diet (nutrients), intestinal microbiota, among others (Hanson and Godfrey, 2015; Stančáková and Laakso, 2016; Sircana et al., 2018; Zhang and Pollin, 2018). T2DM is the most common type of diabetes. T2DM is characterized by presenting various defects at a biochemical and pathophysiological level, which are associated with peripheral insulin resistance, increased hepatic glucose production, altered levels of intestinal hormones that regulate insulin and glucagon function, decrease and failure of pancreatic β cells function, as well as additional mechanisms that are related to inflammation (Defronzo, 2009; Brunton, 2016; Javeed and Matveyenko, 2018). In the context of T2DM, insulin plays an essential role in the regulation of immunocellular function, acting as a critical link between metabolic dysfunction and the immune response (Berbudi et al., 2025). Insulin resistance, a central feature of T2DM, disrupts immunological homeostasis by affecting the functionality of innate and adaptive immune cells, resulting in an imbalance between pro-inflammatory and anti-inflammatory responses (Dror et al., 2017). This state favors the overproduction of proinflammatory cytokines and adipokines, including tumor necrosis factor alpha (TNF)-α, interleukin (IL)-6, leptin, and resistin, which not only exacerbate insulin resistance but also contribute to the establishment of a chronic low-grade inflammatory microenvironment (Gerrits et al., 2012; Villarreal-Pérez et al., 2014; Sun et al., 2018). This persistent inflammation constitutes a key pathogenic factor in the progression of T2DM, further impairing insulin signaling and compromising carbohydrate metabolism (Dror et al., 2017).

Several studies have associated T2DM with periodontitis, suggesting a bidirectional association between both pathologies (Santos et al., 2015; Turner, 2022), since patients with T2DM have a greater probability of developing periodontitis, and in those patients who present this comorbidity, between both pathologies, they show worse blood glucose control (Tsai et al., 2002; Guzman et al., 2003; Liccardo et al., 2019). In this context, T2DM leads to an increase in the expression of proinflammatory cytokines in periodontal tissues (Polak and Shapira, 2018), such as IL-1β and prostaglandin (PG)-E_2 in gingival crevicular fluid. Likewise, an increase in the expression of TNF-α, IL-1β, IL-6, IL-17, and IL-23 in the gingiva has been reported, both in patients and in animal models with diabetes (Salvi et al., 1997; Salvi et al., 1998), which influences the vascular and cellular phenomena of inflammation (Domingueti et al., 2016), stimulating greater bone resorption, through an increase and reduction in the expression of the receptor activator of nuclear factor-κ B ligand (RANKL) and osteoprotegerin, respectively (Santos et al., 2010). On the other hand, inflammation also induces an increase in the production and activation of matrix metalloproteinases, which leads to the destruction of connective tissue, induction of apoptosis in fibroblasts and osteoblasts, thus limiting the repair capacity of the periodontal tissues (Pacios et al., 2013; Sarkar et al., 2013; Xiao et al., 2016). Furthermore, a decrease in the production of anti-inflammatory lipid mediators and cytokines such as IL-4, IL-10 and transforming growth factor (TGF)-β has been reported, potentially contributing to the development and aggravation of periodontal inflammation in patients with T2DM (Andriankaja et al., 2012; Acharya et al., 2017; Van Dyke, 2017).

Another important factor during T2DM is the role of blood glucose concentration, since high blood glucose levels contribute to the development and evolution of inflammation, through the activation of various intracellular signaling pathways. For example, mitogen-activated protein kinase (MAPK) and nuclear factor (NF)-κB pathways, which results in an increase in the production of proinflammatory mediators, such as cytokines and reactive oxygen species (Coughlan and Sharma, 2016; Fakhruddin et al., 2017; Lim et al., 2017; Zheng et al., 2018). Furthermore, it has been observed that patients with T2DM show an increase in both the expression of inducible nitric oxide synthase (iNOS) and the levels of lipid peroxides in the periodontium and crevicular fluid, respectively, which contributes to a more severe course of the periodontal inflammation (Shaker et al., 2013).

The COVID-19 disease, caused by SARS-CoV-2, has caused alarming numbers of infections and deaths around the world (Zhang et al., 2023). The clinical characteristics of the COVID-19 disease are very diverse, which can present from an asymptomatic state, or mild symptoms can manifest (Ullah et al., 2021); until progressing to pneumonia, developing acute respiratory distress syndrome (ARDS), multiple organ dysfunction and death (Ye et al., 2020). The pathophysiology of COVID-19 disease may not be limited exclusively to pulmonary manifestations, including pneumonia and ARDS (Gupta et al., 2020), since SARS-CoV-2 is able to infect other cell types which express its binding receptor, angiotensin-converting enzyme (ACE)-2 (Muniyappa and Gubbi, 2020), such as cells of the upper respiratory system, alveolar epithelial cells in lungs, enterocytes, endothelial cells (Gurwitz,

2020), from heart (Zheng et al., 2020), tubular epithelium kidney (Diao et al., 2021) and pancreas (Liu et al., 2020), causing organ-specific extrapulmonary clinical manifestations associated with harmful effects on many other systems of the human body, such as neurological, thrombotic, endocrine, cardiac, dermatological, hepatic, renal and gastrointestinal (Gupta et al., 2020). Although it is known that the majority of people with COVID-19 do not develop symptoms or only have mild manifestations of the disease, approximately 14% of infected people develop the disease with a severe course (Zhou et al., 2020), where advanced age and some comorbidities, such as diabetes (Abdi et al., 2020), have been associated as potential risk factors for triggering more severe disease and death (Zhou et al., 2020). Diabetic patients who suffer from COVID-19 have a prevalence of death between 22 to 31%, compared to patients without diabetes (Singh et al., 2020). Elements that could influence in patients with diabetes mellitus to increase susceptibility to COVID-19 disease include: greater ease for the virus to adhere and efficiently enter cells, less effectiveness of the immune system in eliminating the virus, greater probability of suffering severe complications due to the excessive release of proinflammatory cytokines causing hyperinflammation, and presence of diseases associated with the heart (Muniyappa and Gubbi, 2020). Likewise, it has been shown that there is high expression of ACE-2 in the lung, kidney, heart, and pancreas in rodent models of diabetes mellitus (Wysocki et al., 2006; Roca-Ho et al., 2017), and a higher pulmonary expression of ACE-2 in humans (Rao et al., 2020). In this context, diverse studies support the hypothesis that patients with diabetes mellitus have greater susceptibility to SARS-CoV-2 infection, since they are not able to efficiently eliminate the virus. This is due, on the one hand, to the fact that patients with diabetes mellitus have high levels of furin, a protease involved in cleaving the S1 and S2 domains of the virus spike protein, which facilitates the entry of the virus into the cell (Fernandez et al., 2018). Furthermore, patients with diabetes mellitus present alterations in the immune system, which inhibit neutrophil chemotaxis, phagocytosis, and intracellular destruction of pathogens, as well as delaying both the activation of Th1 cells and the hyperinflammatory response (Hodgson et al., 2015; Cuschieri and Grech, 2020). On the other hand, patients with COVID-19 present, at a peripheral level, low counts of CD4+ and CD8+ T cells, but with a higher proportion of pro-inflammatory CD4+ Th17 T cells, along with high levels of pro-inflammatory cytokines (Yang et al., 2020).

Currently, there is not enough scientific evidence on the relationship between periodontitis and T2DM and the risk of SARS-CoV-2 infection. Therefore, a more extensive and exhaustive search is necessary to identify additional literature; and in this way provide a more reliable and accurate hypothesis and conclusion about the association of these three pathologies. In this context, the aim of this research was to provide a systematized narrative review to contrast the existing evidence on the relationship between periodontitis, T2DM and COVID-19 disease. In this narrative review, a systematic methodology was applied (Page et al., 2021), without date restrictions, indexed in the electronic databases of PubMed, for the inclusion of articles in English, and LILACS for the inclusion of articles in Spanish, through the use of the Boolean operators AND, OR and NOT; using the following DeCS/MeSH terms: "periodontal disease", "periodontitis", "type 2 diabetes mellitus", "SARS-CoV-2" and "COVID-19".

2 Periodontitis and type 2 diabetes mellitus

Periodontitis is considered the sixth complication of diabetes mellitus (Acharya et al., 2017), because several studies have shown a strong bidirectional relationship between these diseases, since it has been observed that in subjects with T2DM (controlled or not) present a significant increase in the prevalence of chronic or severe periodontitis, compared to healthy subjects (Susanto et al., 2011; Shamala et al., 2017; Alasqah et al., 2018; Trentin et al., 2018; Wu et al., 2020; Monod Nuñez et al., 2022). This bidirectional relationship between periodontitis and T2DM is also because both diseases share pathogenic inflammatory mechanisms (Figure 1). On the one hand, periodontitis can influence the development and state of chronic systemic inflammation, through the aberrant increase in proinflammatory cytokines, such as IL-1β, IL-6 and TNF-α, affecting endothelial function, and substantially contributing to the development of insulin resistance, causing a homeostatic imbalance in blood glucose regulation (Acharya et al., 2017). On the other hand, T2DM is closely related to vascular endothelial dysfunction, affecting the protective balance and permeability of the endothelium, enhancing chronic systemic inflammation (Janket et al., 2008; Gurav, 2014; Li et al., 2022).

TNF-α plays a crucial role in regulating the expression of endocan, a soluble proteoglycan that is highly produced by vascular endothelium during endothelial activation and inflammatory processes (Sarrazin et al., 2006). This dual characteristic allows that the endocan may act as both an inflammatory mediator and a marker of endothelial activation (van Eijk et al., 2014). Interestingly, studies have shown a correlation between elevated endocan levels and worsening glycemic control; while improvements in glycemic control lead to a decrease in endocan expression. Furthermore, endocan expression has been detected in systemically healthy individuals with periodontal disease (Arman et al., 2016; Türer et al., 2017), suggesting a potential link beyond glycemic status. In this context, endocan could be a promising biomarker for the early diagnosis and prognosis of chronic inflammatory states in T2DM and periodontal disease, due to its ability to reflect the impact of endothelial activation in these pathological conditions. Furthermore, endocan could serve as an indicator for monitoring the response to treatment in patients with T2DM and periodontal disease, since the alteration of its levels is associated with the inflammatory state and glycemic control in individuals with these pathologies (Kumar et al., 2020).

On the other hand, a hallmark of metabolic disorders, particularly T2DM, is the abnormal activation of both the innate and adaptive immune systems, through the recruitment of immune

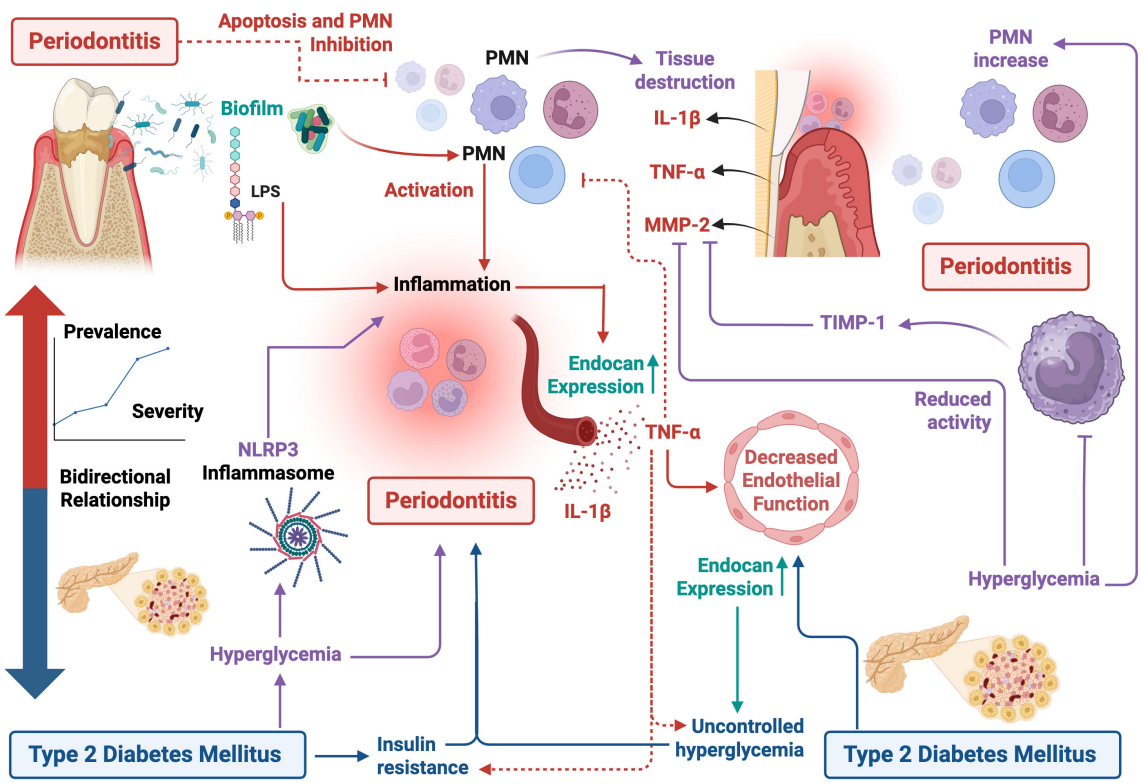

FIGURE 1
Pathogenic inflammatory mechanisms between periodontitis and type 2 diabetes mellitus. The figure represents the bidirectional interaction between both pathologies, in which periodontal inflammation contributes to a systemic proinflammatory state, characterized by an increase in the release of proinflammatory cytokines (such as TNF-α and IL-1β), which induce insulin resistance and worsen glycemic control. In parallel, chronic hyperglycemia typical of T2DM generates oral dysbiosis, immune dysfunction, endothelial dysfunction, and increased susceptibility to periodontal disease progression. This inflammatory and immunometabolic responses establishes a pathogenetic cycle that enhances the severity of both conditions. Figure created with BioRender.com by Muñoz-Carrillo et al.

cells in the affected tissues, even in the absence of external pathogens or antigens (Coelho et al., 2013; Zhou et al., 2018). The direct consequences of these responses and the modulation of immune cell populations depend largely on the metabolic system, altering cellular functionality, increasing the secretion of cytokines and chemokines, as well as the recruitment and activation of leukocyte populations (Lackey and Olefsky, 2016). Therefore, the hyperglycemia in patients with T2DM favors the increase of polymorphonuclear neutrophil leukocytes (PMNs) within the tissues, altering several functions such as cell adhesion, chemotaxis, phagocytosis, and the degradation of antigens, generating tissue damage by these cells. Because periodontitis and T2DM share a complex relationship involving inflammation, hyperinflammation, especially caused by hyperreactive PMNs, plays a crucial role in host tissue destruction in the pathogenesis of periodontitis, since the different phenotypes that present by PMNs act as an important link in both diseases, influencing in their pathogenesis (Figure 1) (Ling et al., 2015).

Bacteria residing in the gingival sulcus trigger the activation of PMNs, resulting in an increase in the release of molecules with bactericidal properties. These molecules, in turn, are considered responsible for the hallmark characteristics that mark the progression of periodontal disease, including the destruction of periodontal (Nussbaum and Shapira, 2011) tissue and inflammation, which may contribute to metabolic dysregulation (Ling et al., 2015). In this context, Herrmann et al. found that patients with periodontitis and T2DM showed a significant increase in gingival PMNs, compared to individuals who only had periodontitis, indicating a hyperinflammatory reaction in the gingival tissue, probably due to T2DM. Therefore, it is suggested that inflammation may be a bilateral factor that can increase the severity and progression of both diseases (Herrmann et al., 2020). The research by Manosudprasit et al. corroborates these findings. In their study, it was observed that the apoptosis of PMNs in the peripheral blood was altered in individuals with T2DM. Furthermore, periodontal disease acted as a confounding factor, meaning that it exerted an additive effect, significantly delaying spontaneous PMNs apoptosis in patients with T2DM and periodontitis. These findings suggest that periodontal disease not only affects the apoptosis of PMNs at the site of periodontal infection but also has a systemic impact on the resolution of inflammation and clearance of PMNs. This may contribute to the exacerbation of other systemic inflammatory conditions, such as T2DM. In fact, it has been shown that apoptosis of PMNs is delayed in periodontal disease due to the action of TNF-α (Figure 1) (Manosudprasit et al., 2017).

Furthermore, T2DM is considered a significant risk factor for the development of periodontitis (Dhir et al., 2018), because T2DM intensifies the inflammatory response in periodontal tissues, significantly increasing the levels of proinflammatory mediators such as IL-1β and TNF-α, as well as an increase in the activity of matrix metalloproteinases (MMP) (Mesia et al., 2016). On the other hand, high blood glucose levels attenuate the immune response in patients with T2DM, affecting the recovery of periodontal tissue, which alters the etiopathology of diverse diseases, such as periodontitis (Grover and Luthra, 2013). MMPs are enzymes that play a crucial role in tissue remodeling and the breakdown of the extracellular matrix (ECM) (Sapna et al., 2014). Furthermore, they are involved in the regulation of the activity of various biologically active substrates (Collazos et al., 2015), such as pro- and anti-inflammatory cytokines, chemokines, growth factors, serum components, complement components and cell signaling molecules, which modulate immune responses (Heikkinen et al., 2016). MMP-2 is a highly active MMP present in saliva, which plays a crucial role in the degradation of periodontal tissues (Woessner, 1991). Recent studies have established a connection between MMP-2 and periodontitis, since its activity is controlled by tissue inhibitors of matrix metalloproteinases (TIMPs) (Bătăiosu et al., 2015), mainly TIMP-1, a natural inhibitor of MMP-2 produced by periodontal cells, macrophages and monocytes (Figure 1) (da Costa Fernandes and Zambuzzi, 2020).

During periodontal tissue inflammation, an overexpression of MMP-2 has been observed in saliva and gingival crevicular fluid (Lira-Junior et al., 2017; Barreiros et al., 2018). In the study carried out by Arreguin-Cano et al. (2019), the periodontal status, HbA1c levels, MMP-2 and TIMP-1 activity, and percentage of PMNs in patients with T2DM were compared and analyzed. In this study, an increase in the enzymatic activity of MMP-2 was observed, as well as the expression of TMP-1 according to the severity of periodontitis, this increase being significant in severe periodontitis. In addition, a significant increase in glycosylated hemoglobin (HbA1c) levels was found in patients with moderate and severe periodontitis, suggesting that poor glycemic control is associated with the severity of periodontitis. Likewise, it was observed that in patients with poor glycemic control, there was a significant increase in PMNs, along with a significant decrease in MMP-2 and TMP-1 activity. These findings suggest that in patients with T2DM and poor glycemic control there is an imbalance in MMP-2/TIMP-1, and that the process of inhibition of MMP-2 activity by TIMP-1 is lost in severe periodontitis (Figure 1) (Arreguin-Cano et al., 2019).

On the other hand, the NLRP3 inflammasome plays an important role during the inflammatory response against infections or cellular stress (Schroder and Tschopp, 2010). In this context, studies have reported a high expression of the NLRP3 inflammasome, both in the gingival tissues of patients with periodontitis (Bostanci et al., 2009; Park et al., 2014), as well as in cells of the innate immune system and pancreatic β-cells in patients with T2DM (Schroder et al., 2010; Jourdan et al., 2013). In this context, Huang et al. (2015) reported that, both in patients with chronic periodontitis and T2DM, as well as human gingival epithelial cells (HGEC) stimulated with lipopolysaccharide (LPS) and high concentrations of glucose, showed a significant increase in the expression of the NLRP3 inflammasome and IL-1β. These findings suggest that hyperglycemia can exacerbate the inflammatory response of gingival tissue through the NLRP3 pathway, contributing to greater tissue degradation (Huang et al., 2015), because high levels of IL-1β were significantly associated with periodontitis immunopathology, causing periodontal tissue degradation, mainly in alveolar bone absorption and damage to the lamina propria (Figure 1) (Liu et al., 1996).

3 Periodontitis and COVID-19

At a clinical level, studies have established an association between periodontitis and adverse outcomes of COVID-19 (Brock et al., 2022). Patients with periodontal disease have been shown to be at increased risk of severe COVID-19, including hospitalization, intensive care unit admission, and mortality. Furthermore, periodontal disease may contribute to the severity of COVID-19 by elevating levels of inflammatory biomarkers (Marouf et al., 2021; Gupta et al., 2022). Conversely, COVID-19 can exacerbate periodontal disease, leading to increased gingival bleeding, dental plaque accumulation, and periodontal pocket deepening (Figure 2) (Anand et al., 2022; Kalsi et al., 2022). Although there is currently no clear causal relationship, periodontitis represents a risk factor for increasing the severity of COVID-19 (Sánchez Sánchez et al., 2022), by causing microbial dysbiosis, bacterial super-infection, hyperreactivity of the host, and over stimulation of the immune system. Probably due to the set of environmental, microbial and inflammatory factors, which contribute to the progression of the disease (Sukumar and Tadepalli, 2021). According to Campisi et al. (2021) two interrelated mechanisms may underlie the association between periodontitis and COVID-19. The first mechanism involves a direct viral infection of periodontal tissues, facilitated by the high expression of the ACE-2 receptor in these tissues. The second mechanism involves a shared inflammatory response (overexpression of inflammatory cytokines) characterized by a cytokine storm, a condition associated with severe COVID-19 (Campisi et al., 2021) (Figure 2).

Direct contact of the SARS-CoV-2 with periodontal tissues. Periodontitis-induced ulceration of the gingival epithelium may compromise its protective function, increasing the risk of SARS-CoV-2 invasion. The main route of entry of SARS-CoV-2 into human cells is through the ACE-2 receptor, present in diverse tissues such as the lungs, nasal passages, salivary glands, and oral cavity (Huang et al., 2021). In the mouth, ACE-2 is mainly found in tongue cells, fibroblasts, periodontal tissues, and gingival crevices (Mancini et al., 2020). Notably, the salivary glands of the oral cavity have higher expression of ACE-2 than the lungs, making them an important reservoir of the virus and facilitating effective infection (Jiménez et al., 2022). In addition to ACE-2, other molecules such as TMPRSS-2, and furin, are required for SARS-CoV-2 infection (Sakaguchi et al., 2020). These molecules are highly expressed in the oral cavity, especially in the oral lining, gingival cells, periodontal tissue, and gingival fluid (Pascolo et al., 2020). Their

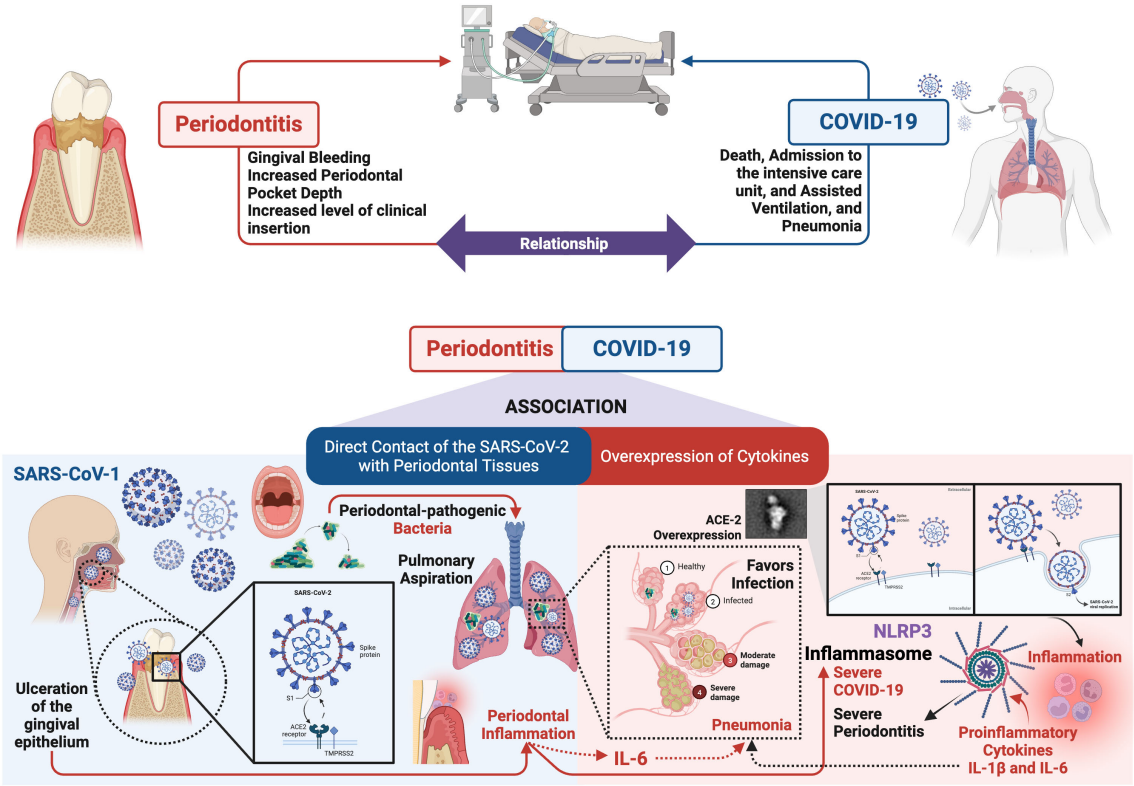

FIGURE 2
Relationship between periodontitis and COVID-19. The figure illustrates the potential immunopathological mechanisms linking periodontal disease with SARS-CoV-2 infection. Periodontitis induces a chronic systemic inflammatory state characterized by the overproduction of proinflammatory cytokines (such as IL-6), which may contribute to an exacerbated immune response in COVID-19 patients, favoring the development of a "cytokine storm." Additionally, the oral dysbiosis associated with periodontitis may facilitate opportunistic colonization by respiratory pathogens, increasing susceptibility to severe pulmonary infections. Furthermore, it has been suggested that periodontal inflammation may upregulate the expression of receptors such as ACE-2, potentially enhancing viral entry. This evidence supports the hypothesis that periodontal status could influence the clinical severity of COVID-19. Figure created with BioRender.com by Muñoz-Carrillo et al.

combined presence is crucial for the activation of the the S protein of SARS-CoV-2, allowing it to bind to host cells and enhance its ability to infect the oral cavity (Campisi et al., 2021; Sukumar and Tadepalli, 2021). In this context, periodontal-pathogenic bacteria, such as *Porphyromonas gingivalis*, can induce the overexpression of ACE-2, TMPRSS2, and furin in cells of the oral cavity (Sena et al., 2021). This overexpression of ACE-2, on the one hand, negatively regulates the production of proinflammatory cytokines, such as IL-1β, IL-6, and TNF-α (Mancini et al., 2020); while on the other hand, it favors the entry of SARS-CoV-2 into the oral cavity (Brock et al., 2022). Once SARS-CoV-2 infection occurs, ACE-2 expression is downregulated, leading to an increase in proinflammatory cytokines, favoring the inflammatory response (Iwasaki et al., 2020). In this sense, local inflammation promotes the spread of SARS-CoV-2 infection and its replication in periodontal tissues, with possible further systemic expansion. Therefore, it is deduced that aspiration of periodontal-pathogenic bacteria could increase the risk of SARS-CoV-2 infection, since these can increase the expression of ACE-2 in the oral cavity, lungs, and bronchi; inducing the production of inflammatory cytokines, such as interleukin IL-6, by alveolar and bronchial epithelial cells, which promotes SARS-CoV-2 infection, and inflammation of the lower respiratory tract can become severe in the presence of pneumonia viral, contributing to the development of cytokine storm and acute respiratory distress syndrome (Figure 2) (Campisi et al., 2021; Brock et al., 2022).

Overexpression of cytokines. IL-6, a cytokine overexpressed in periodontitis, has been implicated in the pathogenesis of COVID-19 (Silvestre and Márquez-Arrico, 2022). SARS-CoV-2 infection induces the release of proinflammatory cytokines, including IL-1β and IL-6, which may contribute to the development of interstitial pneumonia, a hallmark of severe COVID-19. While the causal role of IL-6 in COVID-19 severity remains under investigation, it has been proposed as a potential biomarker for early disease detection and progression monitoring (Figure 2) (Campisi et al., 2021). In this context, serum IL-6 levels have been correlated with the stage of COVID-19 disease, particularly in patients experiencing respiratory failure. Therefore, elevated IL-6 levels can be used as a predictive biomarker to identify patients at risk for disease progression. Furthermore, increased expression of the IL-6 receptor (IL-6R) and higher levels of IL-6 have been observed in COVID-19 patients who did not survive compared to patients who survived throughout the clinical course of the disease. These findings suggest a potential role of IL-6 in the pathogenesis and progression of COVID-19 (Qi et al., 2023).

Periodontitis and COVID-19 share several common inflammatory pathways, such as the NLRP3/IL-1β and IL-6 signaling pathway (Figure 2). NF-κB induces the transcriptional expression of NLRP3 and pro-IL-1β (Liu et al., 2017; Chen et al., 2021). Activation of the NLRP3 inflammasome results in the release of pro-inflammatory cytokines IL-1β and IL-18 (Brodin, 2021), thereby promoting inflammation and other associated disorders. Inflammatory cytokines can promote the development of low-grade systemic inflammation, leading to the abnormal activation of the NLRP3 inflammasome. This, in turn, can drive chronic inflammatory conditions and influence the pathophysiology of inflammation-related diseases (Sharma and Kanneganti, 2021). It has been observed that patients with periodontitis exhibit significantly higher levels of NLRP3, in both blood and saliva. NLRP3 inflammasome-related proteins, such as IL-1β, have been proposed as potential biomarkers for periodontal clinical status (Qi et al., 2023). Studies have reported that the expression of these proteins is associated with alveolar bone loss, a hallmark of periodontal disease, and an increase in proinflammatory cytokines, which can contribute to the severity of periodontal disease (Figure 2) (Mainas et al., 2022). COVID-19 severity has been correlated with NLRP3 inflammasome activation. Post-mortem analysis of COVID-19 patients has revealed persistent NLRP3 inflammasome activation in various tissues and PMNs from peripheral blood (Qi et al., 2023). This is because, after viral replication, ACE-2 decreases its activity, activating ACE1, leading to elevated levels of PMN, reactive oxygen species, NF-κB, and proinflammatory cytokines, ultimately resulting in inflammatory cell death and tissue damage (Ariana Dalys and Fabricio Miltom, 2023).

4 Type 2 diabetes mellitus and COVID-19

Retrospective studies of this group of patients indicate that poor glycemic control is associated with increased morbidity and mortality from COVID-19. However, the severity of COVID-19 is closely correlated with the age of patients, which is often also the case for T2DM (Turk Wensveen et al., 2021). It has been reported that hospitalized patients with COVID-19 and T2DM have almost double the risk of mortality compared to their counterparts without diabetes (Shenoy et al., 2020). In addition, COVID-19 positive patients with T2DM had worse clinical outcomes, exhibiting a severe inflammatory response with a higher risk of admission to the intensive care unit, receiving mechanical ventilation, and in-hospital mortality than those without diabetes (Figure 3) (Shenoy et al., 2020; You et al., 2020).

The underlying molecular mechanism of how T2DM leads to more severe COVID-19 disease is currently unclear (Turk Wensveen et al., 2021). However, this susceptibility of patients with T2DM to adverse outcomes associated with SARS-CoV-2 infection is due to impaired immune system function, and possible up regulation of enzymes that mediate viral invasion. Chronic inflammation caused by diabetes, coupled with the acute inflammatory reaction caused by SARS-CoV-2, results in a propensity for inflammatory storm (Figure 3) (Yin et al., 2021); which is characterized by the following successive stages: 1) Infection of lung cells by SARS-CoV-2; 2) immune cells, including macrophages, identify the virus and produce cytokines; 3) cytokines attract more immune cells, such as white blood cells, which in turn produce more cytokines, creating a cycle of inflammation that damages lung cells; 4) damage can occur through fibrin formation; and 5) weakened blood vessels allow fluid to leak and fill the lung cavities, causing respiratory failure (Figure 3).

Likewise, it has been reported that patients with T2DM and COVID-19 had a higher count of white blood cells, neutrophils, and proinflammatory cytokines (such as IL-6 and TNF-α), suggesting an increased inflammatory response compared to patients without diabetes (Shenoy et al., 2020). In addition to this, the severity of hyperglycemia was associated with the intensity of the cytokine storm, which is a clear indication that immunological triggers are responsible for changes in blood glucose regulation in the context of a severe disease. Furthermore, a fundamental role of alveolar macrophages has been indicated, which increase their glycolytic rate after activation. In this context, SARS-CoV-2 can infect macrophages and benefit from the increase in the glycolytic rate in these cells. Therefore, the presence of a hyperglycemic state in patients with T2DM further facilitates viral replication in macrophages, promoting disease progression (Figure 3) (Turk Wensveen et al., 2021).

5 Relationship between periodontitis, type 2 diabetes mellitus and COVID-19

In the current scientific literature, there is only one systematic review, whose purpose was to carry out a systematic review of the literature, which included 12 studies, to contrast the existing evidence on the relationship between periodontal disease and diabetes mellitus, and the risk of SARS-CoV-2 infection, as well as to establish a hypothesis that explains the ways in which this interaction could occur. Casillas Santana et al. (2021) hypothesize that the relationship between these three pathologies is because T2DM is a metabolic disorder characterized by hyperglycemia in the blood, the result of altered secretion or action of insulin. Likewise, periodontitis and diabetes mellitus are inflammatory disorders with a bidirectional association, which share a similar immunomodulatory cascade and cytokine profile. On the other hand, ACE-2 is a crucial component of the renin-angiotensin system, and a key entry factor into SARS-CoV-2 cells. ACE-2 is widely distributed in various tissues including the oral cavity, mainly in the tongue and periodontal tissue. ACE-2 expression is modified by chronic uncontrolled glycemia in T2DM. Therefore, uncontrolled hyperglycemia increases the risk of developing periodontitis and triggers an overexpression of ACE-2 in the periodontal tissue of patients with T2DM, these events being potentially essential for SARS-CoV-2 infection and the

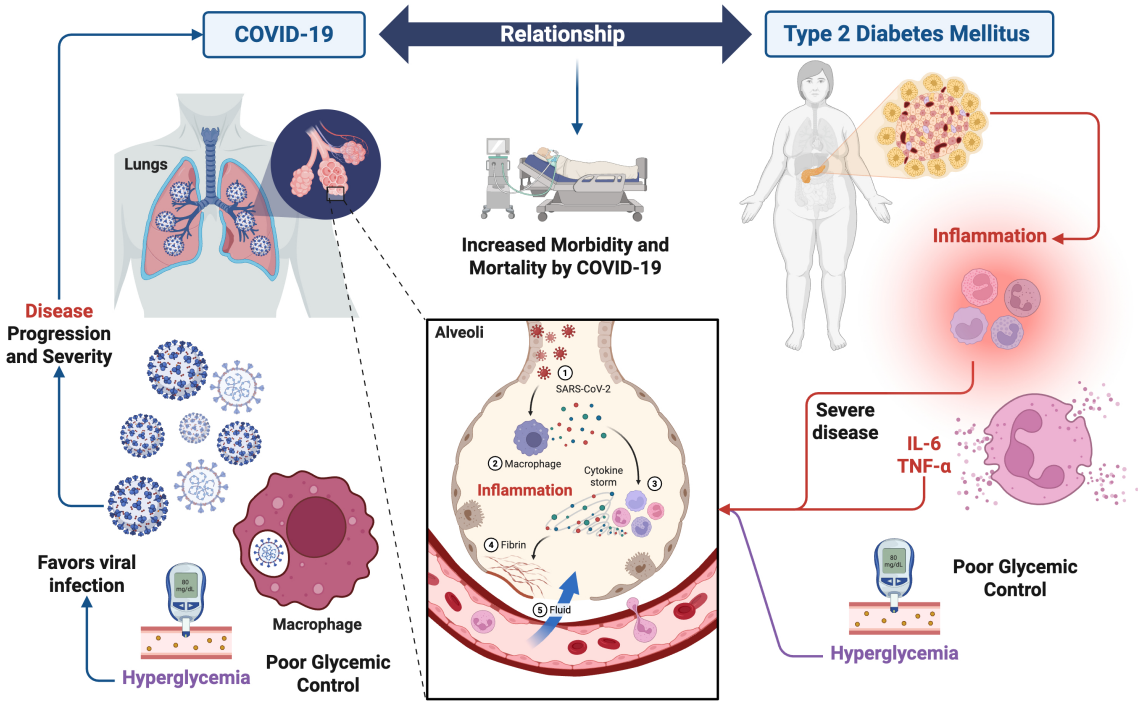

FIGURE 3
Relationship between type 2 diabetes mellitus and COVID-19. The figure depicts the pathophysiological mechanisms by which T2DM may influence the clinical course of SARS-CoV-2 infection. Chronic hyperglycemia in individuals with diabetes contributes to persistent inflammatory state marked by elevated levels of proinflammatory cytokines such as IL-6, and TNF-α. These factors can amplify the dysregulated immune response characteristic of severe COVID-19, promoting cytokine storm, acute lung injury, and adverse clinical outcomes. This interaction suggests that T2DM is not only a risk factor for severe COVID-19 but also actively contributes to its immunopathological progression. Figure created with BioRender.com by Muñoz-Carrillo et al.

development of the mild to severe form of COVID-19 (Casillas Santana et al., 2021). However, this systematic review was carried out in 2021, and has certain limitations, mainly in the search strategy, since the studies evaluated are limited to the English language, excluding studies conducted in Spanish. Therefore, a broader and more exhaustive search is necessary to identify additional literature; and in this way provide a more reliable and precise hypothesis and conclusion on the association of these three pathologies. In this context, this review provides a comprehensive, original and exhaustive perspective on the influence and association of COVID-19 disease with T2DM and periodontitis, through three axes, which interrelate these three pathologies.

Currently, there is very little scientific literature on the relationship between periodontitis, T2DM, and COVID-19. In the present study, we first sought to explain the relationship between the following comorbidities: 1) periodontitis and T2DM; 2) periodontitis and COVID-19; and 3) T2DM and COVID-19. Based on the systematized reviewed literature, in addition to the few published scientific studies on the relationship between these three pathologies, we can hypothesize that the three diseases share important cofactors (Table 1), which focus on three important axes (Figure 4): 1) a clinicopathological axis; 2) an axis associated with glycemia; and 3) an immune axis associated with inflammation.

Clinicopathological axis. Regarding this axis, studies have reported that patients who suffer from T2DM are more susceptible to developing periodontitis, even in a more severe course of this disease. In turn, patients with poorly controlled T2DM have a higher prevalence of periodontitis with a more severe course (Tsai et al., 2002; Susanto et al., 2011; Shamala et al., 2017; Alasqah et al., 2018; Trentin et al., 2018; Monod Nuñez et al., 2022), evidencing a bidirectional relationship between both pathologies (Wu et al., 2020). In turn, poor control of T2DM is associated with high morbidity and mortality by COVID-19, increasing the risk of death, admission to the intensive care unit, and receiving mechanical ventilation (Shenoy et al., 2020; You et al., 2020; Turk Wensveen et al., 2021). Likewise, it has been reported that patients with COVD-19 show a more severe course of periodontitis, and that this, in turn, is associated with complications during COVID-19 disease, including death, admission to the care unit intensive care, need for assisted ventilation and pneumonia (Marouf et al., 2021; Anand et al., 2022; Brock et al., 2022; Gupta et al., 2022; Kalsi et al., 2022).

Axis associated with glycemia. One of the main characteristics of T2DM is the lack of control of blood glucose, since, if the disease is not controlled, patients who suffer from it, present hyperglycemia. In this context, hyperglycemia triggers many negative effects on the health of patients, including making them more prone to the development of comorbidities with other diseases. On the one hand, hyperglycemia in patients with T2DM favors inflammatory mechanisms that, in turn, can induce insulin resistance (Acharya

TABLE 1 Interrelated cofactors between periodontitis, type 2 diabetes mellitus, and COVID-19.

Co-factor	Periodontitis	Type 2 Diabetes Mellitus (T2DM)	COVID-19	Ref
Impact on the immune system	Chronic inflammation weakens immune defense.	T2DM leads to immune dysfunction and impaired inflammatory response.	COVID-19 exacerbates immune dysfunction and inflammation.	(Coelho et al., 2013; Mira et al., 2017; Zhou et al., 2018; Berbudi et al., 2025)
Effect on inflammation	Inflammation in periodontal tissues can spread to other parts of the body.	Chronic inflammation from T2DM worsens the response of the body to infections.	COVID-19 triggers systemic inflammation, which can worsen comorbid conditions.	(Moreno Caicedo et al., 2018; Muniyappa and Gubbi, 2020; Turk Wensveen et al., 2021; Yin et al., 2021)
Glycemic control	Poor oral health can negatively affect glycemic control.	Poorly controlled T2DM worsens COVID-19 outcomes due to impaired immune function.	Inflammatory responses from COVID-19 may disrupt glucose metabolism.	(Tsai et al., 2002; Guzman et al., 2003; Grover and Luthra, 2013; Acharya et al., 2017; Dror et al., 2017; Liccardo et al., 2019; Turk Wensveen et al., 2021)
Role of oral bacteria	Periodontitis is caused by pathogenic oral bacteria, which may enter the bloodstream.	T2DM can increase the risk of periodontal disease due to immune dysfunction.	Oral bacteria may contribute to systemic inflammation, increasing COVID-19 severity.	(Nussbaum and Shapira, 2011; Ling et al., 2015; Sukumar and Tadepalli, 2021; Yin et al., 2021)
Risk of complications	Increased risk of systemic diseases.	Patients with T2DM are at higher risk for severe COVID-19 outcomes.	COVID-19 can worsen outcomes in patients with existing comorbidities, including periodontitis and T2DM.	(Acharya et al., 2017; Moreno Caicedo et al., 2018; Shenoy et al., 2020; You et al., 2020; Brock et al., 2022)
Risk of co-infection	Periodontitis can increase the risk of respiratory infections.	T2DM patients are at higher risk of infections, including periodontitis and respiratory infections.	COVID-19 can increase susceptibility to secondary bacterial infections, including oral infections.	(Dhir et al., 2018; Anand et al., 2022; Brock et al., 2022; Kalsi et al., 2022; Sánchez Sánchez et al., 2022)

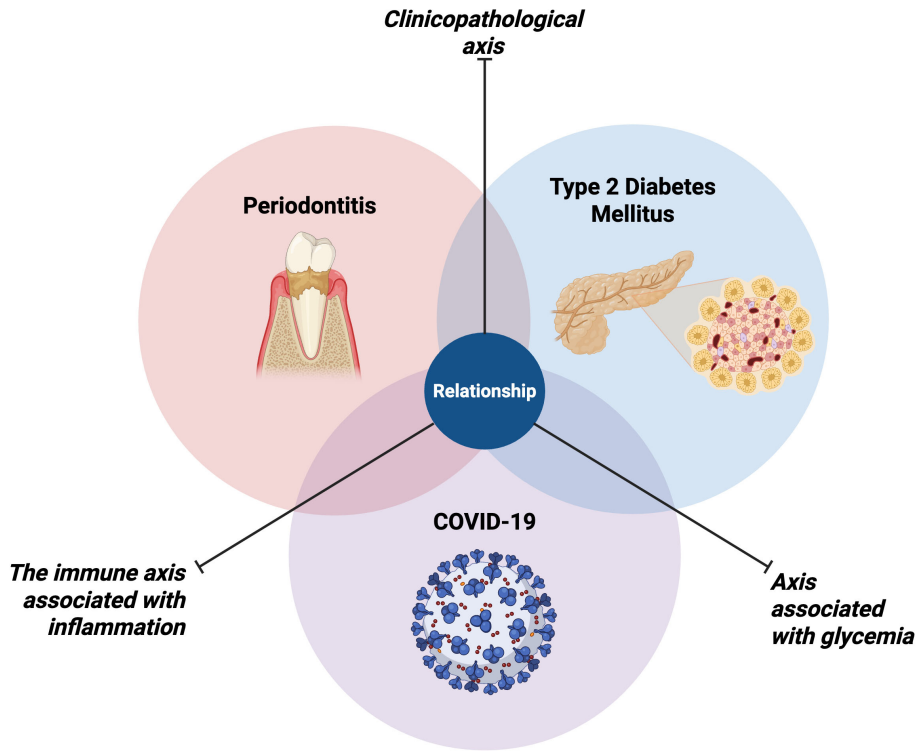

FIGURE 4
Relationship between periodontitis, type 2 diabetes mellitus, and COVID-19. The figure illustrates the complex interplay between these three chronic conditions, which share three important axes that interconnect them: 1) a clinicopathological axis; 2) an axis associated with glycemia; and 3) an immune axis associated with inflammation. Figure created with BioRender.com by Muñoz-Carrillo et al.

et al., 2017), decreased endothelial function (Kumar et al., 2020), and an increase in PMN (Herrmann et al., 2020). These factors influence in periodontitis, enhancing the destruction of periodontal tissues, due to the exacerbation of the inflammatory response, generating a more serious course of the disease (Arreguin-Cano et al., 2019). In this context, these conditions favor the infectious capacity of SARS-CoV-2 (Sukumar and Tadepalli, 2021). This is because hyperglycemia is a key factor in the development of T2DM. Therefore, high glucose levels can make patients with T2DM more susceptible to COVID-19, as hyperglycemia can affect the production of enzymes that help the SARS-CoV-2 infect and multiply in the body (Michaels et al., 2024). Furthermore, hyperglycemia can worsen the inflammatory response of the body to the virus. Furthermore, periodontal-pathogenic bacteria, if aspirated into the lungs, induce the overexpression of ACE-2 in the alveoli (Campisi et al., 2021; Sukumar and Tadepalli, 2021), which favors lung inflammation and exacerbated production of proinflammatory cytokines, generating a cytokine storm that induces the destruction of the resident tissue (Campisi et al., 2021; Brock et al., 2022). This phenomenon is also closely related to T2DM, since hyperglycemia further enhances the cytokine storm at the lung level, thus increasing the inflammatory response, due to a deterioration of the immune system (Yin et al., 2021), caused by T2DM, which favors the severity of COVID-19 disease (Turk Wensveen et al., 2021).

The immune axis associated with inflammation. The integration of this axis is even more complex, due to the interconnected pathways between periodontitis, T2DM and COVID-19 disease. However, the common denominator within the axis is inflammation. Periodontitis is caused, mainly, by the inflammatory response induced by periodontal-pathogenic bacteria residing in dental plaque (Kinane, 2001). The chronicity of this inflammatory response is characterized by an increase in proinflammatory cytokines, such as TNF-α, IL-1β and IL-6, and immune system cell populations (Acharya et al., 2017). Particularly, the aberrant production of TNF-α, on the one hand, generates decreased vascular function (Kumar et al., 2020). On the other hand, it induces the increase and survival of PMN in the periodontal tissue (Manosudprasit et al., 2017; Herrmann et al., 2020), which in turn produces MMP-2, which leads to the destruction of periodontal tissue (Arreguin-Cano et al., 2019). Likewise, TNF-α modulates the expression of endocan, a proteoglycan that acts as a pro-inflammatory mediator, which is associated with the most severe course of the disease (Kumar et al., 2020). Regarding IL-1β, this proinflammatory cytokine is associated with the activation of the inflammasome (they are over expression of NLRP3), amplifying the inflammatory response and therefore the destruction of gingival tissue (Huang et al., 2015). The intersection between periodontitis, T2DM and COVID-19 disease (Sukumar and Tadepalli, 2021; Brock et al., 2022), occurs when during diabetes mellitus, there is an increase in blood glucose levels (hyperglycemia) and together with the viral infection, an exacerbated inflammatory response is triggered, increasing the production of TNF-α. IL-1β, IL-6, endocan, NLRP3 inflammasome and an increase in the PMN population, amplifying their effects and leading to a more severe course of comorbidity between these three pathologies (Huang et al., 2015; Acharya et al., 2017; Kumar et al., 2020; Qi et al., 2023). In turn, during COVID-19 disease, periodontitis facilitates the passage of periodontal-pathogenic bacteria, invading the lung, which increase the expression of ACE-2, favoring SARS-CoV-2 infection (Campisi et al., 2021; Sukumar and Tadepalli, 2021); which in turn produces a strong inflammatory response, also characterized by the aberrant production of proinflammatory cytokines (TNF-α, IL-1β and IL-6) (Torres-Tamayo et al., 2020; Silvestre and Márquez-Arrico, 2022; Qi et al., 2023), and the activation of alveolar macrophages, which leads to a cytokine storm (Yin et al., 2021), which ultimately induces tissue destruction at the lung level (Campisi et al., 2021), generating respiratory failure (Campisi et al., 2021; Brock et al., 2022). However, this cytokine storm manages to reach the systemic circulation, which reaches the periodontal tissues, also favoring their destruction (Ariana Dalys and Fabricio Miltom, 2023)

6 Conclusion

Currently, scientific evidence that jointly analyzes the relationship between periodontitis, T2DM and the risk of developing COVID-19 remains limited. However, based on a systematic review of available studies, it is possible to propose a well-founded hypothesis that suggests the existence of three key axes linking these conditions. The three diseases share similar clinical characteristics, such as chronic inflammation, progressive tissue deterioration, and dysregulated immune responses, suggesting common pathological mechanisms that could enhance their interaction. Both T2DM and periodontitis are closely related to glycemic control. Persistent hyperglycemia creates an environment conducive to the development of infections and exacerbates inflammatory processes, which can increase susceptibility to complications in the event of SARS-CoV-2 infection. Therefore, these three diseases involve an alteration of the immune system, characterized by an excessive or dysregulated inflammatory response. This condition could explain why patients with T2DM and periodontitis are at greater risk of developing severe forms of COVID-19, as they generate a more intense and damaging immune response to the virus. Taken together, this interrelationship suggests that comorbidity between periodontitis and T2DM not only increases vulnerability to COVID-19 infection but can also lead to a more severe clinical course of the disease.

Author contributions

JM: Conceptualization, Data curation, Formal Analysis, Investigation, Methodology, Project administration, Software, Supervision, Validation, Visualization, Writing – original draft, Writing – review & editing. PP: Conceptualization, Investigation, Methodology, Resources, Supervision, Validation, Visualization, Writing – original draft, Writing – review & editing. MV: Conceptualization, Investigation, Methodology, Resources,

Supervision, Validation, Visualization, Writing – original draft, Writing – review & editing. OG: Conceptualization, Formal Analysis, Investigation, Methodology, Project administration, Resources, Supervision, Validation, Visualization, Writing – original draft, Writing – review & editing. FC: Formal Analysis, Investigation, Methodology, Resources, Validation, Visualization, Writing – review & editing. SV: Formal Analysis, Investigation, Methodology, Resources, Validation, Visualization, Writing – review & editing. PV: Formal Analysis, Investigation, Methodology, Resources, Validation, Visualization, Writing – review & editing. JP: Formal Analysis, Investigation, Methodology, Resources, Validation, Visualization, Writing – review & editing.

Funding

The author(s) declare that no financial support was received for the research and/or publication of this article.

Acknowledgments

The first and corresponding author thanks the other authors for their collaboration in this work. Special thanks to the International University of Ecuador and University Center of the Lagos, University of Guadalajara.

Conflict of interest

The authors declare that the research was conducted in the absence of any commercial or financial relationships that could be construed as a potential conflict of interest.

Generative AI statement

The author(s) declare that no Generative AI was used in the creation of this manuscript.

Publisher's note

All claims expressed in this article are solely those of the authors and do not necessarily represent those of their affiliated organizations, or those of the publisher, the editors and the reviewers. Any product that may be evaluated in this article, or claim that may be made by its manufacturer, is not guaranteed or endorsed by the publisher.

References

Abdi, A., Jalilian, M., Sarbarzeh, P. A., and Vlaisavljevic, Z. (2020). Diabetes and COVID-19: A systematic review on the current evidences. *Diabetes Res. Clin. Pract.* 166, 108347. doi: 10.1016/j.diabres.2020.108347

Acharya, A. B., Thakur, S., Muddapur, M. V., and Kulkarni, R. D. (2017). Cytokine ratios in chronic periodontitis and type 2 diabetes mellitus. *Diabetes Metab. Syndr.* 11, 277–278. doi: 10.1016/J.DSX.2016.12.007

Alasqah, M., Mokeem, S., Alrahlah, A., Al-Hamoudi, N., Abduljabbar, T., Akram, Z., et al. (2018). Periodontal parameters in prediabetes, type 2 diabetes mellitus, and non-diabetic patients. *Braz. Oral. Res.* 32, e81. doi: 10.1590/1807-3107BOR-2018.VOL32.0081

Anand, P. S., Jadhav, P., Kamath, K. P., Kumar, S. R., Vijayalaxmi, S., and Anil, S. (2022). A case-control study on the association between periodontitis and coronavirus disease (COVID-19). *J. Periodontol* 93, 584–590. doi: 10.1002/JPER.21-0272

Andriankaja, O. M., Galicia, J., Dong, G., Xiao, W., Alawi, F., and Graves, D. T. (2012). Gene expression dynamics during diabetic periodontitis. *J. Dent. Res.* 91, 1160–1165. doi: 10.1177/0022034512465292

Ariana Dalys, C. L., and Fabricio Miltom, L. (2023). Periodontal disease and COVID-19: Prognosis and potential pathways of association in their pathogenesis. *Can. J. Dent. Hyg* 57, 44–51.

Arman, Y., Akpinar, T. S., Kose, M., Emet, S., Yuruyen, G., Akarsu, M., et al. (2016). Effect of glycemic regulation on endocan levels in patients with diabetes: A preliminary study. *Angiology* 67, 239–244. doi: 10.1177/0003319715585664

Arreguin-Cano, J. A., Ayerdi-Nájera, B., Tacuba-Saavedra, A., Navarro-Tito, N., Dávalos-Martínez, A., Emigdio-Vargas, A., et al. (2019). MMP-2 salivary activity in type 2 diabetes mellitus patients. *Diabetol. Metab. Syndr.* 11, 1–8. doi: 10.1186/S13098-019-0510-2

Barreiros, D., Nelson-Filho, P., Paula-Silva, F. W. G., de Oliveira, K. M. H., Lucisano, M. P., de Rossi, A., et al. (2018). MMP2 and MMP9 are associated with apical periodontitis progression and might be modulated by TLR2 and myD88. *Braz. Dent. J.* 29, 43–47. doi: 10.1590/0103-6440201801731

Bătăiosu, M., Taisescu, C. I., Pisoschi, C. G., Pascu, E. I., Țuculină, M. J., Dăguci, L., et al. (2015). Effects of therapy with two combinations of antibiotics on the imbalance of MMP-2÷TIMP-2 in chronic periodontitis. *Rom J. Morphol Embryol* 56, 77–83.

Berbudi, A., Khairani, S., and Tjahjadi, A. (2025). Interplay between insulin resistance and immune dysregulation in type 2 diabetes mellitus: implications for therapeutic interventions. *ImmunoTargets Ther.* 14, 359–382. doi: 10.2147/ITT.S499605

Bostanci, N., Emingil, G., Saygan, B., Turkoglu, O., Atilla, G., Curtis, M. A., et al. (2009). Expression and regulation of the NALP3 inflammasome complex in periodontal diseases. *Clin. Exp. Immunol.* 157, 415–422. doi: 10.1111/J.1365-2249.2009.03972.X

Brock, M., Bahammam, S., and Sima, C. (2022). The relationships among periodontitis, pneumonia and COVID-19. *Front. Oral. Heal* 2. doi: 10.3389/FROH.2021.801815

Brodin, P. (2021). Immune determinants of COVID-19 disease presentation and severity. *Nat. Med.* 27, 28–33. doi: 10.1038/S41591-020-01202-8

Brunton, S. (2016). Pathophysiology of type 2 diabetes: the evolution of our understanding. *J. Fam. Pract.* 65 (4 Suppl), supp_az_0416.

Campisi, G., Bizzoca, M. E., and Lo Muzio, L. (2021). COVID-19 and periodontitis: reflecting on a possible association. *Head Face Med.* 17, 1–6. doi: 10.1186/S13005-021-00267-1

Casillas Santana, M. A., Arreguín Cano, J. A., Dib Kanán, A., Dipp Velázquez, F. A., Munguía, P. D. C. S., Martínez Castañón, G. A., et al. (2021). Should we be concerned about the association of diabetes mellitus and periodontal disease in the risk of infection by SARS-coV-2? A systematic review and hypothesis. *Medicina (Kaunas)* 57, 1–16. doi: 10.3390/MEDICINA57050493

Chapple, I. L. C., Mealey, B. L., Van Dyke, T. E., Bartold, P. M., Dommisch, H., Eickholz, P., et al. (2018). Periodontal health and gingival diseases and conditions on an intact and a reduced periodontium: Consensus report of workgroup 1 of the 2017 World Workshop on the Classification of Periodontal and Peri-Implant Diseases and Conditions. *J. Periodontol* 89 Suppl 1, S74–S84. doi: 10.1002/JPER.17-0719

Chen, Y., Yang, Q., Lv, C., Chen, Y., Zhao, W., Li, W., et al. (2021). NLRP3 regulates alveolar bone loss in ligature-induced periodontitis by promoting osteoclastic differentiation. *Cell Prolif* 54, 1–14. doi: 10.1111/CPR.12973

Coelho, M., Oliveira, T., and Fernandes, R. (2013). Biochemistry of adipose tissue: an endocrine organ. *Arch. Med. Sci.* 9, 191–200. doi: 10.5114/AOMS.2013.33181

Collazos, J., Asensi, V., Martin, G., Montes, A. H., Suárez-Zarracina, T., and Valle-Garay, E. (2015). The effect of gender and genetic polymorphisms on matrix metalloprotease (MMP) and tissue inhibitor (TIMP) plasma levels in different infectious and non-infectious conditions. *Clin. Exp. Immunol.* 182, 213–219. doi: 10.1111/CEI.12686

Coughlan, M. T., and Sharma, K. (2016). Challenging the dogma of mitochondrial reactive oxygen species overproduction in diabetic kidney disease. *Kidney Int.* 90, 272–279. doi: 10.1016/J.KINT.2016.02.043

Cuschieri, S., and Grech, S. (2020). COVID-19 and diabetes: The why, the what and the how. *J. Diabetes Complications* 34, 107637. doi: 10.1016/J.JDIACOMP.2020.107637

da Costa Fernandes, C. J., and Zambuzzi, W. F. (2020). Fibroblast-secreted trophic factors contribute with ECM remodeling stimulus and upmodulate osteocyte gene markers in osteoblasts. *Biochimie* 168, 92–99. doi: 10.1016/J.BIOCHI.2019.10.013

Defronzo, R. A. (2009). From the triumvirate to the ominous octet: A new paradigm for the treatment of type 2 diabetes mellitus. *Diabetes* 58, 773. doi: 10.2337/DB09-9028

Dhir, S., Wangnoo, S., and Kumar, V. (2018). Impact of glycemic levels in type 2 diabetes on periodontitis. *Indian J. Endocrinol. Metab.* 22, 672–677. doi: 10.4103/IJEM.IJEM_566_17

Diao, B., Wang, C., Wang, R., Feng, Z., Zhang, J., Yang, H., et al. (2021). Human kidney is a target for novel severe acute respiratory syndrome coronavirus 2 infection. *Nat. Commun.* 12, 1–9. doi: 10.1038/S41467-021-22781-1

Domingueti, C. P., Dusse, L. M. S. A., Carvalho, M. D. G., De Sousa, L. P., Gomes, K. B., and Fernandes, A. P. (2016). Diabetes mellitus: The linkage between oxidative stress, inflammation, hypercoagulability and vascular complications. *J. Diabetes Complications* 30, 738–745. doi: 10.1016/J.JDIACOMP.2015.12.018

Dror, E., Dalmas, E., Meier, D. T., Wueest, S., Thévenet, J., Thienel, C., et al. (2017). Postprandial macrophage-derived IL-1β stimulates insulin, and both synergistically promote glucose disposal and inflammation. *Nat. Immunol.* 18, 283–292. doi: 10.1038/NI.3659

Fakhruddin, S., Alanazi, W., and Jackson, K. E. (2017). Diabetes-induced reactive oxygen species: mechanism of their generation and role in renal injury. *J. Diabetes Res.* 2017, 1–30. doi: 10.1155/2017/8379327

Fernandez, C., Rysä, J., Almgren, P., Nilsson, J., Engström, G., Orho-Melander, M., et al. (2018). Plasma levels of the proprotein convertase furin and incidence of diabetes and mortality. *J. Intern. Med.* 284, 377–387. doi: 10.1111/JOIM.12783

Gerrits, A. J., Gitz, E., Koekman, C. A., Visseren, F. L., van Haeften, T. W., and Akkerman, J. W. N. (2012). Induction of insulin resistance by the adipokines resistin, leptin, plasminogen activator inhibitor-1 and retinol binding protein 4 in human megakaryocytes. *Haematologica* 97, 1149–1157. doi: 10.3324/HAEMATOL.2011.054916

Grover, H., and Luthra, S. (2013). Molecular mechanisms involved in the bidirectional relationship between diabetes mellitus and periodontal disease. *J. Indian Soc. Periodontol* 17, 292–301. doi: 10.4103/0972-124X.115642

Gupta, A., Madhavan, M. V., Sehgal, K., Nair, N., Mahajan, S., Sehrawat, T. S., et al. (2020). Extrapulmonary manifestations of COVID-19. *Nat. Med.* 26, 1017–1032. doi: 10.1038/S41591-020-0968-3

Gupta, S., Mohindra, R., Singla, M., Khera, S., Sahni, V., Kanta, P., et al. (2022). The clinical association between Periodontitis and COVID-19. *Clin. Oral. Investig.* 26, 1361–1374. doi: 10.1007/S00784-021-04111-3

Gurav, A. N. (2014). The implication of periodontitis in vascular endothelial dysfunction. *Eur. J. Clin. Invest.* 44, 1000–1009. doi: 10.1111/ECI.12322

Gurwitz, D. (2020). Angiotensin receptor blockers as tentative SARS-CoV-2 therapeutics. *Drug Dev. Res.* 81, 537–540. doi: 10.1002/DDR.21656

Guzman, S., Karima, M., Wang, H.-Y., and Van Dyke, T. E. (2003). Association between interleukin-1 genotype and periodontal disease in a diabetic population. *J. Periodontol* 74, 1183–1190. doi: 10.1902/JOP.2003.74.8.1183

Hanson, M. A., and Godfrey, K. M. (2015). Genetics: Epigenetic mechanisms underlying type 2 diabetes mellitus. *Nat. Rev. Endocrinol.* 11, 261–263. doi: 10.1038/NRENDO.2015.31

Heikkinen, A. M., Kettunen, K., Kovanen, L., Haukka, J., Elg, J., Husu, H., et al. (2016). Inflammatory mediator polymorphisms associate with initial periodontitis in adolescents. *Clin. Exp. Dent. Res.* 2, 208–215. doi: 10.1002/CRE2.40

Herrmann, J. M., Sonnenschein, S. K., Groeger, S. E., Ewald, N., Arneth, B., and Meyle, J. (2020). Refractory neutrophil activation in type 2 diabetics with chronic periodontitis. *J. Periodontal Res.* 55, 315–323. doi: 10.1111/JRE.12717

Hodgson, K., Morris, J., Bridson, T., Govan, B., Rush, C., and Ketheesan, N. (2015). Immunological mechanisms contributing to the double burden of diabetes and intracellular bacterial infections. *Immunology* 144, 171–185. doi: 10.1111/IMM.12394

Huang, N., Pérez, P., Kato, T., Mikami, Y., Okuda, K., Gilmore, R. C., et al. (2021). SARS-CoV-2 infection of the oral cavity and saliva. *Nat. Med.* 27, 892–903. doi: 10.1038/S41591-021-01296-8

Huang, X., Yang, X., Ni, J., Xie, B., Liu, Y., Xuan, D., et al. (2015). Hyperglucose contributes to periodontitis: involvement of the NLRP3 pathway by engaging the innate immunity of oral gingival epithelium. *J. Periodontol* 86, 327–335. doi: 10.1902/JOP.2014.140403

Iwasaki, M., Saito, J., Zhao, H., Sakamoto, A., Hirota, K., and Ma, D. (2020). Inflammation triggered by SARS-coV-2 and ACE2 augment drives multiple organ failure of severe COVID-19: molecular mechanisms and implications. *Inflammation* 44, 13. doi: 10.1007/S10753-020-01337-3

Janket, S. J., Jones, J. A., Meurman, J. H., Baird, A. E., and Van Dyke, T. E. (2008). Oral infection, hyperglycemia, and endothelial dysfunction. *Oral. Surg. Oral. Med. Oral. Pathol. Oral. Radiol. Endod.* 105, 173. doi: 10.1016/J.TRIPLEO.2007.06.027

Javeed, N., and Matveyenko, A. V. (2018). Circadian etiology of type 2 diabetes mellitus. *Physiology* 33, 138. doi: 10.1152/PHYSIOL.00003.2018

Jiménez, D., Martínez-Sanz, J., Sainz, T., Calvo, C., Méndez-Echevarría, A., Moreno, E., et al. (2022). Differences in saliva ACE2 activity among infected and non-infected adult and pediatric population exposed to SARS-CoV-2. *J. Infect.* 85, 86. doi: 10.1016/J.JINF.2022.04.041

Jourdan, T., Godlewski, G., Cinar, R., Bertola, A., Szanda, G., Liu, J., et al. (2013). Activation of the Nlrp3 inflammasome in infiltrating macrophages by endocannabinoids mediates beta cell loss in type 2 diabetes. *Nat. Med.* 19, 1132–1140. doi: 10.1038/NM.3265

Kalsi, R., Ahmad, Z., Siddharth, M., Vandana, K., Arora, S., and Saurav, K. (2022). Correlation of COVID-19 with severity of periodontitis-A clinical and biochemical study. *Indian J. Dent. Res.* 33, 307–312. doi: 10.4103/IJDR.IJDR_1168_21

Kedlaya, M. N., Puzhankara, L., Prasad, R., and Raj, A. (2023). Periodontal disease pathogens, pathogenesis, and therapeutics: the CRISPR-cas effect. *Cris J.* 6, 90–98. doi: 10.1089/CRISPR.2022.0094

Kinane, D. F. (2001). Causation and pathogenesis of periodontal disease. *Periodontol* 2000, 25. doi: 10.1034/J.1600-0757.2001.22250102.X

Kumar, G., Ponnaiyan, D., Parthasarathy, H., Tadepalli, A., and Veeramani, S. (2020). Evaluation of endocan and tumor necrosis factor-α as inflammatory biomarkers in type 2 diabetes and periodontal disease. *Genet. Test Mol. Biomarkers* 24, 431–435. doi: 10.1089/GTMB.2020.0037

Lackey, D. E., and Olefsky, J. M. (2016). Regulation of metabolism by the innate immune system. *Nat. Rev. Endocrinol.* 12, 15–20. doi: 10.1038/NRENDO.2015.189

Li, Q., Ouyang, X., and Lin, J. (2022). The impact of periodontitis on vascular endothelial dysfunction. *Front. Cell Infect. Microbiol.* 12. doi: 10.3389/FCIMB.2022.998313

Liccardo, D., Cannavo, A., Spagnuolo, G., Ferrara, N., Cittadini, A., Rengo, C., et al. (2019). Periodontal disease: A risk factor for diabetes and cardiovascular disease. *Int. J. Mol. Sci.* 20, 1–14. doi: 10.3390/IJMS20061414

Lim, J. C., Ko, K. I., Mattos, M., Fang, M., Zhang, C., Feinberg, D., et al. (2017). TNFα contributes to diabetes impaired angiogenesis in fracture healing. *Bone* 99, 26–38. doi: 10.1016/J.BONE.2017.02.014

Ling, M. R., Chapple, I. L. C., and Matthews, J. B. (2015). Peripheral blood neutrophil cytokine hyper-reactivity in chronic periodontitis. *Innate Immun.* 21, 714–725. doi: 10.1177/1753425915589387

Lira-Junior, R., Öztürk, VÖ, Emingil, G., Bostanci, N., and Boström, E. A. (2017). Salivary and serum markers related to innate immunity in generalized aggressive periodontitis. *J. Periodontol* 88, 1339–1347. doi: 10.1902/JOP.2017.170287

Liu, C. M., Hou, L. T., Wong, M. Y., and Rossomando, E. F. (1996). Relationships between clinical parameters, Interleukin 1B and histopathologic findings of gingival tissue in periodontitis patients. *Cytokine* 8, 161–167. doi: 10.1006/CYTO.1996.0023

Liu, F., Long, X., Zhang, B., Zhang, W., Chen, X., and Zhang, Z. (2020). ACE2 expression in pancreas may cause pancreatic damage after SARS-coV-2 infection. *Clin. Gastroenterol. Hepatol.* 18, 2128–2130.e2. doi: 10.1016/J.CGH.2020.04.040

Liu, T., Zhang, L., Joo, D., and Sun, S. C. (2017). NF-κB signaling in inflammation. *Signal Transduct Target Ther.* 2, 1–9. doi: 10.1038/SIGTRANS.2017.23

Mainas, G., Nibali, L., Ide, M., Mahmeed, W., Al-Rasadi, K., Al-Alawi, K., et al. (2022). Associations between periodontitis, COVID-19, and cardiometabolic complications: molecular mechanisms and clinical evidence. *Metabolites* 13, 1–17. doi: 10.3390/METABO13010040

Mancini, L., Quinzi, V., Mummolo, S., Marzo, G., and Marchetti, E. (2020). Angiotensin-converting enzyme 2 as a possible correlation between COVID-19 and periodontal disease. *Appl. Sci.* 10, 6224. doi: 10.3390/APP10186224

Manosudprasit, A., Kantarci, A., Hasturk, H., Stephens, D., and Van Dyke, T. E. (2017). Spontaneous PMN apoptosis in type 2 diabetes and the impact of periodontitis. *J. Leukoc. Biol.* 102, 1431–1440. doi: 10.1189/JLB.4A0416-209RR

Marouf, N., Cai, W., Said, K. N., Daas, H., Diab, H., Chinta, V. R., et al. (2021). Association between periodontitis and severity of COVID-19 infection: A case-control study. *J. Clin. Periodontol* 48, 483–491. doi: 10.1111/JCPE.13435

Mesia, R., Gholami, F., Huang, H., Clare-Salzler, M., Aukhil, I., Wallet, S. M., et al. (2016). Systemic inflammatory responses in patients with type 2 diabetes with chronic periodontitis. *BMJ Open Diabetes Res. Care* 4, 1–7. doi: 10.1136/BMJDRC-2016-000260

Michaels, T. M., Essop, M. F., and Joseph, D. E. (2024). Potential effects of hyperglycemia on SARS-coV-2 entry mechanisms in pancreatic beta cells. *Viruses* 16, 1–35. doi: 10.3390/V16081243

Mira, A., Simon-Soro, A., and Curtis, M. A. (2017). Role of microbial communities in the pathogenesis of periodontal diseases and caries. *J. Clin. Periodontol* 44 Suppl 18, S23–S38. doi: 10.1111/JCPE.12671

Monod Nuñez, M. S., Aransibia, L. V., Blanco Fernández, M. J., Hernández Oropesa, T., and Linari, M. A. (2022). Frecuencia de enfermedad periodontal en pacientes adultos con diabetes mellitus tipo 2 en la Ciudad Autónoma de Buenos Aires y la Provincia de Buenos Aires. *Rev. Soc. Argent Diabetes* 56, 19–30. doi: 10.47196/DIAB.V56I1.516

Moreno Caicedo, L. F., Amaya Sánchez, S., and Cruz Olivo, E. A. (2018). Factores de riesgo modificables e inmodificables de la periodontitis: revisión narrativa. *Univ Odontol* 37, 1–28. doi: 10.11144/JAVERIANA.UO37-79.FRMI

Muniyappa, R., and Gubbi, S. (2020). COVID-19 pandemic, coronaviruses, and diabetes mellitus. *Am. J. Physiol. Endocrinol. Metab.* 318, E736–E741. doi: 10.1152/AJPENDO.00124.2020

Muñoz-Carrillo, J. L., Hernández-Reyes, V. E., García-Huerta, O. E., Chávez-Ruvalcaba, F., Chávez-Ruvalcaba, M. I., Chávez-Ruvalcaba, K. M., et al. (2019). "Pathogenesis of periodontal disease," in *Diagnostic and adjunctive non-surgical considerations*. Ed. Y. Nermin (IntechOpen, London), 1–14. doi: 10.5772/INTECHOPEN.86548

Nussbaum, G., and Shapira, L. (2011). How has neutrophil research improved our understanding of periodontal pathogenesis? *J. Clin. Periodontol* 38 Suppl 11, 49–59. doi: 10.1111/J.1600-051X.2010.01678.X

Pacios, S., Andriankaja, O., Kang, J., Alnammary, M., Bae, J., De Brito Bezerra, B., et al. (2013). Bacterial infection increases periodontal bone loss in diabetic rats through enhanced apoptosis. *Am. J. Pathol.* 183, 1928–1935. doi: 10.1016/J.AJPATH.2013.08.017

Page, M. J., Moher, D., Bossuyt, P. M., Boutron, I., Hoffmann, T. C., Mulrow, C. D., et al. (2021). PRISMA 2020 explanation and elaboration: updated guidance and exemplars for reporting systematic reviews. *BMJ* 372, 1–36. doi: 10.1136/BMJ.N160

Park, E., Na, H. S., Song, Y. R., Shin, S. Y., Kim, Y. M., and Chung, J. (2014). Activation of NLRP3 and AIM2 inflammasomes by Porphyromonas gingivalis infection. *Infect. Immun.* 82, 112–123. doi: 10.1128/IAI.00862-13

Pascolo, L., Zupin, L., Melato, M., Tricarico, P. M., and Crovella, S. (2020). TMPRSS2 and ACE2 coexpression in SARS-coV-2 salivary glands infection. *J. Dent. Res.* 99, 1120–1121. doi: 10.1177/0022034520933589

Polak, D., and Shapira, L. (2018). An update on the evidence for pathogenic mechanisms that may link periodontitis and diabetes. *J. Clin. Periodontol* 45, 150–166. doi: 10.1111/JCPE.12803

Qi, M., Sun, W., Wang, K., Li, W., Lin, J., Gong, J., et al. (2023). Periodontitis and COVID-19: immunological characteristics, related pathways, and association. *Int. J. Mol. Sci.* 24, 1–18. doi: 10.3390/IJMS24033012

Rao, S., Lau, A., and So, H. C. (2020). Exploring diseases/traits and blood proteins causally related to expression of ACE2, the putative receptor of SARS-coV-2: A mendelian randomization analysis highlights tentative relevance of diabetes-related traits. *Diabetes Care* 43, 1416–1426. doi: 10.2337/DC20-0643

Roca-Ho, H., Riera, M., Palau, V., Pascual, J., and Soler, M. J. (2017). Characterization of ACE and ACE2 expression within different organs of the NOD mouse. *Int. J. Mol. Sci.* 18, 1–13. doi: 10.3390/IJMS18030563

Sakaguchi, W., Kubota, N., Shimizu, T., Saruta, J., Fuchida, S., Kawata, A., et al. (2020). Existence of SARS-coV-2 entry molecules in the oral cavity. *Int. J. Mol. Sci.* 21, 1–16. doi: 10.3390/IJMS21176000

Salvi, G. E., Beck, J. D., and Offenbacher, S. (1998). PGE2, IL-1 beta, and TNF-alpha responses in diabetics as modifiers of periodontal disease expression. *Ann. Periodontol* 3, 40–50. doi: 10.1902/ANNALS.1998.3.1.40

Salvi, G. E., Yalda, B., Collins, J. G., Jones, B. H., Smith, F. W., Arnold, R. R., et al. (1997). Inflammatory mediator response as a potential risk marker for periodontal diseases in insulin-dependent diabetes mellitus patients. *J. Periodontol* 68, 127–135. doi: 10.1902/JOP.1997.68.2.127

Sánchez Sánchez, R. J., Sigcho Romero, C. R., and Niño Peña, A. (2022).Una díada de riesgo: periodontitis y COVID-19. In: *Gac méd espirit*. Available online at: http://scielo.sld.cu/scielo.php?script=sci_arttext&pid=S1608–89212022000200014 (Accessed April 11, 2023).

Santos, V. R., Lima, J. A., Gonçalves, T. E. D., Bastos, M. F., Figueiredo, L. C., Shibli, J. A., et al. (2010). Receptor activator of nuclear factor-kappa B ligand/osteoprotegerin ratio in sites of chronic periodontitis of subjects with poorly and well-controlled type 2 diabetes. *J. Periodontol* 81, 1455–1465. doi: 10.1902/JOP.2010.100125

Santos, C. M. M. L., Lira, R., Fischer, R. G., Santos, A. P. P., and Oliveira, B. H. (2015). Systemic antibiotics in periodontal treatment of diabetic patients: A systematic review. *PloS One* 10, 1–11. doi: 10.1371/JOURNAL.PONE.0145262

Sapna, G., Gokul, S., and Bagri-Manjrekar, K. (2014). Matrix metalloproteinases and periodontal diseases. *Oral. Dis.* 20, 538–550. doi: 10.1111/ODI.12159

Sarkar, P. D., Choudhury, A. B., and Choudhury, A. B. (2013). Relationships between serum osteocalcin levels versus blood glucose, insulin resistance and markers of systemic inflammation in central Indian type 2 diabetic patients. *Eur. Rev. Med. Pharmacol. Sci.* 17, 1631–1635.

Sarrazin, S., Adam, E., Lyon, M., Depontieu, F., Motte, V., Landolfi, C., et al. (2006). Endocan or endothelial cell specific molecule-1 (ESM-1): a potential novel endothelial cell marker and a new target for cancer therapy. *Biochim. Biophys. Acta* 1765, 25–37. doi: 10.1016/J.BBCAN.2005.08.004

Schroder, K., and Tschopp, J. (2010). The inflammasomes. *Cell* 140, 821–832. doi: 10.1016/J.CELL.2010.01.040

Schroder, K., Zhou, R., and Tschopp, J. (2010). The NLRP3 inflammasome: a sensor for metabolic danger? *Science* 327, 296–300. doi: 10.1126/SCIENCE.1184003

Sena, K., Furue, K., Setoguchi, F., and Noguchi, K. (2021). Altered expression of SARS-CoV-2 entry and processing genes by Porphyromonas gingivalis-derived lipopolysaccharide, inflammatory cytokines and prostaglandin E2 in human gingival fibroblasts. *Arch. Oral. Biol.* 129, 1–9. doi: 10.1016/J.ARCHORALBIO.2021.105201

Shaker, O.s, Ghallab, N. A., Hamdy, E., and Sayed, S. (2013). Inducible nitric oxide synthase (iNOS) in gingival tissues of chronic periodontitis with and without diabetes: immunohistochemistry and RT-PCR study. *Arch. Oral. Biol.* 58, 1397–1406. doi: 10.1016/J.ARCHORALBIO.2013.05.003

Shamala, A., Al-Hajri, M., Ali Al-Wesabi, M., and Shamala De-, A. (2017). Risk factors for periodontal diseases among Yemeni type II diabetic patients. *A case-control study. J. Oral. Res.* 6, 176–181. doi: 10.17126/%x

Sharma, B. R., and Kanneganti, T. D. (2021). NLRP3 inflammasome in cancer and metabolic diseases. *Nat. Immunol.* 22, 550–559. doi: 10.1038/S41590-021-00886-5

Shenoy, A., Ismaily, M., and Bajaj, M. (2020). Diabetes and covid-19: a global health challenge. *BMJ Open Diabetes Res. Care* 8, 1–2. doi: 10.1136/BMJDRC-2020-001450

Silvestre, F. J., and Márquez-Arrico, C. F. (2022). COVID-19 and periodontitis: A dangerous association? *Front. Pharmacol.* 12. doi: 10.3389/FPHAR.2021.789681

Singh, A. K., Gupta, R., Ghosh, A., and Misra, A. (2020). Diabetes in COVID-19: Prevalence, pathophysiology, prognosis and practical considerations. *Diabetes Metab. Syndr. Clin. Res. Rev.* 14, 303–310. doi: 10.1016/J.DSX.2020.04.004

Sircana, A., Framarin, L., Leone, N., Berrutti, M., Castellino, F., Parente, R., et al. (2018). Altered gut microbiota in type 2 diabetes: just a coincidence? *Curr. Diabetes Rep.* 18, 1–11. doi: 10.1007/S11892-018-1057-6

Stančáková, A., and Laakso, M. (2016). Genetics of type 2 diabetes. *Endocr. Dev.* 31, 203–220. doi: 10.1159/000439418

Sukumar, K., and Tadepalli, A. (2021). Nexus between COVID-19 and periodontal disease. *J. Int. Med. Res.* 49, 1–11. doi: 10.1177/03000605211002695

Sun, Y., Shi, H., Yin, S., Ji, C., Zhang, X., Zhang, B., et al. (2018). Human mesenchymal stem cell derived exosomes alleviate type 2 diabetes mellitus by reversing peripheral insulin resistance and relieving β-cell destruction. *ACS Nano* 12, 7613–7628. doi: 10.1021/ACSNANO.7B07643

Susanto, H., Nesse, W., Dijkstra, P. U., Agustina, D., Vissink, A., and Abbas, F. (2011). Periodontitis prevalence and severity in Indonesians with type 2 diabetes. *J. Periodontol* 82, 550–557. doi: 10.1902/JOP.2010.100285

Torres-Tamayo, M., Caracas-Portillo, N. A., Peña-Aparicio, B., Juárez-Rojas, J. G., Medina-Urrutia, A. X., Martínez-Alvarado M del, R., et al. (2020). Infección por coronavirus en pacientes con diabetes. *Arch. Cardiol. México* 90, 67–76. doi: 10.24875/ACM.M20000068

Trentin, M. S., de Carli, J. P., Ferreira M de, C., Gambin, D. J., da Silva, S. O., and Lisboa, H. (2018). Prevalence and severity of periodontal disease in type 2 diabetes mellitus patients: a cross-sectional study. *Biosci. J.* 34, 1114–1123. doi: 10.14393/BJ-V34N1A2018-41485

Tsai, C., Hayes, C., and Taylor, G. W. (2002). Glycemic control of type 2 diabetes and severe periodontal disease in the US adult population. *Community Dent. Oral. Epidemiol.* 30, 182–192. doi: 10.1034/J.1600-0528.2002.300304.X

Türer, Ç. C., Durmuş, D., Balli, U., and Güven, B. (2017). Effect of non-surgical periodontal treatment on gingival crevicular fluid and serum endocan, vascular endothelial growth factor-A, and tumor necrosis factor-alpha levels. *J. Periodontol* 88, 493–501. doi: 10.1902/JOP.2016.160279

Turk Wensveen, T., Gašparini, D., Rahelić, D., and Wensveen, F. M. (2021). Type 2 diabetes and viral infection; cause and effect of disease. *Diabetes Res. Clin. Pract.* 172, 1–13. doi: 10.1016/J.DIABRES.2020.108637

Turner, C. (2022). Diabetes mellitus and periodontal disease: the profession's choices. *Br. Dent. J.* 233, 537–538. doi: 10.1038/S41415-022-5029-5

Ullah, H., Ullah, A., Gul, A., Mousavi, T., and Khan, M. W. (2021). Novel coronavirus 2019 (COVID-19) pandemic outbreak: A comprehensive review of the current literature. *Vacunas* 22, 106–113. doi: 10.1016/J.VACUN.2020.09.009

Van Dyke, T. E. (2017). Pro-resolving mediators in the regulation of periodontal disease. *Mol. Aspects Med.* 58, 21–36. doi: 10.1016/J.MAM.2017.04.006

van Eijk, L. T., Cox, L. A. E., Ramakers, B. P. C., Dorresteijn, M. J., Gerretsen, J., Kox, M., et al. (2014). Plasma endocan levels are associated with endothelial dysfunction during experimental human endotoxemia. *Intensive Care Med. Exp.* 2, 1–2. doi: 10.1186/2197-425X-2-S1-P52

Villarreal-Pérez, J. Z., Villarreal-Martínez, J. Z., Lavalle-González, F. J., Torres-Sepúlveda, M. D. R., Ruiz-Herrera, C., Cerda-Flores, R. M., et al. (2014). Plasma and urine metabolic profiles are reflective of altered beta-oxidation in non-diabetic obese subjects and patients with type 2 diabetes mellitus. *Diabetol. Metab. Syndr.* 6, 1–8. doi: 10.1186/1758-5996-6-129

Woessner, J. F. (1991). Matrix metalloproteinases and their inhibitors in connective tissue remodeling. *FASEB J.* 5, 2145–2154. doi: 10.1096/FASEBJ.5.8.1850705

Wu, C. Z., Yuan, Y. H., Liu, H. H., Li, S. S., Zhang, B. W., Chen, W., et al. (2020). Epidemiologic relationship between periodontitis and type 2 diabetes mellitus. *BMC Oral. Health* 20, 1–15. doi: 10.1186/S12903-020-01180-W

Wysocki, J., Ye, M., Soler, M. J., Gurley, S. B., Xiao, H. D., Bernstein, K. E., et al. (2006). ACE and ACE2 activity in diabetic mice. *Diabetes* 55, 2132–2139. doi: 10.2337/DB06-0033

Xiao, W., Wang, Y., Pacios, S., Li, S., and Graves, D. T. (2016). Cellular and molecular aspects of bone remodeling. *Front. Oral. Biol.* 18, 9–16. doi: 10.1159/000351895

Yang, X., Yu, Y., Xu, J., Shu, H., Xia, J., Liu, H., et al. (2020). Clinical course and outcomes of critically ill patients with SARS-CoV-2 pneumonia in Wuhan, China: a single-centered, retrospective, observational study. *Lancet Respir. Med.* 8, 475–481. doi: 10.1016/S2213-2600(20)30079-5

Ye, Z., Zhang, Y., Wang, Y., Huang, Z., and Song, B. (2020). Chest CT manifestations of new coronavirus disease 2019 (COVID-19): a pictorial review. *Eur. Radiol.* 30, 4381–4389. doi: 10.1007/S00330-020-06801-0

Yin, Y., Rohli, K. E., Shen, P., Lu, H., Liu, Y., Dou, Q., et al. (2021). The epidemiology, pathophysiological mechanisms, and management toward COVID-19 patients with Type 2 diabetes: A systematic review. *Prim Care Diabetes* 15, 899–909. doi: 10.1016/J.PCD.2021.08.014

You, J. H., Lee, S. A., Chun, S. Y., Song, S. O., Lee, B. W., Kim, D. J., et al. (2020). Clinical outcomes of COVID-19 patients with type 2 diabetes: A population-based study in korea. *Endocrinol. Metab. (Seoul Korea)* 35, 901–908. doi: 10.3803/ENM.2020.787

Zhang, H., and Pollin, T. I. (2018). Epigenetics variation and pathogenesis in diabetes. *Curr. Diabetes Rep.* 18, 1–9. doi: 10.1007/S11892-018-1091-4

Zhang, H., Sun, Y., Wang, Y., Yazici, D., Azkur, D., Ogulur, I., et al. (2023). Recent developments in the immunopathology of COVID-19. *Allergy* 78, 369–388. doi: 10.1111/ALL.15593

Zheng, J., Chen, S., Albiero, M. L., Vieira, G. H. A., Wang, J., Feng, J. Q., et al. (2018). Diabetes activates periodontal ligament fibroblasts via NF-κB. *In Vivo. J. Dent. Res.* 97, 580–588. doi: 10.1177/0022034518755697

Zheng, Y. Y., Ma, Y. T., Zhang, J. Y., and Xie, X. (2020). COVID-19 and the cardiovascular system. *Nat. Rev. Cardiol.* 17, 259–260. doi: 10.1038/S41569-020-0360-5

Zhou, T., Hu, Z., Yang, S., Sun, L., Yu, Z., and Wang, G. (2018). Role of adaptive and innate immunity in type 2 diabetes mellitus. *J. Diabetes Res.* 2018, 1–9. doi: 10.1155/2018/7457269

Zhou, F., Yu, T., Du, R., Fan, G., Liu, Y., Liu, Z., et al. (2020). Clinical course and risk factors for mortality of adult inpatients with COVID-19 in Wuhan, China: a retrospective cohort study. *Lancet (London England)* 395, 1054–1062. doi: 10.1016/S0140-6736(20)30566-3

frontiers | Frontiers in Cellular and Infection Microbiology

TYPE Original Research
PUBLISHED 27 May 2025
DOI 10.3389/fcimb.2025.1586121

OPEN ACCESS

EDITED BY
Rommel Chacon-Salinas,
Instituto Politécnico Nacional, Mexico

REVIEWED BY
Adriana Muñoz,
National Autonomous University of Mexico, Mexico
Ismael Martínez Cortés,
Universidad Autónoma Metropolitana, Mexico

*CORRESPONDENCE
Xiurong Xu
xuxiurong@nwafu.edu.cn

RECEIVED 02 March 2025
ACCEPTED 25 April 2025
PUBLISHED 27 May 2025

CITATION
Yan F, Zhang Z, Zhan X, Yang W, Yao J and Xu X (2025) Immune pre-stimulation by injected yeast beta-glucan as a strategy to prevent calf diarrhea and bovine respiratory disease during the first 74 days of age. *Front. Cell. Infect. Microbiol.* 15:1586121. doi: 10.3389/fcimb.2025.1586121

Immune pre-stimulation by injected yeast beta-glucan as a strategy to prevent calf diarrhea and bovine respiratory disease during the first 74 days of age

Fang Yan[1], Zhihong Zhang[2], Xiaorong Zhan[1], Wenqian Yang[1], Junhu Yao[1] and Xiurong Xu[1]*

[1]College of Animal Science and Technology, Northwest A&F University, Yangling, Shaanxi, China,
[2]Animal Husbandry Division, Junlebao Dairy Co. Ltd., Shijiazhuang, Hebei, China

Introduction: The complexity of intestinal pathogens poses a great challenge to the prevention of infectious diarrhea in calves. Studies have shown that immune stimulants such as yeast beta-glucan can induce the innate immune system to acquire memory and improve their non-specific defense functions. This trial was conducted to evaluate the prophylactic effect of intraperitoneal injection of yeast β-glucan after birth on diarrhea in Holstein calves during the first 74 days of age.

Methods: A total of 52 healthy newborn Holstein calves (body weight 39.3 ± 0.82 kg) were enrolled and randomly assigned into two groups (n = 26 in per group): 1) placebo group (CON), and 2) intraperitoneal injection with yeast β-glucan solution (0.1 g/mL, 50 mg/kg body weight) at 3 and 6 days of age (IP). The CON group received an equal volume of sterile saline at the same time. Body weight was measured monthly, and health checks and fecal consistency were evaluated daily for every calf. Jugular blood and rectal feces were collected at 7 and 30 days of age.

Results: IP induced inflammation in calves, which was manifested as obvious increased levels of serum cytokines (IL-1β, IL-6, and TNF-a), immunoglobulin (IgG and IgM), and oxidative stress after 24 h, and the antimicrobial substance (defensin and secreted immunoglobulin A) in feces also significantly increased, but stimulation didn't lead to a higher level of serum diamine oxidase (DAO). The pre-stimulation had no positive effect on growth performance or feed efficiency, but reduced the frequencies of diarrhea and bovine respiratory disease, especially during 31-60 d. Furthermore, the pre-stimulation increased the levels of serum IL-6, fecal defensin and secreted immunoglobulin A, while decreased the levels of serum DAO and malonaldehyde at 30 d. In addition, compared with the ones in the CON group, calves in the IP group showed a better rectal bacterial structure at 30 d, with a more enrichment of beneficial bacteria such as *Bifidobacterium*.

Discussion: Our findings suggested that early stimulation with yeast β-glucan could be a promising strategy for reducing the frequencies of both diarrhea and BRD in calves.

KEYWORDS

yeast β-glucan, trained immunity, calves, diarrhea, bovine respiratory disease

Introduction

The prevalence of diarrhea and bovine respiratory disease (BRD) was 18.9% and 11.3% in the United States of America, 29% and 39% in Canada, and 17.9% and 6.0% in Australia, respectively (Windeyer et al., 2014; Urie et al., 2018; Abuelo et al., 2019). Those two diseases accounted for 56.0% and 33.4% of the incidence of calves, respectively, and were the main diseases of calves. The number of calf deaths caused by diarrhea or BRD accounts for 32.0% and 14.1% of the total number of deaths, respectively (Urie et al., 2018).

Pathogen infections are the primary reason behind calf diarrhea, involving a diverse range of pathogens such as viruses, pathogenic bacteria, and parasites (Kolenda et al., 2015), including some newly discovered pathogens (Netea et al., 2016). This complexity makes it challenging to comprehensively vaccinate against infective diarrhea in calves. In recent years, the theory of trained immunity has been deeply studied, which brings new strategies to the prevention of unpredictable or complex infections in animals, especially young ones. Trained immunity refers to the development of immune memory by innate immune cells in response to infection by a pathogen or stimulation of its antigenic components to provide enhanced protection against later exposure to homologous or heterologous infections (Netea et al., 2020). This process is distinct from adaptive immunity, which involves the production of specific antibodies and memory T cells. The inducers of trained immunity include some pathogens (Quintin et al., 2012; Schrum et al., 2018) and their attenuated strains (Ifrim et al., 2014; Saeed et al., 2014), non-live ones (Brandi et al., 2022; Juste et al., 2022), or cell wall components (Briard et al., 2021; Brandi et al., 2022; Vuscan et al., 2024). In addition, yeast β-glucan, a cell wall component of fungi with β-1,3/1, 6- glycosidic linkages (Han et al., 2020), has also been shown to have the function of inducing immune memory in innate immune cells. Yeast β-glucan or beta-glucans from other organisms have been extensively studied as a prebiotic when added to animal feed daily (Ding et al., 2019; Pornanek and Phoemchalard, 2021; Goh et al., 2023). Reis et al (Reis et al., 2022) found that adding 2 g/d algal beta-glucan to milk replacer increased the weight of calves at 8 weeks and reduced the fecal scores during the first 28 days of age in Holstein dairy calves. As trained immunity inducers, studies have confirmed that two-time injections of yeast β-glucan induced macrophages in the blood of goats to acquire immune memory (Angulo et al., 2020). In newborn calves, in vivo β-glucan oral administration induced a trained phenotype in innate immune cells, leading to immune metabolic changes, upon ex vivo challenge with Escherichia coli (Angulo and Angulo, 2023). However, the effect of yeast β-glucan-induced trained immunity on the prevention of diarrhea and bovine respiratory disease (BRD) in dairy calves is unclear.

Therefore, this study aimed to evaluate the effects of intraperitoneal injection of yeast beta-glucan at birth on diarrhea and BRD frequency in Holstein dairy calves during lactation and early weaning. In addition, the differences of three inflammatory factors in serum and defense proteins secreted by intestinal epithelial cells in feces between the two groups after immune stimulation and combined stress were detected, to explore whether the effect of pre-stimulation on the intestinal health of calves involved the mechanism of trained immunity. Our study may provide a new strategy for improving calf health.

Materials and methods

Animal feeding and experimental design

A total of 52 healthy Holstein heifer calves (3 d of age; BW = 39.3 ± 0.82 kg) were weighed, and housed in a naturally ventilated barn with individual shelter (3.0 m × 1.2 m × 1.8 m; length × width × height). At enrollment, the calf ID, date, and time of day (morning or evening) were recorded. Buckets with water and calf starter were available in each shelter. Screened wood shavings with a minimum theoretical length cut of 50 mm were used to minimize dustiness in the housing environment. The bedding was refreshed every 7 d to keep the pens visibly clean and dry. Calves were equally divided into two groups (n = 26 in per group) and randomly assigned to one of 2 treatments as follows: 1) placebo group (CON), and 2) intraperitoneal injection with yeast β-glucan solution (0.1 g/mL, 50 mg/kg body weight) at 3 and 6 days of age (IP). The CON group received an intraperitoneally equal volume of sterile saline at the same time. The experiment lasted until the 74th day of age. The experimental design is shown in Figure 1A.

Calves were fed milk 2 times daily (06:00 and 16:00) with 6 L/d, 10 L/d, and 12 L/d offered from d 2-7, d 8-20, d 21-50, respectively. At 20–23 days of age, 155 g/L commercial milk replacer with 23.4% crude protein (CP) and 13.7% fat is used to gradually replace milk according to the actual dry matter of milk. Calves were weaned over

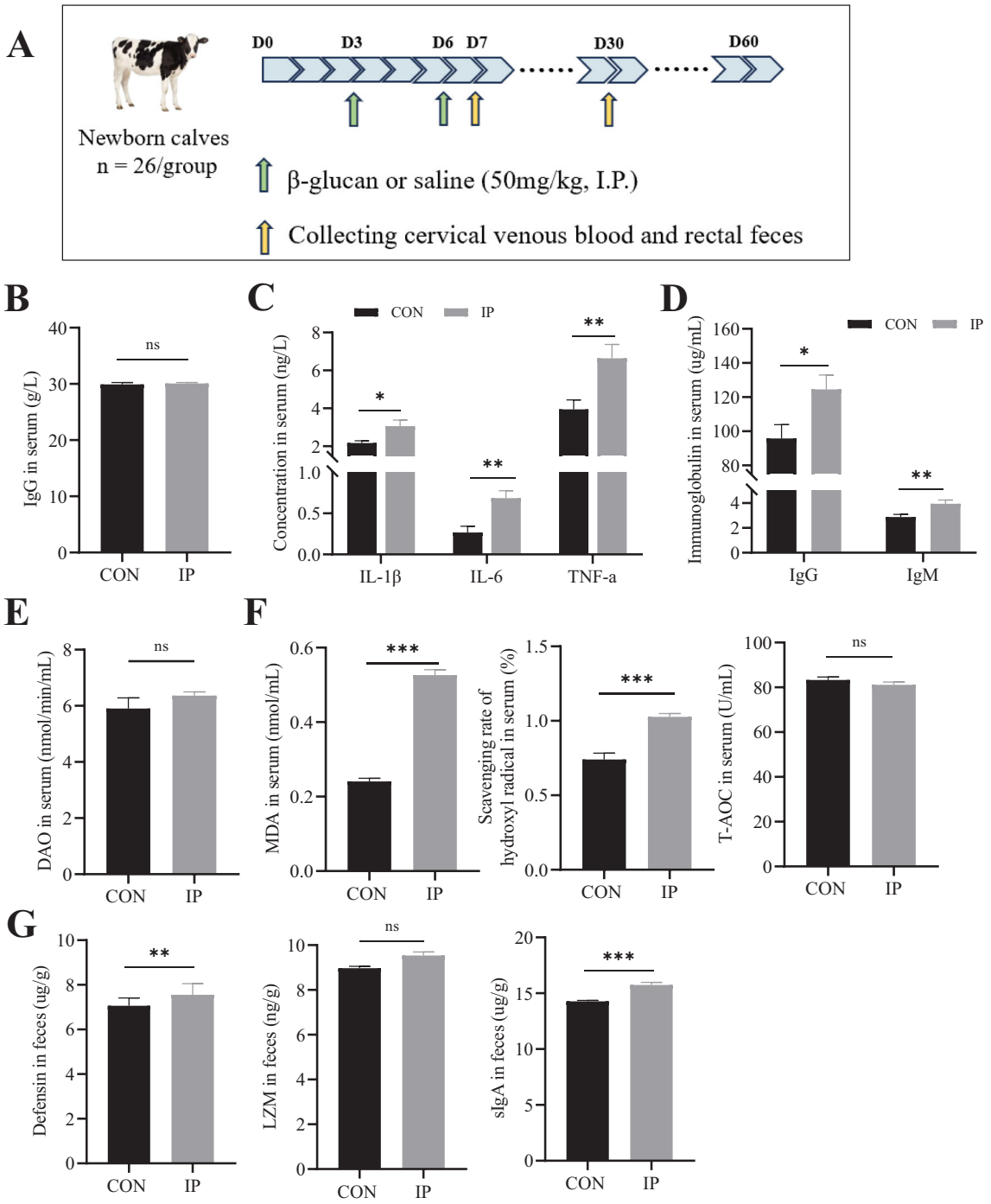

FIGURE 1
The effect of intraperitoneal injection of yeast β-glucan on calves after 24 h. **(A)** Schematic diagram of the experimental procedure. **(B)** The concentration of IgG in the serum of calves at 2 days of age. **(C)** The concentration of IL-1β, IL-6, and TNF-a in the serum of calves after intraperitoneal injection 24 h. **(D)** The immunoglobulin levels in the serum of calves after intraperitoneal injection 24 h. **(E)** The serum DAO levels were measured by ELISA to evaluate the degree of intestinal injury. **(F)** The antioxidant status of calves after intraperitoneal injection 24 h. **(G)** The Defensin, LZM, and sIgA levels in the rectal contents of calves were measured by ELISA to evaluate the degree of immune response. All data is shown as mean values ± standard error of the mean (SEM). Control group n = 12, IP group n = 15; Statistical significance was determined by the unpaired, two-tailed Student's t-test with a 95% confidence interval, *$P < 0.05$, **$P < 0.01$, ***$P < 0.001$. CON, control group, IP, Intraperitoneal injection group; IL, interleukin, TNF-a, tumor necrosis factor-a; IgG, immunoglobulin G, IgM, immunoglobulin M; MDA, malonaldehyde, T-AOC, total antioxidant capacity; DAO, diamine oxidase; LZM, lysozyme; sIgA, the secreted immunoglobulin A. ns, no significance.

10 d from d 51-60, receiving a total of 10 L in 2 meals/d from d 51-52, 8 L from d 53-54, 6 L from d 55-56, 4 L from d 57-58, and 2 L from d 59–60 until weaned. The composition of the milk replacer and starter concentrate is shown in Table 1 and Table 2.

TABLE 1 Nutrient compositions (%, DM basis) of the milk replacer (MR).

Items	Value[1]
DM (%, as fed)	94.1
Ash	6.50
Gross energy (GE, MJ/kg of DM)	19.5
CP	23.4
EE	13.7
Ca	0.98
P	0.71

[1]Commercial milk replacer (Beijing Precision Animal Nutrition Research Center).
Items: DM, Dry matter; CP, Crude protein; EE, Ether extract.

Samples collection and handling

At 7 and 30 days of age, blood samples were collected from all calves by jugular venipuncture using tubes (BD Vacutainer, Franklin Lakes, NJ) at 08:00 h, subsequently centrifuged at 3000 × g for 15 min at 4°C to obtain serum. Fecal samples were collected by rectal massage in a 5 mL frozen tube at the same time. The serum and fecal samples were quickly frozen in liquid nitrogen and then kept at -40°C for subsequent analysis.

TABLE 2 Ingredients and nutrient composition of the starter feed (%, DM basis).

Items	Value[2]
Ingredients	
Corn	36.5
Soybean meal	30.0
Wheat bran	23.4
Limestone	0.1
Premix[1]	10.0
Nutrition composition	
DM	87.63
CP	23.06
EE	3.41
CF	4.92
Ca	1.06
P	0.73

[1]Provided per kg of diet: VA 15–000 IU, VD3 5–000 IU, VE 50 mg, Fe 9 mg, Cu 12.5 mg, Mn 130 mg, Zn 100 mg, Se 0.3 mg, I 1.5 mg and Co 0.5 mg.
[2]Commercial calf starter feed (Charoen Pokphand Group agriculture and animal husbandry food enterprises).
Items: DM, Dry matter; CP, Crude protein; EE, Ether extract; CF, Crude fiber.

Growth performance and health recording

To avoid the stress associated with weighing, we minimized animal weighing, and calves were weighed with mechanical scales (ICS-300; Coimma Limited) at birth, 30, and 60 days of age before the morning feeding. Milk replacer intake, Calf-starter intake, fecal consistency, and BRD score were measured daily. Feed refusals were removed before the provision of fresh starter feed. Individual feed intake was determined daily by weighing the amounts of starter feed offered and the amounts refused using a calibrated electronic scale (model PX3000; Pand Iran Co., Isfahan, Iran). Average Daily Gain (ADG) was calculated as the difference between body weight (BW) taken at 30-d intervals divided by 30. The total dry matter (DM) intake was calculated as the milk replacer DM plus the starter feed DM. The estimation of feed efficiency was calculated as the ratio of ADG to the total DM intake.

The health status of the calves was performed daily during the entire experimental period. Diarrhea was diagnosed based on fecal consistency. All calves were rectally stimulated to defecate, and fecal consistency was scored on a scale of 0 to 3, where 0 = normal consistency, 1 = semiformed or pasty, 2 = loose feces, and 3 = watery feces (Renaud et al., 2020). A fecal score ≥ 2 was considered as diarrhea. BRD and interventions were performed daily on all calves by the same trained veterinarian after the morning feeding. Signs of BRD were scored daily on each calf according to the previous study (McGuirk and Peek, 2014). Briefly, abnormal nasal discharge, coughing, ear tilt, eye discharge, and an elevated rectal temperature (TS-101 Colors Techline digital, Techline São Paulo) were recorded. The presence of at least 2 categories of abnormal scores was required for a diagnosis of BRD. The cumulative frequency of diarrhea for each group was calculated as previously described (Zou et al., 2021): The frequency of diarrhea (%) = (number of calves with diarrhea × days of diarrhea)/(total number of calves × examined days) × 100. Antimicrobial therapy was administered only when the animal showed fever or depression symptoms, such as recumbence, and decreased or refused milk intake. All calves with a positive diarrhea bout received antimicrobial intervention on the day of initial diagnosis; sulfamethoxazole and trimethoprim were administered intramuscularly with a dosage calculated by BW (1 mL/15 kg; Trissulfim, Ourofino Animal Health) according to the herd veterinarian protocol. For BRD, florfenicol + flunixin meglumine was administered intramuscularly with the dosage calculated by BW (1 mL/15 kg florfenicol; Florkem, Ceva Sante Animale; 1 mL/45 kg flunixin meglumine; Flumax, J.A. Saúde Animal) according to the herd veterinarian protocol. Medications used, dosage, and duration of treatments were recorded for individual calves.

Detection of serum oxidative stress indicators

After removing the serum from -40°C, thaw it on ice.

The Malonaldehyde (MDA) concentration in the serum was determined using a commercially available kit (Nanjing Jiancheng

Bioengineering Institute, A003-1, Nanjing, China) based on thiobarbituric acid (TBA) reactivity. Briefly, after mixing trichloroacetic acid with the homogenate and centrifuging, a supernatant was obtained, and TBA was added. The developed red color of the resulting reaction was measured at 532 nm with a spectrophotometer. Other procedures were carried out following the manufacturer's protocols. Total antioxidant capacity (T-AOC) was detected by a colorimetry kit (Nanjing Jiancheng Bioengineering Institute, A015-1, Nanjing, China) following the manufacturer's protocols. Hydroxy free radical scavenging activity in the serum was determined using a commercially available kit (Angle Gene Biotechnology, AK319, Nanjing, China) based on the fenton microplate process. The developed color of the resulting reaction was measured at 536 nm with a spectrophotometer.

Detection of serum cytokines, immunoglobulins, and diamine oxidase concentrations

Cytokines (IL-1β, IL-6, and TNF-α), immunoglobulins (immunoglobulin G (IgG) and immunoglobulin M (IgM)), and diamine oxidase (DAO) in the serum were detected using a double-antibody one-step sandwich commercial ELISA kits (Jining Biotechnology, Nanjing, China) with the batch numbers JN21039, JN21752, JN20906, JN7372, and JN7340 respectively. The assays were performed using a double-antibody one-step sandwich ELISA format. The antibody was pre-coated with respective trapping antibodies sourced from commercial producer. The procedures were carried out following the manufacturer's protocols. The absorbance (OD value) is measured at a wavelength of 450 nm using a microplate reader to calculate the sample concentration.

Detection of intestinal antimicrobial substance concentrations

After taking the fecal samples out from a -80°C environment, thaw them on ice. After weighing, add them to the corresponding volume of sterile PBS (generally at a weight-to-volume ratio of 1:9, for example, 1 g of rectal feces sample corresponds to 9 mL of PBS) in a sterile centrifuge tube, and grind thoroughly on ice. Finally, centrifuge the homogenate at 5000×g for 5 to 10 minutes, and collect the supernatant for detection.

Defensin, LZM, and secreted immunoglobulin A (sIgA) in the rectal feces were detected using commercial ELISA kits (Jining Biotechnology, Nanjing, China) with the batch numbers JN1350, JN2132, and JN2203 respectively according to the manufacturer's instructions.

16S rRNA gene sequencing of intestinal bacteria

Fifteen healthy calves that had not been treated with antibiotics before 30 days of age were randomly selected in each group for detecting the bacterial structure in the rectal feces of calves on 30 d. Bacterial genomic DNA from rectal feces samples was extracted using the CTAB according to the manufacturer's instructions. The barcoded PCR primers F341 (5′-CCTAYGGGRBGCASCAG-3′) and R806 (5′-GGAC TACNNGGGTATCTAAT-3′) were used to amplify the V3-V4 region of the 16S rRNA gene. PCR amplification was performed in a total volume of 25 μL reaction mixture containing 25 ng of template DNA, 12.5 μL PCR Premix, 2.5 μL of each primer, and PCR-grade water to adjust the volume. The PCR conditions to amplify the prokaryotic 16S fragments consisted of an initial denaturation at 98°C for 30 s; 32 cycles of denaturation at 98°C for 10 s, annealing at 54°C for 30 s, and extension at 72°C for 45 s; and then final extension at 72°C for 10 min. The PCR products were detected with 2% agarose gel electrophoresis. Throughout the DNA extraction process, ultrapure water, instead of a sample solution, was used to exclude the possibility of false-positive PCR results as a negative control. The PCR products were purified by AMPure XT beads (Beckman Coulter Genomics, Danvers, MA, USA) and quantified by Qubit (Invitrogen, USA). The amplicon pools were prepared for sequencing and the size and quantity of the amplicon library were assessed on Agilent 2100 Bioanalyzer (Agilent, USA) and with the Library Quantification Kit for Illumina (Kapa Biosciences, Woburn, MA, USA), respectively. The libraries were sequenced on the NovaSeq PE250 platform according to the manufacturer's recommendations, provided by LC-Bio. Alpha diversity and beta diversity were calculated by normalizing to the same sequences randomly. For alpha diversity, Chao1 and Shannon's indices were used to evaluate the differences in microbial richness and diversity, and PCA based on unweighted UniFrac distances and PCoA based on bray-Curtis metrics were to examine the community structures of the feces microbiotas. The graphs were computed using normalized data in R (version 4.1.2) with the vegan package. To compare the abundances of the microbiome between the CON group and IP group, a Linear Discriminant Analysis Effect Size (LEfSe) was performed with LDA > 3 ($P < 0.05$) as the critical value. These data are available in NCBI with PRJNA1155013.

Statistical analyses

Data were managed in Excel (Microsoft) spreadsheets. All statistical analyses were performed considering the calf as the experimental unit and using SPSS Statistics V21.0. The experimental design used was a randomized block, considering birth date, and birth weight as blocking factors. Baseline measurements were compared using one-way ANOVA after confirming normality (Shapiro-Wilk test $P > 0.05$ for all variables) and homogeneity of variances (Levene's test). No significant differences were observed between groups for any baseline parameter (all ANOVA $P > 0.05$). Measurements for serum analytes, rectal temperature, and respiration frequency at all time points were analyzed for normality using a Shapiro-Wilk test, with Q-Q plots visually confirming distributions, for homogeneity of the variances using the Levene test. The

treatment means were compared using the Tukey-Kramer adjustment test. The threshold of significance was set at $P < 0.05$. The figures for data visualization were performed using GraphPad Prism 9.0 (GraphPad Software Inc., San Diego, CA). The data were presented as mean ± SEM. A $P < 0.05$ was considered as statistically significant, and P-values between 0.05 and 0.10 represent a statistical trend. The asterisks indicate statistical significance (∗, $P < 0.05$; ∗∗, $P < 0.01$; ∗∗∗, $P < 0.001$).

Result

Animal inclusion/exclusion criteria

Inclusion Criteria: A total of 52 Holstein heifer calves (3 d of age; body weighing 38–40 kg at enrollment. Clinically healthy (no diarrhea/respiratory) with normal rectal temperature (<39.5°C) and success-of-passive-transfer (IgG >10 g/L). Exclusion Criteria: Animals with congenital defects, or fecal score >2 at baseline. No animals died during the experiment, and all animals were included in the statistics of diarrhea and BRD incidence frequency (n = 52). However, animal individuals with more than 2 cases illness requiring antibiotics were excluded and the final sample size during laboratory testing was: control group: n = 12 (original n= 26–14 exclusions). IP Group: n= 15 (original n = 26–11 exclusions). Excluded animals are not included in statistical analyses.

Transient inflammatory response

We first measured the serum IgG levels of all the calf subjects at the time of their inclusion in the trial. The results are shown in Figure 1B, and there was no significant difference in the initial immune status between calves in the IP and CON group ($P > 0.05$). The short-term effects (24 hours after the second injection) of IP are shown in Figures 1C-F. In the IP group, the cytokines IL-1β ($P = 0.019$), IL-6 ($P = 0.001$), and TNF-a ($P = 0.005$), and the IgG ($P = 0.020$) and IgM ($P = 0.007$) were significantly increased. Additionally, serum MDA content and hydroxyl free radical scavenging ability were also significantly elevated ($P < 0.001$) (Figure 1F), but there was no significant difference in DAO content between the two groups ($P = 0.263$) (Figure 1E). In the rectal contents, the levels of antibacterial substances secreted by intestinal epithelial cells, namely defensin ($P = 0.005$) and sIgA ($P < 0.001$), were significantly increased, while there was no significant difference in LZM content ($P > 0.05$).

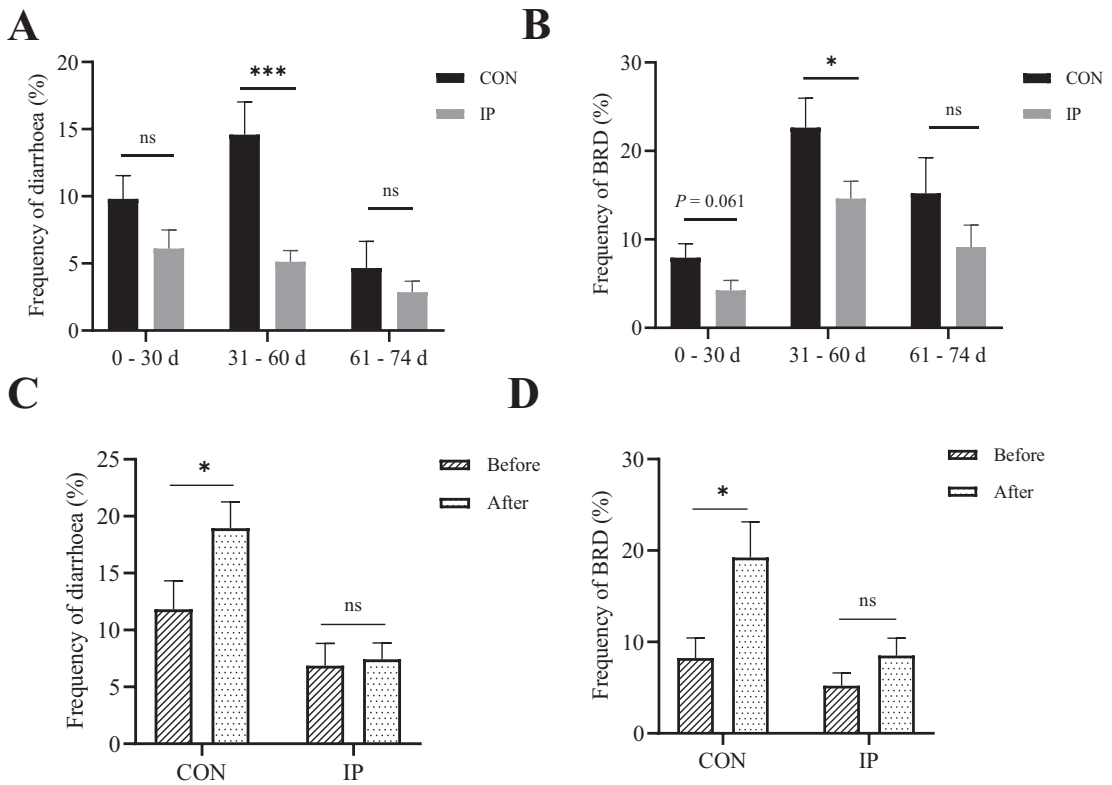

FIGURE 2
Pre-stimulation with yeast β-glucans decreased the frequency of diarrhea and BRD in calves. **(A)** The frequency of diarrhea and **(B)** BRD during 0–74 days of age. **(C)** The frequency of diarrhea and **(D)** BRD 2 weeks before and after 30 days of calves. All data is shown as mean values ± standard error (SEM). n = 26 in per group; Statistical significance was determined by the Chi-squared test with a 95% confidence interval, *$P < 0.05$, ***$P < 0.001$. CON, control group, IP, intraperitoneal injection group, BRD, Bovine Respiratory Disease. ns, no significance.

TABLE 3 Effects of prestimulation with yeast β-glucans on the growth performance of calves.

Items	Experimental groups		SEM	*P*-value
	CON	IP		
0-30d				
Milk replacer intake, L/d	8.509	8.431	0.086	0.372
Calf-starter intake, kg/d	0.035	0.039	0.005	0.680
Total DM intake*, kg/d	1.272	1.263	0.015	0.566
ADG(kg)	0.945	0.954	0.031	0.879
Feed efficiency[1]	0.744	0.756	0.051	0.801
31-60d				
Milk replacer intake, L/d	9.356	9.562	0.117	0.086
Calf-starter intake, kg/d	0.120	0.085	0.009	0.056
Total DM intake*, kg/d	1.467	1.464	0.028	0.918
ADG(kg)	1.037	1.031	0.030	0.917
Feed efficiency	0.698	0.703	0.048	0.934
0-60d				
Milk replacer intake, L/d	8.945	8.997	0.081	0.524
Calf-starter intake, kg/d	0.078	0.060	0.012	0.154
Total DM intake*, kg/d	1.366	1.356	0.019	0.609
ADG(kg)	0.991	1.002	0.015	0.465
Feed efficiency	0.723	0.733	0.013	0.445

*Total DM intake = milk replacer DM + starter feed DM.
[1]Feed efficiency was calculated by dividing ADG by average total DMI (milk replacer DM + starter feed DM).
Items: DM, Dry matter; ADG, Average Daily Gain. Experimental groups: CON, Control group; IP, Intraperitoneal injection group.

Frequency of diarrhea and BRD

As presented in Figures 2A, B, the overall frequency of diarrhea and BRD were both reduced by IP, especially from 31–60 days period the frequencies of both diseases were observed significantly lower ($P < 0.001$). Moreover, the frequency of diarrhea ($P = 0.041$) and BRD ($P = 0.019$) in the CON group of calves significantly increased when comparing the 2 weeks before and after reaching 30 days of age. Whereas in the IP group, the frequency of both diseases remained stable with no significant increase during the same period ($P > 0.05$) (Figures 2C, D).

Growth performance

As outlined in Table 3, there were no significant differences in the intake (milk replacer, calf-starter feed, and total DM), ADG, and feed efficiency between the CON group and the IP group throughout the entire 0–60 d period ($P > 0.05$).

Oxidative stress status

The difference in oxidative stress levels between the two groups at 30 days of age was shown in Figures 3A-C. The hydroxyl radical scavenging ability of calves in the IP group was significantly higher than that in the CON group ($P < 0.001$) (Figure 3A), while the level of MDA in the IP group was lower than CON group ($P = 0.076$) (Figure 3B), but there was no obvious difference in serum total antioxidant capacity (T-AOC) between the two groups ($P > 0.05$) (Figure 3C).

Concentrations of serum cytokines, immunoglobulins, diamine oxidase, and defensive proteins in rectal contents

At 30 days of age, the serum IL-6 level in the IP group was significantly higher than that in the CON group ($P < 0.001$), while the serum DAO content was significantly lower ($P = 0.023$)

(Figures 4A, C). There were no differences in serum levels of IL-1β, TNF-α, IgG, and IgM between the two groups (Figures 4A, B), but in the rectal contents, the levels of defensin ($P = 0.047$) and sIgA ($P = 0.043$) were significantly higher than that in the CON group.

Rectal bacterial communities

As shown in Figure 5A, there was no significant difference in the richness ($P = 0.13$) and diversity ($P = 0.25$). However, as presented in Figure 5B, the IP group was separated from the CON group ($P < 0.01$), and the individuals of the IP group clustered together, while those of the CON group scattered.

The relative abundance and composition of the top 10 abundance at the phylum level are shown in Figure 5C. The rectal bacterial community in calves was dominated by *Firmicutes* and *Bacteroidota*, followed by *Actinobacteriota*. At the genus level, *Faecalibacterium* was the main genera, followed by *Collinsella*, *Bacteroides*, *Clostridium*, *Alloprevotella*, *Blautia*, *Bifidobacterium*, *Escherichia-Shigella*, *UCG-005*, and *Parabacteroides*. As shown in Figure 5D, it was found that *Bifidobacterium*, *megamonas*, and *Erysipelatoclostridium* were significantly enriched in the IP group ($P < 0.05$), while *Alistipes*, *Pedobacter*, *Colidextribacter*, *Odoribacter*, *Intestinimonas*, *Fusobacterium*, and *UCG-005* in the CON group were significantly more abundant than those in the IP group ($P < 0.05$).

Functional prediction

The results in Figure 6 showed that at level 3 of the Kyoto Encyclopedia of Genes and Genomes (KEGG) pathway, bacterial functional characteristics were mainly enriched in immune pathways, such as signal transduction mechanisms, bacterial secretion system, replication, recombination, and repair proteins. The differences in metabolic pathways of functional genes in bacterial flora between the two groups showed that the two functional pathways of butyrate metabolism ($P < 0.05$) and tryptophan metabolism ($P < 0.01$) in the IP group were significantly weakened. At the same time, amino acid degradation pathways, including valine, leucine, and isoleucine degradation ($P < 0.05$), and lysine degradation ($P < 0.01$) in the IP group were less active.

Discussion

The suckling period is critical for calves. The immune system of animals at this period is undeveloped, therefore, animals are very susceptible to infection at this stage. Pathogenic infection often leads to diarrhea and BRD in calves despite the use of several vaccines and antibiotic alternatives (Vlasova and Saif, 2021). These two diseases are the most common ones in calves and are the leading causes of mortality (Abuelo et al., 2019). Moreover, severe diarrhea or pneumonia, even if well treated, may affect a calf's later growth performance and milk production in adulthood (Abuelo et al., 2019). Therefore, research on the effective prevention of intestinal or respiratory infections in calves is urgent for both dairy and beef cattle farming. In this study, we investigated the effect of twice intraperitoneal injection of yeast β-glucan during the first week of birth on the prevention of diarrhea and BRD of dairy calves and proved that the treatment decreased both the frequency of diarrhea and BRD during the first 74 days of age.

Yeast β-glucan is generally considered both a prebiotic and immune-modulator. Several studies have shown the positive effects of oral supplementation on calf health and growth performance as prebiotics (Ma et al., 2015; Xiao et al., 2016);. Based on the theory of trained immunity of fungal β-glucan (Kalafati et al., 2020), we hypothesized that intraperitoneal injection of it early in life might induce the innate immune system to produce immune memory and

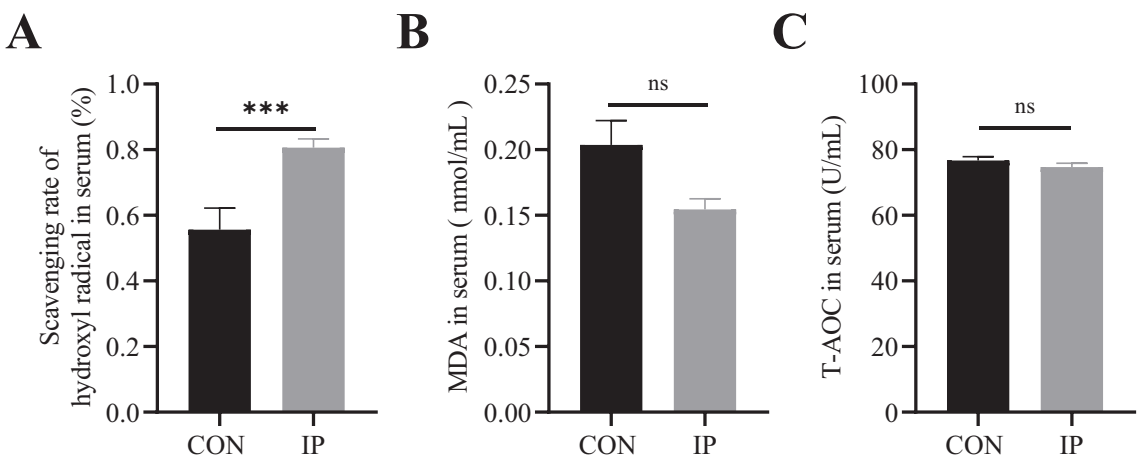

FIGURE 3
The effect of pre-stimulation with yeast β-glucans on oxidative stress level of calves. **(A-C)** The antioxidant status in the serum of calves. All data is shown as mean values ± standard error (SEM). Control group n = 12, IP group n = 15; Statistical significance was determined by the unpaired, two-tailed Student's t-test with a 95% confidence interval or One-way ANOVA analysis, ***$P < 0.001$. CON, control group, IP, intraperitoneal injection group. MDA, Malonaldehyde, T-AOC, total antioxidant capacity. ns, no significance.

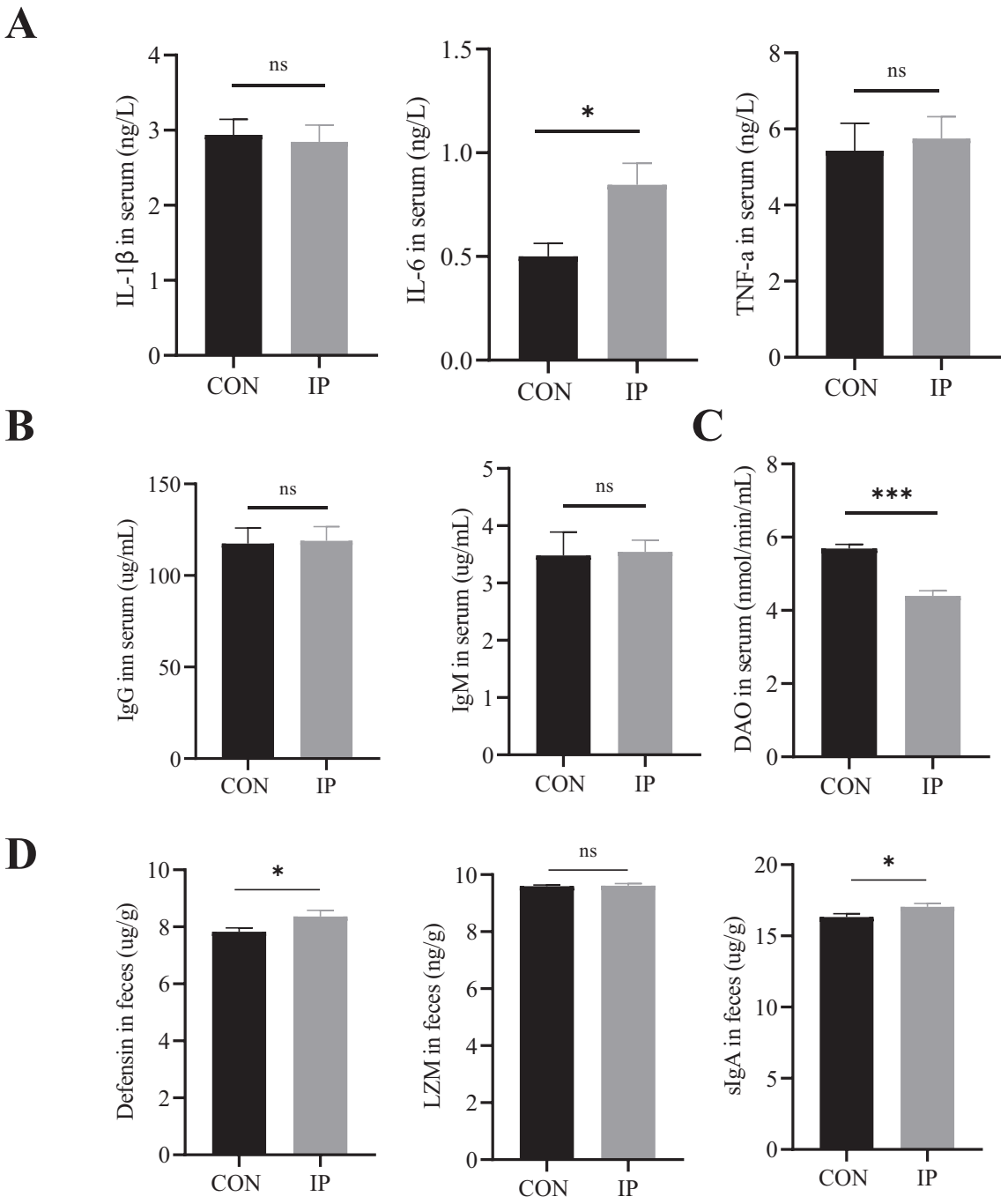

FIGURE 4
The effect of pre-stimulation with yeast β-glucans on the cytokines, immunoglobulins, DAO in serum, and intestinal antimicrobial substance Levels in rectal contents. **(A)** The concentrations of IL-1β, IL-6, and TNF-a in the serum were measured by ELISA to evaluate the degree of immune response. **(B)** The immunoglobulin levels and **(C)** DAO levels in the serum of calves were measured by ELISA to evaluate the degree of immune response and intestinal injury. **(D)** The Defensin, LZM, and sIgA levels in the rectal contents of calves were measured by ELISA to evaluate the degree of immune response. All data is shown as mean values ± standard error (SEM). Control group n = 12, IP group n = 15; Statistical significance was determined by the unpaired, two-tailed student's t-test with a 95% confidence interval or One-way ANOVA analysis, $^{*}P < 0.05$, $^{***}P < 0.001$. CON, control group, IP, intraperitoneal injection group. TNF-a, Tumor necrosis factor-a; IL, Interleukin; DAO, diamine oxidase; LZM, lysozyme; sIgA, the secreted immunoglobulin A. ns, no significance.

effectively prevent intestinal infections, thereby reducing the frequency of diarrhea and even BRD during the early life of calves. As expected, yeast beta-glucan pre-stimulation had a positive effect, significantly reducing the frequency of diarrhea between 31 and 60 days of age. From the detected intestinal damage marker, it can be inferred that pre-stimulation with yeast β-glucan showed a systemic prophylactic effect, which improved the intestinal health status of calves later.

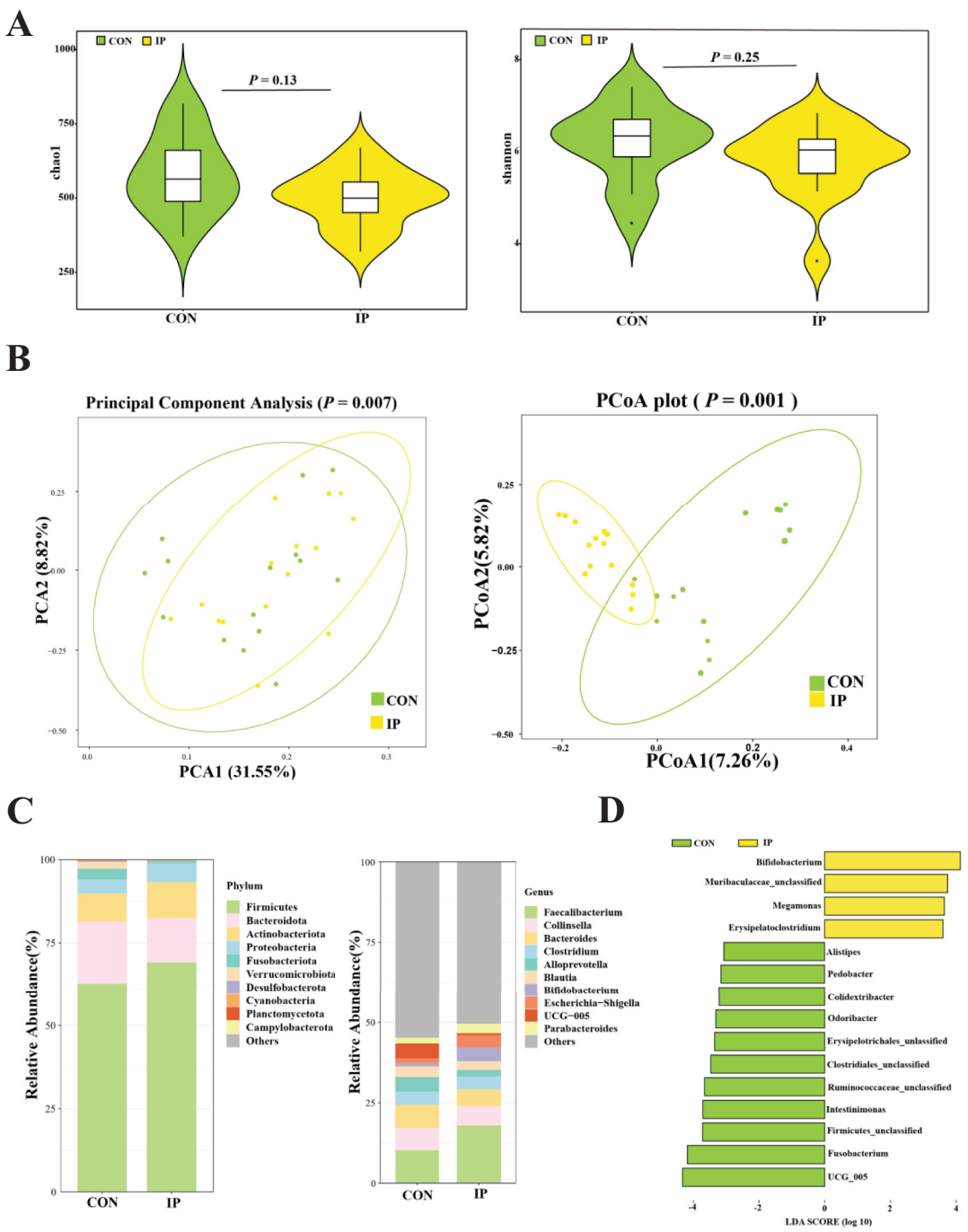

FIGURE 5
The effect of pre-stimulation with yeast β-glucans on the rectal bacterial community of calves. **(A)** Chao1 and Shannon index on the ASVs level. **(B)** Principal Component Analysis (PCA) and Principal coordinate analysis (PCoA) based on bray-curtis. **(C)** Microbial composition at the phylum level and genus level. **(D)** Linear discriminant analysis effect size of fecal bacterial microbiota (LDA > 3, $P < 0.05$).

The systemic preventive mechanism might be complex but should include the immune memory acquired by the body's innate immune cells due to the pre-stimulation. Studies in experimental mice or rats have shown that pre-stimulation with special antigens enables bone marrow stem cells and progenitor cells to acquire immune memory for several months to a year (for the PROMISE- EBF Study Group et al., 2015), and the acquired memory can be passed on to differentiated bone marrow cells including innate immune cells in the blood and resident ones in tissues (Mitroulis et al., 2018; Wang et al., 2023), such as ILC3 in

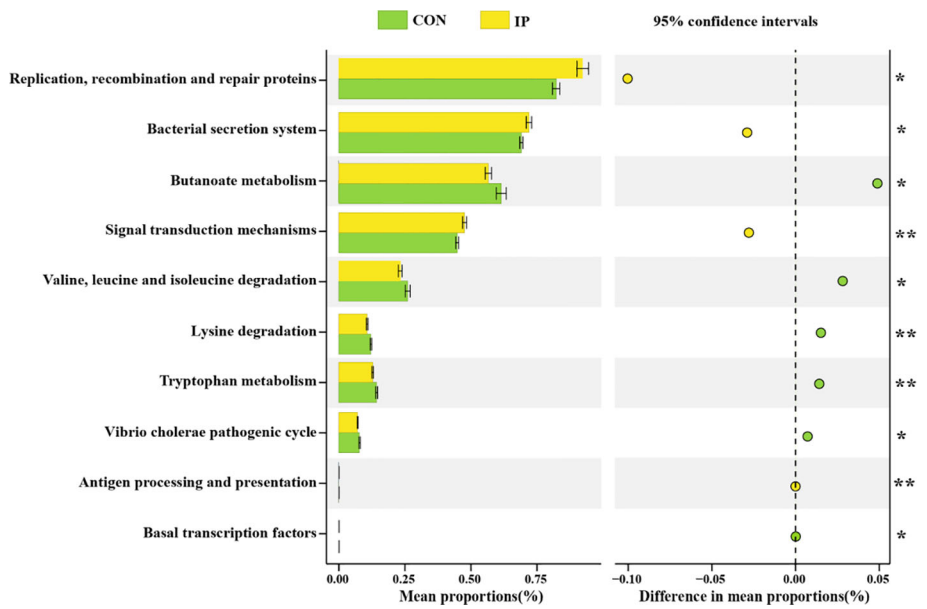

FIGURE 6
The functional prediction of rectal bacterial community of calves. Differential species T-test analysis of rectal bacterial community of calves at the phylum level. Statistical significance was determined by the unpaired, two-tailed student's t-test with a 95% confidence interval or One-way ANOVA analysis. *$P < 0.05$, **$P < 0.01$.

intestine (Serafini et al., 2022) and alveolar macrophages in lung (Jeyanathan et al., 2022), and thus improve the ability of various tissues to fight later infections. Guerra-Maupome et al (Guerra-Maupome et al., 2019) reported that *in vivo* stimulation with Bacille Calmette-Guerin induced a trained innate immune phenotype in calves, characterized by increased levels of several inflammatory factors upon re-stimulation. In the present study, the levels of serum IL-6 and rectal defensin secreted by intestinal epithelial cells in pre-stimulated calves were significantly higher than those in the CON group at 30 days of age, suggesting that pre-stimulation might induce related cells to acquire immune memory in calves.

The classical study of trained immunity consists of three stages, namely pre-stimulation, resting period, and re-stimulation (Netea et al., 2020). In feeding experiments, it is difficult to determine when infection occurs after pre-stimulation in each calf. However, in our experiment, all of the investigated calves underwent a series of stresses before and after 30 days of age, including milk replacement, abrupt drop in temperature, and taking off the waistcoat. The frequency of diarrhea and BRD in the CON group increased significantly two weeks after 30 days of age, indicating that this series of stresses worsened the intestinal and respiratory health of the calves. Stresses been proven to be associated with an increased risk of infection (Nabenishi and Yamazaki, 2017; Qiao et al., 2023), and thus the combined stress could be considered as the re-stimulation phase of the classical trained immunity studies. Elevated pro-inflammatory factors generally indicate an inflammatory response, but are also often a signal of a positively enhanced defense response of innate immune cells, as proven by trained immunity studies, where increased gene expression and release of cytokines, such as TNF-α, IL-1β, and IL-6 indicates a more effective defense response (Arts et al., 2018). In this study, the lower frequency of diarrhea and BRD and higher serum IL-6, defensin, and sIgA levels in the pre-stimulation group suggested that pre-stimulation increased the immune response of calves to above stresses, and thus improved their intestinal and respiratory health. Previous studies detected that *in vitro* training with yeast β-glucan enhanced the production of TNF-α and IL-6 in macrophages and monocytes upon secondary stimulation (Angulo et al., 2020; Paris et al., 2020). Similarly, an *in vivo* study showed up-regulation of gene transcription and higher production levels of TNF-a and IL-6 in mice trained with β-glucan upon an ex vivo challenge with *E. coli* (Geervliet et al., 2020). Although the fact that the expression of TNF-α at 30 days of life was unaffected by our treatment seemed to make it complicated to explain, there is evidence that the inflammatory factors that are elevated in response to later re-stimulation vary from one trained immune study to another, due to different stimulants, different cell types, different hosts, or different re-challenge studied (Mitroulis et al., 2018; Jeyanathan et al., 2022).

Pieces of evidence proved that oral administration of yeast β-glucan daily results in an improved gut microbial balance. For instance, Zhou et al. (Horneck Johnston et al., 2024) observed the counts of pathogenic *E. coli* decreased and the counts of commensal Lactobacillus increased in yeast β-glucan supplemented calves compared with controls, and Virginio Junior et al (Virginio Junior et al., 2021) reported that the administration of β-glucan daily increased the abundance of *Alloprevotella*, a genus associated with improved intestinal barriers and tighter epithelial junctions in the lower gut. Our study also showed that pre-stimulation with yeast β-glucan optimized the bacterial structure in the rectal content

of calves, including enhancing the abundance of some beneficial bacteria and stabilizing the bacterial community, as the intestinal bacterial structure tended to be consistent among individual calves in the pre-stimulated group. However, the addition of yeast β-glucan as an immune stimulant and prebiotics has different mechanisms of influence on the intestinal microflora. The former affects the intestinal microflora mainly by regulating the immune response of the intestine and even the body (Novak and Vetvicka, 2008; Quintin et al., 2012), while the latter's main function is to promote the proliferation of beneficial bacteria as a fermentation substrate, although some studies have reported that it is also involved in regulating the intestinal mucosal immunity (Samuelsen et al., 2014; So et al., 2021). Despite the improved intestinal health status, the present study found that ADG and feed efficiency of calves were not improved by the pre-stimulation with yeast β-glucan. However, positive effects of oral administration with β-glucan daily on ADG and feed efficiency were found (Abo Ghanima et al., 2020; Reis et al., 2022). We speculated that the reasons for the different effects of the two supply modes of beta-glucan on growth performance may involve the following aspects: firstly, as an immune stimulant, the total amount of β-glucan consumed during the present trial is far lower than the total amount as a daily supplement of prebiotics; Secondly, compared with the CON group, the obvious immune response of the pre-stimulated calves was induced during the stimulation period, and the immune level of the calves was also higher when they were affected by the combined stress at about 30 days of age. This meant that during both phases, the pre-stimulated calves might expend more energy for the immune response, but the daily feed intake does not increase, and this probably resulted in no increase in daily gain despite the improved health of the pre-stimulated calf. Nevertheless, it is necessary to compare the effects of two yeast β-glucan supply modes on the prevention of diarrhea and BRD in calves in the same feeding trial, as well as subsequent effects on calves, including their adult performance.

Pre-stimulation through intraperitoneal injection will induce inflammatory response. As we observed, the level of the three detected inflammatory factors in serum increased 24 h after the stimulation with yeast β-glucan. From the theory of trained immunity and its research reports, the inflammatory response caused by pre-stimulation is a condition for the relevant cells to acquire trained immunity (Netea et al., 2020; Ochando et al., 2023). Studies in mice and rats showed that the induced inflammatory response is generally transitory and disappears within two or three days (Cheng et al., 2014; Horneck Johnston et al., 2024). It can be seen that the stimulation did not cause the increase of DAO in serum, and it was speculated that the inflammatory response induced by pre-stimulation did not cause damage to the intestinal tissue of calves in the present study. However, the sharply increased MDA level in serum indicated that the oxidative stress level of the body increased due to the stimulation. Of course, the level of serum oxidative stress in our pre-stimulated calves tended to be lower than that in control calves at 30 days of age, indicating better physical health of pre-stimulated calves later. Nevertheless, whether the transitory negative effects of pre-stimulation on calves are related to the absence of positive effects on growth performance, and whether reducing the injected dose of yeast beta-glucan can achieve the same defensive effect while eliminating oxidative stress in calves, remains to be explored.

In summary, the present study showed that intraperitoneal injection of yeast-derived β-glucan early in life effectively reduced the frequency of diarrhea and BRD from d 31 to 60, improved the intestinal health status of suckling Holstein dairy calves and suggested the involvement of trained immunity. However, more works are needed to investigate whether pre-stimulation with yeast β-glucan or other stimulants has long-term health benefits or future product performance of calves. In addition, the cytokine changes caused by training immunity may not only be manifested in IL-1β, IL-6, and TNF-a, but also may include IL-8, IL-10, and IFN, etc. The selection of markers for training immunity needs further optimization. Furthermore, the better supplementation method, time, and dosage of stimulants, etc. all need further studies.

Data availability statement

\The datasets presented in this study can be found in online repositories. The names of the repository/repositories and accession number(s) can be found below: https://www.ncbi.nlm.nih.gov/, PRJNA1155013.

Ethics statement

The animal studies were approved by This study was performed in strict accordance with the recommended guidelines from the Administration of Affairs Concerning Experimental Animals (Ministry of Science and Technology, China, revised 2004). The protocol was approved by the Institutional Animal Care and Use Committee of the Northwest A&F University. The studies were conducted in accordance with the local legislation and institutional requirements. Written informed consent was obtained from the owners for the participation of their animals in this study.

Author contributions

FY: Data curation, Software, Writing – original draft, Writing – review & editing. ZZ: Resources, Supervision, Writing – review & editing. XZ: Data curation, Methodology, Formal Analysis, Investigation, Software, Writing – review & editing. WY: Data curation, Investigation, Methodology, Validation, Writing – review & editing. JY: Conceptualization, Funding acquisition, Investigation, Project administration, Supervision, Writing – review & editing. XX: Conceptualization, Data curation, Funding acquisition, Project administration, Resources, Supervision, Writing – review & editing.

Funding

The author(s) declare that financial support was received for the research and/or publication of this article. This study was substantially supported by the Chinese Universities Scientific Fund (award number: 2452022252).

Acknowledgments

We sincerely acknowledge Jiamin Wang for her invaluable assistance in experimental sampling.

Conflict of interest

Author ZZ was employed by Junlebao Dairy Co. Ltd.

The remaining authors declare that the research was conducted in the absence of any commercial or financial relationships that could be construed as a potential conflict of interest.

Generative AI statement

The author(s) declare that no Generative AI was used in the creation of this manuscript.

Publisher's note

All claims expressed in this article are solely those of the authors and do not necessarily represent those of their affiliated organizations, or those of the publisher, the editors and the reviewers. Any product that may be evaluated in this article, or claim that may be made by its manufacturer, is not guaranteed or endorsed by the publisher.

References

Abo Ghanima, M. M., Abd El-Aziz, A. H., Noreldin, A. E., Atta, M. S., Mousa, S. A., and El-Far, A. H. (2020). β-glucan administration improves growth performance and gut health in New Zealand White and APRI rabbits with different breed responses. *PloS One* 15, e0234076. doi: 10.1371/journal.pone.0234076

Abuelo, A., Havrlant, P., Wood, N., and Hernandez-Jover, M. (2019). An investigation of dairy calf management practices, colostrum quality, failure of transfer of passive immunity, and occurrence of enteropathogens among Australian dairy farms. *J. Dairy Sci.* 102, 8352–8366. doi: 10.3168/jds.2019-16578

Angulo, M., and Angulo, C. (2023). Immunometabolic changes of β-glucan-trained immunity induction and inhibition on neonatal calf immune innate cells. *Mol. Immunol.* 159, 58–68. doi: 10.1016/j.molimm.2023.05.008

Angulo, M., Reyes-Becerril, M., Cepeda-Palacios, R., and Angulo, C. (2020). Oral administration of Debaryomyces hansenii CBS8339-β-glucan induces trained immunity in newborn goats. *Dev. Comp. Immunol.* 105, 103597. doi: 10.1016/j.dci.2019.103597

Arts, R. J. W., Moorlag, SJCFM, Novakovic, B., Li, Y., Wang, S.-Y., Oosting, M., et al. (2018). BCG Vaccination Protects against Experimental Viral Infection in Humans through the Induction of Cytokines Associated with Trained Immunity. *Cell Host Microbe* 23, 89–100.e5. doi: 10.1016/j.chom.2017.12.010

Brandi, P., Conejero, L., Cueto, F. J., Martínez-Cano, S., Dunphy, G., Gómez, M. J., et al. (2022). Trained immunity induction by the inactivated mucosal vaccine MV130 protects against experimental viral respiratory infections. *Cell Rep.* 38, 110184. doi: 10.1016/j.celrep.2021.110184

Briard, B., Fontaine, T., Kanneganti, T.-D., Gow, N. A. R., and Papon, N. (2021). Fungal cell wall components modulate our immune system. *Cell Surface* 7, 100067. doi: 10.1016/j.tcsw.2021.100067

Cheng, S.-C., Quintin, J., Cramer, R. A., Shepardson, K. M., Saeed, S., Kumar, V., et al. (2014). mTOR- and HIF-1α–mediated aerobic glycolysis as metabolic basis for trained immunity. *Science* 345, 1250684. doi: 10.1126/science.1250684

Ding, B., Zheng, J., Wang, X., Zhang, L., Sun, D., Xing, Q., et al. (2019). Effects of dietary yeast beta-1,3-1,6-glucan on growth performance, intestinal morphology and chosen immunity parameters changes in Haidong chicks. *Asian-Australas J. Anim. Sci.* 32, 1558–1564. doi: 10.5713/ajas.18.0962

for the PROMISE- EBF Study Group, Nankabirwa, V., Tumwine, J. K., Mugaba, P. M., Tylleskär, T., and Sommerfelt, H. (2015). Child survival and BCG vaccination: a community based prospective cohort study in Uganda. *BMC Public Health* 15, 175. doi: 10.1186/s12889-015-1497-8

Geervliet, M., Lute, L. C. P., Jansen, C. A., Rutten, V. P. M. G., Savelkoul, H. F. J., and Tijhaar, E. (2020). Differential immunomodulation of porcine bone marrow derived dendritic cells by E. coli Nissle 1917 and β-glucans. *PloS One* 15, e0233773. doi: 10.1371/journal.pone.0233773

Goh, T. W., Kim, H. J., Moon, K., Kim, C. S., and Kim, Y. Y. (2023). Effects of β-glucan with vitamin E supplementation on the growth performance, blood profiles, immune response, fecal microbiota, fecal score, and nutrient digestibility in weaning pigs. *Anim. Biosci.* 36, 642–653. doi: 10.5713/ab.22.0311

Guerra-Maupome, M., Vang, D. X., and McGill, J. L. (2019). Aerosol vaccination with Bacille Calmette-Guerin induces a trained innate immune phenotype in calves. *PloS One* 14, e0212751. doi: 10.1371/journal.pone.0212751

Han, B., Baruah, K., Nguyen, D. V., Williams, D. L., Devriendt, B., Cox, E., et al. (2020). Beta-glucan's varying structure characteristics modulate survival and immune-related genes expression from Vibrio harveyi-infected Artemia franciscana in gnotobiotic conditions. *Fish. Shellfish Immunol.* 102, 307–315. doi: 10.1016/j.fsi.2020.04.062

Horneck Johnston, C. J. H., Ledwith, A. E., Lundahl, M. L. E., Charles-Messance, H., Hackett, E. E., O'Shaughnessy, S. D., et al. (2024). Recognition of yeast β-glucan particles triggers immunometabolic signaling required for trained immunity. *iScience* 27, 109030. doi: 10.1016/j.isci.2024.109030

Ifrim, D. C., Quintin, J., Joosten, L. A. B., Jacobs, C., Jansen, T., Jacobs, L., et al. (2014). Trained immunity or tolerance: opposing functional programs induced in human monocytes after engagement of various pattern recognition receptors. *Clin. Vaccine Immunol.* 21, 534–545. doi: 10.1128/CVI.00688-13

Jeyanathan, M., Vaseghi-Shanjani, M., Afkhami, S., Grondin, J. A., Kang, A., D'Agostino, M. R., et al. (2022). Parenteral BCG vaccine induces lung-resident memory macrophages and trained immunity via the gut–lung axis. *Nat. Immunol.* 23, 1687–1702. doi: 10.1038/s41590-022-01354-4

Juste, R. A., Ferreras-Colino, E., de la Fuente, J., Domínguez, M., Risalde, M. A., Domínguez, L., et al. (2022). Heat inactivated mycobacteria, alpha-Gal and zebrafish: Insights gained from experiences with two promising trained immunity inductors and a validated animal model. *Immunology* 167, 139–153. doi: 10.1111/imm.13529

Kalafati, L., Kourtzelis, I., Schulte-Schrepping, J., Li, X., Hatzioannou, A., Grinenko, T., et al. (2020). Innate immune training of granulopoiesis promotes anti-tumor activity. *Cell* 183, 771–785.e12. doi: 10.1016/j.cell.2020.09.058

Kolenda, R., Burdukiewicz, M., and Schierack, P. (2015). A systematic review and meta-analysis of the epidemiology of pathogenic Escherichia coli of calves and the role of calves as reservoirs for human pathogenic E. coli. *Front. Cell Infect. Microbiol.* 5. doi: 10.3389/fcimb.2015.00023

Ma, T., Tu, Y., Zhang, N., Guo, J., Deng, K., Zhou, Y., et al. (2015). Effects of dietary yeast β-glucan on nutrient digestibility and serum profiles in pre-ruminant Holstein calves. *J. Integr. Agric.* 14, 749–757. doi: 10.1016/S2095-3119(14)60843-1

McGuirk, S. M., and Peek, S. F. (2014). Timely diagnosis of dairy calf respiratory disease using a standardized scoring system. *Anim. Health Res. Rev.* 15, 145–147. doi: 10.1017/S1466252314000267

Mitroulis, I., Ruppova, K., Wang, B., Chen, L.-S., Grzybek, M., Grinenko, T., et al. (2018). Modulation of myelopoiesis progenitors is an integral component of trained immunity. *Cell* 172, 147–161.e12. doi: 10.1016/j.cell.2017.11.034

Nabenishi, H., and Yamazaki, A. (2017). Effects of temperature–humidity index on health and growth performance in Japanese black calves. *Trop. Anim. Health Prod.* 49, 397–402. doi: 10.1007/s11250-016-1207-2

Netea, M. G., Domínguez-Andrés, J., Barreiro, L. B., Chavakis, T., Divangahi, M., Fuchs, E., et al. (2020). Defining trained immunity and its role in health and disease. *Nat. Rev. Immunol.* 20, 375–388. doi: 10.1038/s41577-020-0285-6

Netea, M. G., Joosten, L. A. B., Latz, E., Mills, K. H. G., Natoli, G., Stunnenberg, H. G., et al. (2016). Trained immunity: A program of innate immune memory in health and disease. *Science* 352, aaf1098. doi: 10.1126/science.aaf1098

Novak, M., and Vetvicka, V. (2008). β -glucans, history, and the present: immunomodulatory aspects and mechanisms of action. *J. Immunotoxicol.* 5, 47–57. doi: 10.1080/15476910802019045

Ochando, J., Mulder, W. J. M., Madsen, J. C., Netea, M. G., and Duivenvoorden, R. (2023). Trained immunity — basic concepts and contributions to immunopathology. *Nat. Rev. Nephrol.* 19, 23–37. doi: 10.1038/s41581-022-00633-5

Paris, S., Chapat, L., Pasin, M., Lambiel, M., Sharrock, T. E., Shukla, R., et al. (2020). β-glucan-induced trained immunity in dogs. *Front. Immunol.* 11. doi: 10.3389/fimmu.2020.566893

Pornanek, P., and Phoemchalard, C. (2021). Dietary supplementation of beta-glucan-rich molasses yeast powder on antibody response to swine fever virus and hematology of starter–grower pigs. *Trop. Anim. Health Prod.* 53, 43. doi: 10.1007/s11250-020-02431-2

Qiao, B., Li, X., Peng, M., Hui, H., and Tan, Z. (2023). Alteration of intestinal mucosal microbiota in mice with Chinese dampness-heat syndrom diarrhea by improper diet combined with high temperature and humidity environments. *Front. Cell Infect. Microbiol.* 12. doi: 10.3389/fcimb.2022.1096202

Quintin, J., Saeed, S., Martens, J. H. A., Giamarellos-Bourboulis, E. J., Ifrim, D. C., Logie, C., et al. (2012). Candida albicans Infection Affords Protection against Reinfection via Functional Reprogramming of Monocytes. *Cell Host Microbe* 12, 223–232. doi: 10.1016/j.chom.2012.06.006

Reis, M. E., De Toledo, A. F., Da Silva, A. P., Poczynek, M., Cantor, M. C., Virgínio Júnior, G. F., et al. (2022). Effect of supplementation with algae β-glucans on performance, health, and blood metabolites of Holstein dairy calves. *J. Dairy Sci.* 105, 7998–8007. doi: 10.3168/jds.2022-21838

Renaud, D. L., Buss, L., Wilms, J. N., and Steele, M. A. (2020). Technical note: Is fecal consistency scoring an accurate measure of fecal dry matter in dairy calves? *J. Dairy Sci.* 103, 10709–10714. doi: 10.3168/jds.2020-18907

Saeed, S., Quintin, J., Kerstens, H. H. D., Rao, N. A., Aghajanirefah, A., Matarese, F., et al. (2014). Epigenetic programming of monocyte-to-macrophage differentiation and trained innate immunity. *Science* 345, 1251086. doi: 10.1126/science.1251086

Samuelsen, A. B. C., Schrezenmeir, J., and Knutsen, S. H. (2014). Effects of orally administered yeast-derived beta-glucans: A review. *Mol. Nutr. Food Res.* 58, 183–193. doi: 10.1002/mnfr.201300338

Schrum, J. E., Crabtree, J. N., Dobbs, K. R., Kiritsy, M. C., Reed, G. W., Gazzinelli, R. T., et al. (2018). Cutting edge: *plasmodium falciparum* induces trained innate immunity. *J. Immunol.* 200, 1243–1248. doi: 10.4049/jimmunol.1701010

Serafini, N., Jarade, A., Surace, L., Goncalves, P., Sismeiro, O., Varet, H., et al. (2022). Trained ILC3 responses promote intestinal defense. *Science* 375, 859–863. doi: 10.1126/science.aaz8777

So, S. Y., Wu, Q., Leung, K. S., Kundi, Z. M., Savidge, T. C., and El-Nezami, H. (2021). Yeast β-glucan reduces obesity-associated Bilophila abundance and modulates bile acid metabolism in healthy and high-fat diet mouse models. *Am. J. Physiol-Gastrointestinal Liver Physiol.* 321, G639–G655. doi: 10.1152/ajpgi.00226.2021

Urie, N. J., Lombard, J. E., Shivley, C. B., Kopral, C. A., Adams, A. E., Earleywine, T. J., et al. (2018). Preweaned heifer management on US dairy operations: Part V. Factors associated with morbidity and mortality in preweaned dairy heifer calves. *J. Dairy Sci.* 101, 9229–9244. doi: 10.3168/jds.2017-14019

Virginio Junior, G. F., Reis, M. E., Da Silva, A. P., De Toledo, A. F., Cezar, A. M., Mendes, L. W., et al. (2021). Does algae β-glucan affect the fecal bacteriome in dairy calves? *PloS One* 16, e0258069. doi: 10.1371/journal.pone.0258069

Vlasova, A. N., and Saif, L. J. (2021). Bovine immunology: implications for dairy cattle. *Front. Immunol.* 12. doi: 10.3389/fimmu.2021.643206

Vuscan, P., Kischkel, B., Hatzioannou, A., Markaki, E., Sarlea, A., Tintoré, M., et al. (2024). Potent induction of trained immunity by Saccharomyces cerevisiae β-glucans. *Front. Immunol.* 15. doi: 10.3389/fimmu.2024.1323333

Wang, T., Zhang, J., Wang, Y., Li, Y., Wang, L., Yu, Y., et al. (2023). Influenza-trained mucosal-resident alveolar macrophages confer long-term antitumor immunity in the lungs. *Nat. Immunol.* 24, 423–438. doi: 10.1038/s41590-023-01428-x

Windeyer, M. C., Leslie, K. E., Godden, S. M., Hodgins, D. C., Lissemore, K. D., and LeBlanc, S. J. (2014). Factors associated with morbidity, mortality, and growth of dairy heifer calves up to 3 months of age. *Prev. Veterinary Med.* 113, 231–240. doi: 10.1016/j.prevetmed.2013.10.019

Xiao, J. X., Alugongo, G. M., Chung, R., Dong, S. Z., Li, S. L., Yoon, I., et al. (2016). Effects of Saccharomyces cerevisiae fermentation products on dairy calves: Ruminal fermentation, gastrointestinal morphology, and microbial community. *J. Dairy Sci.* 99, 5401–5412. doi: 10.3168/jds.2015-10563

Zou, T., Yang, J., Guo, X., He, Q., Wang, Z., and You, J. (2021). Dietary seaweed-derived polysaccharides improve growth performance of weaned pigs through maintaining intestinal barrier function and modulating gut microbial populations. *J. Anim. Sci. Biotechnol.* 12, 28. doi: 10.1186/s40104-021-00552-8

frontiers | Frontiers in Cellular and Infection Microbiology

TYPE Original Research
PUBLISHED 03 June 2025
DOI 10.3389/fcimb.2025.1555307

OPEN ACCESS

EDITED BY
José Luis Muñoz-Carrillo,
University of Guadalajara, Mexico

REVIEWED BY
Georgia Damoraki,
National and Kapodistrian University of Athens, Greece
Aikaterini Pistiki,
Leibniz Institute of Photonic Technology (IPHT), Germany

*CORRESPONDENCE
Pingsen Zhao
zhaopingsen01@163.com;
zhaopingsen@hotmail.com

†These authors have contributed equally to this work

RECEIVED 04 January 2025
ACCEPTED 11 April 2025
PUBLISHED 03 June 2025

CITATION
Chen J, Liu Z, Zhou F, Sun Y, Jiang Z and Zhao P (2025) Assessment of S100A8/A9 and resistin as predictive biomarkers for mortality in critically ill patients with sepsis. *Front. Cell. Infect. Microbiol.* 15:1555307. doi: 10.3389/fcimb.2025.1555307

Assessment of S100A8/A9 and resistin as predictive biomarkers for mortality in critically ill patients with sepsis

Jing Chen[1,2,3,4,5,6†], Zhengquan Liu[1,2,3,4,5,6†], Fan Zhou[1,2,3,4,5,6], Ye Sun[7], Zhenyou Jiang[8] and Pingsen Zhao[1,2,3,4,5,6*]

[1]Department of Laboratory Medicine, Yuebei People's Hospital Affiliated to Shantou University Medical College, Shaoguan, China, [2]Laboratory for Diagnosis of Clinical Microbiology and Infection, Yuebei People's Hospital Affiliated to Shantou University Medical College, Shaoguan, China, [3]Research Center for Interdisciplinary & High-quality Innovative Development in Laboratory Medicine, Shaoguan, China, [4]Shaoguan Municipal Quality Control Center for Laboratory Medicine, Yuebei People's Hospital Affiliated to Shantou University Medical College, Shaoguan, China, [5]Shaoguan Municipal Quality Control Center for Surveillance of Bacterial Resistance, Yuebei People's Hospital Affiliated to Shantou University Medical College, Shaoguan, China, [6]Shaoguan Engineering Research Center for Research and Development of Molecular and Cellular Technology in Rapid Diagnosis of Infectious Diseases and Cancer, Yuebei People's Hospital Affiliated to Shantou University Medical College, Shaoguan, China, [7]Intensive Care Medicine Department, Yuebei People's Hospital Affiliated to Shantou University Medical College, Shaoguan, China, [8]Key Laboratory of Viral Pathogenesis & Infection Prevention and Control (Jinan University), Ministry of Education, Guangzhou, China

Introduction: Sepsis is associated with high mortality. Early intervention is crucial to reducing sepsis-related mortality. This study aims to assess the clinical potential of S100A8/A9 and resistin as novel biomarkers for predicting mortality risk in sepsis patients.

Method: Serum samples were collected and analyzed from 141 adult sepsis patients (discovery cohort), 43 non-sepsis intensive care units (ICU) patients, 15 healthy volunteers, and 55 sepsis patients along with 17 non-sepsis ICU patients (validation cohort). The 28-day mortality and sequential organ failure assessment (SOFA) scores of the participants were compared. Additionally, the predictive ability of S100A8/A9 and resistin for sepsis mortality was evaluated using the area under the receiver operating characteristic curve at ICU admission.

Results: The concentrations of S100A8/A9 and resistin in sepsis patients were noticeably increased relative to non-sepsis patients and healthy controls. Serum S100A8/A9 concentrations in surviving sepsis patients were significantly higher than in non-surviving patients. On the day of admission, serum resistin concentrations in Gram-negative (G-) sepsis patients were considerably elevated relative to Gram-positive (G+) infected sepsis patients. Among sepsis patients admitted to the ICU, the AUC for S100A8/A9 in predicting 28-day mortality was 0.617 (P = 0.032; 95% confidence bounds 0.513–0.721), and for SOFA was 0.750 (P < 0.0001; 95% confidence bounds 0.660–0.840). Sepsis patients with high serum S100A8/A9 concentrations (≥ 377.53 ng/mL) had a higher survival rate relative to those with low concentrations (<377.53 ng/mL). In the validation cohort, the AUC for S100A8/A9 and 28-day mortality was 0.708 (P = 0.032; 95% confidence bounds 0.563–0.854), and for SOFA was 0.698 (P = 0.025; 95% confidence bounds 0.550–0.845). Additionally, sepsis patients with

high serum S100A8/A9 concentrations (≥ 377.53 ng/mL) also had a higher survival rate relative to those with lower concentrations (< 377.53 ng/mL). Furthermore, serum resistin levels in patients with a normal phenotype and mixed phenotype with hyperinflammation were predictive of mortality, with an AUC of 0.810 (P = 0.034; 95% confidence bounds 0.605–1.00) and 0.708 (P = 0.015; 95% confidence bounds 0.571–0.846). In patients with a normal sepsis phenotype, those with high serum resistin levels (≥ 63.695 ng/mL) had a lower survival rate compared to those with low resistin levels (< 63.695 ng/mL). In contrast, in patients with a mixed phenotype with hyperinflammation, those with high serum resistin levels (≥ 107.64 ng/mL) had a higher survival rate compared to those with lower resistin levels (< 107.64 ng/mL).

Discussion: Sepsis, the leading cause of death in intensive care unit patients. Identifying reliable biomarkers is essential for improving both the diagnosis and treatment of sepsis. We found that serum S100A8/A9 concentration at ICU admission is a significant predictor of 28-day mortality risk in sepsis patients. Additionally, resistin levels at ICU admission play an important role in predicting 28-day mortality risk in patients with both normal and mixed phenotypes with hyperinflammation. These findings suggest that S100A8/A9 and resistin could serve as effective biomarkers. Moreover, these findings could guide early clinical decisions in the treatment of sepsis patients.

KEYWORDS

28-day mortality, biomarkers, immunophenotype, resistin, S100A8/A9, sepsis

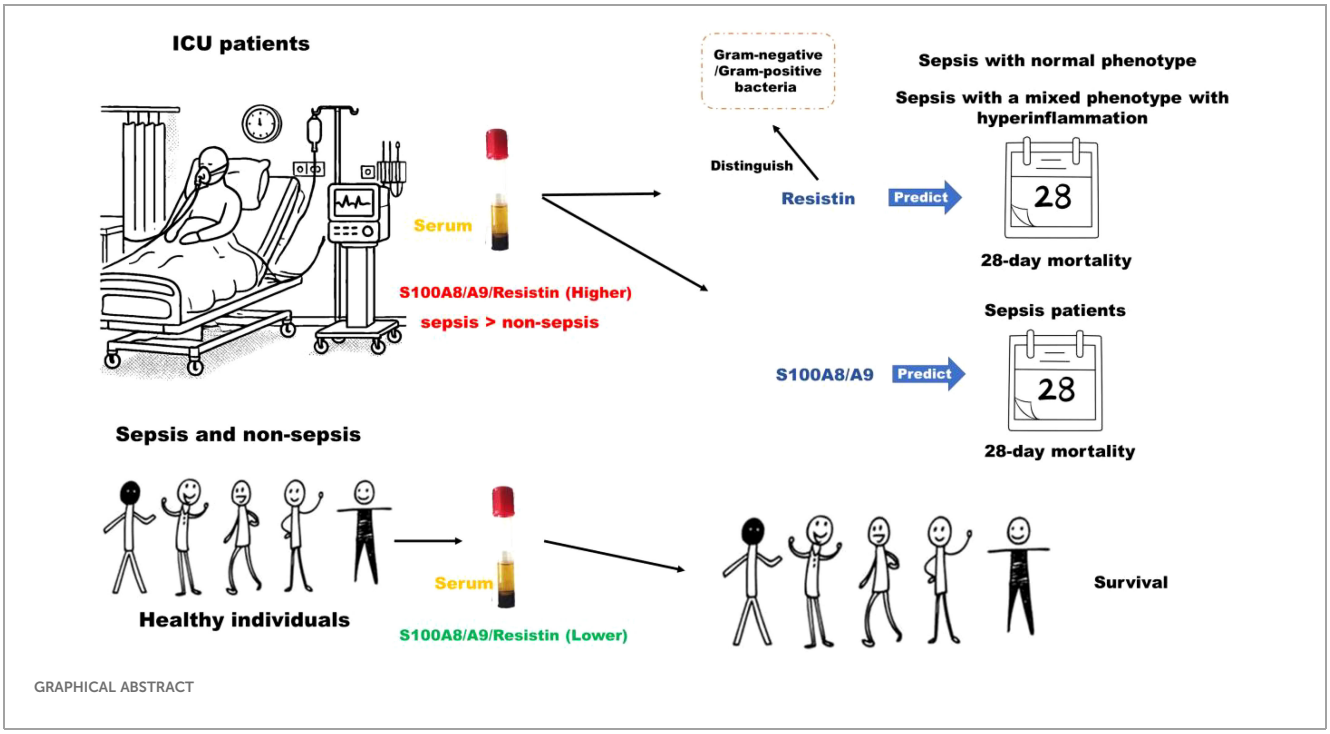

GRAPHICAL ABSTRACT

Introduction

Sepsis is a life-threatening syndrome of organ dysfunction caused by a homeostatic failure in anti-pathogen defenses, with a mortality exceeding 25% (Seymour et al., 2016; Rhodes et al., 2017; Niederman et al., 2021). It poses a significant risk of death in intensive care units (ICUs) and has been recognized as a global health priority (Seymour et al., 2016; Rhodes et al., 2017; Niederman et al., 2021). Immune reaction indicators play critical roles in disease identification, timely recognition of multiorgan impairment, prognostic classification, clinical trajectory assessment, and therapeutic decision-making. Additionally, biomarkers can enhance clinical trials by identifying suitable patients and categorizing intervention risks (Hamilton et al., 2018; Barichello et al., 2022).

Researchers have been striving to identify more effective biomarkers for clinical sepsis patients, aiming to rapidly predict and assess sepsis prognosis and provide clearer treatment expectations to patients. The cytokine network plays a critical role in host defense, immune regulation, and the inflammatory response (Wu et al., 2021). Sepsis is a highly heterogeneous syndrome. This complexity has driven the emergence of endotype-driven approaches, which stratify septic patients through biomarker profiling, thereby facilitating tailored immunomodulatory interventions. Moreover, the simultaneous assessment of multiple biomarkers may address the limitations inherent in using a single biomarker for diagnosis or prognosis (Pierrakos et al., 2020).

Sepsis is characterized by cytokine-mediated excessive inflammation and a sustained decline in immune response. This process leads to the release of intracellular mediators known as damage-associated molecular patterns (DAMPs) (Lu et al., 2014; Wiersinga et al., 2014). Numerous DAMPs have been validated, some of which are currently used as inflammatory biomarkers (Lu et al., 2014; Wiersinga et al., 2014). Examples include proteins and cellular molecules associated with nucleic acids, such as heat shock proteins (HSPs), high mobility group protein 1 (HMGB-1), and members of the S100 family (Kataoka et al., 2014; Kigerl et al., 2014; Wiersinga et al., 2014). Recently, S100A8/A9 has emerged as a promising biomarker for sepsis, and it is a pathogenic molecule with both pro-inflammatory and immunosuppressive properties, primarily found in myeloid cells, including neutrophils and monocytes (Wang et al., 2023).

During sepsis, the S100A8/A9 complex activates the classical Toll-like receptor 4 (TLR4) signaling pathway in monocytes, inducing the expression of pro-inflammatory mediators related to NF-κB, and can be released as a DAMP (Odink et al., 1987; Lagasse and Weissman, 1992). Recent studies have also identified a distinct subpopulation of monocytes, referred to as low HLA-DR and high S100A monocytes. These cells are associated with the immunosuppressive state following sepsis. Inhibiting this subset of monocytes significantly improves sepsis-induced immunosuppression (Wang et al., 2023; Yao et al., 2023).

Resistin, another key pro-inflammatory cytokine (Bostrom et al., 2009; Johansson et al., 2009; Singbartl et al., 2016), plays a crucial role in metabolic inflammation and atherosclerosis, with human resistin expression increasing under inflammatory pathological conditions (Macdonald et al., 2014; Rachakonda et al., 2014; Macdonald et al., 2017). Moreover, growing evidence indicates that resistin serves as a key mediator in the immunosuppressive processes of sepsis (Koch et al., 2009; Vassiliadi et al., 2012; Macdonald et al., 2014; Miller et al., 2019).

Many potential biomarkers for sepsis have been proposed, but they have significant limitations in diagnosing the condition. Biomarkers such as C-reactive protein (CRP) and procalcitonin (PCT), which are the most widely used and studied, do not have the ability to predict mortality in sepsis patients (Pierrakos et al., 2020). Moreover, the Sepsis-3 consensus definition highlights that the role of biomarkers in diagnosing sepsis remains unclear (Singer et al., 2016). Additionally, growing evidence suggests that the morbidity and mortality associated with sepsis are increasingly linked to systemic immune dysfunction, including immunosuppression (Boomer et al., 2011; Hotchkiss et al., 2013). However, there are currently no effective markers to identify a patient's immune status or predict mortality in sepsis patients with excessive inflammation or immunosuppression. Given that immune dysfunction biomarkers in sepsis are often associated with immune paralysis, relying on a single biomarker is not a completely reliable approach for guiding immune stimulation therapies. Measuring multiple biomarkers simultaneously may help address the limitations posed by any single biomarker (Pierrakos et al., 2020).

Early intervention is crucial to reducing sepsis-related mortality. Predicting mortality, assessing disease severity, guiding antibiotic use, and evaluating immune status in sepsis patients can enable timely proactive treatment, optimize therapeutic strategies, and improve patient outcomes, thereby increasing survival rates. Studies have demonstrated that both S100A8/A9 and resistin promote inflammatory responses by activating the TLR4 pathway and play key roles in immune suppression. Therefore, in this study, S100 family members S100A8/A9 and resistin were selected as biological targets. Preclinical identification of sepsis is critical. To this end, serum samples were collected from sepsis patients, non-sepsis patients on the day of admission, and healthy individuals. Along with factors such as CRP, PCT, IL-6, and white blood cell (WBC), we compared and analyzed the potential of resistin and S100A8/A9 as biomarkers for diagnosing sepsis, predicting mortality, generating survival curves, identifying Gram-negative bacteria (G-) and Gram-positive bacteria (G+), and immune subtype identification. A validation cohort was also included for further confirmation, with the aim of identifying new and effective targets for early sepsis intervention.

Materials and methods

Study population and parameters

On the day of ICU admission at Guangdong Yuebei People's Hospital, 141 adult sepsis patients meeting the Sepsis-3 clinical criteria were enrolled in the discovery cohort (within 24h following ICU admission), whereas the validation cohort comprised 55 adult individuals with sepsis fulfilling identical inclusion criteria. After a

28-day follow-up period, patient survival during their ICU stay was recorded until discharge or death. In addition, 43 and 17 age-/gender-matched critically ill non-sepsis ICU patients were recruited as control groups for the discovery and validation cohorts, respectively. Including cases of burns, shock, road traffic injuries, consciousness disorders, falls, and major surgeries. Furthermore, healthy volunteers with 15 age/gender matching were also recruited from the physical examination center of Guangdong Yuebei People's Hospital to serve as a healthy control group. A detailed flowchart of the study population is provided in Supplementary Figures S1 and S2.

Inclusion criteria for patients with sepsis: (1) Patients must meet the Sepsis-3 diagnostic criteria, including confirmed or highly suspected infection, with a sequential organ failure assessment (SOFA) score ≥2 (Shankar-Hari et al., 2016; Singer et al., 2016); (2) Age ≥18 years; (3) Complete clinical records for all patients.

In addition to these diagnostic criteria, patients with septic shock must meet the following conditions: (1) Persistent hypotension requiring vasopressors to maintain a mean arterial pressure above 65 mmHg; or (2) Blood lactate levels exceeding 2 mmol/L in the absence of hypotension (6).

Exclusion criteria for sepsis patients: (1) patients re-admitted to the ICU; (2) Patients with severe liver or renal insufficiency, heart failure, cancer, acquired immunodeficiency syndrome (AIDS) or severe blood diseases; (3) Pregnant or postpartum patients.; (4) Patients with autoimmune diseases receiving immunosuppressant or glucocorticoid therapy; (5) Death within 24 hours of registration (6).

The experimental protocol was approved by the ethics committee of Guangdong Yuebei People's Hospital, Shantou University School of Medicine, China (No. YBEC-KY(2021)-110), and informed consent was obtained from all participants or their legal representatives in accordance with the Declaration of Helsinki.

Sample processing

Clinical parameters collected include WBC (BC-5800 automatic blood cell counter), PCT (Roche Cobas E801), CRP (Roche Cobas 8000), blood and bacterial cultures and other indicators. were measured on the day of enrollment, samples of blood were simultaneously collected, centrifuged at 350×g for 5 min within 30 min to isolate serum, aliquoted into 300 μL to minimize freeze-thaw degradation, and stored at -80°C (Sun S et al., 2021).

Samples underwent standardized preparation per the R&D Systems ELISA kit protocol prior to analytical procedures. Frozen specimens were gradually thawed at 4°C, followed by centrifugation to remove precipitates. Each analytical batch incorporated low, medium, and high concentration, and the calibration curve for ELISA demonstrated a coefficient of determination (R^2) ≥ 0.99. Additionaly, hemolyzed samples were excluded. S100A8/A9 (R&D Systems, DS8900), resistin (R&D Systems, DRSN00), IL-6 (R&D Systems, D6050), interleukin-1β (IL-1β) (R&D Systems, DLB50), TNF-α (R&D Systems, QK225), interleukin-10 (IL-10) (R&D Systems, D1000B), and soluble programmed death-ligand 1 (sPD-L1) (Abcam, ab277712).

Identification criteria for immune status of sepsis patients

To characterize inflammatory and immunosuppressive states in sepsis patients, we analyzed four pro-inflammatory cytokines (IL-6, IL-1β, TNF-α, and CRP) and two anti-inflammatory mediators (IL-10 and sPD-L1) (Zhou F et al., 2024). Biomarker reference thresholds were established using dual criteria: the 95th percentile of healthy volunteers and the 50th percentile (median) of septic patients in our cohort, with the higher value selected as the study-specific cut-off (Zhou F et al., 2024). Concentrations exceeding this threshold were defined as positive (+), while others as negative (-). Based on positivity counts, sepsis patients were categorized into five phenotypes: (1) Normal phenotype (negative for all cytokines), (2) Hyperinflammation only (≥ 1 pro-inflammatory positive, anti-inflammatory negative), (3) Immunosuppression only (pro-inflammatory negative, ≥ 1 anti-inflammatory positive), (4) Mixed phenotype with hyperinflammation (≥ 1 pro-inflammatory positive with single anti-inflammatory positivity), and (5) Mixed phenotype with Immunosuppression (≥ 1 pro-inflammatory positive with dual anti-inflammatory positivity) (Zhou F et al., 2024).

Data processing and statistical methods

Statistical analyses and graph generation were conducted using GraphPad Prism (GraphPad Software 6.02) and IBM SPSS Statistics 26.0 (IBM Corp). Non normally distributed variables are represented by median (interquartile range), and comparison of skewed data between groups is conducted using non parametric Mann Whitney U test or one-way analysis of variance (Wu et al., 2021).To evaluate the predictive efficacy of S100A8/A9 for 28-day mortality, we constructed receiver operating characteristic (ROC) curves based on S100A8/A9 and resistin levels at admission, and calculated the area under the curve (AUC) with 95% confidence intervals. The 28 day cumulative mortality rate was analyzed using Kaplan Meier method with the log-rank *post hoc* test (Wu et al., 2021).The optimal cut-off point was determined by the Youden index, with sensitivity (SE) and specificity (SP) weighted accordingly (Wu et al., 2021). Additionally, survival curves for S100A8/A9 and resistin over 28 days were also plotted. Student's t-test or the Mann-Whitney U test is used to compare normally distributed continuous variables, while chi-square test or Fisher's exact probability method is used for categorical variables. Comparing multiple sets of quantitative data, choose one-way ANOVA or Kruskal-Wallis test based on distribution characteristics (Wu et al., 2021; Lan Y et al., 2024; Zhou F et al., 2024). All tests were bilateral, with a significance threshold set at $P < 0.05$ (Wu et al., 2021; Lan Y et al., 2024; Zhou F et al., 2024).

Results

Clinical characteristics of patients

141 adult sepsis patients, 43 non-septic ICU patients, and 15 healthy control volunteers were included in the discovery cohort. The validation cohort comprised 55 adult sepsis patients, 17 non-septic ICU patients. The basic demographic and clinical characteristics of these subjects are summarized in Supplementary Table S1. On the day of admission, non-survivors exhibited significantly higher acute physiological scores and SOFA scores, as well as a greater extent of organ damage compared to survivors. Additionally, sepsis patients had markedly increased median levels of CRP, PCT, and IL-6 compared to healthy controls (Supplementary Figure S2A-C).

Serum levels of S100A8/A9 and resistin in sepsis patients

On the day of admission, elevated serum concentrations of S100A8/A9 were observed in patients with sepsis. Meanwhile, the S100A8/A9 levels in non-septic ICU patients were noticeably increased relative to healthy standard group (Figure 1A). The median S100A8/A9 concentration at admission was 368.5 ng/mL

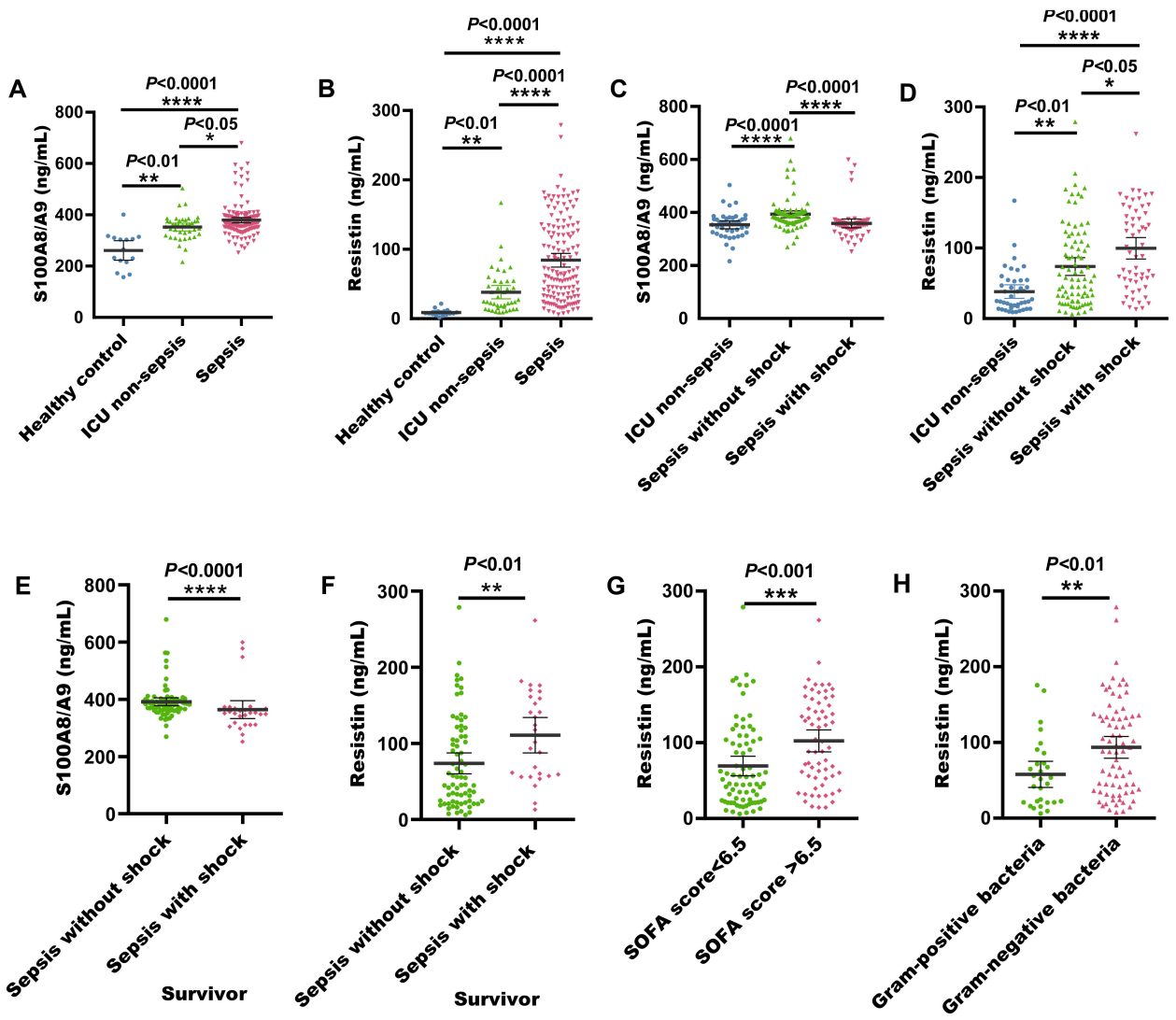

FIGURE 1
Serum S100A8/A9 and resistin levels at admission in the discovery cohort of adult sepsis patients. **(A)** S100A8/A9 concentrations in serum samples from healthy individuals, ICU non-sepsis patients, and sepsis patients. **(B)** Resistin concentrations in serum samples from healthy individuals, ICU non-sepsis patients, and sepsis patients. **(C)** S100A8/A9 concentrations in serum samples from patients with and without septic shock in the discovery cohort. **(D)** Resistin concentrations in serum samples from patients with and without septic shock in the discovery cohort. **(E)** S100A8/A9 concentrations in serum samples from sepsis with shock and sepsis without shock survivors. **(F)** Resistin concentrations in serum samples from sepsis with shock and sepsis without shock survivors. **(G)** Resistin concentrations in serum samples from sepsis patients with SOFA scores <6.5 and >6.5. **(H)** Resistin concentrations in serum samples from sepsis patients with G- and G+ bacterial infections. G+, Gram-positive; G-, Gram-negative; $^{*}P < 0.05$, $^{**}P < 0.01$, $^{***}P < 0.001$, $^{****}P < 0.0001$ (Kruskal-Wallis and Mann-Whitney U test).

(252.6-679.4 ng/mL) in sepsis patients, 356.8 ng/mL (216.1-503.9 ng/mL) in non-septic ICU patients, and 265.0 ng/mL (157.3-401.2 ng/mL) in healthy controls. Similarly, serum resistin concentrations were also substantially raised in sepsis patients in comparison with both non-septic ICU patients and healthy controls. And resistin concentrations in non-septic ICU patients were higher than healthy comparator group (Figure 1B). The median resistin concentration at admission was 66.93 ng/mL (6.15-278.9 ng/mL) in sepsis patients, 24.91 ng/mL (9.01-167.2 ng/mL) in non-septic ICU patients, and 7.63 ng/mL (1.93-21.68 ng/mL) in the healthy comparison group.

Among these 141 sepsis patients, serum S100A8/A9 concentrations were considerably elevated in those with non-shock sepsis (84 cases) relative to those with septic shock ($P < 0.0001$). In contrast, serum resistin concentrations were substantially reduced in non-shock sepsis patients ($P < 0.05$) (Figures 1C, D). Additionally, surviving patients with sepsis without shock demonstrated significantly elevated serum S100A8/A9 levels ($P < 0.0001$), whereas those with septic shock showed markedly increased resistin concentrations ($P < 0.001$) (Figures 1E, F). And nonsurvivors with sepsis without shock demonstrated significantly elevated serum S100A8/A9 levels ($P < 0.001$), whereas resistin levels remained comparable between septic shock and non-shock sepsis nonsurvivors ($P = 0.38$) (Supplementary Figures S2D, E). When stratified by a SOFA score threshold of 6.5, there was no difference in serum S100A8/A9 levels between patients with scores ≥ 6.5 and those with scores < 6.5 ($P = 0.35$) (Supplementary Figure S2F). However, patients with SOFA scores ≥ 6.5 had significantly elevated serum resistin concentrations ($P < 0.01$) (Figure 1G).

Among the 141 sepsis patients, 121 had confirmed bacterial infections, while 20 were diagnosed without bacterial infection. A total of 121 bacterial strains were isolated, including 29 G- bacteria, 75 G+ bacteria, 29 fungal strains, and 31 cases of mixed bacterial infections. The serum levels of S100A8/A9 and resistin were increased in sepsis patients upon admission. However, there was no noticeable difference in S100A8/A9 levels between patients with G- and G+ bacterial infections ($P > 0.5$) (Supplementary Figure S2G). In contrast, serum resistin levels were noticeably increased in patients with G- bacterial infections in comparison with those with gram-positive infections ($P < 0.01$) (Figure 1H).

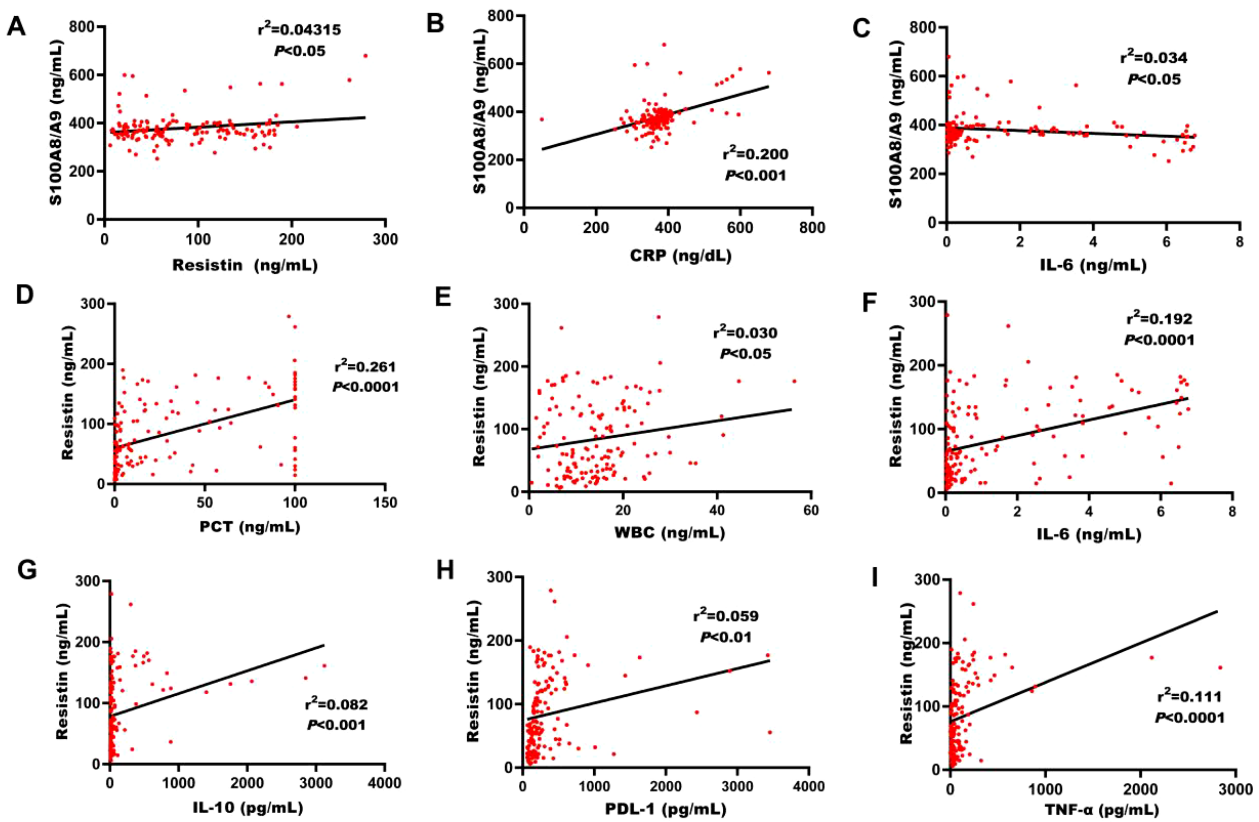

FIGURE 2
Correlation between S100A8/A9, resistin, and various biomarkers. **(A)** Correlation between S100A8/A9 levels and resistin in the discovery cohort of adult sepsis patients upon ICU admission. **(B)** Correlation of S100A8/A9 levels with CRP counts in the discovery cohort of adult patients with sepsis on ICU admission. **(C)** Correlation between S100A8/A9 levels and IL-6 in the discovery cohort. **(D)** Correlation between resistin levels and PCT in the discovery cohort. **(E)** Correlation between resistin levels and WBC in the discovery cohort. **(F)** Correlation between resistin levels and IL-6 in the discovery cohort. **(G)** Correlation between resistin levels and IL-10 in the discovery cohort. **(H)** Correlation between resistin levels and PDL-1 in the discovery cohort. **(I)** Correlation between resistin levels and TNF-α in the discovery cohort. CRP, C-reactive protein; IL-6, interleukin-6; IL-1β, interleukin-1β; TNF-α, tumor necrosis factor-alpha; IL-10, interleukin-10; PDL-1, programmed death-ligand-1. (Spearman's rank correlation coefficient).

Correlation of S100A8/A9 and resistin with other biomolecules

S100A8/A9 showed a significant correlation with resistin (r^2 = 0.043, $P < 0.05$, Figure 2A). Additionally, S100A8/A9 was markedly correlated with CRP and the immune molecule IL-6 ($P < 0.05$, Figures 2B, C). Resistin was noticeably correlated with PCT (r^2 = 0.261, $P < 0.0001$), WBC (r^2 = 0.030, $P < 0.05$), IL-6 (r^2 = 0.192, $P < 0.0001$), IL-10 (r^2 = 0.082, $P < 0.001$), PDL-1 (r^2 = 0.059, $P < 0.01$), and TNF-α (r^2 = 0.111, $P < 0.0001$, Figures 2D–I).

Prognostic value for 28-day survival in sepsis patients

Among the 141 sepsis patients, the 28-day mortality rate was 27.7% (39/141). To identify better predictors of 28-day mortality, various parameters measured at admission were analyzed. The area under the curve (AUC) for SOFA, S100A8/A9, resistin, PCT, CRP, IL-6, and WBC in predicting 28-day mortality were 0.751 (P = 0.000, 95% confidence bounds 0.668–0.853), 0.617 (P = 0.034, 95% confidence bounds 0.513–0.721), 0.521 (P = 0.585, 95% confidence bounds 0.418–0.625), 0.562 (P = 0.225, 95% confidence bounds 0.458–0.667), 0.542 (P = 0.441, 95% confidence bounds 0.438–0.646), 0.554 (P = 0.321, 95% confidence bounds 0.448–0.660), and 0.447 (P = 0.335, 95% confidence bounds 0.345–0.550), respectively (Figure 3A; Table 1). The cut-off value for S100A8/A9 predicting 28-day mortality was 377.53 ng/mL. Kaplan-Meier survival analysis showed a substantial difference ($P < 0.01$) in survival between patients with high (≥ 377.53 ng/mL) and low S100A8/A9 levels. Patients with higher serum S100A8/A9 levels had a better survival rate than those with lower levels (Figure 3B).

In the validation cohort of 55 sepsis patients, the 28-day mortality rate was 27.7% (15/40). For this cohort, the AUC values for predicting 28-day mortality were 0.698 (P = 0.025, 95% confidence bounds 0.550–0.845) for SOFA, 0.708 (P = 0.032, 95% confidence bounds 0.563–0.854) for S100A8/A9, 0.337 (P = 0.064, 95% confidence bounds 0.166–0.508) for resistin, 0.446 (P = 0.539, 95% confidence bounds 0.287–0.605) for PCT, 0.507 (P = 0.940, 95% confidence bounds 0.458–0.667) for CRP, 0.499 (P = 0.321, 95% confidence bounds 0.299–0.699) for IL-6, and 0.468 (P =0.992, 95% confidence bounds 0.245–0.571) for WBC (Figure 3C; Supplementary Table S3). Consistent with the discovery cohort, in the validation cohort, survival analysis also revealed statistically significant variation ($P < 0.0001$) between patients with high (≥ 377.53 ng/mL) and low S100A8/A9 concentrations. As in the initial cohort, patients with higher serum S100A8/A9 levels demonstrated better survival outcomes (Figure 3D). Additionally, in the discovery cohort, the cut-off value for SOFA scores predicting 28-day mortality was 6.5. Kaplan-Meier survival analysis showed a substantial difference ($P < 0.0001$) in survival between patients with high (≥6.5) and low SOFA scores. Patients with higher serum SOFA scores had a lower survival rate than those with lower levels, and a consistent trend was observed in the validation cohort (Figures 3E, F).

Serum expression levels of S100A8/A9 and resistin in sepsis patients across different immunotypes

A total of 196 sepsis patients were included in both the discovery and validation cohorts. Statistical analysis was performed on serum concentrations of CRP, IL-6, IL-1β, TNF-α, IL-10, and PDL1 from healthy individuals and sepsis patients, using a 95% CI. The highest values in each biomarker were selected as reference values. The reference values for CRP, IL-6, IL-1β, TNF-α, IL-10, and PDL1 were 19.51 ng/mL, 0.51 ng/mL, 27.75 pg/mL, 84.76 pg/mL, 22.11 pg/mL, and 288.55 pg/mL, respectively (Supplementary Table S4). Based on the classification criteria provided in Supplementary Table S5, patients were categorized into five groups: normal phenotype (26 cases), hyperinflammation only (39 cases), immunosuppression only (18 cases), mixed phenotype with hyperinflammation (58 cases), and mixed phenotype with immunosuppression (55 cases). A marked difference in S100A8/A9 expression levels was observed between patients with a normal phenotype and those with a mixed phenotype with hyperinflammation ($P < 0.05$), with the latter group exhibiting higher levels of S100A8/A9 (Figure 4A). In comparison with the normal phenotype, serum concentrations of resistin were significantly increased in patients with hyperinflammation only, immunosuppression only, mixed phenotype with hyperinflammation, and mixed phenotype with immunosuppression ($P < 0.01$) (Figure 4B). Among these groups, patients with a mixed phenotype with immunosuppression had the highest resistin levels, which were substantially higher than those in patients with a mixed phenotype with hyperinflammation (Figure 4B). Furthermore, serum resistin levels in patients with a normal phenotype and those with a mixed phenotype with hyperinflammation were predictive of mortality in this cohort (Figures 4C, D), with AUC of 0.810 (P = 0.034, 95% confidence bounds 0.605-1.00) and 0.708 (P = 0.015, 95% confidence bounds 0.571-0.846), respectively (Supplementary Tables S6, S7).

For sepsis patients with a normal phenotype, the resistin cut-off for predicting 28-day mortality was 63.695 ng/ml. Survival curve analysis revealed that patients with high resistin concentrations (≥ 63.695 ng/mL) had considerably decreased survival rates relative to those with lower resistin levels ($P < 0.01$). Conversely, in patients with a mixed phenotype with hyperinflammation, a higher resistin cut-off of 107.64 ng/ml was associated with improved survival ($P < 0.01$) (Figures 4E, F).

Validation of cohort verification results

In the validation cohort, S100A8/A9 concentrations were substantially raised in sepsis patients in comparison with healthy individuals and non-sepsis patients ($P < 0.05$, Figure 5A). And it is highly expressed in surviving sepsis patients ($P < 0.05$, Figure 5B). Additionally, resistin levels were markedly increased in sepsis

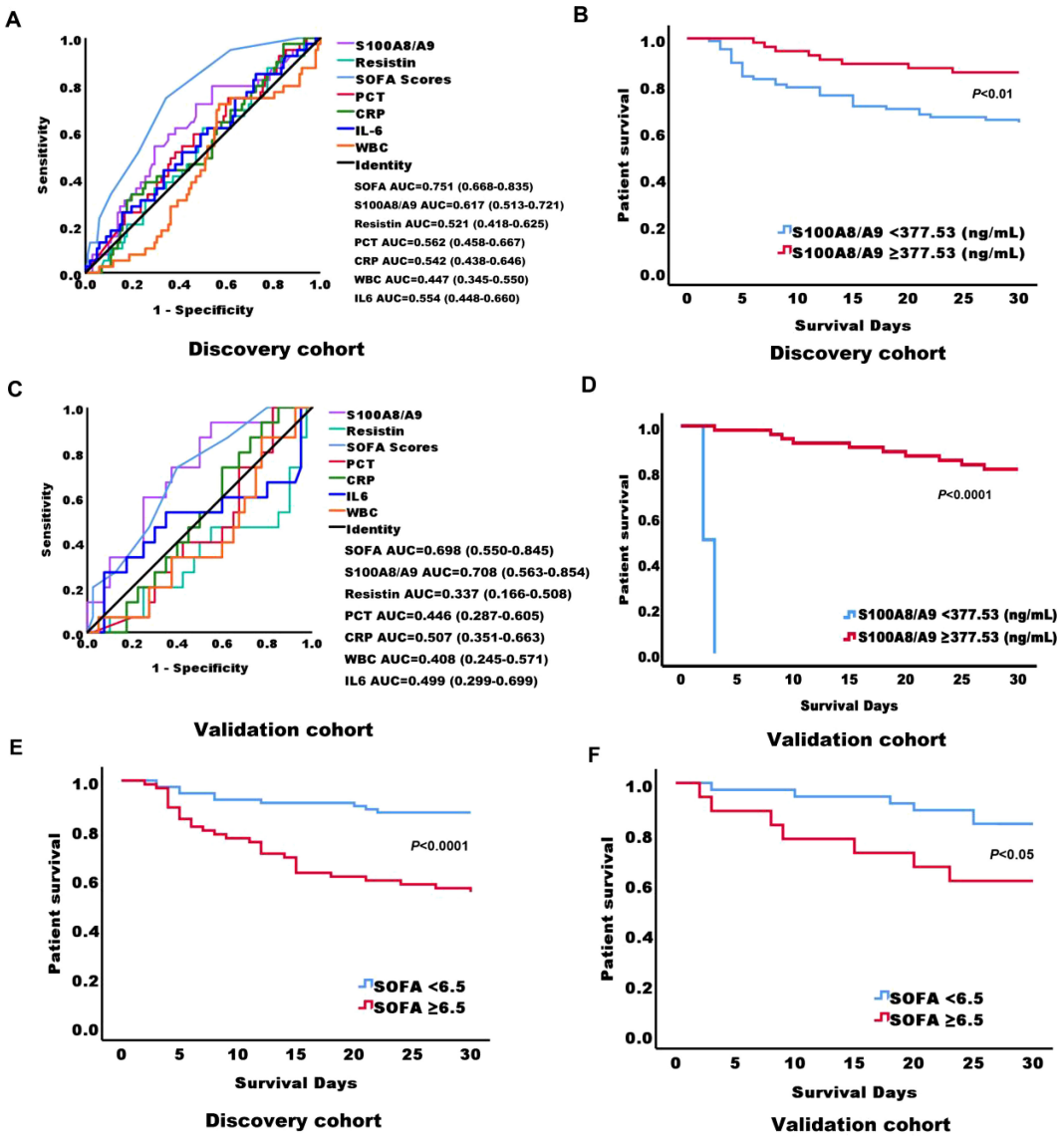

FIGURE 3
Receiver Operating Characteristic (ROC) curves and Kaplan-Meier survival curves for predicting 28-day mortality in adult sepsis patients based on serum biomarkers at admission. **(A)** ROC curves of serum biomarkers at admission in the discovery cohort of adult sepsis patients, predicting 28-day mortality. **(B)** Kaplan-Meier survival curves for 141 adult sepsis patients in the discovery cohort, stratified by S100A8/A9 levels using a cutoff of 377.53 ng/mL at ICU admission. **(C)** ROC curves of serum biomarkers at admission in the validation cohort of adult sepsis patients, predicting 28-day mortality. **(D)** Kaplan-Meier survival curves for 55 adult sepsis patients in the validation cohort, stratified by S100A8/A9 levels using a cutoff of 377.53 ng/mL at ICU admission. **(E)** Kaplan-Meier survival curves for 141 adult sepsis patients in the discovery cohort, stratified by SOFA scores using a cutoff of 6.5 at ICU admission. **(F)** Kaplan-Meier survival curves for 55 adult sepsis patients in the validation cohort, stratified by SOFA scores using a cutoff of 6.5 at ICU admission. AUC, area under the curve; S100A8/A9, S100 calcium-binding protein A8/A9; SOFA, sequential organ failure assessment; PCT, procalcitonin; CRP, C-reactive protein; IL-6, interleukin-6; WBC, white blood cell.

patients ($P < 0.001$, Figure 5C). The serum levels of S100A8/A9 in non-shock sepsis patients were also markedly higher than those in healthy individuals ($P < 0.05$, Figure 5D). Serum resistin concentrations in both non-shock and shock sepsis patients were noticeably increased than those in healthy individuals ($P < 0.01$, Figure 5E). Resistin expression was notably higher in patients with G- bacterial sepsis contrasted with G+ bacterial sepsis ($P < 0.05$, Figure 5F) Furthermore, resistin levels were significantly correlated with PCT, IL-6, and PDL1 ($P < 0.05$, Figures 5G–I).

Discussion

Sepsis, the leading cause of death in intensive care unit patients, is triggered by an uncontrolled systemic response to infection, leading to widespread damage across multiple organs and systems. However, according to the Sepsis-3 consensus definition, the role of biomarkers in diagnosing sepsis remains unclear (Singer et al., 2016; Pierrakos et al., 2020). Identifying reliable biomarkers is essential for improving both the diagnosis and treatment of sepsis.

TABLE 1 AUC, optimal cut-off points, validity indices, and predictive values of severity scores and biomarkers for 28-Day mortality in the discovery cohort.

Paramater	AUC (95% CI)	Cut-off value	SE (%)	SP (%)	P-value	PPV (%)	NPV (%)
S100A8/A9	0.617 (0.513-0.721)	377.53	79.5	46.2	0.032	36.5	85.3
Resistin	0.521 (0.418-0.625)	62.01	61.5	50	0.697	32.4	76.9
SOFA	0.751 (0.668-0.835)	6.5	74.4	65.7	0.000	44.6	87.6
PCT	0.562 (0.458-0.667)	3.22	74.4	39.2	0.225	28.4	82.5
CRP	0.542 (0.438-0.646)	41.32	33.3	80.4	0.441	39.2	78.4
IL-6	0.554 (0.448-0.660)	0.109	84.6	27.5	0.321	29.8	82.3
WBC	0.447 (0.345-0.550)	11.16	71.8	43.1	0.335	30.0	79.4

AUC, area under the curve; S100A8/A9, S100 calcium-binding protein A8/A9; SOFA, sequential organ failure assessment; PCT, procalcitonin; CRP, C-reactive protein; IL-6, interleukin-6; WBC, white blood cell; Cut-off value the optimal value point with the highest sensitivity and specificity; SE, sensitivity; SP, Specificity; NPV, negative predictive value; PPV, positive predictive value.

Both S100A8/A9 and resistin are known to promote inflammatory responses through activation of the TLR4 pathway and have been used as biomarkers for various inflammatory diseases (Donato et al., 2013; Yesudhas et al., 2014; Singbartl et al., 2016; Wang et al., 2023). We found that S100A8/A9 serves as a predictor of mortality in sepsis patients. First, serum S100A8/A9 levels were markedly elevated in sepsis patients relative to non-sepsis patients and healthy individuals, making it a potential diagnostic marker for sepsis (Supplementary Figure S4). Additionally, the serum concentration of S100A8/A9 in septic shock patients was notably lower than in those without shock. Furthermore, S100A8/A9 outperformed traditional biomarkers such as WBC, PCT, CRP, and IL-6 in predicting 28-day mortality at ICU admission. Survival curve analysis revealed that sepsis patients with lower serum S100A8/A9 levels at admission had reduced survival rates compared to those with higher levels. Importantly, the predictive value of S100A8/A9 for 28-day mortality was validated in an independent cohort of 55 sepsis patients. Although resistin did not predict mortality in sepsis patients, it effectively differentiated sepsis patients from non-sepsis patients and healthy individuals, as reflected by its increased serum levels in sepsis. This suggests its potential utility as a diagnostic marker. Moreover, resistin levels were noticeably increased in septic shock patients relative to those without shock, providing insight into the severity of sepsis.

Secondly, the serum S100A8/A9 level in patients with septic shock is significantly lower than that in patients without septic shock, including both survivor and nonsurvivor. In addition, S100A8/A9 outperformed WBC, PCT, CRP, and IL-6 in predicting 28-day mortality upon ICU admission. And according to survival curve analysis, patients with low serum S100A8/A9 admission levels in sepsis had lower survival rates than those with high serum S100A8/A9 admission levels. Most importantly, the role of S100A8/A9 in predicting 28-day mortality from sepsis was validated in an additional 55 adult patients with sepsis. Although resistin cannot predict the death of sepsis patients, it can still effectively distinguish sepsis patients from non-sepsis patients and healthy individuals. This is manifested by an increase in serum resistin expression concentration in sepsis patients, which can also serve as a diagnostic indicator for sepsis.

Additionally, the serum resistin levels in sepsis patients infected with G- and G+ bacteria were notably different. For instance, on the day of admission, resistin levels in patients with G- sepsis were considerably elevated than in those with G+ sepsis. Resistin can thus serve as a distinguishing marker between sepsis caused by G- and G+ infections. Sepsis is characterized by excessive inflammation and immunosuppression (Wu et al., 2021). Both S100A8/A9 and resistin levels were increased in patients with a mixed phenotype and high inflammation. Notably, resistin levels in patients with mixed phenotypes with immunosuppression were significantly higher than in those with mixed phenotypes with hyperinflammation.

Moreover, serum S100A8/A9 levels in sepsis patients show a positive correlation with serum resistin levels. S100A8/A9 is also positively correlated with CRP and the immune molecule IL-6, while resistin levels are positively correlated with PCT, WBC, IL-6, IL-10, PDL-1, and TNF-α. As highlighted, S100A8/A9 and resistin enhances the ability to distinguish sepsis patients from healthy individuals, assess the severity of sepsis, identify the infecting bacterial type, perform immunotyping of sepsis patients, and predict patient survival outcomes.

In conditions of widespread systemic inflammation, such as sepsis, neutrophils and monocytes serve as the immune system's first line of defense against invading pathogens (Borregaard, 2010; Delano and Ward, 2016; Wang et al., 2023). The vesicle-dependent secretion pathway of S100A8/A9 is predominantly found in various immune cells, particularly macrophages and neutrophils. Additionally, inflammatory stimuli can trigger the passive release of S100A8/A9 from necrotic cells into the plasma, with circulating S100A8/A9 levels positively correlated with the extent of cell necrosis or tissue damage (Vogl et al., 2012; Sprenkeler et al., 2022). During sepsis, dysregulated pyroptosis leads to substantial S100A8/A9 release, exacerbating the inflammatory response and inducing platelet pyroptosis. As a result, serum S100A8/A9 concentrations are elevated in sepsis patients, consistent with previous findings (van Zoelen et al., 2009; Wirtz et al., 2020). Studies by have also demonstrated that higher levels of S100A8/A9 in the bloodstream can serve as an early indicator of sepsis and predict a higher risk of ICU admission. Furthermore, a significant positive correlation exists between elevated S100A8/A9 concentrations and poor clinical outcomes, including increased

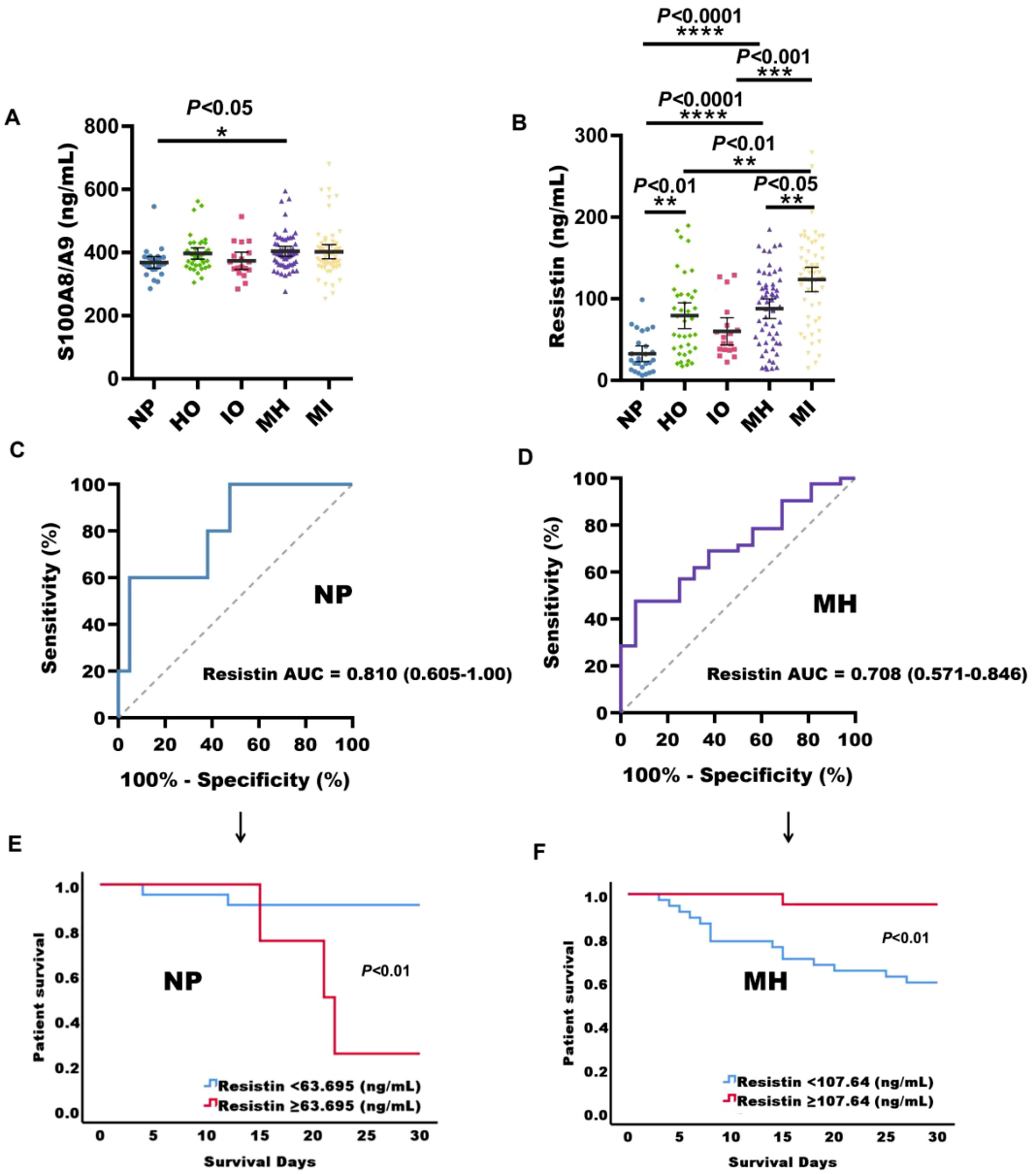

FIGURE 4
Serum S100A8/A9 and resistin expression levels in sepsis patients with different immunotypes. **(A)** S100A8/A9 concentrations in serum samples from sepsis patients with normal phenotype (NP), hyperinflammation only (HO), immunosuppression only (IO), mixed phenotype with hyperinflammation (MH), and mixed phenotype with immunosuppression (MI). **(B)** Resistin concentrations in serum samples from sepsis patients across the same phenotypes. **(C)** Receiver operating characteristic (ROC) curves for serum biomarkers at admission in predicting 28-day mortality in sepsis patients with normal phenotype. **(D)** ROC curves for serum biomarkers at admission in predicting 28-day mortality in sepsis patients with mixed phenotype and hyperinflammation. **(E)** Kaplan-Meier survival curves for 26 sepsis patients with normal phenotype based on the resistin cut-off (63.695 ng/mL) on ICU admission. **(F)** Kaplan-Meier survival curves for 64 sepsis patients with mixed phenotype with hyperinflammation based on the resistin cut-off (107.64 ng/mL) on ICU admission. NP, normal phenotype; HO, hyperinflammation only; IO, immunosuppression only; MH, mixed phenotype with hyperinflammation; MI, mixed phenotype with immunosuppression in sepsis patients; *$P < 0.05$, **$P < 0.01$, ***$P < 0.001$, ****$P < 0.0001$ (Kruskal-Wallis test).

28-day mortality in sepsis patients (Simm et al., 2016; Larsson et al., 2020). However, the results of our current study diverge from previous reports (Wirtz et al., 2020; Gao et al., 2022). While serum S100A8/A9 levels were higher in sepsis patients compared to non-sepsis patients and healthy individuals, severe sepsis cases, including non-survivors, exhibited lower S100A8/A9 expression levels than survivors. Notably, sepsis patients with low baseline calprotectin concentrations had significantly reduced survival rates ($P < 0.01$), contradicting some earlier findings (Wirtz et al., 2020; Gao et al., 2022).

The most likely explanation for this finding is that the majority of non-surviving sepsis patients in this study were in an immunosuppressive state, with compromised immune function, leading to decreased production and release of S100A8/A9.

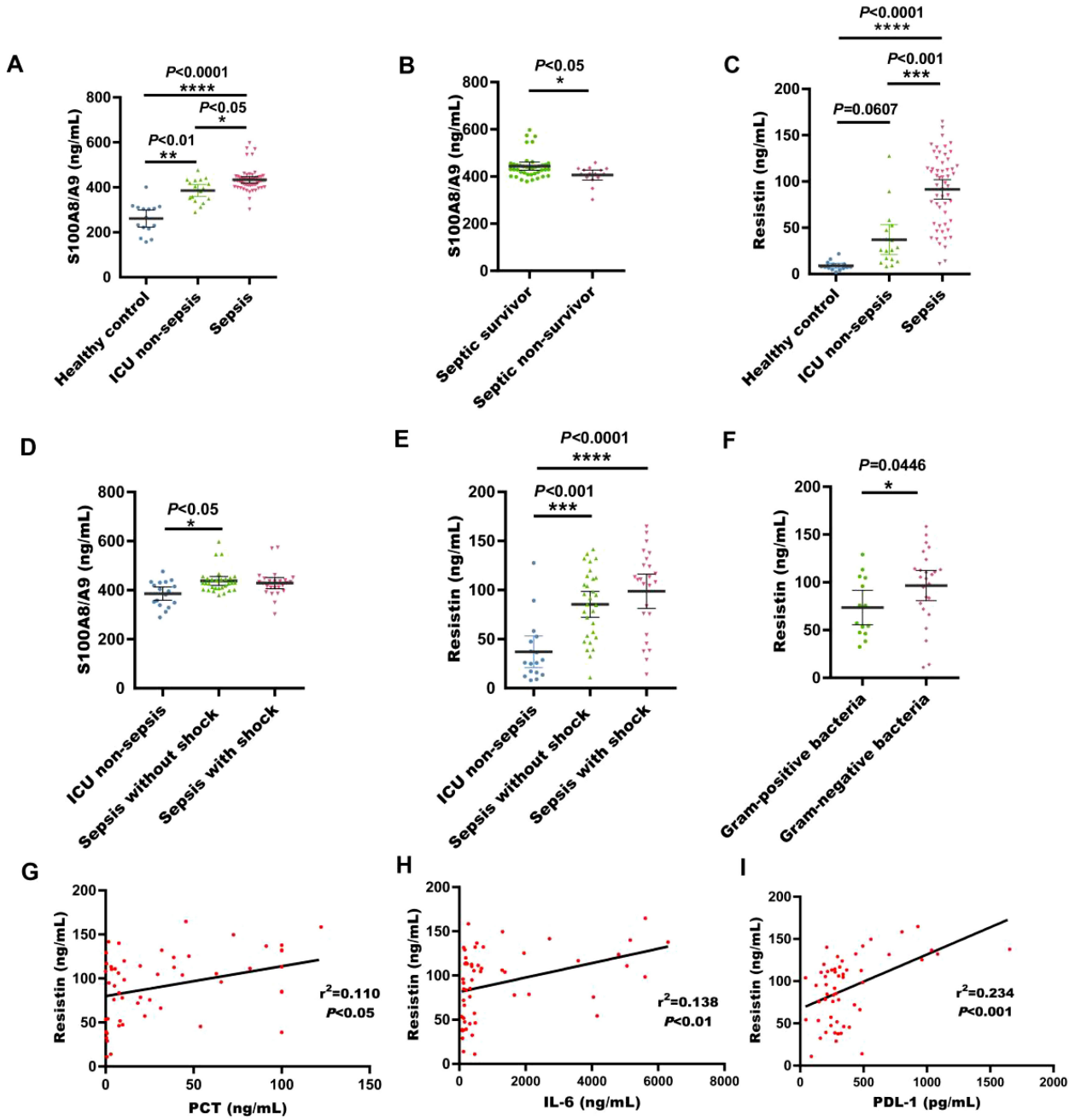

FIGURE 5
Serum S100A8/A9 and resisitin levels at admission were detected in the validation cohort of adult patients with sepsis. **(A)** S100A8/A9 concentrations in serum samples collected from healthy individuals, ICU non-sepsis patients and sepsis patients; **(B)** S100A8/A9 concentrations in serum samples collected from patients with septic shock and patients without shock in the validation cohort; **(C)** Resistin concentrations in serum samples collected from healthy individuals, ICU non-sepsis patients and sepsis patients; **(D)** S100A8/A9 concentrations in serum samples from patients with and without septic shock in the validation cohort. **(E)** Resistin concentrations in serum samples collected from patients with septic shock and patients without shock in the validation cohort; **(F)** Resistin concentrations in serum samples collected from patients with sepsis with G- bacteria and patients with sepsis with G+ bacteria; **(G)** Correlation of resistin levels with PCT counts in the validation cohort of adult patients with sepsis on ICU admission; **(H)** Correlation of resistin levels with IL-6 counts in the validation cohort of adult patients with sepsis on ICU admission; **(I)** Correlation of resistin levels with PDL-1 counts in the validation cohort of adult patients with sepsis on ICU admission; See Figure 1 legend for expansion of abbreviation.*$P < 0.05$, **$P < 0.01$, ***$P < 0.001$, ****$P < 0.0001$ (Kruskal-Wallis and Mann-Whitney U test, Spearman's rank correlation coefficient.).

Previous studies have reported that many sepsis patients survive the initial hyperinflammatory phase but succumb to subsequent immunosuppression (Boomer et al., 2011; Hotchkiss et al., 2013). Traditionally, sepsis has been viewed as a two-stage process, beginning with an excessive inflammatory response followed by a compensatory anti-inflammatory phase. However, growing evidence suggests that immunosuppressive mechanisms may be active from the onset of sepsis (Liu D et al., 2022). This study found

that while the serum concentration of S100A8/A9 in immunosuppressed patients at admission was not significantly different from that in patients with hyperinflammation—possibly due to the limited sample size after immune subtyping—the median levels showed a downward trend (Figure 4A). Moreover, patients with immunosuppressive sepsis exhibited a higher mortality rate compared to those with hyperinflammatory sepsis (Supplementary Table S5). This could provide a plausible explanation for the higher risk of death observed in sepsis patients with relatively low S100A8/A9 levels at hospital admission compared to those who survived.

Resistin has emerged as an important pro-inflammatory cytokine secreted by various cell types (Bostrom et al., 2009; Johansson et al., 2009; Singbartl et al., 2016). Its role as an acute-phase protein is closely linked to the severity of sepsis and septic shock, as well as to elevated levels of inflammatory cytokines, lactate, and serum creatinine (Koch et al., 2009; Vassiliadi et al., 2012; Macdonald et al., 2014). Studies have reported that serum resistin concentrations are significantly higher in patients with severe sepsis compared to those with milder forms of the condition (Singbartl et al., 2016; Lan Y et al., 2024), aligning with this study's findings of increased resistin levels in patients with septic shock Additionally, consistent with the results of this study, Lehrke et al. observed that resistin levels in non-surviving patients were higher than in survivors, although the difference was not statistically significant (Lehrke et al., 2004). Sepsis results from a dysregulated host response to severe infection, with bacteria being the most common cause (Niederman et al., 2021). Rapid differentiation between G- and G+ pathogens is critical for guiding antibiotic therapy and improving patient outcomes. Currently, few biomarkers are recommended for distinguishing G-/G+ bacterial sepsis or improving sepsis prognosis (Huang et al., 2022). However, this study found that resistin expression levels were substantially raised in patients with Gram-negative sepsis, suggesting its potential use in identifying G-/G+ bacterial sepsis. Although resistin expression levels did not reach statistical significance in patients with excessive inflammation or immunosuppression, it was found that resistin levels were substantially raised in patients with inflammation only and mixed phenotype with immunosuppression compared to those with a normal phenotype. Interestingly, within the mixed phenotype group, patients with hyperinflammation had significantly lower resistin levels than those with immunosuppression. Resistin is a pro-inflammatory factor that is typically highly expressed during inflammation (Bostrom et al., 2009; Johansson et al., 2009; Singbartl et al., 2016). In our immune phenotyping results, the concentration of resistin was significantly higher in the inflammation-only compared to patients with normal phenotypes. Although no significant difference was observed between the inflammation-only and the immunosuppression-only - possibly due to the limited sample size, resistin still exhibited an upward trend in the former group. This is also evident from the significantly higher levels observed in patients with mixed inflammatory conditions compared to those with immunosuppression-only. Resistin is secreted not only by immune cells such as macrophages but also by adipocytes. In patients with mixed inflammation and immunosuppression, the anti-inflammatory/pro-inflammatory balance is severely disrupted, causing significant metabolic dysregulation, which may lead to increased adipocyte-derived resistin. Thus, the mixed immune group shows higher resistin levels than the inflammation-only group. Additionally, elevated resistin in mixed immunosuppression patients might further promote immune balance. However, these observations remain preliminary and necessitate additional experimental confirmation.

Notably, serum resistin concentrations in patients with both normal and mixed phenotypes with hyperinflammation were predictive of mortality. Additionally, this study demonstrated significant correlations between resistin, S100A8/A9, CRP, and IL-6 in sepsis patients. CRP is a well-established biomarker for sepsis, while IL-6, a proinflammatory factor, is strongly associated with disease severity and mortality in sepsis (Wu et al., 2021). Furthermore, resistin was significantly correlated with PD-L1 and TNF-α. PD-L1, an immune checkpoint molecule, suppresses T-cell activation by binding to its receptor PD-1, thereby reducing immune aggression and preventing tissue damage from excessive immune responses (Durrechou et al., 2020). TNF-α, a multifunctional cytokine primarily, plays a crucial role in inflammation, apoptosis, immune cell activation, and the acute phase response (Delgado and Brunner, 2019). The correlation of resistin with PD-L1 and TNF-α helps explain its elevated concentration in immunosuppressed patients. Additionally, resistin was significantly correlated with S100A8/A9, suggesting that the combination of these biomarkers could be useful for immune typing of sepsis patients. This approach not only facilitates targeted treatments based on immune profiles but also improves the prediction of mortality risk in sepsis patients.

Biomarkers have been extensively studied for their potential applications in sepsis patients, including diagnosis, prognosis, and guiding treatment decisions. However, the heterogeneity of sepsis at the individual level poses a significant challenge to the development of standardized care (Pierrakos et al., 2020). This complexity has spurred efforts to categorize patients into more homogeneous subgroups based on shared biological characteristics, which could facilitate the creation of tailored sepsis therapies (Liu D et al., 2022). Additionally, measuring multiple biomarkers simultaneously may help address the limitations of relying on any single biomarker. Currently, CRP and PCT are the most widely researched and utilized biomarkers in sepsis (Pierrakos et al., 2020). Both show transient increases during sepsis; however, they primarily reflect the intensity of inflammation and do not effectively predict mortality risk (Wu et al., 2021). In contrast, S100A8/A9 and resistin as sepsis biomarkers not only aids in diagnosing sepsis but also distinguishes between severe sepsis, G- and G+ infections, and different immune subtypes of sepsis patients. Furthermore, these markers can predict 28-day mortality in sepsis patients, particularly those with a normal phenotype or mixed phenotype with hyperinflammation.

While these findings provide valuable insights, our study has several limitations. First, it included only patients from North Guangdong People's Hospital in Guangdong Province, China, which may limit the generalizability of the results. Further multi-center studies are necessary to account for regional and individual

variability. Second, the study focused exclusively on adult sepsis patients. Additionally, we measured the serum levels of S100A8/A9 and resistin only on the first day of admission and assessed their association with short-term sepsis mortality risk. Expanding the observation period and evaluating long-term mortality risk would provide more comprehensive insights into sepsis prognosis. Moreover, as the clinical condition of sepsis patients can evolve and require varied supportive treatments, it remains unclear whether different treatment strategies may influence the study outcomes. Further research is needed to determine the impact of appropriate antibiotic therapy and other interventions on the daily serum levels of S100A8/A9 and resistin. In future studies, we plan to investigate the relationship between different treatment regimens and the dynamic changes in these biomarkers.

Conclusion

Serum S100A8/A9 concentration at ICU admission is a significant predictor of 28-day mortality risk in sepsis patients. Additionally, resistin levels at ICU admission play an important role in predicting 28-day mortality risk in patients with both normal and mixed phenotypes with hyperinflammation. These findings suggest that S100A8/A9 and resistin could serve as effective biomarkers. Moreover, these findings could guide early clinical decisions in the treatment of sepsis patients.

Data availability statement

The original contributions presented in the study are included in the article/Supplementary Material. Further inquiries can be directed to the corresponding author.

Ethics statement

The studies involving humans were approved by Clinical Research Ethics Committee of Yuebei People's Hospital Affiliated to Shantou University Medical College. The studies were conducted in accordance with the local legislation and institutional requirements. The participants and their legal representatives provided their written informed consent to participate in this study.

Author contributions

JC: Conceptualization, Data curation, Formal Analysis, Methodology, Resources, Software, Writing – original draft. ZL: Methodology, Resources, Software, Writing – review & editing. FZ: Methodology, Resources, Software, Writing – review & editing. YS: Resources, Software, Writing – review & editing. ZJ: Methodology, Resources, Software, Writing – review & editing. PZ: Conceptualization, Data curation, Formal Analysis, Funding acquisition, Investigation, Methodology, Project administration, Resources, Software, Supervision, Validation, Visualization, Writing – original draft, Writing – review & editing.

Funding

The author(s) declare that financial support was received for the research and/or publication of this article. This study was supported by Open Research Project of the Key Laboratory of Viral Pathogenesis & Infection Prevention and Control of the Ministry of Education, China (Grant No.: 2024VPPC-R03 to PZ), Natural Science Foundation of Guangdong Province, China (Grant No.: 2025A1515010579 to PZ), Shaoguan Municipal Science and Technology Program, China (Grant No.: 211102114530659 to PZ). Shaoguan Municipal Science and Technology Program, China (Grant No.: 220610154531525 to PZ). Shaoguan Engineering Research Center for Research and Development of Molecular and Cellular Technology in Rapid Diagnosis of Infectious Diseases and Cancer Program, China (Grant No.: 220525096180441 to PZ). Research Fund for Joint Laboratory for Digital and Precise Detection of Clinical Pathogens, Yuebei People's Hospital Affiliated to Shantou University Medical College, China (Grant No.: KEYANSHEN (2023) 01 to PZ). Research Project for Outstanding Scholar of Yuebei People's Hospital Affiliated to Shantou University Medical College, China (Grant No.: RS202001 to PZ).

Conflict of interest

The authors declare that the research was conducted in the absence of any commercial or financial relationships that could be construed as a potential conflict of interest.

Generative AI statement

The author(s) declare that no Generative AI was used in the creation of this manuscript.

Publisher's note

Supplementary material

The Supplementary Material for this article can be found online at: https://www.frontiersin.org/articles/10.3389/fcimb.2025.1555307/full#supplementary-material

SUPPLEMENTARY FIGURE 1
The flowchart of the study population. ROC, receiver operating characteristic.

SUPPLEMENTARY FIGURE 2
Serum biomarker levels at admission were measured in the discovery cohort of adult sepsis patients. **(A)** CRP concentrations in serum samples from healthy individuals, ICU non-sepsis patients, and sepsis patients. **(B)** PCT concentrations in serum samples from healthy individuals, ICU non-sepsis patients, and sepsis patients. **(C)** IL-6 concentrations in serum samples from healthy individuals, ICU non-sepsis patients, and sepsis patients. **(D)** S100A8/A9 concentrations in serum samples from sepsis with shock and sepsis without shock nonsurvivors. **(E)** Resistin concentrations in serum samples from sepsis with shock and sepsis without shock nonsurvivors. **(F)** S100A8/A9 concentrations in serum samples from adult sepsis patients with SOFA scores < 6.5 and > 6.5. **(G)** S100A8/A9 concentrations in serum samples from sepsis patients with Gram-positive and Gram-negative bacteria. CRP, C-reactive protein; IL-6, interleukin-6; IL-1β, interleukin-1β; *$P < 0.05$, **$P < 0.01$, ***$P < 0.001$, ****$P < 0.0001$ (Kruskal-Wallis and Mann-Whitney U test).

SUPPLEMENTARY FIGURE 3
Receiver operating characteristic curves of serum biomarkers at admission in diagnosis of adult sepsis. **(A)** Receiver operating characteristic curves of serum biomarkers at admission in diagnosis of adult sepsis in discovery queue; **(B)** Receiver operating characteristic curves of serum biomarkers at admission in diagnosis of adult sepsis in validation queue. AUC, area under the curve; S100A8/A9, S100 calcium-binding protein A8/A9; SOFA, sequential organ failure assessment; PCT, procalcitonin; CRP, C-reactive protein; IL-6, interleukin-6; WBC, white blood cell.

References

Barichello, T., Generoso, J. S., Singer, M., and Dal-Pizzol, F. (2022). Biomarkers for sepsis: more than just fever and leukocytosis-a narrative review. *Crit. Care* 26, 14. doi: 10.1186/s13054-021-03862-5

Boomer, J. S., To, K., Chang, K. C., Takasu, O., Osborne, D. F., Walton, A. H., et al. (2011). Immunosuppression in patients who die of sepsis and multiple organ failure. *Jama* 306, 2594–2605. doi: 10.1001/jama.2011.1829

Borregaard, N. (2010). Neutrophils, from marrow to microbes. *Immunity* 33, 657–670. doi: 10.1016/j.immuni.2010.11.011

Bostrom, E. A., Tarkowski, A., and Bokarewa, M. (2009). Resistin is stored in neutrophil granules being released upon challenge with inflammatory stimuli. *Biochim. Biophys. Acta* 1793, 1894–1900. doi: 10.1016/j.bbamcr.2009.09.008

Delano, M. J., and Ward, P. A. (2016). The immune system's role in sepsis progression, resolution, and long-term outcome. *Immunol. Rev.* 274, 330–353. doi: 10.1111/imr.12499

Delgado, M. E., and Brunner, T. (2019). The many faces of tumor necrosis factor signaling in the intestinal epithelium. *Genes immun.* 20, 609–626. doi: 10.1038/s41435-019-0057-0

Donato, R., Cannon, B. R., Sorci, G., Riuzzi, F., Hsu, K., Weber, D. J., et al. (2013). Functions of S100 proteins. *Curr. Mol. med.* 13, 24–57. doi: 10.2174/156652413804486214

Durrechou, Q., Domblides, C., Sionneau, B., Lefort, F., Quivy, A., Ravaud, A., et al. (2020). Management of immune checkpoint inhibitor toxicities. *Cancer Manage. Res.* 12, 9139–9158. doi: 10.2147/CMAR.S218756

Gao, R. Y., Jia, H. M., Han, Y. Z., Qian, B. S., You, P., Zhang, X. K., et al. (2022). Calprotectin as a diagnostic marker for sepsis: A meta-analysis. *Front. Cell Infect. Microbiol.* 12. doi: 10.3389/fcimb.2022.1045636

Hamilton, F., Arnold, D., Baird, A., Albur, M., and Whiting, P. (2018). Early Warning Scores do not accurately predict mortality in sepsis: A meta-analysis and systematic review of the literature. *J. infect.* 76, 241–248. doi: 10.1016/j.jinf.2018.01.002

Hotchkiss, R. S., Monneret, G., and Payen, D. (2013). Immunosuppression in sepsis: a novel understanding of the disorder and a new therapeutic approach. *Lancet Infect. dis.* 13, 260–268. doi: 10.1016/S1473-3099(13)70001-X

Huang, C., Xiong, H., Li, W., Peng, L., Zheng, Y., Liao, W., et al. (2022). T cell activation profiles can distinguish gram negative/positive bacterial sepsis and are associated with ICU discharge. *Front. Immunol.* 13. doi: 10.3389/fimmu.2022.1058606

Johansson, L., Linner, A., Sunden-Cullberg, J., Haggar, A., Herwald, H., Lore, K., et al. (2009). Neutrophil-derived hyperresistinemia in severe acute streptococcal infections. *J. Immunol.* 183, 4047–4054. doi: 10.4049/jimmunol.0901541

Kataoka, H., Kono, H., Patel, Z., Kimura, Y., and Rock, K. L. (2014). Evaluation of the contribution of multiple DAMPs and DAMP receptors in cell death-induced sterile inflammatory responses. *PloS One* 9, e104741. doi: 10.1371/journal.pone.0104741

Kigerl, K. A., de Rivero Vaccari, J. P., Dietrich, W. D., Popovich, P. G., and Keane, R. W. (2014). Pattern recognition receptors and central nervous system repair. *Exp. neurol.* 258, 5–16. doi: 10.1016/j.expneurol.2014.01.001

Koch, A., Gressner, O. A., Sanson, E., Tacke, F., and Trautwein, C. (2009). Serum resistin levels in critically ill patients are associated with inflammation, organ dysfunction and metabolism and may predict survival of non-septic patients. *Crit. Care* 13, R95. doi: 10.1186/cc7925

Lagasse, E., and Weissman, I. L. (1992). Mouse MRP8 and MRP14, two intracellular calcium-binding proteins associated with the development of the myeloid lineage. *Blood* 79, 1907–1915. doi: 10.1182/blood.V79.8.1907.1907

Lan Y, G. W., Chen, W., Chen, M., and Li, S. (2024). Resistin as a potential diagnostic biomarker for sepsis: insights from DIA and ELISA analyses. *Clin. Proteom.* 21, 46. doi: 10.1186/s12014-024-09498-1

Larsson, A., Tyden, J., Johansson, J., Lipcsey, M., Bergquist, M., Kultima, K., et al. (2020). Calprotectin is superior to procalcitonin as a sepsis marker and predictor of 30-day mortality in intensive care patients. *Scand. J. Clin. Lab. investig.* 80, 156–161. doi: 10.1080/00365513.2019.1703216

Lehrke, M., Reilly, M. P., Millington, S. C., Iqbal, N., Rader, D. J., and Lazar, M. A. (2004). An inflammatory cascade leading to hyperresistinemia in humans. *PloS med.* 1, e45. doi: 10.1371/journal.pmed.0010045

Liu D, H. S., Sun, J. H., Zhang, H. C., Cai, Q. L., Gao, C., Li, L., et al. (2022). Sepsis-induced immunosuppression: mechanisms, diagnosis and current treatment options. *Military Med. Res.* 9, 56. doi: 10.1186/s40779-022-00422-y

Lu, B., Wang, C., Wang, M., Li, W., Chen, F., Tracey, K. J., et al. (2014). Molecular mechanism and therapeutic modulation of high mobility group box 1 release and action: an updated review. *Expert Rev. Clin. Immunol.* 10, 713–727. doi: 10.1586/1744666X.2014.909730

Macdonald, S. P. J., Bosio, E., Neil, C., Arendts, G., Burrows, S., Smart, L., et al. (2017). Resistin and NGAL are associated with inflammatory response, endothelial activation and clinical outcomes in sepsis. *Inflammation Res.* 66, 611–619. doi: 10.1007/s00011-017-1043-5

Macdonald, S. P., Stone, S. F., Neil, C. L., van Eeden, P. E., Fatovich, D. M., Arendts, G., et al. (2014). Sustained elevation of resistin, NGAL and IL-8 are associated with severe sepsis/septic shock in the emergency department. *PloS One* 9, e110678. doi: 10.1371/journal.pone.0110678

Miller, L., Singbartl, K., Chroneos, Z. C., Ruiz-Velasco, V., Lang, C. H., and Bonavia, A. (2019). Resistin directly inhibits bacterial killing in neutrophils. *Intens. Care Med. experiment.* 7, 30. doi: 10.1186/s40635-019-0257-y

Niederman, M. S., Baron, R. M., Bouadma, L., Calandra, T., Daneman, N., DeWaele, J., et al. (2021). Initial antimicrobial management of sepsis. *Crit. Care* 25, 307. doi: 10.1186/s13054-021-03736-w

Odink, K., Cerletti, N., Bruggen, J., Clerc, R. G., Tarcsay, L., Zwadlo, G., et al. (1987). Two calcium-binding proteins in infiltrate macrophages of rheumatoid arthritis. *Nature* 330, 80–82. doi: 10.1038/330080a0

Pierrakos, C., Velissaris, D., Bisdorff, M., Marshall, J. C., and Vincent, J. L. (2020). Biomarkers of sepsis: time for a reappraisal. *Crit. Care* 24, 287. doi: 10.1186/s13054-020-02993-5

Rachakonda, V., Gabbert, C., Raina, A., Li, H., Malik, S., DeLany, J. P., et al. (2014). Stratification of risk of death in severe acute alcoholic hepatitis using a panel of adipokines and cytokines. *Alcohol. Clin. Exp. Res.* 38, 2712–2721. doi: 10.1111/acer.12558

Rhodes, A., Evans, L. E., Alhazzani, W., Levy, M. M., Antonelli, M., Ferrer, R., et al. (2017). Surviving sepsis campaign: international guidelines for management of sepsis and septic shock: 2016. *Crit. Care med.* 45, 486–552. doi: 10.1097/CCM.0000000000002255

Seymour, C. W., Liu, V. X., Iwashyna, T. J., Brunkhorst, F. M., Rea, T. D., Scherag, A., et al. (2016). Assessment of clinical criteria for sepsis: for the third international consensus definitions for sepsis and septic shock (Sepsis-3). *Jama* 315, 762–774. doi: 10.1001/jama.2016.0288

Shankar-Hari, M., Phillips, G. S., Levy, M. L., Seymour, C. W., Liu, V. X., Deutschman, C. S., et al. (2016). Developing a new definition and assessing new clinical criteria for septic shock: for the third international consensus definitions for sepsis and septic shock (Sepsis-3). *Jama* 315, 775–787. doi: 10.1001/jama.2016.0289

Simm, M., Soderberg, E., Larsson, A., Castegren, M., Nilsen, T., Eriksson, M., et al. (2016). Performance of plasma calprotectin as a biomarker of early sepsis: a pilot study. *Biomarkers med.* 10, 811–818. doi: 10.2217/bmm-2016-0032

Singbartl, K., Miller, L., Ruiz-Velasco, V., and Kellum, J. A. (2016). Reversal of acute kidney injury-induced neutrophil dysfunction: A critical role for resistin. *Crit. Care med.* 44, e492–e501. doi: 10.1097/CCM.0000000000001472

Singer, M., Deutschman, C. S., Seymour, C. W., Shankar-Hari, M., Annane, D., Bauer, M., et al. (2016). The third international consensus definitions for sepsis and septic shock (Sepsis-3). *Jama* 315, 801–810. doi: 10.1001/jama.2016.0287

Sprenkeler, E. G. G., Zandstra, J., van Kleef, N. D., Goetschalckx, I., Verstegen, B., Aarts, C. E. M., et al. (2022). S100A8/A9 is a marker for the release of neutrophil extracellular traps and induces neutrophil activation. *Cells* 11 (2), 236. doi: 10.3390/cells11020236

Sun S, C. Y., Liu, Z., Tian, R., Liu, J., Chen, E., Mao, E., et al. (2021). Serum-soluble PD-L1 may be a potential diagnostic biomarker in sepsis. *Scand. J. Immunol.* 94, e13049. doi: 10.1111/sji.13049

van Zoelen, M. A., Vogl, T., Foell, D., Van Veen, S. Q., van Till, J. W., Florquin, S., et al. (2009). Expression and role of myeloid-related protein-14 in clinical and experimental sepsis. *Am. J. respiratory Crit. Care med.* 180, 1098–1106. doi: 10.1164/rccm.200810-1552OC

Vassiliadi, D. A., Tzanela, M., Kotanidou, A., Orfanos, S. E., Nikitas, N., Armaganidis, A., et al. (2012). Serial changes in adiponectin and resistin in critically ill patients with sepsis: associations with sepsis phase, severity, and circulating cytokine levels. *J. Crit. Care* 27, 400–409. doi: 10.1016/j.jcrc.2012.04.007

Vogl, T., Gharibyan, A. L., and Morozova-Roche, L. A. (2012). Pro-inflammatory S100A8 and S100A9 proteins: self-assembly into multifunctional native and amyloid complexes. *Int. J. Mol. Sci.* 13, 2893–2917. doi: 10.3390/ijms13032893

Wang, Q., Long, G., Luo, H., Zhu, X., Han, Y., Shang, Y., et al. (2023). S100A8/A9: An emerging player in sepsis and sepsis-induced organ injury. *Biomed. pharmacother. = Biomed. pharmacother.* 168, 115674. doi: 10.1016/j.biopha.2023.115674

Wiersinga, W. J., Leopold, S. J., Cranendonk, D. R., and van der Poll, T. (2014). Host innate immune responses to sepsis. *Virulence* 5, 36–44. doi: 10.4161/viru.25436

Wirtz, T. H., Buendgens, L., Weiskirchen, R., Loosen, S. H., Haehnsen, N., Puengel, T., et al. (2020). Association of serum calprotectin concentrations with mortality in critically ill and septic patients. *Diagnostics* 10 (11), 990. doi: 10.3390/diagnostics10110990

Wu, C., Ma, J., Yang, H., Zhang, J., Sun, C., Lei, Y., et al. (2021). Interleukin-37 as a biomarker of mortality risk in patients with sepsis. *J. infect.* 82, 346–354. doi: 10.1016/j.jinf.2021.01.019

Yao, R. Q., Zhao, P. Y., Li, Z. X., Liu, Y. Y., Zheng, L. Y., Duan, Y., et al. (2023). Single-cell transcriptome profiling of sepsis identifies HLA-DR(low)S100A(high) monocytes with immunosuppressive function. *Military Med. Res.* 10, 27. doi: 10.1186/s40779-023-00462-y

Yesudhas, D., Gosu, V., Anwar, M. A., and Choi, S. (2014). Multiple roles of toll-like receptor 4 in colorectal cancer. *Front. Immunol.* 5. doi: 10.3389/fimmu.2014.00334

Zhou F, C. M., Liu, Y., Xia, X., and Zhao, P. (2024). Serum mitochondrial-encoded NADH dehydrogenase 6 and Annexin A1 as novel biomarkers for mortality prediction in critically ill patients with sepsis. *Front. Immunol.* 14. doi: 10.3389/fimmu.2024.1486322

Glossary

AIDS	Acquired immunodeficiency syndrome
ANOVA	One-way analysis of variance
AUC	area under the curve
COPD	Chronic Obstructive Pulmonary Disease
CRP	C-reactive protein
DAMPs	Damage-associated molecular patterns
G-	Gram-negative bacteria
G+	Gram-positive bacteria
HBP	Heparin-Binding Protein
HLA-DR	Human leukocyte antigen DR
HMGB-1	High mobility group protein 1
HSPs	Heat shock proteins
ICU	Intensive care unit
IL-1β	Interleukin-1β
IL-6	Interleukin-6
IL-10	Interleukin-10
IQR	Inter quartile range
NPV	Negative predictive value
PCT	Procalcitonin
PDL-1	Programmed death-ligand-1
PPV	Positive predictive value
ROC	Receiver operating characteristic
SE	Sensitivity
SOFA	Sequential organ failure assessment
SP	Specificity
TLR4	Toll-like receptor 4
TNF-α	Tumor necrosis factor-alpha
WBC	White Blood Cell
sPD-L1	Soluble programmed death-ligand 1
95% CI	95% confidence intervals

frontiers | Frontiers in Cellular and Infection Microbiology

TYPE Original Research
PUBLISHED 12 June 2025
DOI 10.3389/fcimb.2025.1573511

OPEN ACCESS

EDITED BY
Rommel Chacon-Salinas,
Instituto Politécnico Nacional, Mexico

REVIEWED BY
Rosendo Luria-Perez,
Children's Hospital of Mexico Federico Gomez, Mexico
Martha Pedraza-Escalona,
National Council of Science and Technology (CONACYT), Mexico

*CORRESPONDENCE
Jun Li
huosu2014@163.com
Caixia Ye
807612383@qq.com
Xing Zhang
zhichi828@126.com

†These authors have contributed equally to this work

RECEIVED 14 March 2025
ACCEPTED 29 May 2025
PUBLISHED 12 June 2025

CITATION
Chen Y, Yuan Y, Liu X, Li B, Meng L, Xiao Y, Su Z, Han L, Li H, Deng L, Li J, Ye C and Zhang X (2025) Alterations in BCR heavy chain CDR3 repertoire characteristics in pediatric mycoplasma pneumoniae infection. *Front. Cell. Infect. Microbiol.* 15:1573511. doi: 10.3389/fcimb.2025.1573511

Alterations in BCR heavy chain CDR3 repertoire characteristics in pediatric mycoplasma pneumoniae infection

Yanfei Chen[1†], Yi Yuan[2†], Xingzhu Liu[1†], Bin Li[1], Lijuan Meng[1], Ying Xiao[1], Zhongjian Su[1], Linfei Han[1], Hong Li[1], Lili Deng[1], Jun Li[2*], Caixia Ye[3*] and Xing Zhang[1*]

[1]Department of Cardiology, Kunming Children's Hospital, Kunming, Yunnan, China, [2]Department of Immunology, Center of Immunomolecular Engineering, Innovation and Practice Base for Graduate Students Education, Zunyi Medical University, Zunyi, China, [3]Department of Pediatrics 1, Yunyang Maternal and Child Health Hospital, Chongqing, China

Introduction: Mycoplasma pneumoniae (MP) infection is a leading cause of pediatric pneumonia, triggering a complex immune response in which B cells play a critical role. This study aimed to analyze B cell receptor (BCR) heavy chain CDR3 repertoires in MP patients.

Methods: Clinical data from 202 children diagnosed with MP were retrospectively analyzed. Flow cytometry was used to assess B cell counts in 99 MP patients and 25 healthy controls (HC). Multiplex PCR was used to construct BCR heavy chain CDR3 repertoires from peripheral blood samples of 8 MP patients and 9 HC.

Results: Serological analysis revealed elevated levels of inflammatory markers, including C-reactive protein, interleukin-6, and ferritin, indicating an active immune response. Flow cytometry showed significantly increased B cell counts in MP patients compared to HC. Immunoglobulin levels were elevated in several patients, indicating immune fluctuations during infection. BCR repertoire analysis revealed increased diversity and altered clonotype distribution in MP patients, with preferential usage of IGHV1-18, IGHV7-4-1, and IGHJ6. MP patients exhibited a bimodal distribution of CDR3 lengths, with significantly longer CDR3 regions. Sixty-eight MP-exclusive clonotypes were identified, with evidence of clonal expansion.

Conclusion: These findings suggest that alterations in the BCR heavy chain CDR3 repertoire play a crucial role in the immune response to MP infection and may offer insight into disease progression and therapeutic targets.

KEYWORDS

Mycoplasma pneumoniae, B cell receptor, CDR3 repertoire, flow cytometry, clonal expansion

Introduction

Mycoplasma pneumoniae (MP) is a leading cause of community-acquired pneumonia in children, often resulting in significant morbidity and prolonged hospitalization (Kutty et al., 2019; Li et al., 2021). While MP infections are generally self-limiting, severe and refractory cases have been increasingly reported (Choi et al., 2022; Li et al., 2023), raising concerns about disease pathogenesis and immune response dynamics. Pediatric MP infections can manifest in a spectrum of clinical presentations, ranging from mild upper respiratory symptoms to severe pneumonia with extrapulmonary complications (Atkinson et al., 2008; Waites et al., 2017). The immune response to MP is a critical determinant of disease severity, with excessive inflammation and immune dysregulation contributing to more severe manifestations (Waites and Talkington, 2004; Zhu et al., 2023).

Humoral immunity, particularly the B cell response, plays a central role in host defense against infection, including those caused by bacteria (Fan et al., 2021), viruses (Miwa et al., 2023), and fungi (Casadevall et al., 2002). B cells mediate immunity through antibody production, antigen presentation, and cytokine secretion. The B cell receptor (BCR) repertoire, particularly the diversity and clonality of immunoglobulin heavy chain complementarity-determining region 3 (CDR3), provides insights into the adaptive immune response to infection (He et al., 2022; Kotagiri et al., 2022; Mai et al., 2023). The BCR repertoire is shaped by V(D)J recombination, somatic hypermutation, and clonal selection, generating a highly diverse set of antigen-specific receptors (Papavasiliou et al., 1997; Ollila and Vihinen, 2005; Spisak et al., 2024). This diversity enables the immune system to recognize and respond to a wide range of pathogens. The alterations in BCR repertoire characteristics, such as skewed V and J gene usage, abnormal CDR3 length distribution, and the presence of disease-specific clonotypes, may be associated with immune dysfunction and the host's response to specific pathogens.

Despite the known involvement of B cells in MP infections (Zhang et al., 2022; Li et al., 2024), comprehensive analyses of the BCR heavy chain CDR3 repertoire in pediatric MP patients remain limited. Understanding the characteristics of the BCR repertoire in these patients could provide valuable insights into disease mechanisms, immune evasion strategies of MP, and potential biomarkers for disease severity. In this study, we analyzed the BCR heavy chain CDR3 repertoire in pediatric MP patients, focusing on serological characteristics, B cell activation, V and J gene usage, CDR3 length distribution, amino acid composition, and disease-specific clonotypes. Our findings offer new perspectives on the adaptive immune response to MP and contribute to a deeper understanding of immune dynamics in pediatric respiratory infections.

Materials and methods

Participant demographics and sample collection

This study aimed to examine the serological characteristics, B cell response, and BCR heavy chain CDR3 repertoire in pediatric patients diagnosed with MP infection. A total of 202 MP patients, aged 4–6 years, were enrolled from the pediatric department at Kunming Children's Hospital in Yunnan Province, China. All participants were diagnosed with MP infection based on Mycoplasma pneumoniae nucleic acid testing and clinical symptoms.

Blood samples (2 mL) were collected in EDTA tubes from 8 participant during their hospital admission. Additionally, 9 healthy children, matched for age and sex, served as controls, with blood samples drawn at Kunming Children's Hospital. Detailed clinical data, including age, sex, clinical manifestations, and laboratory parameters were retrospectively collected from the participants' medical records. The study was approved by the Institutional Review Board (IRB) of Kunming Children's Hospital (Approval No: 2023-03-246-K01), and written consent was obtained from the parents or guardians of all pediatric patients. This research adhered to the ethical principles set forth in the Declaration of Helsinki.

RNA extraction, cDNA synthesis, and quality control

Total RNA were extracted using the Tiangen RNA extraction kit (Tiangen Biotech, China), following the manufacturer's instructions. RNA was then reverse transcribed into cDNA libraries using a standard reverse transcription kit. The final cDNA were collected and stored at -80°C until further analysis. The concentration and purity of the extracted nucleic acids were assessed using a NanoDrop 2000 Spectrophotometer (Thermo Fisher Scientific, USA), and the RNA integrity was evaluated by electrophoresis on a 1% agarose gel. Only samples with an RNA integrity number (RIN) greater than 7.0 were used for library construction and sequencing.

Library preparation and sequencing

Library preparation was performed using a multiplex PCR-based method. Briefly, cDNA samples were subjected to multiplex PCR amplification using primers designed to target the IGH CDR3 regions. The PCR products were then purified and assessed for quality before being used for library construction. After preparing the libraries, they were sent to BGI Genomics (Shenzhen, China) for next-generation sequencing. High-throughput sequencing was performed using an Illumina NovaSeq 6000 platform to generate paired-end 150-bp reads.

Pre-processing of raw sequencing data

We utilized the cDNA library sequencing data in FASTQ format for the multiplex PCR-based BCR repertoire analysis. Initial quality assessment was performed using FastQC to evaluate the overall sequencing quality, checking for issues such as low-quality reads (phred score <20) and adapter contamination.

Reads that failed the quality assessment were trimmed using Trimmomatic v.0.39 to remove unwanted sequences. After ensuring the data quality, we used MiXCR software to identify BCR clonotypes, converting raw sequencing data into quantitative clonotype information. The MiXCR analysis pipeline included aligning the sequencing reads to the V, D, J, and C genes of B cell receptors from the IMGT (International ImMunoGeneTics) database. The aligned reads were then assembled to extract the CDR3 gene regions, essential for BCR repertoire analysis. Clonotypes were defined based on identical CDR3 nucleotide sequences in combination with V and J gene usage, following the software's default clonotype grouping parameters. To ensure quality and biological relevance, CDR3 amino acid sequences containing stop codons ("*") or gaps ("-") were excluded from downstream analysis. Each remaining clonotype thus represented a unique and productive BCR rearrangement. For further analysis, we utilized Immunarch to convert MiXCR's output into a text file formatted for downstream analysis of BCR repertoire dynamics and diversity.

Analysis of CDR3 sequences and diversity estimation

Comprehensive analyses of BCR CDR3 sequences were performed using the Immunarch package with default parameters. Key assessments included basic statistics, CDR3 length distribution, V(D)J gene segment usage, amino acid composition, clonotype richness, and evenness. BCR clonal diversity was estimated using D50 index. To identify conserved sequence motifs among the dominant MP-specific clonotypes, CDR3 amino acid sequences were submitted to the MEME Suite web server (https://meme-suite.org/meme/tools/meme). Motif discovery was conducted using default parameters, specifying the identification of up to three motifs.

Data statistics and visualization

All statistical analyses were performed using R. The Wilcoxon rank-sum test was applied for non-parametric comparisons to assess statistical significance between groups, as the data either did not follow a normal distribution or had a small sample size. P-values < 0.05 were considered statistically significant. For data visualization, various plots, including boxplots and bar charts, were generated using the ggplot2 package in R. Significant p-values were manually annotated on the plots using the ggpubr package.

Results

Serological characteristics and activated B Cell response in pediatric MP patients

A total of 202 patients diagnosed with MP infection were included in the study. The clinical characteristics of MP patients are summarized in Table 1. Among them, 197 patients had available data on white blood cell count, lymphocyte count, monocyte count, lymphocyte percentage, and monocyte percentage. The mean WBC count was $8.7 \pm 4.32 \times 10^9$/L. The lymphocyte count averaged $3.15 \pm 2.87 \times 10^9$/L, while the monocyte count was $0.65 \pm 0.39 \times 10^9$/L. The lymphocyte percentage was 35.41 ± 14.3%, and the monocyte percentage was 7.88 ± 3.73%, both within their respective reference ranges. Inflammatory markers were also assessed. C-reactive protein levels were available for 171 patients, with a mean value of 10.86 ± 15.87 mg/L, slightly exceeding the upper reference limit. Serum interleukin-6 levels were elevated, with a mean of 11.49 ± 11.58 pg/ml in 129 patients. Ferritin levels, measured in 171 patients, averaged 148.43 ± 94.18 μg/L, exceeding the reference range. Complement levels were measured in a subset of patients, with C3 at 1.19 ± 0.26 g/L and C4 at 0.29 ± 0.11 g/L, both within reference ranges.

The serological indicators of MP patients suggest an active state of immune response and inflammation. Flow cytometry analysis of peripheral blood B cell counts in 99 MP patients and 25 healthy children revealed that B cell numbers were significantly higher in MP patients compared to the HC group (Figures 1A, B), indicating that B cells may play an important role in the immune response during MP infection. A further retrospective analysis of immunoglobulin levels in 173 MP patients (Figures 1C–E) showed that the immunoglobulin levels were elevated in some patients, with 81, 34 and 11 patients having IgM, IgA, or IgG levels exceeding the reference range respectively. This suggests that MP infection may lead to abnormal fluctuations in immunoglobulin levels, providing further evidence for the involvement of B cells in the immune response to MP infection and potentially contributing to the progression of the disease.

TABLE 1 Clinical characteristics of patients diagnosed with MP infection.

Test Item	Measured Value	Reference Range	Sample Size
White Blood Cell Count (10^9/L)	8.7 ± 4.32	4.3-11.3	197
Lymphocyte Count (10^9/L)	3.15 ± 2.87	1.5-4.6	197
Monocyte Count (10^9/L)	0.65 ± 0.39	0.13-0.76	197
Lymphocyte Percentage (%)	35.41 ± 14.3	23-59	197
Monocyte Percentage (%)	7.88 ± 3.73	2-11	197
C-Reactive Protein (mg/L)	10.86 ± 15.87	0-10	171
Complement C4 (g/L)	0.29 ± 0.11	0.125-0.425	172
Complement C3 (g/L)	1.19 ± 0.26	0.8-1.5	157
Interleukin-6 (pg/ml)	11.49 ± 11.58	0-7	129
Ferritin (ug/L)	148.43 ± 94.18	7-142	171

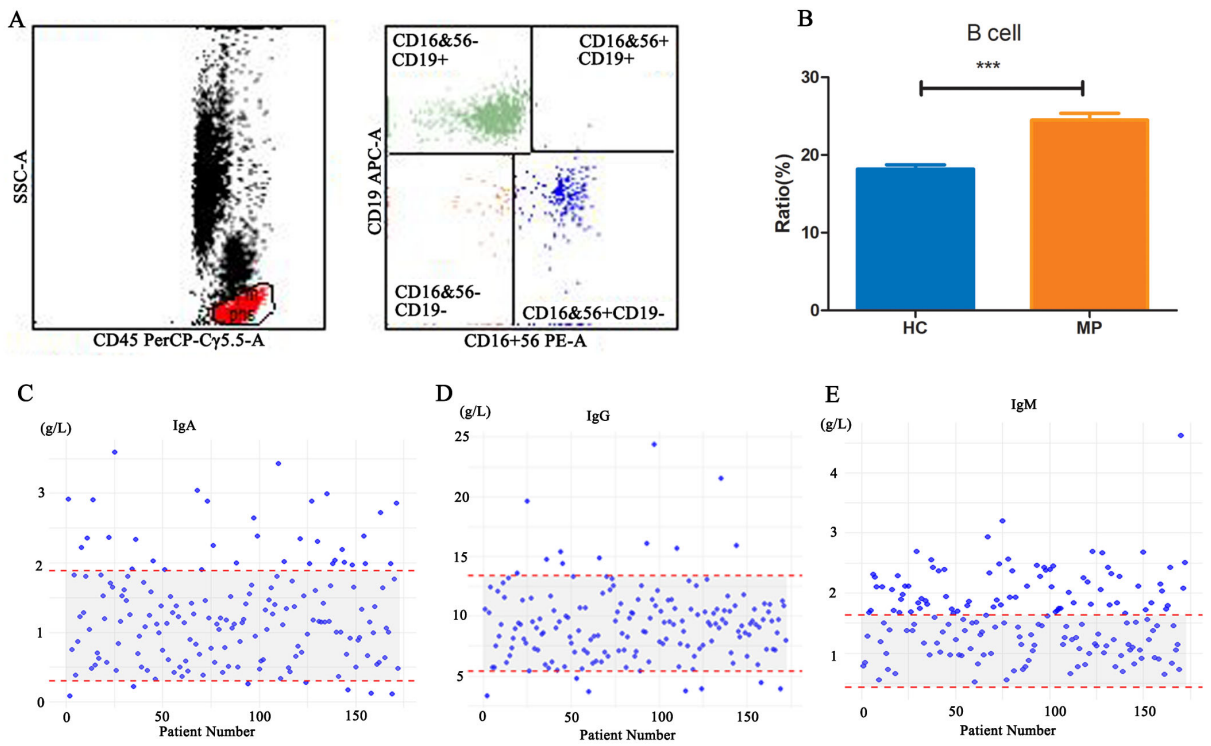

FIGURE 1
B cell counts and immunoglobulin levels in MP patients. **(A)** Representative flow cytometry gating strategy for identifying B cells in peripheral blood. **(B)** Comparison of peripheral blood B cell counts between MP patients (n=99) and healthy controls (HC, n=25). **(C-E)** Retrospective analysis of serum immunoglobulin levels (IgA, IgG, and IgM) in 173 MP patients. MP: Mycoplasma pneumoniae. HC: Healthy control. Data are presented as mean ± SEM. Statistical significance was determined using unpaired two-tailed Student's t-test. ***$p < 0.001$.

BCR heavy chain CDR3 repertoire analysis in pediatric MP patients

To further investigate BCR repertoire characteristics in pediatric MP patients, we analyzed the BCR heavy chain CDR3 repertoires from peripheral blood samples of eight MP patients and nine HC. After filtering the raw sequencing data, we randomly selected 100,000 clones from each sample for analysis. The proportion of unique clones relative to the total clone count was approximately 40% in both groups, with a higher percentage observed in the MP group compared to the HC group, though the difference was not statistically significant (Figure 2A).

Diversity analysis revealed a significantly higher diversity in the MP group than in the HC group (Figure 2B). Examination of the relative clone abundance indicated that both groups were predominantly composed of clones with Small and Medium frequencies (Figure 2C). Furthermore, analysis of the top clones demonstrated a high degree of similarity within each group (Figure 2D). Notably, the occupied repertoire space corresponding to clonotype indices of 101–1000 was significantly lower in the MP group than in the HC group, whereas the repertoire space occupied by clonotype indices exceeding 1000 was significantly higher in the MP group (Figure 2E). These findings suggest distinct BCR repertoire characteristics in MP patients, with increased diversity and alterations in clonotype distribution.

Preferential V and J gene usage in pediatric MP patients

To determine whether specific V or J gene segments exhibit preferential usage in pediatric MP patients, we analyzed their involvement in clonotype patterns compared to healthy controls. A total of 96 V genes were detected, and after filtering out those with low detection rates, we visualized the top 13 most frequently used V genes across all 17 samples using a heatmap (Figure 3A). The heatmap demonstrated distinct selective usage patterns of V genes between MP and HC groups, suggesting preferential selection of specific V segments in MP patients.

Further comparative analysis identified significant differences in the usage frequencies of IGHV1-18, IGHV4-39, IGHV4-4, IGHV5-10-1, and IGHV7-4–1 between the two groups (Figure 3B). Specifically, IGHV1–18 and IGHV7-4–1 were significantly enriched in the MP group compared to the HC group, whereas IGHV4-39, IGHV4-4, and IGHV5-10–1 showed significantly lower usage in MP patients. Principal component analysis (PCA) based on V gene usage frequencies further demonstrated a clear separation between MP and HC samples (Figure 3C).

Similarly, analysis of J gene usage revealed seven detectable J segments (Figure 3D). Among them, five J genes exhibited comparable usage frequencies between the two groups, whereas IGHJ4 was significantly underrepresented in the MP group, and

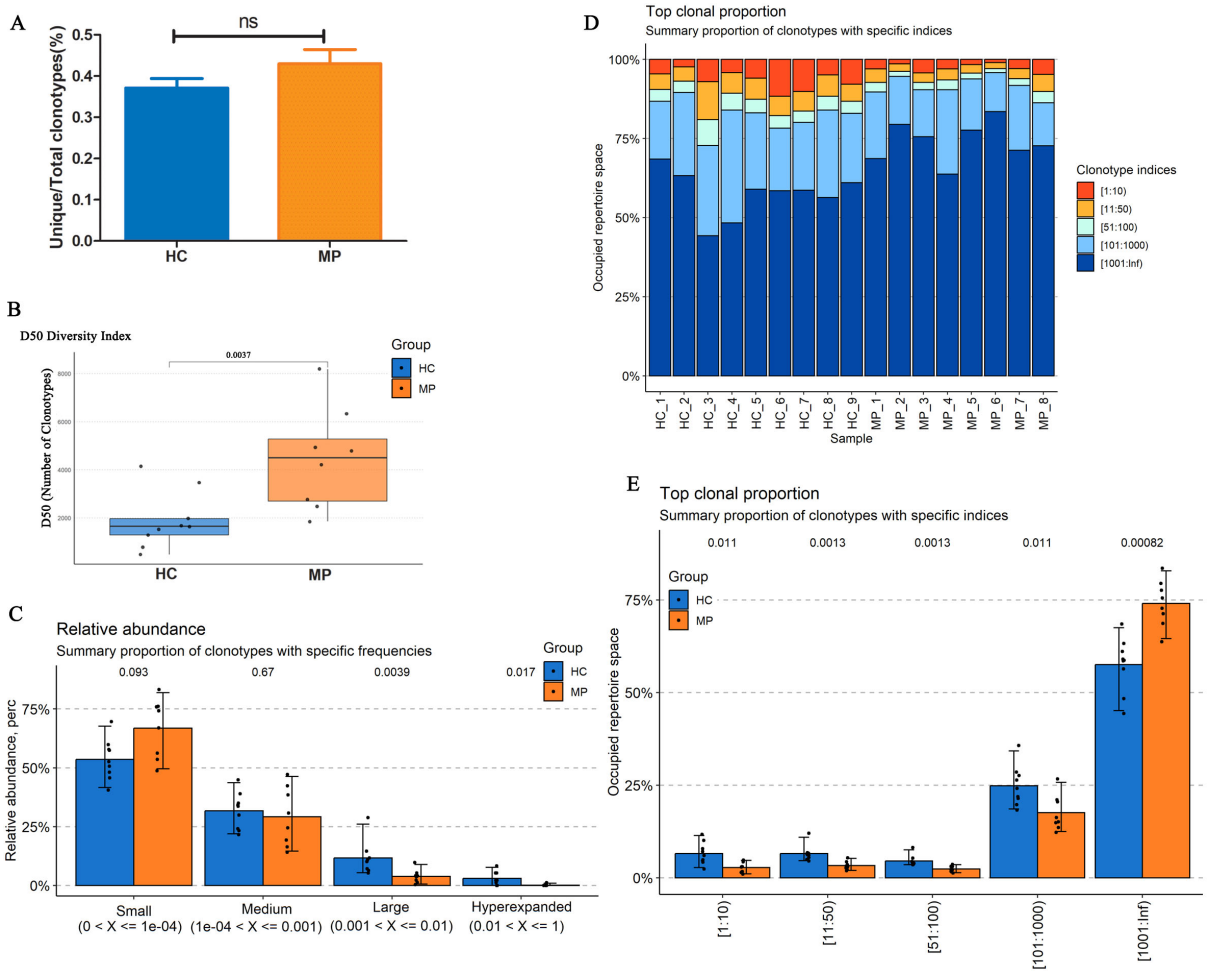

FIGURE 2
BCR heavy chain CDR3 repertoire diversity and clonotype distribution. **(A)** The proportion of unique BCR clones relative to the total clone count in MP and HC groups. **(B)** Diversity analysis revealed significantly increased BCR repertoire diversity in MP patients compared to HC. **(C)** Relative abundance distribution of BCR clonotypes. **(D)** Top clone analysis demonstrated a high degree of intra-group similarity. **(E)** Clonotype occupancy analysis. MP: Mycoplasma pneumoniae. HC: Healthy control. ns indicates no statistical difference. Data are presented as mean ± SEM. Statistical significance was determined using unpaired two-tailed Student's t-test. ns indicates no statistical difference. $P < 0.05$ indicates statistical difference.

IGHJ6 was significantly overrepresented in MP patients compared to HC (Figure 3E). PCA analysis based on J gene usage frequencies also showed a clear distinction between MP and HC groups, further reinforcing the presence of disease-associated differences in BCR repertoire composition (Figure 3F).

CDR3 length distribution and amino acid usage in pediatric MP patients

To further investigate the structural characteristics of the BCR heavy chain CDR3 repertoire, we analyzed the CDR3 length distribution and amino acid usage in MP patients and HC. The length distribution of unique CDR3 clonotypes exhibited distinct patterns between the two groups (Figure 4A). As expected, the HC group displayed a conventional bell-shaped distribution, with a peak at 15–17 amino acids. Interestingly, the MP group exhibited a bimodal distribution, with one peak at 15–17 amino acids, similar to the HC group, and an additional peak at 20–22 amino acids. Moreover, the average CDR3 length was significantly longer in MP patients (19.63 amino acids) compared to HC (17.27 amino acids), suggesting an altered selection process in the MP immune response.

Further quantitative analysis of CDR3 clonotype proportions at key length intervals revealed significant differences between the groups (Figure 4B). The proportion of CDR3 clonotypes with 15 and 16 amino acids was significantly higher in the HC group than in MP patients. In contrast, MP patients exhibited a significantly higher proportion of 21 and 22 amino acid-long CDR3 clonotypes, reinforcing the presence of an extended CDR3 repertoire in MP. Additionally, we analyzed amino acid usage within the CDR3 regions of both groups (Figure 4C). While the overall amino acid composition was largely similar, the frequency of methionine (M) usage was significantly different between MP and HC groups. These findings suggest that MP patients exhibit a distinct BCR repertoire characterized by an expanded CDR3

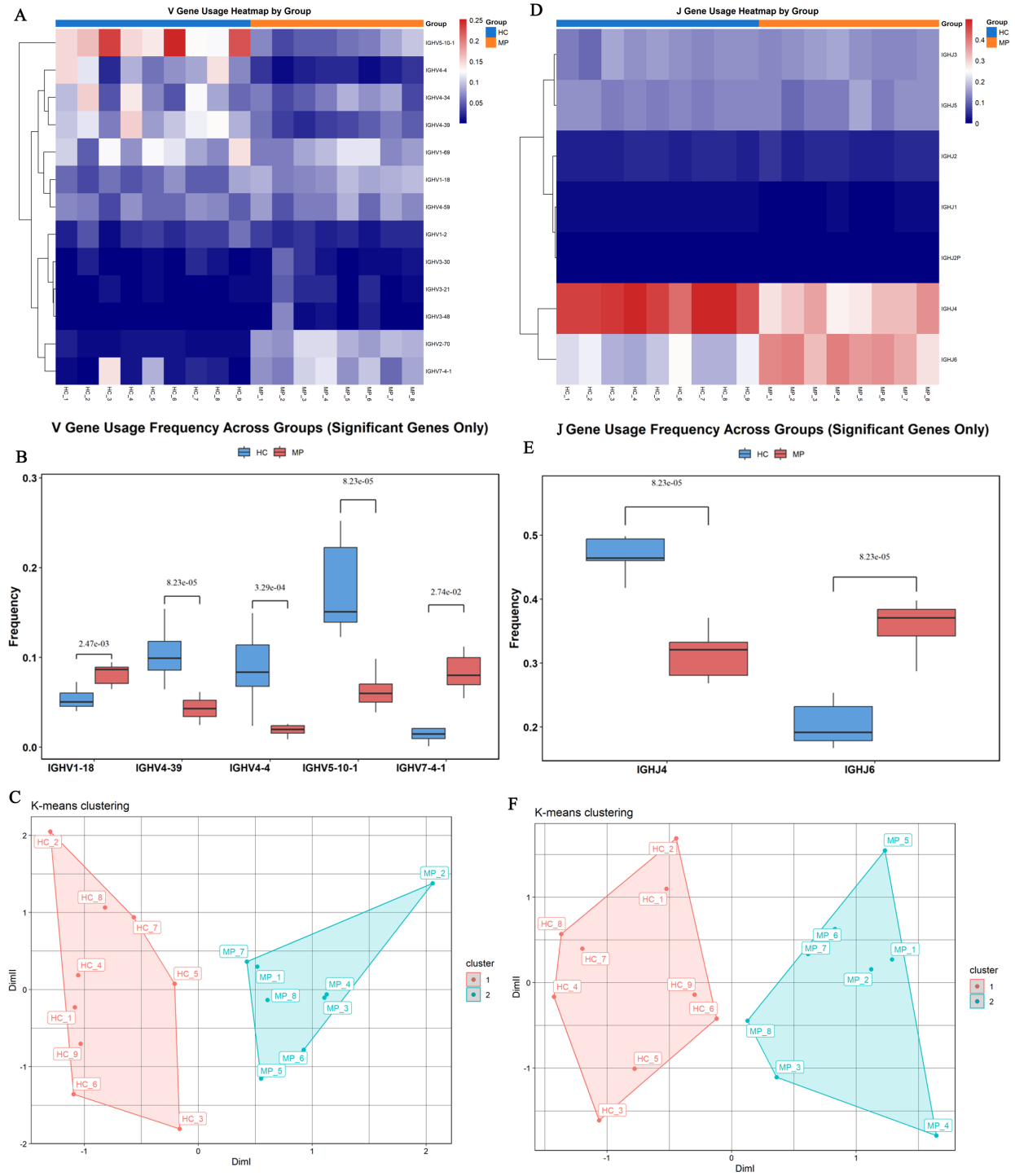

FIGURE 3
Preferential V and J gene usage. **(A)** Heatmap visualization of the top 13 most frequently used V genes across 17 samples. **(B)** Significant differences in V gene usage of top 13 most frequently used V genes. **(C)** Principal component analysis based on V gene usage showed clear separation between MP and HC samples. **(D)** Heatmap of J gene usage frequencies across all samples. **(E)** Identified significant differences in J gene usage. **(F)** Principal component analysis based on J gene usage demonstrated a clear distinction between MP and HC groups. MP, Mycoplasma pneumoniae; HC, Healthy control. Data are presented as mean ± SEM. Statistical significance was determined using unpaired two-tailed Student's t-test. $P < 0.05$ indicates statistical difference.

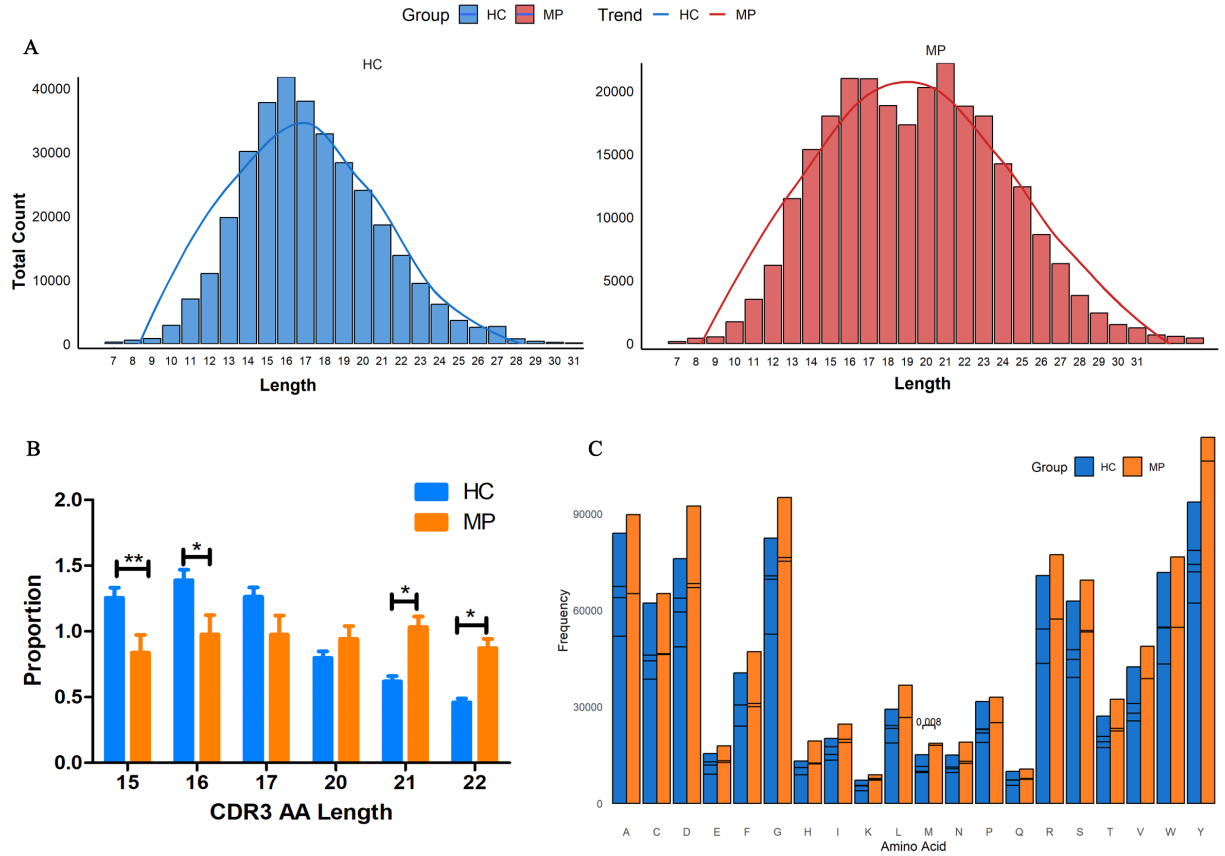

FIGURE 4
Altered CDR3 length distribution and amino acid usage. **(A)**CDR3 length distribution analysis revealed a conventional bell-shaped pattern in HC, whereas MP patients exhibited a bimodal distribution with an additional peak at 20–22 amino acids. **(B)** Quantification of CDR3 clonotypes at key length intervals. **(C)** Amino acid usage analysis within CDR3 regions between MP and HC groups. MP, Mycoplasma pneumoniae; HC, Healthy control. Data are presented as mean ± SEM. Statistical significance was determined using unpaired two-tailed Student's t-test. $P < 0.05$ indicates statistical difference. *$p < 0.05$, **$p < 0.001$.

length distribution and altered amino acid usage, which may contribute to disease-associated immune responses.

Disease-specific clonotypes in MP patients

To further explore the clonal architecture of the BCR repertoire in MP patients, we analyzed the degree of repertoire overlap among different samples (Figure 5A). The repertoire overlap heatmap revealed that certain clonotypes were shared among individuals, with the highest level of clonal sharing observed within the HC group, followed by the MP group. This suggests that healthy individuals maintain a more conserved BCR repertoire, whereas MP patients exhibit a more individualized immune response with distinct clonotypic expansions. To quantify the extent of shared and unique clonotypes between the two groups, we constructed an UpSet plot (Figure 5B), which demonstrated that 11,796 clonotypes were shared between MP and HC groups. This substantial overlap suggests the presence of a common baseline BCR repertoire that exists in both healthy and diseased states.

Next, we specifically examined intra-group clonal sharing within the MP cohort using another UpSet plot (Figure 5C). The results showed that the highest degree of sharing between two MP samples reached 2,213 clonotypes, while the maximum number of clonotypes shared across three MP samples was 559. Notably, a core set of 121 clonotypes was detected in all MP samples, suggesting a potential disease-associated repertoire.

To determine whether these 121 MP-specific clonotypes were also present in the HC group, we cross-referenced them against the HC dataset (Figure 5D). Among these, 53 clonotypes were also found in HC samples, leaving 68 clonotypes that were exclusively shared among MP patients but absent in HC individuals. These MP-specific clonotypes could represent disease-associated B cell expansions or antigen-driven immune responses unique to MP pathology. Further analysis of the 68 MP-exclusive clonotypes revealed substantial clonal amplification, suggesting their potential involvement in the immune response against MP. Among these, Figure 5E highlights the top 20 expanded clonotypes, with four clonotypes exhibiting extreme expansion (clone count >1,000). The most highly expanded clonotypes included: CARARAAAGFWYFDLW, CARPRDGFDIW, CARDDVHSWTTTGSFW, CAHVTYYDYVWGTSRPVHFDYW. To investigate whether these sequences shared common structural features, we performed motif analysis. Two conserved amino acid

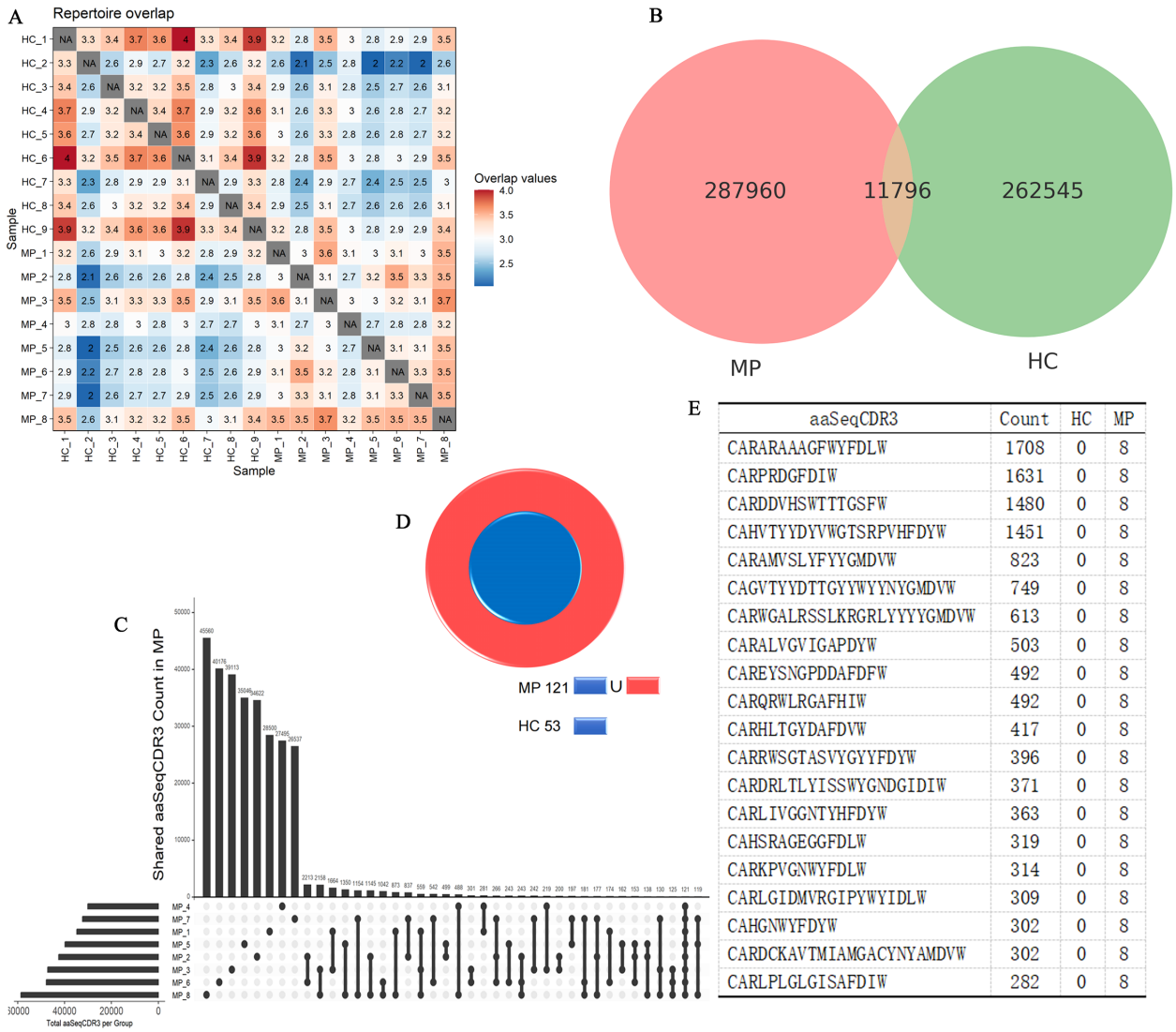

aaSeqCDR3	Count	HC	MP
CARARAAAGFWYFDLW	1708	0	8
CARPRDGFDIW	1631	0	8
CARDDVHSWTTTGSFW	1480	0	8
CAHVTYYDYVWGTSRPVHFDYW	1451	0	8
CARAMVSLYFYYGMDVW	823	0	8
CAGVTYYDTTGYYWYYNYGMDVW	749	0	8
CARWGALRSSLKRGRLYYYYGMDVW	613	0	8
CARALVGVIGAPDYW	503	0	8
CAREYSNGPDDAFDFW	492	0	8
CARQRWLRGAFHIW	492	0	8
CARHLTGYDAFDVW	417	0	8
CARRWSGTASVYGYYFDYW	396	0	8
CARDRLTLYISSWYGNDGIDIW	371	0	8
CARLIVGGNTYHFDYW	363	0	8
CAHSRAGEGGFDLW	319	0	8
CARKPVGNWYFDLW	314	0	8
CARLGIDMVRGIPYWYIDLW	309	0	8
CAHGNWYFDYW	302	0	8
CARDCKAVTMIAMGACYNYAMDVW	302	0	8
CARLPLGLGISAFDIW	282	0	8

FIGURE 5
Disease-specific BCR clonotypes in MP patients. **(A)** Heatmap of BCR repertoire overlap among MP and HC individuals. **(B)** UpSet plot illustrating shared and unique clonotypes between MP and HC groups. **(C)** UpSet plot illustrating shared and unique clonotypes among MP cohort. **(D)** Cross-referencing analysis identified 68 clonotypes exclusive to MP patients. **(E)** The top 20 expanded clonotypes that are shared among MP patients and absent in the HC group. MP, Mycoplasma pneumoniae; HC, Healthy control.

motifs, GNYGFDVW and CARARV, were identified among the dominant CDR3 sequences (Supplementary Figure S1). These motifs may reflect structural or functional convergence driven by antigen selection. The presence of such motifs, along with highly expanded clones, supports the notion of an antigen-driven B cell response in MP, potentially offering insights into MP-specific immunological memory or diagnostic biomarkers.

Discussion

The composition and diversity of the BCR repertoire play a crucial role in shaping the humoral immune response and influencing disease outcomes following bacterial infections (Hoehn et al., 2016; Guo et al., 2019). Previous studies have highlighted dynamic alterations in the BCR repertoire in response to various pathogens, such as Streptococcus pneumoniae (Morgan et al., 2024) and Haemophilus influenzae (Truck et al., 2015). Moreover, the expansion and persistence of specific BCR clonotypes during chronic infections illustrate the evolving nature of the adaptive immune response (Florova et al., 2024; Jin et al., 2024). Our study demonstrates significant changes in the BCR repertoire of MP-infected children, suggesting that Mycoplasma pneumoniae infection induces a highly dynamic B cell response. Understanding BCR diversity and clonal expansion in this context may provide valuable insights into disease severity, immune protection, and potential therapeutic strategies.

Our findings demonstrate a significant increase in total B cell counts and serum immunoglobulin levels in MP-infected patients, indicating an enhanced humoral immune response. This is

consistent with previous studies suggesting that MP infection triggers robust B cell activation and antibody production as a critical component of host defense (Simecka et al., 1993; Meyer Sauteur et al., 2020). Notably, we observed abnormalities in immunoglobulin levels, with IgM showing the most significant changes. This predominance of IgM elevation may be due to the early and primary nature of the humoral immune response against Mycoplasma pneumoniae infection. Since IgM is the first antibody isotype produced during an initial immune response (Jones et al., 2020), its higher levels likely reflect active B cell stimulation in response to persistent MP antigens (Dong et al., 2017). However, fewer abnormalities were observed in IgG and IgA levels, likely due to their limited antigen exposure history and immature germinal center reactions, which delay efficient IgG class-switching. In contrast, adults typically mount faster IgG-dominated responses owing to pre-existing memory B cells and well-developed secondary lymphoid structures (Semmes et al., 2020).

BCR repertoire analysis revealed significant differences in diversity indices between MP-infected and control groups. Notably, the BCR diversity in MP patients exhibited an overall increase, as reflected by the higher D50 index. This finding contrasts with the commonly observed decrease in diversity following SARS-CoV-2 (Xiao et al., 2024) or Pneumocystis (Sun et al., 2021) infections, where immune responses are often characterized by a contraction of the repertoire due to clonal expansion of pathogen-specific B cells. This could suggest that MP infection triggers the activation of a wider range of B cell clones, potentially to generate antibodies against a diverse array of epitopes on the pathogen. Further investigations into the specific characteristics of these expanded B cell clones, including their functional roles and antigen specificity, are needed to better understand the nature of the immune response in MP-infected individuals and how it differs from other bacterial or viral infections.

Our study identified distinct V and J gene usage patterns in MP-infected patients compared to healthy controls. Several V gene families, including IGHV1-18, IGHV3–23 and IGHV7-4, exhibited significantly higher usage frequencies, suggesting preferential selection in response to MP infection. The enrichment of these specific V gene families aligns with previous studies reporting their involvement in immune responses against pathogens. For example, IGHV1–18 has been identified as the germline origin of HmAb64, an antibody with a 15-amino-acid CDR H3, which neutralized 10% (20 out of 208) of cross-clade HIV-1 pseudoviruses, including tier 2 strains from clades B, BC, C, and G (Wang et al., 2024). Additionally, IGHV1–18 usage was significantly elevated in human B cells following dengue virus infection (Godoy-Lozano et al., 2016). IGHV3-23-IGHJ4 pairing has been associated with a monoclonal response specific to SARS-CoV-2 infection (Wen et al., 2020). Transcriptomic analysis of mixed peripheral blood mononuclear cells from moderate and severe SARS-CoV-2 patients revealed a significant upregulation of IGHV7–4 expression (Khalid et al., 2022). Furthermore, the observed differences in J gene segment usage, particularly the increased utilization of IGHJ6 and decreased utilization of IGHJ4. Both IGHJ4 and IGHJ6 have been reported to exhibit CDR-H3 loop length-dependent usage in the natural human immune repertoire (Wang et al., 2021), indicating their involvement in shaping antigen specificity. Notably, IGHJ6 has also been reported to be highly utilized in patients with SARS-CoV-2 infection (Zhou et al., 2021). Interestingly, while previous studies have shown that IGHJ4 is preferentially utilized across various immune-related conditions, including autoimmune diseases (Hirokawa et al., 2019), cancers (Katsibardi et al., 2011), and infectious diseases (Andreano et al., 2021), our study found a distinct pattern. Although IGHJ4 still exhibited biased usage in MP-infected patients, its overall frequency was lower than in healthy controls. Further investigations are needed to determine whether the altered IGHJ4 and IGHJ6 usage impacts BCR functionality and contributes to the immune response differences observed in MP infection.

The value of CDR3 length analysis lies in its ability to reflect the diversity of the TCR and Ig repertoire, revealing immune clone distribution patterns across individuals and over time (Miqueu et al., 2007). In this study, CDR3 length distribution analysis revealed a shift towards longer CDR3 sequences in MP-infected patients, which is commonly associated with increased antigen specificity and affinity maturation. For example, in IgG4-related disease (IgG4-RD), the length distribution of IgG4-RD-specific CDR3 amino acid sequences was skewed towards longer fragments (Wang et al., 2019). Notably, ultra-long CDR3 regions have been observed in certain species, such as cattle, where extensive somatic hypermutation generates a high degree of diversity. These long CDR3 sequences enable cattle to mount particularly strong immune responses against viral antigens, including broadly neutralizing responses to stable HIV gp140 trimers (Stanfield et al., 2018; Deiss et al., 2019). The shift towards longer CDR3 sequences in MP-infected patients observed in our study may similarly reflect an adaptive mechanism to enhance antigen recognition and immune response effectiveness.

During pathogen infection, the expansion and proliferation of BCRs are driven by interactions with pathogen-specific antigens (Tian et al., 2017; St John and Rathore, 2019). The immune response is triggered by both bacterial proteins and host-derived factors, leading to the selective proliferation of specific BCR clonotypes (Ngono and Shresta, 2018; Lee et al., 2022). The key finding of our study is the identification of disease-specific clonotypes that were significantly enriched in MP-infected patients. Several high-frequency clonotypes were exclusively detected in the MP group, suggesting their potential role as biomarkers for MP infection. The persistence of these clonotypes in multiple patients implies a conserved immune response to MP, which may be leveraged for diagnostic or therapeutic purposes. Additionally, the expanded clones exhibited convergent recombination patterns, indicating a shared immune response across individuals (Nielsen et al., 2020). These results highlight the potential of BCR repertoire analysis for identifying infection-specific immune signatures and advancing our understanding of host-pathogen interactions in MP infection.

Despite providing valuable insights into the IGH CDR3 repertoire of MP-infected patients, several limitations must be acknowledged to contextualize our findings. First, the sample size

in this study was relatively small, which may limit the statistical power and generalizability of the results. Additionally, our study was cross-sectional, which restricts the ability to assess the temporal dynamics of TCR and Ig repertoires over the course of infection. Longitudinal studies are needed to track changes in immune repertoire diversity and its correlation with clinical outcomes over time. Addressing these limitations in future research would improve the robustness of the findings and provide a more comprehensive understanding of immune responses in MP infection.

In conclusion, our study provides novel insights into the humoral immune response to *Mycoplasma pneumoniae* infection by integrating serological markers, B cell counts, and BCR heavy chain CDR3 repertoire analysis. We identified increased B cell activation, elevated inflammatory and immunoglobulin markers, and significant changes in BCR diversity, gene usage preferences, CDR3 length distribution, and disease-specific clonotypes. These alterations, particularly the identification of MP-exclusive clonotypes and biased usage of IGHV and IGHJ genes, enhance our understanding of the immunopathology of MP infection. Importantly, these findings may contribute to the development of improved diagnostic and therapeutic strategies. For instance, the MP-specific public clonotypes or stereotyped BCR features identified in this study may serve as potential biomarkers for early diagnosis or disease monitoring. Additionally, repertoire characteristics associated with disease could inform precision immunotherapy design and provide novel targets for B cell–modulating interventions in pediatric MP.

Data availability statement

The datasets presented in this study can be found in online repositories. The names of the repository/repositories and accession number(s) can be found in the article/Supplementary Material.

Ethics statement

The study was approved by the Institutional Review Board of Kunming Children's Hospital (Approval No: 2023-03-246-K01), and written consent was obtained from the parents or guardians of all pediatric patients. This research adhered to the ethical principles set forth in the Declaration of Helsinki. The studies were conducted in accordance with the local legislation and institutional requirements. Written informed consent for participation in this study was provided by the participants' legal guardians/next of kin.

Author contributions

YC: Conceptualization, Data curation, Formal Analysis, Methodology, Project administration, Software, Writing – original draft. YY: Data curation, Formal Analysis, Investigation, Methodology, Software, Writing – original draft. XL: Data curation, Formal Analysis, Resources, Software, Writing – original draft. BL: Data curation, Investigation, Methodology, Software, Writing – original draft. LM: Data curation, Formal Analysis, Methodology, Resources, Writing – review & editing. YX: Data curation, Methodology, Resources, Software, Writing – review & editing. ZS: Conceptualization, Data curation, Investigation, Validation, Writing – review & editing. LH: Data curation, Investigation, Resources, Writing – review & editing. HL: Investigation, Methodology, Resources, Writing – review & editing. LD: Data curation, Formal Analysis, Investigation, Writing – review & editing. JL: Conceptualization, Project administration, Supervision, Writing – review & editing, Writing – original draft. CY: Conceptualization, Investigation, Project administration, Supervision, Validation, Visualization, Writing – review & editing. XZ: Conceptualization, Funding acquisition, Investigation, Supervision, Visualization, Writing – original draft, Writing – review & editing.

Funding

The author(s) declare that financial support was received for the research and/or publication of this article. This study was supported by Health research project of Kunming Health Commission (No.2023-06-01-004), Kunming "Spring City Plan" High-level talent introduced by the Engineering Young Talents Special Project, and Basic Research Special General Project of Yunnan Provincial Department of Science and Technology (No.202401AT070263).

Acknowledgments

The authors would like to thank the medical staff and researchers at Kunming Children's Hospital for their support in patient recruitment and sample collection. We also sincerely appreciate the volunteers who generously provided samples for this study.

Conflict of interest

The authors declare that the research was conducted in the absence of any commercial or financial relationships that could be construed as a potential conflict of interest.

Generative AI statement

The author(s) declare that no Generative AI was used in the creation of this manuscript.

Publisher's note

All claims expressed in this article are solely those of the authors and do not necessarily represent those of their affiliated

organizations, or those of the publisher, the editors and the reviewers. Any product that may be evaluated in this article, or claim that may be made by its manufacturer, is not guaranteed or endorsed by the publisher.

Supplementary material

The Supplementary Material for this article can be found online at: https://www.frontiersin.org/articles/10.3389/fcimb.2025.1573511/full#supplementary-material

References

Andreano, E., Paciello, I., Piccini, G., Manganaro, N., Pileri, P., Hyseni, I., et al. (2021). Hybrid immunity improves B cells and antibodies against SARS-CoV-2 variants. *Nature* 600, 530–535. doi: 10.1038/s41586-021-04117-7

Atkinson, T. P., Balish, M. F., and Waites, K. B. (2008). Epidemiology, clinical manifestations, pathogenesis and laboratory detection of Mycoplasma pneumoniae infections. *FEMS Microbiol. Rev.* 32, 956–973. doi: 10.1111/j.1574-6976.2008.00129.x

Casadevall, A., Feldmesser, M., and Pirofski, L. A. (2002). Induced humoral immunity and vaccination against major human fungal pathogens. *Curr. Opin. Microbiol.* 5, 386–391. doi: 10.1016/s1369-5274(02)00337-5

Choi, Y. J., Chung, E. H., Lee, E., Kim, C. H., Lee, Y. J., Kim, H. B., et al. (2022). Clinical characteristics of macrolide-refractory mycoplasma pneumoniae pneumonia in korean children: A multicenter retrospective study. *J. Clin. Med.* 11 (2), 306. doi: 10.3390/jcm11020306

Deiss, T. C., Vadnais, M., Wang, F., Chen, P. L., Torkamani, A., Mwangi, W, et al. (2019). Immunogenetic factors driving formation of ultralong VH CDR3 in Bos taurus antibodies. *Cell Mol. Immunol.* 16, 53–64. doi: 10.1038/cmi.2017.117

Dong, Y., Lv, W., and Lin, Z. (2017). Value of serum Mycoplasma pneumoniae immunoglobulin in the diagnosis of mycoplasma-related pneumonia in newborns. *Exp. Ther. Med.* 14, 1445–1449. doi: 10.3892/etm.2017.4654

Fan, X., Li, N., Xu, M., Yang, D., and Wang, B. (2021). Intrapulmonary vaccination induces long-lasting and effective pulmonary immunity against *staphylococcus aureus* pneumonia. *J. Infect. Dis.* 224, 903–913. doi: 10.1093/infdis/jiab012

Florova, M., Abreu-Mota, T., Paesen, G. C., Beetschen, A. S., Cornille, K., Marx, A. F., et al. (2024). Central tolerance shapes the neutralizing B cell repertoire against a persisting virus in its natural host. *Proc. Natl. Acad. Sci. U.S.A.* 121, e2318657121. doi: 10.1073/pnas.2318657121

Godoy-Lozano, E. E., Tellez-Sosa, J., Sanchez-Gonzalez, G., Sámano Sánchez, H., Aguilar Salgado, A., Salinas Rodríguez, A., et al. (2016). Lower IgG somatic hypermutation rates during acute dengue virus infection is compatible with a germinal center-independent B cell response. *Genome Med.* 8, 23. doi: 10.1186/s13073-016-0276-1

Guo, Y., Chen, K., Kwong, P. D., Shapiro, L., and Sheng, Z. (2019). cAb-rep: A database of curated antibody repertoires for exploring antibody diversity and predicting antibody prevalence. *Front. Immunol.* 10. doi: 10.3389/fimmu.2019.02365

He, B., Liu, S., Xu, M., Hu, Y., Lv, K., Wang, Y., et al. (2022). Comparative global B cell receptor repertoire difference induced by SARS-CoV-2 infection or vaccination via single-cell V(D)J sequencing. *Emerg. Microbes Infect.* 11, 2007–2020. doi: 10.1080/22221751.2022.2105261

Hirokawa, M., Fujishima, N., Togashi, M., Saga, A., Omokawa, A., Saga, T., et al. (2019). High-throughput sequencing of IgG B-cell receptors reveals frequent usage of the rearranged IGHV4-28/IGHJ4 gene in primary immune thrombocytopenia. *Sci. Rep.* 9, 8645. doi: 10.1038/s41598-019-45264-2

Hoehn, K. B., Fowler, A., Lunter, G., and Pybus, O. G. (2016). The diversity and molecular evolution of B-cell receptors during infection. *Mol. Biol. Evol.* 33, 1147–1157. doi: 10.1093/molbev/msw015

Jin, Y., He, Y., Liu, B., Zhang, X., Song, C., Wu, Y., et al. (2024). Single-cell RNA sequencing reveals the dynamics and heterogeneity of lymph node immune cells during acute and chronic viral infections. *Front. Immunol.* 15. doi: 10.3389/fimmu.2024.1341985

Jones, K., Savulescu, A. F., Brombacher, F., and Hadebe, S. (2020). Immunoglobulin M in health and diseases: how far have we come and what next? *Front. Immunol.* 11. doi: 10.3389/fimmu.2020.595535

Katsibardi, K., Braoudaki, M., Papathanasiou, C., Karamolegou, K., and Tzortzatou-Stathopoulou, F. (2011). Clinical significance of productive immunoglobulin heavy chain gene rearrangements in childhood acute lymphoblastic leukemia. *Leuk Lymphoma* 52, 1751–1757. doi: 10.3109/10428194.2011.582907

Khalid, Z., Huan, M., Sohail Raza, M., Abbas, M., Naz, Z., Kombe Kombe, A. J., et al. (2022). Corrigendum: Identification of novel therapeutic candidates against SARS-CoV-2 infections: An application of RNA sequencing toward mRNA based nanotherapeutics. *Front. Microbiol.* 13. doi: 10.3389/fmicb.2022.1059437

Kotagiri, P., Mescia, F., Rae, W. M., Bergamaschi, L., Tuong, Z. K., Turner, L., et al. (2022). B cell receptor repertoire kinetics after SARS-CoV-2 infection and vaccination. *Cell Rep.* 38, 110393. doi: 10.1016/j.celrep.2022.110393

Kutty, P. K., Jain, S., Taylor, T. H., Bramley, A. M., Diaz, M. H., Ampofo, K., et al. (2019). Mycoplasma pneumoniae among children hospitalized with community-acquired pneumonia. *Clin. Infect. Dis.* 68, 5–12. doi: 10.1093/cid/ciy419

Lee, M. F., Voon, G. Z., Lim, H. X., Chua, M. L., and Poh, C. L. (2022). Innate and adaptive immune evasion by dengue virus. *Front. Cell Infect. Microbiol.* 12. doi: 10.3389/fcimb.2022.1004608

Li, M., Wei, X., Zhang, S. S., Li, S., Chen, S. H., Shi, S. J., et al. (2023). Recognition of refractory Mycoplasma pneumoniae pneumonia among Myocoplasma pneumoniae pneumonia in hospitalized children: development and validation of a predictive nomogram model. *BMC Pulm Med.* 23, 383. doi: 10.1186/s12890-023-02684-1

Li, Y., Wu, M., Liang, Y., Yang, Y., Guo, W., Deng, Y., et al. (2024). Mycoplasma pneumoniae infection outbreak in Guangzhou, China after COVID-19 pandemic. *Virol. J.* 21, 183. doi: 10.1186/s12985-024-02458-z

Li, Z. J., Zhang, H. Y., Ren, L. L., Lu, Q. B., Ren, X., Zhang, C. H., et al. (2021). Etiological and epidemiological features of acute respiratory infections in China. *Nat. Commun.* 12, 5026. doi: 10.1038/s41467-021-25120-6

Mai, G., Zhang, C., Lan, C., Zhang, J., Wang, Y., Tang, K., et al. (2023). Characterizing the dynamics of BCR repertoire from repeated influenza vaccination. *Emerg. Microbes Infect.* 12, 2245931. doi: 10.1080/22221751.2023.2245931

Meyer Sauteur, P. M., Truck, J., van Rossum, A. M. C., and Berger, C. (2020). Circulating antibody-secreting cell response during mycoplasma pneumoniae childhood pneumonia. *J. Infect. Dis.* 222, 136–147. doi: 10.1093/infdis/jiaa062

Miqueu, P., Guillet, M., Degauque, N., Doré, J. C., Soulillou, J. P., and Brouard, S. (2007). Statistical analysis of CDR3 length distributions for the assessment of T and B cell repertoire biases. *Mol. Immunol.* 44, 1057–1064. doi: 10.1016/j.molimm.2006.06.026

Miwa, H., Antao, O. Q., Kelly-Scumpia, K. M., Baghdasarian, S., Mayer, D. P., Shang, L., et al. (2023). Improved humoral immunity and protection against influenza virus infection with a 3d porous biomaterial vaccine. *Adv. Sci. (Weinh)* 10, e2302248. doi: 10.1002/advs.202302248

Morgan, D. M., Zhang, Y. J., Kim, J. H., Murillo, M., Singh, S., Loschko, J., et al. (2024). Full-length single-cell BCR sequencing paired with RNA sequencing reveals convergent responses to pneumococcal vaccination. *Commun. Biol.* 7, 1208. doi: 10.1038/s42003-024-06823-0

Ngono, A. E., and Shresta, S. (2018). Immune response to dengue and zika. *Annu. Rev. Immunol.* 36, 279–308. doi: 10.1146/annurev-immunol-042617-053142

Nielsen, S. C. A., Yang, F., Jackson, K. J. L., Hoh, R. A., Röltgen, K., Jean, G. H., et al. (2020). Human B cell clonal expansion and convergent antibody responses to SARS-cov-2. *Cell Host Microbe* 28, 516–25.e5. doi: 10.1016/j.chom.2020.09.002

Ollila, J., and Vihinen, M. (2005). B cells. *Int. J. Biochem. Cell Biol.* 37, 518–523. doi: 10.1016/j.biocel.2004.09.007

Papavasiliou, F., Casellas, R., Suh, H., Qin, X. F., Besmer, E., Pelanda, R., et al. (1997). V(D)J recombination in mature B cells: a mechanism for altering antibody responses. *Science* 278, 298–301. doi: 10.1126/science.278.5336.298

Semmes, E. C., Chen, J. L., Goswami, R., et al. (2020). Understanding early-life adaptive immunity to guide interventions for pediatric health. *Front. Immunol.* 11. doi: 10.3389/fimmu.2020.595297

Simecka, J. W., Ross, S. E., Cassell, G. H., and Davis, J. K. (1993). Interactions of mycoplasmas with B cells: antibody production and nonspecific effects. *Clin. Infect. Dis.* 17 Suppl 1, S176–S182. doi: 10.1093/clinids/17.supplement_1.s176

Spisak, N., Athenes, G., Dupic, T., Mora, T., and Walczak, A. M. (2024). Combining mutation and recombination statistics to infer clonal families in antibody repertoires. *Elife* 13 (2), 306. doi: 10.7554/eLife.86181

Stanfield, R. L., Haakenson, J., Deiss, T. C., Criscitiello, M. F., Wilson, I. A., and Smider, V. V. (2018). The unusual genetics and biochemistry of bovine immunoglobulins. *Adv. Immunol.* 137, 135–164. doi: 10.1016/bs.ai.2017.12.004

St John, A. L., and Rathore, A. P. S. (2019). Adaptive immune responses to primary and secondary dengue virus infections. *Nat. Rev. Immunol.* 19, 218–230. doi: 10.1038/s41577-019-0123-x

Sun, H., Yang, H. Q., Zhai, K., and Tong, Z. H. (2021). Signatures of B cell receptor repertoire following pneumocystis infection. *Front. Microbiol.* 12. doi: 10.3389/fmicb.2021.636250

Tian, Y., Babor, M., Lane, J., Schulten, V., Patil, V. S., Seumois, G., et al. (2017). Unique phenotypes and clonal expansions of human CD4 effector memory T cells re-expressing CD45RA. *Nat. Commun.* 8, 1473. doi: 10.1038/s41467-017-01728-5

Truck, J., Ramasamy, M. N., Galson, J. D., Rance, R., Parkhill, J., Lunter, G., et al. (2015). Identification of antigen-specific B cell receptor sequences using public repertoire analysis. *J. Immunol.* 194, 252–261. doi: 10.4049/jimmunol.1401405

Waites, K. B., and Talkington, D. F. (2004). Mycoplasma pneumoniae and its role as a human pathogen. *Clin. Microbiol. Rev.* 17, 697–728. doi: 10.1128/CMR.17.4.697-728.2004

Waites, K. B., Xiao, L., Liu, Y., Balish, M. F., and Atkinson, T. P. (2017). Mycoplasma pneumoniae from the respiratory tract and beyond. *Clin. Microbiol. Rev.* 30, 747–809. doi: 10.1128/CMR.00114-16

Wang, S., Chan, K. W., Wei, D., Ma, X., Liu, S., Hu, G., et al. (2024). Human CD4-binding site antibody elicited by polyvalent DNA prime-protein boost vaccine neutralizes cross-clade tier-2-HIV strains. *Nat. Commun.* 15, 4301. doi: 10.1038/s41467-024-48514-8

Wang, H., Yan, K., Wang, R., Yang, Y., Shen, Y., Yu, C., et al. (2021). Antibody heavy chain CDR3 length-dependent usage of human IGHJ4 and IGHJ6 germline genes. *Antib Ther.* 4, 101–108. doi: 10.1093/abt/tbab010

Wang, L., Zhang, P., Li, J., et al. (2019). High-throughput sequencing of CD4(+) T cell repertoire reveals disease-specific signatures in IgG4-related disease. *Arthritis Res. Ther.* 21, 295. doi: 10.1186/s13075-019-2069-6

Wen, W., Su, W., Tang, H., Le, W., Zhang, X., Zheng, Y., et al. (2020). Immune cell profiling of COVID-19 patients in the recovery stage by single-cell sequencing. *Cell Discov.* 6, 31. doi: 10.1038/s41421-020-0168-9

Xiao, J., Luo, Y., Li, Y., and Yao, X. (2024). The characteristics of BCR-CDR3 repertoire in COVID-19 patients and SARS-CoV-2 vaccinated volunteers. *J. Med. Virol.* 96, e29488. doi: 10.1002/jmv.29488

Zhang, Z., Dou, H., Tu, P., Shi, D., Wei, R., Wan, R., et al. (2022). Serum cytokine profiling reveals different immune response patterns during general and severe Mycoplasma pneumoniae pneumonia. *Front. Immunol.* 13. doi: 10.3389/fimmu.2022.1088725

Zhou, Y., Zhang, J., Wang, D., Wang, D., Guan, W., Qin, J., et al. (2021). Profiling of the immune repertoire in COVID-19 patients with mild, severe, convalescent, or retesting-positive status. *J. Autoimmun* 118, 102596. doi: 10.1016/j.jaut.2021.102596

Zhu, Y., Luo, Y., Li, L., Jiang, X., Du, Y., Wang, J., et al. (2023). Immune response plays a role in Mycoplasma pneumoniae pneumonia. *Front. Immunol.* 14, 1189647. doi: 10.3389/fimmu.2023.1189647

frontiers | Frontiers in Cellular and Infection Microbiology

TYPE Mini Review
PUBLISHED 23 July 2025
DOI 10.3389/fcimb.2025.1547525

OPEN ACCESS

EDITED BY
Oscar Gutierrez-Coronado,
University of Guadalajara, Mexico

REVIEWED BY
Mairaj Ahmed Ansari,
Jamia Hamdard University, India
Paula Pérez,
CONICET Instituto de Investigaciones Biomédicas en Retrovirus y SIDA (INBIRS), Argentina

*CORRESPONDENCE
Yan Ran
164013043@qq.com

RECEIVED 18 December 2024
ACCEPTED 02 July 2025
PUBLISHED 23 July 2025

CITATION
Yuan X, Huang C and Ran Y (2025) Exosome in HBV infection: current concepts and future perspectives. *Front. Cell. Infect. Microbiol.* 15:1547525. doi: 10.3389/fcimb.2025.1547525

Exosome in HBV infection: current concepts and future perspectives

XueLan Yuan[1], ChunXia Huang[2] and Yan Ran[3]*

[1]Health Management Center, Fengdu General Hospital, Fengdu County, Chongqing, China,
[2]Department of Gastroenterology, Fengdu General Hospital, Fengdu County, Chongqing, China,
[3]Department of Infectious Diseases, Fengdu General Hospital, Fengdu County, Chongqing, China

Exosomes are nanoparticles delimited by a lipid bilayer that are secreted by a wide variety of cells. They play a significant role in the pathophysiological processes associated with HBV infection, which poses huge burdens for public health. Emerging evidence has been demonstrated that exosomes are extensively associated with the replication and transmission processes of HBV. In this review, we outline the process of exosome production, composition and function. Moreover, we elaborate on the essential role of exosomes in the pathology processes of HBV infection. Exosomes could serve as essential biomarkers for early detection of HBV infection and HBV-related diseases. Finally, we outline the therapeutic potential of exosomes in anti-HBV therapy, which may provide novel insights into the prevention and treatment of HBV.

KEYWORDS

HBV, exosome, immune response, virus infection, therapy

1 Introduction

Hepatitis B virus (HBV) is a specific small hepatotropic DNA virus responsible for hepatitis B, currently recognized as the most prevalent serious liver infection worldwide (Shih et al., 2018; Zheng et al., 2024). Chronic hepatitis B virus infections impact approximately 250 million individuals worldwide (Lai-Hung Wong and Lemoine, 2024). As a hepatotropic virus, HBV often progresses to cirrhosis and hepatocellular carcinoma (HCC) in patients with high HBV DNA (Starnawski et al., 2025). Globally, 60% to 80% of HCC cases are attributed to HBV infection (Starnawski et al., 2025). Additionally, approximately 70% of cirrhosis cases are caused by HBV (Zhang S. et al., 2025). Despite the development of effective preventive vaccines and oral antiviral medications, chronic HBV infection continues to be a significant underlying or contributing factor to a considerable health burden (Bixler et al., 2019).

Extracellular vesicles (EVs) are nanoscale membrane vesicles released actively by cells (Colombo et al., 2014). Based on their biogenesis, size, and biophysical properties, they can be further classified into subtypes such as exosomes and microvesicles (Wang et al., 2025). Initially regarded merely as cellular debris, EVs are increasingly recognized as important mediators of intercellular communication and significant carriers of circulating biomarkers for disease

diagnosis and prognosis (Lorite et al., 2024; Zhang L. et al., 2025). Exosomes are derived from endosomal origins and typically range in size from approximately 40 to 160 nm in diameter, with an average size of around 100 nm (Krylova and Feng, 2023). All exosomes carry a variety of active substances, including proteins, lipids, and nucleic acids, and are crucial for intercellular communication when released into the extracellular environment (Colombo et al., 2014; Welsh et al., 2024). They function as cargo vehicles in various biological fluids, such as serum, plasma, urine, saliva, breast milk, pleural effusions, bronchoalveolar lavage fluid, epididymal fluid, and amniotic fluid (Kalluri and LeBleu, 2020). The current characterization of the biological activities of exosomes primarily relies on non-physiological readouts generated from tissue cultures, which may be amplified, as well as various EVs isolation methods that require further refinement (Zhang et al., 2023). Nevertheless, the role of exosomes in cellular function appears to extend beyond mere protein recycling and varies according to the cellular origin, metabolic status, and environment (Liang et al., 2021). Molecules contained within exosomes, such as signaling proteins and RNA, can be internalized by recipient cells, thereby influencing their physiological state and function (Kim et al., 2024). This enables effective information transfer between the originating and receiving cells (Kim et al., 2024). Exosomes play a crucial role in mediating communication among immune cells and regulating immune responses (Li et al., 2025). For instance, exosomes released by tumor cells can suppress immune system activity, aiding tumor cells in evading immune surveillance (Liu et al., 2025). Additionally, exosomes are important in the processes of tissue repair and regeneration; they facilitate the proliferation and migration of adjacent cells by delivering growth factors and cytokines (Khalilzad et al., 2025). The investigation of exosomes and the mechanisms that regulate their cellular bioactivities and functions encompasses a wide range of processes (Hu et al., 2023). Exosome research is driven by its potential to function as biomarkers for treating numerous human diseases including: cardiovascular dysfunction, neurodegenerative disorders, and tumors (Barile and Vassalli, 2017). Recently, emerging evidence has revealed the essential role of exosomes in HBV infection, which is attributed to their structural and functional similarities (Liu et al., 2023; Peng et al., 2023). Given that exosomes are found in all biological fluids and possess the potential for multicomponent analyses, their application as liquid biopsies are particularly promising (Li et al., 2024).

In this review, we provide an overview of our current knowledge regarding the pathogenesis of HBV, with an emphasis on the role of exosomes in disease development and their potentially application into anti-HBV therapy. We also underscore the future prospects for clinical translation in this field.

2 The source and function of exosomes

EVs from endosomal origin were initially discovered in sheep reticulocytes in 1983 and subsequently named "exosomes" in 1987 (Pan and Johnstone, 1983; Johnstone et al., 1987). Research has demonstrated that exosomes are secreted *in vitro* by diverse eukaryotic cell types and can be found in bodily fluids, including blood, urine, bile, synovial fluid, breast milk, and semen (Abels and Breakefield, 2016). The protein and nucleic acid components within EVs are shielded from degradation by the vesicular membrane structure, rendering them markedly more stable than their free counterparts in human body fluids (Gupta et al., 2021). Exosomes originate from multivesicular bodies (MVBs), which are formed by the inward budding of the plasma membrane (Arumugam and Kaur, 2017). These early endosomes subsequently mature into late endosomes and MVBs that contain intraluminal vesicles (ILVs) (Han et al., 2022). After the formation of ILVs, some MVBs fuse with the cell membrane, releasing exosomes into the extracellular space, while others are degraded by lysosomes (Liu et al., 2021). The secretion of exosomes is mediated by the endosomal sorting complex required for transport (ESCRT), a family of proteins composed of four distinct complexes: ESCRT-0, ESCRT-I, ESCRT-II, and ESCRT-III (La Torre et al., 2024). Different ESCRT complexes display distinct functions in biological activities. ESCRT-0 mediates cargo aggregation through a ubiquitination-dependent pathway, while ESCRT-I and ESCRT-II initiate membrane budding. ESCRT-III is responsible for vesicle scission, and accessory proteins, such as VPS4 ATPase, facilitate the disassembly and recycling of the ESCRT complex (Aseervatham, 2023; Rivera-Cuevas and Carruthers, 2023).

These EVs offer significant potential as biomarkers for liquid biopsies and therapeutic applications, functioning as an innovative mechanism for intercellular communication and molecular transport (Čeri et al., 2024). These biovesicles are secreted by nearly all cell types and transport bioactive proteins, lipids, and nucleic acids (including noncoding RNAs) to target cells at distant locations (Palma et al., 2023; Dai Y. et al., 2024). Exosomes have emerged as potential diagnostic and prognostic biomarkers for various diseases, including cardiovascular conditions, cancers and neurodegenerative disorders (Chang et al., 2024; Yang et al., 2024). Recently, emerging evidence has demonstrated that exosomes play critical roles in viral infection (Chavda et al., 2024). During these processes, exosomes are integral to host immunity, as they contribute to the activation of antiviral responses and mediate the transfer of antiviral factors between adjacent cells (Shi et al., 2024). Exosomes influence the viral infection process in two ways: by modulating their cargo and by regulating the immune status of the host, which provides novel insights into the antiviral therapy (Shi et al., 2024) (Figure 1).

3 Exosomes in the pathology processes of HBV infection

Many viruses rely on intracellular trafficking to complete replication, initially interacting with the cell surface and following pathways to endosomes. The assembly and budding of enveloped viruses closely resemble the biogenesis of small exosomes, as both depend on cellular membranes. Thus, it is unsurprising that some viruses disrupt MVB formation and exosome production. The ESCRT system plays a key role in enveloped virus production.

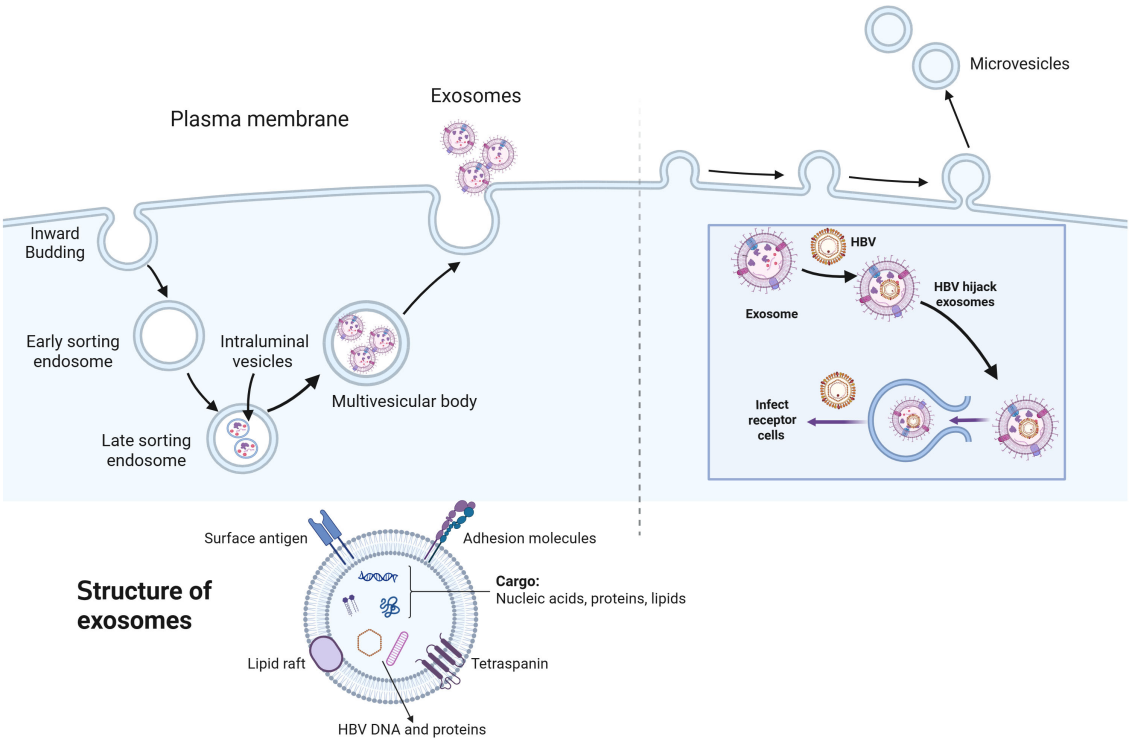

FIGURE 1
The biogenesis of exosomes and the essential role of exosomes in HBV infection. Exosome biogenesis is a multistep process beginning with the inward budding of the plasma membrane, which engulfs extracellular components to generate early endosomes. These early endosomes subsequently merge and mature into early sorting endosomes, which undergo a series of sorting and trafficking events, eventually differentiating into late sorting endosomes (LSEs). Within LSEs, further invagination of the endosomal membrane forms intraluminal vesicles (ILVs), resulting in the development of multivesicular bodies (MVBs). When MVBs fuse with the plasma membrane, ILVs are released as exosomes into the extracellular space via exocytosis. The process of microvesicle formation begins with the generation of outward protrusions at specific locations on the membrane, followed by fission and subsequent release of the vesicle into the extracellular space. Exosomes are small extracellular vesicles ranging from 30 to 150 nanometers in diameter, characterized by a lipid bilayer membrane composed of phospholipids and cholesterol. Their surface is covered with proteins such as tetraspanins and major histocompatibility complex molecules, which facilitate interactions with recipient cells. Internally, exosomes contain a diverse array of biomolecules, including proteins, various types of RNAs, and lipids. Moreover, they also include the hepatitis B virus (HBV) DNA and HB-related proteins upon HBV infection. Additionally, hepatitis B virus (HBV) exploits exosomes as vehicles for its release, transport, and interaction with target cells. Upon infecting host cells, HBV produces viral proteins and nucleic acids, which are subsequently packaged into exosomes, facilitating infecting receptor cells.

Studies have shown that many viruses hijack the ESCRT machinery to promote budding, enhancing their replication and spread (Dai J. et al., 2024; Chen et al., 2025). The hijacking of exosome biogenesis by viruses may further enable them to incorporate key components into exosomes, including their own viral nucleic acids, viral proteins, and even complete virions. This phenomenon is particularly evident in the case of HBV.

Exosomes serve as effective carriers of viral DNA and protein components, enabling the transfer of these materials from infected to uninfected cells and thereby promoting HBV dissemination (Wu et al., 2023). HBV-infected cells secrete exosomes that can be isolated from cell culture supernatants, exhibiting characteristic exosomal markers along with HBV-specific components (Wu et al., 2023). These exosome-enriched fractions can be effectively separated from fractions containing free viral particles. Controlled detergent treatment of exosomes leads to the sequential release of intact HBV virions and non-enveloped capsids. Transmission electron microscopy directly visualizes complete HBV virions encapsulated within exosomes (Wu et al., 2023). Additionally, purified extracellular vesicles derived from HBV-infected primary human hepatocytes derived from humanized chimeric mice (PXB) cells contained detectable HBV DNA and exhibited functional transfer competence of viral genetic material to uninfected PXB cells (Sanada et al., 2017). Research has revealed that HBV particles associated with the membranes of late endosomes and large intracellular compartments, suggesting the involvement of the ESCRT mechanism in HBV envelopment (Wang et al., 2020). Disruptions in the ESCRT system hindered HBV budding and release. For example, The knockdown of ESCRT-II not only suppressed the production and release of enveloped HBV virions but also impaired the formation of intracellular nucleocapsids (Stieler and Prange, 2014). Genetic ablation of TSG101 markedly attenuated viral particle secretion, which was corroborated by transmission electron microscopy analysis demonstrating a substantial reduction in HBV virions within MVBs following either TSG101 or NEDD4 depletion (Zheng Y. et al., 2023). HBV employed a sophisticated ERGIC-53-COPII cooperative mechanism for cellular egress, which represented a novel viral

export pathway (Zeyen et al., 2020). Evidence has indicated that mutations in critical ESCRT-related genes, such as actin-interacting protein (AIP) 1 or VPS4B, can block the formation of MVBs, subsequently preventing the release of enveloped HBV particles (Lambert et al., 2007). Furthermore, HBx mRNA and protein are packaged within exosomal cargo, shielding them from degradation by host nucleases (Kapoor et al., 2017).

4 Exosomes mediate the crosstalk between HBV and immune responses

4.1 Exosomes inhibit immune responses in HBV infection

The pathogenesis of chronic hepatitis B (CHB) results from the interaction between HBV and the host immune response (Lok et al., 2016). Consequently, it is unsurprising that HBV-associated exosomes play a critical role in evading the immune system's defenses. Moreover, exosomes play essential roles in regulating the immune cell function during HBV infection (Liu et al., 2023). Studies have reported that exosomes derived from the serum of CHB patients can facilitate the transmission of HBV to NK cells through the involvement of TGF-β, which leads to impaired NK cell function (Yang Y. et al., 2017). Overexpressed miR-21 and miR-29 in EVs derived from HBV-infected liver cells inhibited the release of IL-12 from dendritic cells and macrophages, leading to impaired NK cell function, inhibited immune response, and progression of liver fibrosis (Kouwaki et al., 2016). Exosomes released from HBV-infected cells have been shown to be endocytosed by monocytes, leading to the upregulation of programmed death-ligand 1 (PD-L1) expression and the simultaneous downregulation of CD69 (Kakizaki et al., 2018). PD-L1, as one of the most critical immune checkpoints, can also be induced by inflammatory cytokines, which ultimately inhibits T cell function (Zhou et al., 2023). CD69 functions as a biomarker of activated immune cells (Yong et al., 2017), which suggests that the depletion and inactivation of T cells in CHB may be attributed to the upregulated PD-L1 expression, which is triggered by HBV-associated exosomes (Kakizaki et al., 2020). In the mouse models of HBV, HBV-derived exosomes significantly suppressed the immune response and exacerbated CHB progression (Kakizaki et al., 2020). These effects were attributed to the impaired clearance of HBV-replicating cells in HBV-infected mice, mediated by HBV-derived EVs (Kakizaki et al., 2020). Moreover, these EVs demonstrated systemic biodistribution, with specific accumulation in multiple organs including the liver, bone marrow (BM), and intestinal tract, suggesting an EV-mediated liver-BM-gut tripartite axis in HBV infection, offering transformative understanding of CHB progression mechanisms (Kakizaki et al., 2020) (Figure 2).

4.2 Exosomes promote immune responses in HBV infection

Several studies have demonstrated that HBV-associated exosomes can enhance immune responses during HBV infection (Liu et al., 2023). For example, Zhao et al. discovered that hepatitis B virus (HBV) produces a microRNA (HBV-miR-3) that inhibited HBV replication by targeting HBV 3.5-kb transcript, leading to the decreased expression of HBsAg, HBeAg and HBc as well as impaired HBV replication (Yang X. et al., 2017). Further investigations have revealed that HBV-miR-3 activated the JAK/STAT signaling pathway by downregulating suppressor of cytokine signaling 5 (SOCS) in hepatocytes, thereby amplifying the interferon (IFN)-gamma-induced anti-HBV response (Zhao et al., 2020). Moreover, HBV-miR-3 in exosomes promoted M1 macrophage polarization (Zhao et al., 2020). Additionally, exosomes carrying HBV-miR-3 enhanced IL-6 secretion by inhibiting SOCS5-mediated Epidermal growth factor receptor (EGFR) ubiquitination, indicating that HBV-miR-3 activated the innate immune response through multiple pathways to potentially mitigate HBV-induced acute liver cell injury and influencing the HBV infection (Zhao et al., 2020).

In line with this, a study has revealed that liver nonparenchymal cells (LNPCs) treated with IFN-α exhibited increased expression of antiviral proteins, including A3G, MyD88, and PKR, which effectively inhibited HBV infection. Notably, exosomes derived from IFN-α-treated LNPCs were enriched with IFN-α and A3G. These antiviral components within the exosomes could be internalized by hepatocytes, leading to suppressed HBV infection (Li et al., 2013). Moreover, miR-106b-3p has been identified as an interferon-responsive miRNA. Furthermore, interferon could suppress viral replication and antigen expression by delivering miR-106b-3p to HBV-positive hepatocytes via macrophage-derived exosomes, which leading to the suppression of its downstream PI3K/AKT signaling pathway (Chen et al., 2024). Additionally, macrophage-derived exosomes rely on T cell immunoglobulin and mucin receptor 1 (TIM-1) to enter hepatocytes and deliver IFN-α-induced anti-HBV activity. Additionally, lysobisphosphatidic acid (LBPA), an anionic lipid associated with viral endosome penetration, facilitated exosome membrane fusion in late endosomes/multivesicular bodies (LEs/MVBs) and cargo release, providing insights into the transmission mechanisms of macrophage exosomes, highlighting similarities with viral entry pathways (Yao et al., 2018).

5 Exosomes as essential biomarkers in HBV-related disease.

HBV infection imposes significant disease burden to public health. Therefore, identifying essential biomarkers to guide treatment decisions and evaluate treatment response are critically important (Wu et al., 2020; Zheng C. et al., 2023). HBV DNA serves as the primary biomarker for viral replication and is the main virological endpoint in clinical trials of nucleos(t)ide analog (NA) therapy (Fung et al., 2022). However, given that current antiviral agents effectively suppress HBV DNA with minimal impact on covalently closed circular DNA (cccDNA), there is a need for additional biomarkers to assess cccDNA transcriptional activity and to evaluate the effects of future antiviral agents (He et al., 2023).

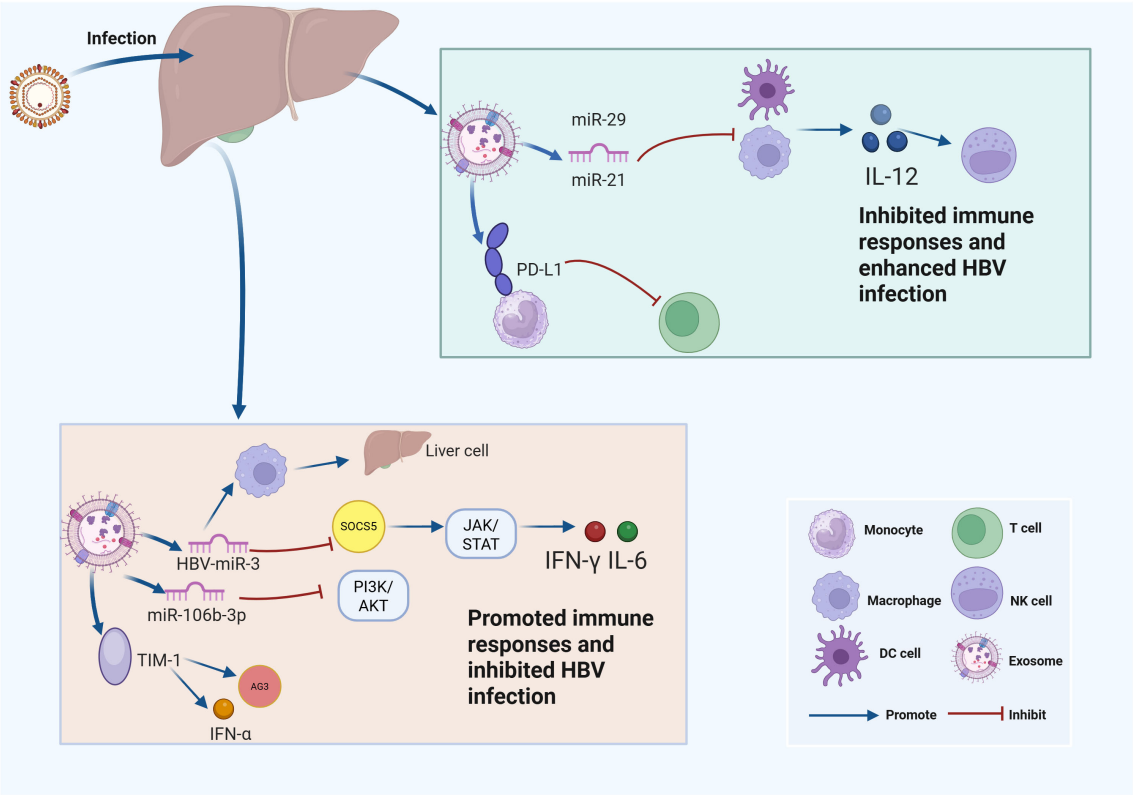

FIGURE 2
Exosomes influence HBV infection through regulating immune responses. This schematic illustrates the molecular mechanisms by which hepatitis B virus (HBV) modulates host immune responses through microRNAs (miRNAs) and key signaling pathways at the cellular level. Upper right panel: After HBV infection, liver immune cells such as monocytes, macrophages, and dendritic cells (DCs) produce microRNAs including miR-29 and miR-21, which are loaded into EVs. These miRNAs inhibit the expression of interleukin-12 (IL-12), leading to suppressed immune responses and facilitating enhanced HBV infection. In addition, the expression of programmed death-ligand 1 (PD-L1) is promoted by EVs released from HBV-infected cells, further contributing to immune evasion. Lower panel: EVs loaded with HBV-derived microRNAs (e.g., HBV-miR-3) and host microRNAs (such as miR-106b-3p) impact immune pathways within liver cells. HBV-miR-3 upregulates suppressor of cytokine signaling 5 (SOCS5), which suppresses the Janus kinase/signal transducer and activator of transcription (JAK/STAT) signaling pathway, while miR-106b-3p inhibits the phosphoinositide 3-kinase/protein kinase B (PI3K/AKT) pathway. Both mechanisms synergistically enhance the production of interferons, including interferon-gamma (IFN-γ) and interleukin-6 (IL-6), thereby promoting immune responses and inhibiting HBV infection. The interaction between T-cell immunoglobulin and mucin-domain containing-1 (TIM-1) and exosome-associated antigen 3 (Ag3) further stimulates the production of interferon-alpha (IFN-α).

Recently, emerging studies have revealed that EVs have functioned as novel diagnostic and prognostic biomarkers for HBV infection (Wu et al., 2024). Gan et al. reported that HBV-miR-3 in serum-derived exosomes from CHB patients had a positive correlation with HBV DNA, and HBsAg levels. In patients who received NA combined with PEG-interferon (PEG-IFN) treatment, the HBsAg, HBV pregenomic (pgRNA), and HBV-miR-3 exhibited a decrease during the 48 weeks of sequential therapy, indicating that HBV-miR-3 could serve as a supplement to current viral markers (Gan et al., 2022).

The progression to cirrhosis is the most common complication of HBV infection, posing huge health burdens to public health (van Bömmel and Berg, 2013). The onset of cirrhosis is primarily driven by inflammatory activity in the liver, which reflects an immune response to the infection; however, this may not always be indicated by elevated ALT levels, as other contributing factors may also play a role (Guerrieri and Levrero, 2023). Serum EV-associated miR-92a-3p and miR-146a-5p have demonstrated superior diagnostic capabilities compared to the fibrosis index based on four factors (FIB-4), and liver stiffness measurement (LSM) for identifying severe fibrosis patients, thus offering a promising non-invasive alternative (Wang Q. et al., 2021). Serum EV-associated adenosylhomocysteinase (AHCY) expression was also positively correlated with the degree of cirrhosis, achieving over 90% rates of specificity, which exceeded the predictive power of Child–Pugh classification system (Tong et al., 2021).

HBV is the main cause of hepatocellular carcinoma (HCC), which poses a significant public health threat, and early detection remains challenging due to the absence of highly sensitive and specific biomarkers for HBV-related HCC (HBV-HCC) (Papatheodoridi et al., 2022). Todorova et al. employed miRNA sequencing analysis and various bioinformatics methods to identify more than 40 dysregulated exosomal miRNAs in HBV-HCC cells. Among them, miR-483-5p exhibited high specificity and serving as the top dysregulated molecules (Todorova et al., 2023). Moreover, other five miRNAs including miR-182, miR-133a, miR-183, miR-155, and miR-34a positively associated with HBV activity and disease development (Todorova et al., 2023), supporting novel

non-invasive biomarkers for the prediction of HBV-HCC. Additionally, exosomal hsa_circ_0028861 was also marked as innovative diagnostic biomarker for HBV-HCC. It exhibited great predictive power for multiple stages and types of HCC including small tumor types, AFP-negative and early-stage phase (Wang Y. et al., 2021).

HBV-related acute-on-chronic liver failure (ACLF) is characterized by elevated short-term mortality rates, highlighting the need for precise prognostic biomarkers for effective early detection and prompt intervention (Wu et al., 2020). By aligning RNA sequencing (RNA-seq), Chen and colleagues revealed that the expression NADPH oxidase 1 (NOX1) and ZSCAN16-AS1 were both upregulated in HBV-ACLF and CHB tissues. Further investigation indicated that both NOX1 and ZSCAN16-AS1 negatively correlated with ALB levels and positively associated with ALT levels, suggesting the promising clinical application of serving as biomarkers for patients with CHB or HBV-ACLF (Chen et al., 2020). In line with this, Xu et al. identified critical small noncoding RNAs (sncRNAs) in HBV-ACLF patients through small RNA-seq approach, which indicating that six sncRNAs including tsRNA-46, tsRNA-20, rsRNA-249, hsa-miR-23b-3p, hsa-miR-223-3p, and hsa-miR-339-5p were uniquely differentially expressed in the plasma exosomes of patients. Moreover, they developed a risk stratification. model called MTR-RNA for HBV-ACLF early detection. The MTR-RNA model exhibited strong predictive power with a 0.787 of C-index, along with more than 70% predictive specificity and sensitivity, which demonstrated that these sncRNAs could function as reliable and feasible biomarkers for HBV-ACLF patients (Xu et al., 2022). Additionally, exosomal lncRNA GAS5 extracted from HBV-ACLF patients exhibited great predictive power of 3-month mortality with achieving AUC of 0.88 (Sun et al., 2023). Exosomal NEAT1 was another biomarker for predicting the 3-month mortality of HBV-ACLF. It exhibited superior predictive power compare to the MELD score system, which attributed to its association with a dysregulated innate immune response that promoted HBV replication, thereby offering a more direct evaluation of the liver microenvironment (Gao et al., 2021). Therefore, exosomes can enhance early diagnosis and offer prognostic insights for HBV-ACLF, assisting in the evaluation of disease progression and informing management adjustments.

Consequently, exosomes have garnered significant attention as potential markers for disease diagnosis. Further exploration of exosomal contents associated with HBV infection is anticipated to facilitate the identification of more promising biomarkers for HBV diagnosis.

6 Applications of exosomes in the anti-HBV therapy

Current antiviral therapies for HBV infection are primarily categorized into two classes: interferons (IFNs) and nucleoside analogs (NAs) (Lee et al., 2020). Although IFNs have been extensively used to treat CHB patients, it exhibited limited clinical effectiveness due to the distributions of its antiviral molecular pathways and not fully activated immune responses (Lei et al., 2024). NAs exert their antiviral functions through suppressing the activity of DNA polymerase and impeding the HBV replication progression. However, the clinical effectiveness of NAs remains suboptimal with low proportion of CHB patients achieved HBsAg loss after NAs treatment (Nishikawa et al., 2024). Therefore, there is the urgent need to develop innovative antiviral drugs for impeding HBV replication and achieving favorable clinical efficacy.

Exosomes play essential roles in HBV pathology processes and mediate complex immune responses (Liu et al., 2023). Moreover, they serve as essential biomarkers for the detection and monitoring of HBV-related diseases, suggesting that exosomes hold immense potential for anti-HBV treatment (Hu et al., 2021; Gan et al., 2022). Exosomes could activate immune cells to exert antiviral effects. For example, exosomes containing HBV-miR-3 secreted by HBV-infected hepatocytes can act on macrophages to promote IL-6 secretion and restrict viral replication (Zhao et al., 2020). Additionally, exosomes derived from immune cells could transfer their antiviral capacity to infected hepatocytes. For instance, Exosomes are capable of transferring IFN-α-related miRNAs (hsa-miR-193a-5p, hsa-miR-25-5p, and hsa-miR-574-5p) from macrophages to hepatocytes infected with HBV, which led to significant antiviral activity. Among them, hsa-miR-574-5p bound to the 2750–2757 region of the HBV genome, leading to a reduction in the levels of pgRNA and polymerase mRNA (Wu et al., 2021). Therefore, exosomes could serve as potential agents for antiviral therapy.

Moreover, exosomes could function as the therapeutic targets for HBV infection and HBV-related liver fibrosis. For example, stress-induced tribbles pseudokinase 3 (TRIB3) interacted with sequestosome 1 (SQSTM1) to enhance the secretion of INHBA/Activin A-rich exosomes from hepatocytes, thereby activating hepatic stellate cells (HSCs) and promoting liver fibrosis (Zhang et al., 2020). HBV-infected hepatocytes could also secrete MiR-222 and HBX, which further facilitated the activation of HSCs. Conversely, Kupffer cells produced endogenous miR-690 and transported it via exosomes to hepatocytes, recruited hepatic macrophages (RHMs), and HSCs, directly inhibiting adipogenesis in hepatocytes, suppressing the inflammation in RHMs, and hindering the activation of HSCs (Zhang et al., 2020). Thus, enhancing the secretion of antifibrotic exosomes, inhibiting the release of profibrotic exosomes, or developing therapeutic exosome-based strategies targeting fibrosis may offer promising approaches for delaying the progression of HBV-associated liver fibrosis.

Notably, exosomes could function as carriers by efficiently delivering nucleic acids and proteins that play essential roles in innate immune responses (Buzas, 2023). Exosomes hold great potential to serve as prophylactic vaccines (Kim and Thapa, 2023; Wang et al., 2023). EVs derived from lipopolysaccharide (LPS)-stimulated human monocytic cell line (THP-1) were systematically characterized and demonstrated dual adjuvant properties. Primarily, these exosomes function as natural immunostimulants by potently inducing the secretion of key proinflammatory cytokines including interleukin 1 beta (IL-1β) and tumor necrosis factor alpha (TNF-α), thereby effectively activating host immune responses (Jesus et al., 2018). Furthermore, when co-administered with hepatitis B surface antigen

(HBsAg) - either in conventional soluble form or encapsulated in innovative HBsAg-loaded poly-ε-caprolactone (PCL)/chitosan nanoparticle delivery systems – the exosomes significantly enhanced vaccine immunogenicity (Jesus et al., 2018). Additionally, Ferrantelli et al. used DNA Vectors to produced engineered exosomes that induced cytotoxic T lymphocyte (CTL) immune responses against HBV-related antigens, which functioned as novel vaccine candidates for anti-HBV treatment (Ferrantelli et al., 2018).

EVs are membrane-delimited nanovesicles derived from biological sources, recognized for their stability, biocompatibility, low immunogenicity, and capacity to traverse biological barriers, which gain recognition as promising vehicles for drug delivery (Kibria et al., 2018). The progress of drug delivery using exosomes is closely associated with advancements in artificial exosome technology and the development of drug-loaded exosomes (Liang et al., 2021). For example, Zeng et al. incorporated vesicular stomatitis virus glycoprotein (VSV-G) onto the EV membrane, which significantly promoted endosomal escape of Clustered Regularly Interspaced Short Palindromic Repeats (CRISPR) -associated protein 9 (Cas9) protein and boosted its gene-editing efficacy in recipient cells. This could effectively reduce viral antigen levels and cccDNA in both HBV replication and infection cell models, indicating that engineered EVs could offer a promising therapeutic approach for the eradication of chronic HBV infection (Zeng et al., 2024).

7 Conclusions and perspectives

Exosomes play crucial roles in essential biological processes related to HBV infection. This review provides an overview of research focused on the role of exosomes in the progression of HBV infection, specifically addressing their involvement in HBV replication, synthesis, and release. Drawing on the characteristics and functions of exosomes, we outline and anticipate the potential uses of exosomes in the context of HBV. However, research on exosomes in HBV-related diseases is still in its early stages. Advancing our understanding of the biology of HBV-derived exosomes through further research may lead to the discovery of novel diagnostic and therapeutic targets. While established guidelines are available for the diagnosis and management of HBV infection, additional studies are necessary to develop innovative therapies aimed at suppressing viral replication and transmission while minimizing adverse effects. As highlighted in this review, exosomes play a crucial role in the formation of HBV particles, facilitate viral spread, and modulate the pathogenicity of HBV infection. Therefore, targeting exosome-associated pathways could represent a promising therapeutic approach for HBV infection. Although research into HBV-derived exosomes is still at an early stage, the potential for exosome-based clinical applications is increasingly evident.

Author contributions

XY: Formal analysis, Investigation, Methodology, Resources, Visualization, Writing – original draft, Writing – review & editing. CH: Conceptualization, Data curation, Formal analysis, Investigation, Project administration, Resources, Software, Supervision, Visualization, Writing – review & editing. YR: Conceptualization, Data curation, Formal analysis, Methodology, Project administration, Supervision, Validation, Writing – review & editing.

Funding

The author(s) declare that no financial support was received for the research and/or publication of this article.

Acknowledgments

We thank the BioRender drawing software (https://www.biorender.com/).

Conflict of interest

The authors declare that the research was conducted in the absence of any commercial or financial relationships that could be construed as a potential conflict of interest.

Generative AI statement

The author(s) declare that no Generative AI was used in the creation of this manuscript.

Publisher's note

All claims expressed in this article are solely those of the authors and do not necessarily represent those of their affiliated organizations, or those of the publisher, the editors and the reviewers. Any product that may be evaluated in this article, or claim that may be made by its manufacturer, is not guaranteed or endorsed by the publisher.

References

Abels, E. R., and Breakefield, X. O. (2016). Introduction to extracellular vesicles: biogenesis, RNA cargo selection, content, release, and uptake. *Cell Mol. Neurobiol.* 36, 301–312. doi: 10.1007/s10571-016-0366-z

Arumugam, S., and Kaur, A. (2017). The lipids of the early endosomes: making multimodality work. *Chembiochem* 18, 1053–1060. doi: 10.1002/cbic.201700046

Aseervatham, J. (2023). Dynamic role of exosome microRNAs in cancer cell signaling and their emerging role as noninvasive biomarkers. *Biol. (Basel)* 12. doi: 10.3390/biology12050710

Barile, L., and Vassalli, G. (2017). Exosomes: Therapy delivery tools and biomarkers of diseases. *Pharmacol. Ther.* 174, 63–78. doi: 10.1016/j.pharmthera.2017.02.020

Bixler, D., Zhong, Y., Ly, K. N., Moorman, A. C., Spradling, P. R., Teshale, E. H., et al. (2019). Mortality among patients with chronic hepatitis B infection: the chronic hepatitis cohort study (CHeCS). *Clin. Infect. Dis.* 68, 956–963. doi: 10.1093/cid/ciy598

Buzas, E. I. (2023). The roles of extracellular vesicles in the immune system. *Nat. Rev. Immunol.* 23, 236–250. doi: 10.1038/s41577-022-00763-8

Čeri, A., Somborac-Bačura, A., Fabijanec, M., Hulina-Tomašković, A., Matusina, M., Detel, D., et al. (2024). Establishment of liquid biopsy procedure for the analysis of circulating cell free DNA, exosomes, RNA and proteins in colorectal cancer and adenoma patients. *Sci. Rep.* 14, 26925. doi: 10.1038/s41598-024-78497-x

Chang, C., Weiping, L., and Jibing, C. (2024). Exosomal miRNA therapy for central nervous system injury diseases. *Cell Mol. Neurobiol.* 45, 3. doi: 10.1007/s10571-024-01522-0

Chavda, V. P., Luo, G., Bezbaruah, R., Kalita, T., Sarma, A., Deka, G., et al. (2024). Unveiling the promise: Exosomes as game-changers in anti-infective therapy. *Explor. (Beijing)* 4, 20230139. doi: 10.1002/exp.20230139

Chen, J., Xu, Q., Zhang, Y., and Zhang, H. (2020). RNA profiling analysis of the serum exosomes derived from patients with chronic hepatitis and acute-on-chronic liver failure caused by HBV. *Sci. Rep.* 10, 1528. doi: 10.1038/s41598-020-58233-x

Chen, J., Yang, H., Wan, M., Cheng, Y., Bai, J., Li, Y., et al. (2025). Classical swine fever virus recruits ALIX and ESCRT-III to facilitate viral budding. *mBio*, e0261824. doi: 10.1128/mbio.02618-24

Chen, J., Yin, Q., Xu, S., Tan, X., Liang, Y., Chen, C., et al. (2024). IFN-treated macrophage-derived exosomes prevents HBV-HCC migration and invasion via regulating miR-106b-3p/PCGF3/PI3K/AKT signaling axis. *Front. Cell Infect. Microbiol.* 14. doi: 10.3389/fcimb.2024.1421195

Colombo, M., Raposo, G., and Théry, C. (2014). Biogenesis, secretion, and intercellular interactions of exosomes and other extracellular vesicles. *Annu. Rev. Cell Dev. Biol.* 30, 255–289. doi: 10.1146/annurev-cellbio-101512-122326

Dai, J., Feng, Y., Liao, Y., Tan, L., Sun, Y., Song, C., et al. (2024). ESCRT machinery and virus infection. *Antiviral Res.* 221, 105786. doi: 10.1016/j.antiviral.2023.105786

Dai, Y., Wang, X., Du, W., Chen, R., Ma, F., Ma, T., et al. (2024). NK cell-derived exosomes inhibit survival of Mycobacterium tuberculosis by promoting apoptosis in mice. *Cytokine* 185, 156820. doi: 10.1016/j.cyto.2024.156820

Ferrantelli, F., Manfredi, F., Chiozzini, C., Anticoli, S., Olivetta, E., Arenaccio, C., et al. (2018). DNA vectors generating engineered exosomes potential CTL vaccine candidates against AIDS, hepatitis B, and tumors. *Mol. Biotechnol.* 60, 773–782. doi: 10.1007/s12033-018-0114-3

Fung, S., Choi, H. S. J., Gehring, A., and Janssen, H. L. A. (2022). Getting to HBV cure: The promising paths forward. *Hepatology* 76, 233–250. doi: 10.1002/hep.32314

Gan, W., Chen, X., Wu, Z., Zhu, X., Liu, J., Wang, T., et al. (2022). The relationship between serum exosome HBV-miR-3 and current virological markers and its dynamics in chronic hepatitis B patients on antiviral treatment. *Ann. Transl. Med.* 10, 536. doi: 10.21037/atm-22-2119

Gao, S., Fan, Y. C., Han, L. Y., and Wang, K. (2021). Serum exosomal long noncoding RNA nuclear-enriched abundant transcript 1 predicts 90-day mortality in acute-on-chronic hepatitis B liver failure. *Expert Rev. Clin. Immunol.* 17, 789–797. doi: 10.1080/1744666x.2021.1933442

Guerrieri, F., and Levrero, M. (2023). HBV, mitochondrial stress, and liver fibrosis: chicken or the egg. *Hepatology* 77, 1088–1089. doi: 10.1097/hep.0000000000000031

Gupta, D., Zickler, A. M., and El Andaloussi, S. (2021). Dosing extracellular vesicles. *Adv. Drug Delivery Rev.* 178, 113961. doi: 10.1016/j.addr.2021.113961

Han, C., Yang, J., Sun, J., and Qin, G. (2022). Extracellular vesicles in cardiovascular disease: Biological functions and therapeutic implications. *Pharmacol. Ther.* 233, 108025. doi: 10.1016/j.pharmthera.2021.108025

He, P., Zhang, P., Fang, Y., Han, N., Yang, W., Xia, Z., et al. (2023). The role of HBV cccDNA in occult hepatitis B virus infection. *Mol. Cell Biochem.* 478, 2297–2307. doi: 10.1007/s11010-023-04660-z

Hu, Q., Wang, Q., Zhang, Y., Tao, S., Zhang, X., Liu, X., et al. (2021). Baseline serum exosome-derived miRNAs predict HBeAg seroconversion in chronic hepatitis B patients treated with peginterferon. *J. Med. Virol.* 93, 4939–4948. doi: 10.1002/jmv.26916

Hu, J., Zhu, J., Chai, J., Zhao, Y., Luan, J., Wang, Y., et al. (2023). Application of exosomes as nanocarriers in cancer therapy. *J. Mater Chem. B* 11, 10595–10612. doi: 10.1039/d3tb01991h

Jesus, S., Soares, E., Cruz, M. T., and Borges, O. (2018). Exosomes as adjuvants for the recombinant hepatitis B antigen: First report. *Eur. J. Pharm. Biopharm* 133, 1–11. doi: 10.1016/j.ejpb.2018.09.029

Johnstone, R. M., Adam, M., Hammond, J. R., Orr, L., and Turbide, C. (1987). Vesicle formation during reticulocyte maturation. Association of plasma membrane activities with released vesicles (exosomes). *J. Biol. Chem.* 262, 9412–9420. doi: 10.1016/S0021-9258(18)48095-7

Kakizaki, M., Yamamoto, Y., Otsuka, M., Kitamura, K., Ito, M., Kawai, H. D., et al. (2020). Extracellular vesicles secreted by HBV-infected cells modulate HBV persistence in hydrodynamic HBV transfection mouse model. *J. Biol. Chem.* 295, 12449–12460. doi: 10.1074/jbc.RA120.014317

Kakizaki, M., Yamamoto, Y., Yabuta, S., Kurosaki, N., Kagawa, T., Kotani, A., et al. (2018). The immunological function of extracellular vesicles in hepatitis B virus-infected hepatocytes. *PloS One* 13, e0205886. doi: 10.1371/journal.pone.0205886

Kalluri, R., and LeBleu, V. S. (2020). The biology, function, and biomedical applications of exosomes. *Science* 367. doi: 10.1126/science.aau6977

Kapoor, N. R., Chadha, R., Kumar, S., Choedon, T., Reddy, V. S., Kumar, V., et al. (2017). The HBx gene of hepatitis B virus can influence hepatic microenvironment via exosomes by transferring its mRNA and protein. *Virus Res.* 240, 166–174. doi: 10.1016/j.virusres.2017.08.009

Khalilzad, M. A., Mohammadi, J., Amirsaadat, S., Najafi, S., Zare, S., Nilforoushzadeh, M. A., et al. (2025). Therapeutic potential of apoptotic vesicles in modulating inflammation, immune responses, and tissue regeneration. *J. Nanobiotechnology* 23, 260. doi: 10.1186/s12951-025-03278-1

Kibria, G., Ramos, E. K., Wan, Y., Gius, D. R., and Liu, H. (2018). Exosomes as a drug delivery system in cancer therapy: potential and challenges. *Mol. Pharm.* 15, 3625–3633. doi: 10.1021/acs.molpharmaceut.8b00277

Kim, J., Ro, J., and Cho, Y. K. (2024). Vascularized platforms for investigating cell communication via extracellular vesicles. *Biomicrofluidics* 18, 051504. doi: 10.1063/5.0220840

Kim, J., and Thapa, N. (2023). Exosome-based COVID-19 vaccine. *Methods Mol. Biol.* 2668, 301–311. doi: 10.1007/978-1-0716-3203-1_20

Kouwaki, T., Fukushima, Y., Daito, T., Sanada, T., Yamamoto, N., Mifsud, E. J., et al. (2016). Extracellular vesicles including exosomes regulate innate immune responses to hepatitis B virus infection. *Front. Immunol.* 7. doi: 10.3389/fimmu.2016.00335

Krylova, S. V., and Feng, D. (2023). The machinery of exosomes: biogenesis, release, and uptake. *Int. J. Mol. Sci.* 24. doi: 10.3390/ijms24021337

Lai-Hung Wong, G., and Lemoine, M. (2024). The 2024 updated WHO guidelines for the prevention and management of chronic hepatitis B: main changes and potential implications for the next major liver society clinical practice guidelines. *J. Hepatol.* doi: 10.1016/j.jhep.2024.12.004

Lambert, C., Döring, T., and Prange, R. (2007). Hepatitis B virus maturation is sensitive to functional inhibition of ESCRT-III, Vps4, and gamma 2-adaptin. *J. Virol.* 81, 9050–9060. doi: 10.1128/jvi.00479-07

La Torre, M., Burla, R., and Saggio, I. (2024). Preserving genome integrity: unveiling the roles of ESCRT machinery. *Cells* 13. doi: 10.3390/cells13151307

Lee, H. W., Lee, J. S., and Ahn, S. H. (2020). Hepatitis B virus cure: targets and future therapies. *Int. J. Mol. Sci.* 22. doi: 10.3390/ijms22010213

Lei, Z., Wang, L., Gao, H., Guo, S., Kang, X., Yuan, J., et al. (2024). Mechanisms underlying the compromised clinical efficacy of interferon in clearing HBV. *Virol. J.* 21, 314. doi: 10.1186/s12985-024-02589-3

Li, J., Liu, K., Liu, Y., Xu, Y., Zhang, F., Yang, H., et al. (2013). Exosomes mediate the cell-to-cell transmission of IFN-α-induced antiviral activity. *Nat. Immunol.* 14, 793–803. doi: 10.1038/ni.2647

Li, D., Shi, Y., Yu, S., Zhang, B., Huang, Z., Ling, F., et al. (2025). NK cellular derived nanovesicles in tumor immunity. *Mol. Immunol.* 182, 54–61. doi: 10.1016/j.molimm.2025.03.018

Li, Y., Wang, Y., Zhao, H., Pan, Q., and Chen, G. (2024). Engineering strategies of plant-derived exosome-like nanovesicles: current knowledge and future perspectives. *Int. J. Nanomedicine* 19, 12793–12815. doi: 10.2147/ijn.S496664

Liang, Y., Duan, L., Lu, J., and Xia, J. (2021). Engineering exosomes for targeted drug delivery. *Theranostics* 11, 3183–3195. doi: 10.7150/thno.52570

Liu, Z., Li, Y., Wang, Y., Bai, X., and Zhang, Y. (2023). Exosomes in HBV infection. *Clin. Chim. Acta* 538, 65–69. doi: 10.1016/j.cca.2022.11.012

Liu, J., Ren, L., Li, S., Li, W., Zheng, X., Yang, Y., et al. (2021). The biology, function, and applications of exosomes in cancer. *Acta Pharm. Sin. B* 11, 2783–2797. doi: 10.1016/j.apsb.2021.01.001

Liu, X., To, K. K. W., Zeng, Q., and Fu, L. (2025). Effect of extracellular vesicles derived from tumor cells on immune evasion. *Adv. Sci. (Weinh)* 12, e2417357. doi: 10.1002/advs.202417357

Lok, A. S., McMahon, B. J., Brown, R. S. Jr., Wong, J. B., Ahmed, A. T., Farrah, W., et al. (2016). Antiviral therapy for chronic hepatitis B viral infection in adults: A systematic review and meta-analysis. *Hepatology* 63, 284–306. doi: 10.1002/hep.28280

Lorite, P., Domínguez, J. N., Palomeque, T., and Torres, M. I. (2024). Extracellular vesicles: advanced tools for disease diagnosis, monitoring, and therapies. *Int. J. Mol. Sci.* 26. doi: 10.3390/ijms26010189

Nishikawa, H., Kim, S. K., and Asai, A. (2024). Liver carcinogenesis suppression in chronic hepatitis B in the nucleoside analogues era. *In Vivo* 38, 40–47. doi: 10.21873/invivo.13408

Palma, L., Gentile, M., and Chun, N. (2023). Exosomes as modulators and biomarkers of transplant immunity. *Curr. Transplant. Rep.* 10, 245–252. doi: 10.1007/s40472-023-00413-5

Pan, B. T., and Johnstone, R. M. (1983). Fate of the transferrin receptor during maturation of sheep reticulocytes *in vitro*: selective externalization of the receptor. *Cell* 33, 967–978. doi: 10.1016/0092-8674(83)90040-5

Papatheodoridi, M., Tampaki, M., Lok, A. S., and Papatheodoridis, G. V. (2022). Risk of HBV reactivation during therapies for HCC: A systematic review. *Hepatology* 75, 1257–1274. doi: 10.1002/hep.32241

Peng, Y., Yang, Y., Li, Y., Shi, T., Luan, Y., Yin, C., et al. (2023). Exosome and virus infection. *Front. Immunol.* 14. doi: 10.3389/fimmu.2023.1154217

Rivera-Cuevas, Y., and Carruthers, V. B. (2023). The multifaceted interactions between pathogens and host ESCRT machinery. *PloS Pathog.* 19, e1011344. doi: 10.1371/journal.ppat.1011344

Sanada, T., Hirata, Y., Naito, Y., Yamamoto, N., Kikkawa, Y., Ishida, Y., et al. (2017). Transmission of HBV DNA mediated by ceramide-triggered extracellular vesicles. *Cell Mol. Gastroenterol. Hepatol.* 3, 272–283. doi: 10.1016/j.jcmgh.2016.10.003

Shi, C., Hu, S., Liu, S., Jia, X., and Feng, Y. (2024). Emerging role of exosomes during the pathogenesis of viral hepatitis, non-alcoholic steatohepatitis and alcoholic hepatitis. *Hum. Cell* 38, 26. doi: 10.1007/s13577-024-01158-8

Shih, C., Yang, C. C., Choijilsuren, G., Chang, C. H., and Liou, A. T. (2018). Hepatitis B virus. *Trends Microbiol.* 26, 386–387. doi: 10.1016/j.tim.2018.01.009

Starnawski, P., Nowak, K., Augustyn, Z., Malicki, D., Piąta, A., Lorek, D., et al. (2025). Role of hepatotropic viruses in promoting hepatocellular carcinoma-current knowledge and recent advances. *Med. Oncol.* 42, 111. doi: 10.1007/s12032-025-02674-9

Stieler, J. T., and Prange, R. (2014). Involvement of ESCRT-II in hepatitis B virus morphogenesis. *PloS One* 9, e91279. doi: 10.1371/journal.pone.0091279

Sun, C. X., Han, L. Y., Wang, K., and Gao, S. (2023). Serum exosomal long noncoding RNA growth arrest-specific 5 predicts 3-month mortality in acute-on-chronic hepatitis B liver failure. *J. Inflammation Res.* 16, 4603–4616. doi: 10.2147/jir.S423321

Todorova, V. K., Byrum, S. D., Mackintosh, S. G., Jamshidi-Parsian, A., Gies, A. J., Washam, C. L., et al. (2023). Exosomal microRNA and protein profiles of hepatitis B virus-related hepatocellular carcinoma cells. *Int. J. Mol. Sci.* 24. doi: 10.3390/ijms241713098

Tong, L., Yan, C., Wang, M., Yang, J., Wang, H., Wang, Y., et al. (2021). Prognostic value of serum exosomal AHCY expression in hepatitis B-induced liver cirrhosis. *Front. Med. (Lausanne)* 8. doi: 10.3389/fmed.2021.777452

van Bömmel, F., and Berg, T. (2013). Treatment of HBV related cirrhosis. *Liver Int.* 33 Suppl 1, 176–181. doi: 10.1111/liv.12074

Wang, J., Cao, D., and Yang, J. (2020). Exosomes in hepatitis B virus transmission and related immune response. *Tohoku J. Exp. Med.* 252, 309–320. doi: 10.1620/tjem.252.309

Wang, Q., Hu, Q., Ying, Y., Lu, C., Li, W., Huang, C., et al. (2021). Using next-generation sequencing to identify novel exosomal miRNAs as biomarkers for significant hepatic fibrosis. *Discov. Med.* 31, 147–159.

Wang, Y., Pei, L., Yue, Z., Jia, M., Wang, H., Cao, L. L., et al. (2021). The potential of serum exosomal hsa_circ_0028861 as the novel diagnostic biomarker of HBV-derived hepatocellular cancer. *Front. Genet.* 12. doi: 10.3389/fgene.2021.703205

Wang, J., Xing, K., Zhang, G., Li, Z., Ding, X., and Leong, D. T. (2025). Surface components and biological interactions of extracellular vesicles. *ACS Nano* 19, 8433–8461. doi: 10.1021/acsnano.4c16854

Wang, R., Zhu, T., Hou, B., and Huang, X. (2023). An iPSC-derived exosome-pulsed dendritic cell vaccine boosts antitumor immunity in melanoma. *Mol. Ther.* 31, 2376–2390. doi: 10.1016/j.ymthe.2023.06.005

Welsh, J. A., Goberdhan, D. C. I., O'Driscoll, L., Buzas, E. I., Blenkiron, C., Bussolati, B., et al. (2024). Minimal information for studies of extracellular vesicles (MISEV2023): From basic to advanced approaches. *J. Extracell Vesicles* 13, e12404. doi: 10.1002/jev2.12404

Wu, Q., Glitscher, M., Tonnemacher, S., Schollmeier, A., Raupach, J., Zahn, T., et al. (2023). Presence of intact hepatitis B virions in exosomes. *Cell Mol. Gastroenterol. Hepatol.* 15, 237–259. doi: 10.1016/j.jcmgh.2022.09.012

Wu, X., Niu, J., and Shi, Y. (2024). Exosomes target HBV-host interactions to remodel the hepatic immune microenvironment. *J. Nanobiotechnology* 22, 315. doi: 10.1186/s12951-024-02544-y

Wu, W., Wu, D., Yan, W., Wang, Y., You, J., Wan, X., et al. (2021). Interferon-induced macrophage-derived exosomes mediate antiviral activity against hepatitis B virus through miR-574-5p. *J. Infect. Dis.* 223, 686–698. doi: 10.1093/infdis/jiaa399

Wu, D., Zhang, S., Xie, Z., Chen, E., Rao, Q., Liu, X., et al. (2020). Plasminogen as a prognostic biomarker for HBV-related acute-on-chronic liver failure. *J. Clin. Invest.* 130, 2069–2080. doi: 10.1172/jci130197

Xu, W., Yu, M., Wu, Y., Jie, Y., Li, X., Zeng, X., et al. (2022). Plasma-derived exosomal sncRNA as a promising diagnostic biomarker for early detection of HBV-related acute-on-chronic liver failure. *Front. Cell Infect. Microbiol.* 12. doi: 10.3389/fcimb.2022.923300

Yang, K., Fu, W., Ma, Y., Wu, M., Li, X., Wang, Y., et al. (2024). A simple capillary isoelectric focusing method as the novel strategy for the isoelectric point measurement of exosomes and its application in disease diagnosis. *Mikrochim Acta* 192, 8. doi: 10.1007/s00604-024-06864-6

Yang, Y., Han, Q., Hou, Z., Zhang, C., Tian, Z., Zhang, J., et al. (2017). Exosomes mediate hepatitis B virus (HBV) transmission and NK-cell dysfunction. *Cell Mol. Immunol.* 14, 465–475. doi: 10.1038/cmi.2016.24

Yang, X., Li, H., Sun, H., Fan, H., Hu, Y., Liu, M., et al. (2017). Hepatitis B virus-encoded microRNA controls viral replication. *J. Virol.* 91. doi: 10.1128/jvi.01919-16

Yao, Z., Qiao, Y., Li, X., Chen, J., Ding, J., Bai, L., et al. (2018). Exosomes exploit the virus entry machinery and pathway to transmit alpha interferon-induced antiviral activity. *J. Virol.* 92. doi: 10.1128/jvi.01578-18

Yong, Y. K., Tan, H. Y., Saeidi, A., Rosmawati, M., Atiya, N., Ansari, A. W., et al. (2017). Decrease of CD69 levels on TCR Vα7.2(+)CD4(+) innate-like lymphocytes is associated with impaired cytotoxic functions in chronic hepatitis B virus-infected patients. *Innate Immun.* 23, 459–467. doi: 10.1177/1753425917714854

Zeng, W., Zheng, L., Li, Y., Yang, J., Mao, T., Zhang, J., et al. (2024). Engineered extracellular vesicles for delivering functional Cas9/gRNA to eliminate hepatitis B virus cccDNA and integration. *Emerg. Microbes Infect.* 13, 2284286. doi: 10.1080/22221751.2023.2284286

Zeyen, L., Döring, T., and Prange, R. (2020). Hepatitis B virus exploits ERGIC-53 in conjunction with COPII to exit cells. *Cells* 9. doi: 10.3390/cells9081889

Zhang, M., Hu, S., Liu, L., Dang, P., Liu, Y., Sun, Z., et al. (2023). Engineered exosomes from different sources for cancer-targeted therapy. *Signal Transduct Target Ther.* 8, 124. doi: 10.1038/s41392-023-01382-y

Zhang, S., Mak, L. Y., Yuen, M. F., and Seto, W. K. (2025). Mechanisms of hepatocellular carcinoma and cirrhosis development in concurrent steatotic liver disease and chronic hepatitis B. *Clin. Mol. Hepatol.* 31, S182–s195. doi: 10.3350/cmh.2024.0837

Zhang, L., Wong, C. Y., and Shao, H. (2025). Integrated technologies for molecular profiling of genetic and modified biomarkers in extracellular vesicles. *Lab. Chip* 25, 2504–2520. doi: 10.1039/d5lc00053j

Zhang, X. W., Zhou, J. C., Peng, D., Hua, F., Li, K., Yu, J. J., et al. (2020). Disrupting the TRIB3-SQSTM1 interaction reduces liver fibrosis by restoring autophagy and suppressing exosome-mediated HSC activation. *Autophagy* 16, 782–796. doi: 10.1080/15548627.2019.1635383

Zhao, X., Sun, L., Mu, T., Yi, J., Ma, C., Xie, H., et al. (2020). An HBV-encoded miRNA activates innate immunity to restrict HBV replication. *J. Mol. Cell Biol.* 12, 263–276. doi: 10.1093/jmcb/mjz104

Zheng, C., Lu, F., Chen, B., Yang, J., Yu, H., Wang, D., et al. (2023). Gut microbiome as a biomarker for predicting early recurrence of HBV-related hepatocellular carcinoma. *Cancer Sci.* 114, 4717–4731. doi: 10.1111/cas.15983

Zheng, S., Qi, W., Xue, T., Zao, X., Xie, J., Zhang, P., et al. (2024). Chinese medicine in the treatment of chronic hepatitis B: The mechanisms of signal pathway regulation. *Heliyon* 10, e39176. doi: 10.1016/j.heliyon.2024.e39176

Zheng, Y., Wang, M., Li, S., Bu, Y., Xu, Z., Zhu, G., et al. (2023). Hepatitis B virus hijacks TSG101 to facilitate egress via multiple vesicle bodies. *PloS Pathog.* 19, e1011382. doi: 10.1371/journal.ppat.1011382

Zhou, Y. J., Li, G., Wang, J., Liu, M., Wang, Z., Song, Y., et al. (2023). PD-L1: expression regulation. *Blood Sci.* 5, 77–91. doi: 10.1097/bs9.0000000000000149

Frontiers in
Cellular and Infection Microbiology

Investigates how microorganisms interact with their hosts

Explores bacteria, fungi, parasites, viruses, endosymbionts, prions and all microbial pathogens as well as the microbiota and its effect on health and disease in various hosts.

Discover the latest Research Topics

See more →

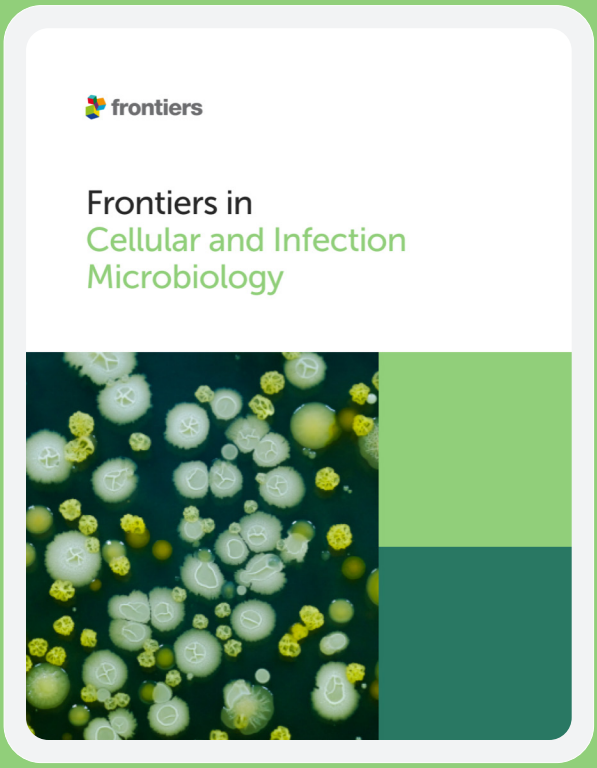

Frontiers

Avenue du Tribunal-Fédéral 34
1005 Lausanne, Switzerland
frontiersin.org

Contact us

+41 (0)21 510 17 00
frontiersin.org/about/contact